# Diversity of microbial communities in biofilms growing on hexachlorohexane and related substrates

Von der Fakultät für Lebenswissenschaften

der Technischen Universität Carolo-Wilhelmina

zu Braunschweig


zur Erlangung des Grades eines

Doktors der Naturwissenschaften

(Dr. rer. nat.)

genehmigte

**Dissertation**

von: Ahmed Shawky El-Housseiny Mohamed Gebreil

aus: El Dakahlia, Ägypten

1. Referent apl. Professor Dr. Dietmar H. Pieper
2. Referent Privatdozent Dr.-Ing. Max Schobert
eingereicht am: 27.07.2011
mündliche Prüfung (Disputation) am: 06.09.2011

Druckjahr 2011

DEDICATED TO:

MY COUNTRY EGYPT,

MY PARENTS,

MY SISTER,

MY DAUGHTER MENNATAALAH

AND MY KIND WIFE

# ACKNOWLEDGEMENT

All deepest thanks are due to **ALLAH** (Almighty), Al-Rahman, the most merciful, and the compassionate for uncountable gifts given to me.

First and foremost I want to thank my supervisor Dr. ***Wolf-Rainer Abraham*** for the support. It has been an honor to be one of his Ph.D. students. He has taught me, how good research in microbial biofilm can be done. I appreciate all his contributions of time, ideas, experience productive and stimulating. I want to thank him for the pleasant and trusting co-operation as well as the possibilities to present the results of my work in national and international conferences. Also I have to show my appreciation to Dr. ***Maximiliano G. Gutierrez*** for the efforts in the microscopic studies. I'd like to thank also Dr. ***Mahmoud B. Riad*** for teaching me how primers design and some basics in molecular biology.

I am very grateful to Prof. Dr. ***Dietmar Pieper*** and PD. Dr.-Ing. ***Max Schobert*** and Prof. Dr. ***Dietmar Schomburg*** of the examination committee for devoting some of their time to read, review and evaluate this study.

Many thanks to the CMIK group, they where more than colleagues, I made very good friends. Special thanks for Dr. ***Sonja Pawelczyk, Jennifer Knaak***, ***Esther Surges*** and ***Bettina Klug***, for being so kind and patient in teaching me how things worked in the lab. I want to thank also Dr. ***Marcela Heck***, ***Andréia Bergamo Estrela,*** and ***Maira Peres de Carvalho*****,** for the helping and friendship.

I am really grateful to all my new friends in HZI and Germany from many parts of the world. I am sure that without these people much more power would have been needed to finish this journey in Germany. Also I would like to thank all my Egyptian friends who are PhD students at the TU Braunschweig. I want to thank them for supporting me and my family to enjoy our stay in Braunschweig.

I wish to extend my gratitude to the Egyptian Government, Ministry of Higher Education, represented by the cultural affairs and missions sector in the Egyptian Embassy in Berlin for financial support during my study in Germany.

Lastly but no least, I would like to thank my family for all their love and encouragement, for my parents who raised me with a love of science and supported me in all my pursuits. I would like also to express my deepest thank and profound gratitude to my kind wife ***Fardous El-Senduny*** and my little daughter ***Mennatallah*** for their support, patience and encouragement during the hard times.

**Ahmed Shawky Gebreil**

Braunschweig, Germany, 2011

## Vorveröffentlichungen der Dissertation

Teilergebnisse aus dieser Arbeit wurden mit Genehmigung der Fakultät für Lebenswissenschaften, vertreten durch den Mentor der Arbeit, in folgenden Beiträgen vorab veröffentlicht:

Tagungsbeiträge

**Ahmed Shawky Gebreil and Wolf-Rainer Abraham** (2010), Diversity of bacterial biofilm communities growing on γ-hexachlorocyclohexane; Biofilms 4 International Conference, Winchester- UK.

**Ahmed Shawky Gebreil and Wolf-RainerAbraham** (2010), Diversity of bacterial communities growing on γ-hexachlorocyclohexane in soils from Egypt; 3rd Joint Conference of the German Society of Hygiene and Microbiology (DGHM) and the Association for General and Applied Microbiology (VAAM), Hannover-Germany.

**Table of Contents**

## List of abbreviations

| | |
|---|---|
| 1,2,4-TCB | 1,2,4-trichlorobenzene |
| 1,4- TCDN | 1,3,4,6-tetrachloro-1,4-cyclohexadiene |
| 2,4,5-DNOL | 2,4,5-trichloro- 2,5-cyclohexadiene-1-ol |
| 2,5- DCP | 2,5-dichlorophenol |
| 2,5-DCHQ | 2,5-dichlorohydroquinone |
| 2,5-DDOL | 2,5-dichloro-2,5-cyclohexadiene-1,4-diol |
| 2-CMA | 2-chloromaleylacetate |
| Acetyl-CoA | Acetyl coenzyme A |
| AFM | Atomic force microscopy |
| AHL | N-Acyl homoserine lactones |
| ARISA | Automated ribosomal intergenic spacer analysis |
| BDE 15 | 4,4'-dibromodiphenyl ether |
| BFRs | Brominated flame retardants |
| BHC | Benzenehexachloride |
| BTBPE | 1,2-bis(2,4,6-tribromophenoxy) ethane |
| CHQ | Chlorohydroquinone |
| CLSM | Confocal laser scanning microscopy |
| DCM | Dichloromethane |
| ddNTP’s | Dideoxynucleosidtriphosphates |
| DDT | Dichlorodiphenyltrichloroethane |
| DGGE | Denaturating gradient gel electrophoresis |
| dNTP’s | Desoxynucleosidtriphosphates |
| EDTA | Ethylene diamine tetraacetic acid |
| EPS | Extracellular polymeric substance |
| FAME | Fatty acid methyl ester |
| FID | Flame ionisation detector |
| FR | Flame retardants |
| GC | Gas chromatography |
| GSH | Glutathione (reduced form) |
| GS-SG | Glutathione (oxidized form) |
| HBCDD | Hexabromocyclododecane |
| HCHs | Hexachlorocyclohexanes |
| HOCs | Hydrophobic organic chemicals |
| HQ | Hydroquinone |
| LB-medium | Luria Bertani medium |
| MA | Maleylacetate |
| MTT | 3-(4,5-Dimethylthiazol-2-yl)-2,5-diphenyltetrazolium bromide |
| NADH | Nicotineamido adenine dinucleotide reduced form |
| NADPH | Nicotineamido adenine dinucleotide phosphate reduced form) |
| NCBI | National Center for Biotechnology Information |
| N-J | Neighbor-joining |
| OCPs | Organochlorine pesticides |
| OTUs | Operational taxonomic units |
| PBBs | Polybrominated biphenyls |
| PBDD/Fs | Polybrominated dibenzo-p-dioxins/di-benzofurans |
| PBDEs | Polybrominated diphenyl ethers |
| PBS | Phosphate buffered saline |

| | |
|---|---|
| PBTs | Persistent, Bioaccumulative and Toxic |
| PCBs | Polychlorinated biphenyls |
| PCCH | Pentachlorocyclohexene |
| PCDDs | Polychlorodibenzo-p-dioxins |
| PCDFs | Polychlorodibenzofurans |
| PCR | Polymerase chain reaction |
| PDA | Potato-dextrose-agar |
| PFA | Paraformaldehyde |
| POPS | Persistent organic pollutants |
| RFLP | Restriction fragment length polymorphism |
| RISA | Ribosomal intergenic spacer analysis |
| SEM | Scanning electron microscopy |
| SSCP | Single-strand conformation polymorphism |
| TBBPA | Tetrabromobisphenol A |
| TBE Buffer | Tris-borate-edta-buffer |
| TCA | Citrate/tricarboxylic acid cycle |
| TEM | Transmission electron microscopy |
| TEMED | N,N,N`,N`tetraethylmethylendiamine |
| TGGE | Temperature gradient gel electrophoresis |
| t-HCH | Technical formulation of HCH |
| TOMPs | Toxic organic micro pollutants |
| T-RFLP | Terminal restriction fragment length polymorphism |
| UNEP | United Nations environment programme |
| VP | Vapor pressures |
| WST-1 | Water-soluble Tetrazolium salts |
| α-HCH | Alpha- hexachlorocyclohexane |
| β-HCH | Beta- hexachlorocyclohexane |
| γ-HCH | Gamma-hexachlorocyclohexane |
| γ-TeCCH | Gamma-3,4,5,6,-tetrachlorocyclohexane |
| δ-HCH | Delta- hexachlorocyclohexane |

# 1 Introduction

Synthetic organic compounds are ubiquitous in our modern environment. They are found in our homes, workplaces, public spaces and in agriculture. A number of toxic synthetic organic compounds have contaminated environmental soil through either local (e.g., industrial) or diffuse (e.g., agricultural) contamination. These organic compounds can enter soil, air and water and can often be found far from their source of origin. Effects of contamination of environmental soil with toxic synthetic organic compounds include the poisoning of animals and plants, altering of ecosystems, and human health risks such as cancer.

Many toxic synthetic organic compounds are persistent and are stored in fat tissue, due to their hydrophobic properties, resulting in bioaccumulation. Therefore, organisms at higher levels in food chains (e.g., humans) tend to have higher concentrations of these bio-accumulated toxins stored in their fat tissue than those at lower levels resulting in bio-magnification of the physiological effects of the toxins in higher organisms. At the highest level in the food chain, i.e., humans, these toxic organic compounds can be passed from mother to child either *in utero* via the placenta or *post-natally* via breast milk.

Synthetic organic compounds of concern as environmental contaminants include polychlorinated biphenyls (PCBs), pesticides, industrial solvents, petroleum products, dioxins, furans, explosives, and brominated flame retardants.

Twelve organic compounds were listed as persistent organic pollutants (POPs) by the Stockholm Convention on Persistent Organic Pollutants, under the auspices of the United Nations Environment Programme (UNEP), an international agreement enforced in 2004. Although the use of these POPs worldwide has been generally phased out because of their toxicity and persistence, they can still be found as contaminants in the natural environment due to their past use and continue to pose a threat to human health [1].

## 1.1 Persistent organic pollutants

Persistent organic pollutants (POPs) are organic compounds that are resistant to environmental degradation through chemical, biological, and photolytic processes. Because of this, they are ubiquitous compounds of great concern due to their toxicity in the environment [2], persistence, long-range transport ability [3], bioaccumulation in human and animal tissue[4], biomagnifications in food chains, and they have potential significant impacts on human health and the environment. POPs bind strongly to soil organic matter and have been shown to become progressively sequestered with time [5]. Due to contaminant's

hydrophobicity, POPs readily bioaccumulate in the lipids of exposed organisms [6]. Subsequent biomagnification within food chains and significant negative impact on top trophic level organisms may then occur [7]. Many POPs are currently or were in the past used as pesticides. Others are used in industrial processes and in the production of a range of goods such as solvents, plastics and pharmaceuticals.

## 1.2 Chemical properties

Some of the chemical characteristics of POPs include low water solubility, high lipophilicity, semi-volatility and high molecular masses [8]. POPs with molecular weights lower than 236 g/mol are less toxic, less persistent in the environment and have more reversible effects than those with higher molecular masses. POPs are frequently halogenated, usually with chlorine. The more chlorine groups a POP has, the more resistant it is to being broken down over time. One important factor of their chemical properties such as lipid solubility results in the ability to pass through biological phospholipid membranes and bioaccumulate in the fatty tissues of living organisms [9].

## 1.3 Long-range transport

The ability of POPs to travel great distances is part of the explanation why countries that banned the use of specific POPs are no longer experiencing a decline in their concentrations; the wind may carry chemicals into the country from places that still use them. POPs entering the marine environment are readily absorbed by organic matter and taken up by plankton at the base of marine food webs. Bioaccumulation of POPs through the food chain is cause for concern, particularly for long-lived, top-level predators, such as marine mammals and humans. Known consequences of POP contamination in mammals include impaired immunity, increased susceptibility to disease, neurotoxicity, and reproductive impairment [10].

Hydrophobic organic chemicals (HOCs), like dieldrin, polycyclic aromatic hydrocarbons and pesticides, tightly adsorb on soil [11-12], which leads to low bioavailability of HOCs in soil [13-14]. However, despite this low bioavailability, the HOCs in soil are taken up by some plants; cucurbits in particular contain a large amount of HOCs in their shoots [15-16]. POPs reach remote oceans by long range atmospheric transport and subsequent deposition. Once in the water column, hydrophobic organic pollutants accumulate in planktonic organisms. It has been shown that planktonic food webs influence the oceanic cycle of POPs at regional and global scales [17-19].

## 1.4 Health concerns

Exposure to POPs can cause death and illnesses including disruption of the endocrine, reproductive and the immune systems, neuro-behavioral disorders and cancers including breast cancer. Exposure to POPs can take place through diet, environmental exposure, or accidents. A study published in 2006 indicated a link between blood serum levels of POPs and diabetes. Halogenated organic pollutants are ubiquitous in the environment. Concerns about their potential for harmful effects on human health such as various disruptions to the endocrine system have led to bans on the use of many of them [20].

## 1.5 Compounds

The groups of compounds that make up POPs are also classed as PBTs (Persistent, Bioaccumulative and Toxic) or TOMPs (Toxic Organic Micro Pollutants). These groups include carcinogenic compounds such as brominated flame-retardants and some organochlorinepesticides (OCPs) such as hexachlorocyclohexanes (HCHs) [9].

## 1.6 Organochlorine pesticides

A large variety of synthetic organic chemicals such as organochlorine pesticides (OCPs), have been released into the environment over the last few decades [21]. As widespread environmental pollutants, OCPs are highly lipophilic and chemically stable compounds that persist in the environment accumulating in the food chain and in human tissues [22].

Pesticides have been extensively used to protect and improve the quality and the quantity of food commodities, building materials and many environmentally important xenobiotics and other chemicals introduced for industrial and agricultural use are halogenated. Halogenation is often implicated as the reason for persistence and toxicity of such compounds. These compounds enter soil, water and food by several routes e.g. land fill, dumping of industrial wastes, by run-off from treated plant surfaces, spillage during application, use of contaminated manure, drift from aerial and ground application, erosion of contaminated soil by wind and water into the aquatic system, accidents in transport of insecticides, etc. One of halogenated insecticide is hexachlorocyclohexane (HCH), a homocyclic (alicyclic) chlorinated hydrocarbon popularly called benzenehexachloride (BHC) [23]. The widespread contamination of the environment, globally, has been caused by extensive and indiscriminate use of hexachlorocyclohexane as an insecticide since the 1940s, threatening the biota including humans [24]. HCH has been banned in technologically

advanced countries. However, it is still in use in tropical countries for mosquito control and thus new areas continue to be contaminated [23].

## 1.7 Hexachlorocyclohexanes (HCHs)

The technical formulation of HCH (t-HCH), was also used as a popular insecticide before the 1990s, mainly contains a mixture of HCH isomers (Figure 1) which include γ- (10–12%), α- (60–70%), β- (5–12%), and δ- (6–10%) isomers [25]. Because only γ-HCH has insecticidal activity among these four HCH isomers, it is generally purified from the rest of the isomers in t-HCH and used as "lindane" (>99% purity); the remaining three isomers are discarded as "HCH muck" [26]. The physical properties and persistence of each isomer differ because of the different chlorine atom orientations on each molecule (axial or equatorial). However, all four isomers are considered as toxic and recalcitrant worldwide pollutants [27].

The chemical structure and polarity of pesticides affect their solubility, volatility and sorption characteristics, factors that contribute to their transport, persistence and biodegradability, and might be used to explain the relative recalcitrance of the four isomers (α, β, γ, and δ) found in technical HCH. These characteristics are also influenced by the orientation of the chlorine atoms on each HCH isomer (Figure 1) [27].

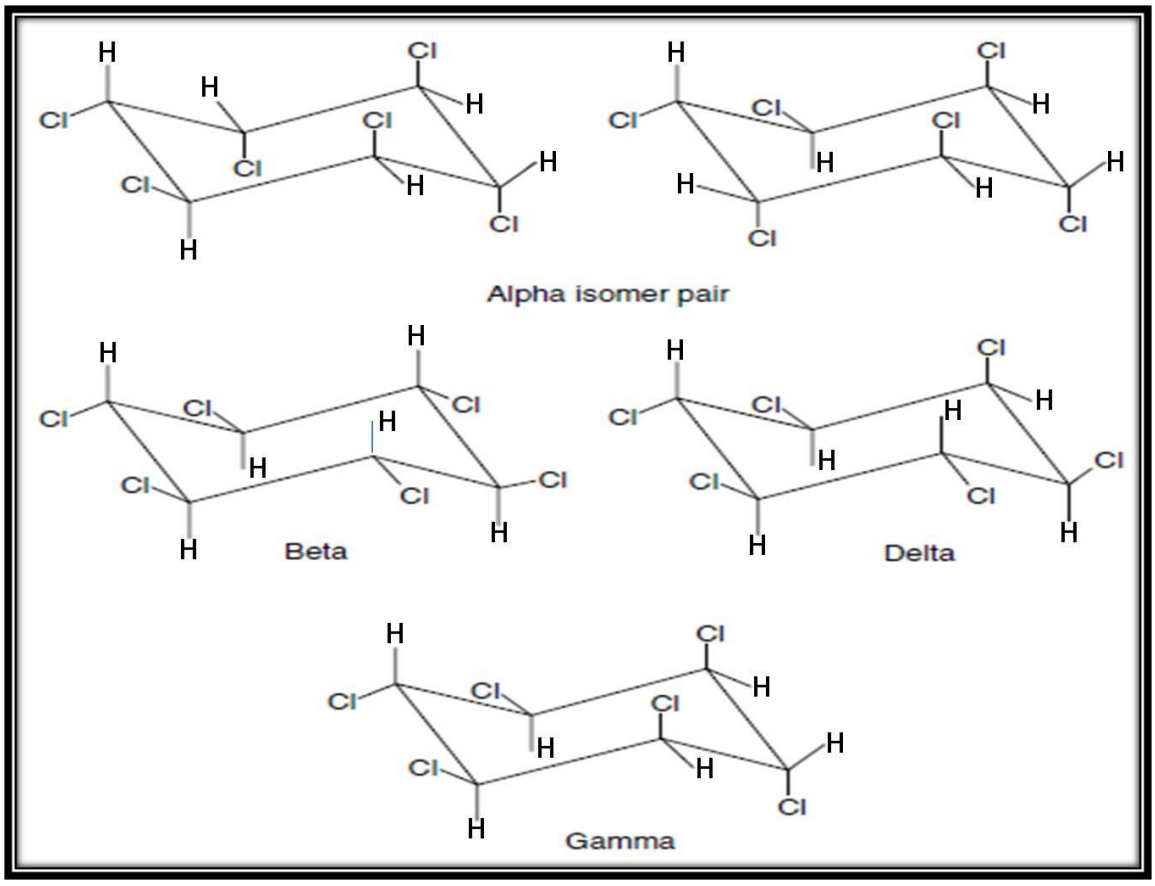


**Figure 1: Structures of HCH isomers, including the two enantiomers of α-HCH [27].**

γ-Hexachlorocyclohexane (γ-HCH, also called γ-BHC ) is a completely man-made halogenated organic insecticide. HCH is commercially manufactured by the photochemical chlorination of benzene in the presence of UV light. It has been used worldwide as a general, broad spectrum insecticide for a variety of purposes including fumigation of household and commercial storage areas, pest control on domestic animals, mosquito control and to kill soil-dwelling and plant-eating insects such as aphids, grasshoppers, flies, boil weevils, mange mites, termites, ants, leafminers, thrips, armyworms and wireworms, on fruits, vegetables and christmas and ornamental trees. It is widely used for stem borer control in rice paddies and is applied in Canada as a seed treatment for crops, such as canola, to protect from flea beetle infestations [26].

Sites heavily contaminated with HCH have been reported from The Netherlands, Brazil, Germany, Spain, China, Greece, Canada, the United States, and India. The 1998 Food and Agriculture Organization (FAO) inventory of obsolete, unwanted, and/or banned pesticides also found unused stockpiles of both technical HCH and lindane (2,785 tons of technical HCH, 304 tons of lindane, and 45 tons of unspecified HCH material) scattered in dump sites in Africa and the Near East [28]. Weber *et al.* estimated that four to six million tons of various HCH materials have been dumped worldwide, which is similar in scale to the combined totals of dumped materials for all other persistent organic pollutants (POPs) defined by the Stockholm Convention [29].

Although only lindane is insecticidal, HCHs as a group are toxic and considered potential carcinogens [27]. Due to their persistence and recalcitrance, however, HCHs continue to pose a serious toxicological problem at industrial sites where past production of lindane along with unsound disposal practices has led to serious contamination. In addition, many countries still allow HCH production and use despite localized limitations. HCH contamination continues to be a global issue, as these compounds have moderate volatility and can be transported by air to remote locations [27].

### 1.7.1 Toxicological effects of hexachlorocyclohexane

The organochlorine pesticides are widely recognized as neurotoxic substances affecting the peripheral and central nervous systems, and causing a hyperexcitability of nerves and muscles [30]. Other harmful effects of HCH deposition in human fat are disturbances of lipid metabolism [31-32], alterations in some membrane-bound proteins and membrane permeability [33-34]. Harmful effects of organochlorines on nonmammalian animals have also been reported. These chemicals enter into aquatic systems by drifting,

runoff, or water application. They accumulate through the food chain. For example, HCH has been reported from the eggs of birds that prey on fishes [35].

### 1.7.2 Degradation of lindane

Chemical, physical, or biological agents may degrade pesticides reaching the soil sediments or water ecosystem. Biological and chemical decomposition of xenobiotic compounds in such environments is always influenced by changes in many physicochemical parameters, such as temperature, pH, ion concentration, and redox potential. However, the microorganisms present in soil and water are a major factor in the degradation of these pesticides [30].

#### 1.7.2.1 Bacterial degradation of lindane

γ-HCH is degraded under both aerobic and anaerobic conditions, but it is generally mineralized only under aerobic conditions [27]. Many γ-HCH-degrading aerobic bacteria have been isolated and characterized [27, 36-38]. Only 60 years have passed since the first release of γ-HCH into the environment [25]. Thus, it is possible that γ-HCH-degrading bacteria have acquired the ability within this short period [27]. Bacteria able to degrade γ-HCH are a good model for helping us understanding how bacteria adapt to their environment.

Isolation of lindane-degrading microorganisms by enrichment culture has confirmed the ability of specific species of bacteria to degrade HCHs either aerobically or anaerobically. Some of these strains are able to grow on HCH as a sole carbon source. Several bacteria capable of degrading lindane have been described. These include *Clostridium sphenoides* UQM780 [39], *Clostridium rectum* S-17 [40], several other *Clostridium sp.* [41], a strain of *E. coli* isolated from rat feces [42], two species of *Bacillus* [27], several *Pseudomonas* [43], *Sphingomonas* [44] species, a *Pandoraea sp.*[45], *Citrobacter freundii* [41], and *Rhodanobacter lindaniclasticus*[46].

HCH-degrading (*Pseudomonas*) *Brevundimonas vesicularis* P59 was isolated in the Netherlands [47] by enrichment culture from contaminated soil slurries. A *Pseudomonas sp.* capable of aerobic growth on minimal salts media containing α- and γ-HCH as sole carbon sources was isolated from sugarcane rhizosphere soil [48-49]. The organism was able to degrade δ- and β-isomers in minimal salts media, but did not proliferate, nor did degrade these isomers in inoculated soil [48]. *Sphingomonas paucimobilis* UT26 is a nalidixic acid-resistant mutant of *Pseudomonas* (reclassified *Sphingomonas*) *paucimobilis* SS86, which was initially isolated from an upland soil in Japan [27]. UT26 is capable of aerobically degrading α-, γ- and δ-HCH isomers and using γ-HCH as a sole carbon source [27].

### 1.7.2.2 Fungal degradation of lindane

Until recently, research into pesticide degradation by microorganisms has focused primarily on bacteria, and fewer studies have been performed with fungi. The main reasons are: bacteria are easy to culture and grow more quickly than fungi, are more amenable to genetic manipulation techniques, are less likely to form mutant revertants, and bacteria use pesticides in laboratory conditions as their sole source of carbon.

Fungi as future bioremedial agents have several advantages over bacteria such as: ability to tolerate low pH values, fewer complex nutritional requirements, capability to degrade and utilize a wide range of complex substrates such as cellulose, hemicellulose, lignin and pectin, white-rot fungi with a wide range of extracellular enzymes degrade organopollutants nonspecifically in soil or water environments and make the resultant metabolites more vulnerable for further microbial attack. White-rot fungi degrade various pesticides including lindane by co-metabolism, and tolerate higher concentrations of toxic pollutants than bacteria [30].

Various white-rot basidiomycetes have been investigated for their lindane-degrading capabilities such as *Phanerochaete chrysosporium* [30], *Pleurotus sajor-caju* [50], *Trametes* ( *Coriolus*) *hirsutus*, *Phanerochaete sordida*, and *Cyathus bulleri* [30]. Pure cultures of the lignin-degrading fungi *Phanerochaete chrysosporium* and *Trametes hirsutus* have been shown to degrade lindane [51-52]. The conditions required for degradation of highly substituted aromatic or aliphatic compounds were similar to those that promoted lignin degradation by these fungi: nitrogen-deficiency and the presence of a co-substrate such as glucose. Therefore, the proposed mechanism of degradation of organochlorine pesticides by the fungus was similar to that of lignin degradation by lignin peroxidases, i.e., multiple non-specific oxidative reactions resulting from generation of carbon-centered free radicals [51]. The ability of several white-rot fungi to degrade lindane was tested by Arisoy 1998[53] who reported that *Phanerochaete chrysosporium*, *Pleurotus sajorcaju*, *Pleurotus florida* and *Pleurotus eryngii* were all able to degrade significant (>10%) amounts of lindane during 20 days incubation in culture media under oxic conditions. A summary of the HCH-degrading microorganisms is provided in Table 1.

**Table 1: Aerobic hexachlorocyclohexane-degrading microorganisms:**

| Microorganism (s) | References |
|---|---|
| **Bacteria** | |
| *Aerobacter aerogenes* | **[30]** |
| *Alcaligenes faecalis* | **[54]** |
| *Anabaena sp* | **[55]** |
| *Arthrobacter citreus* | **[56]** |
| *Bacillus circulans and Bacillus brevis* | **[28]** |
| *Bacillus megaterium* | **[30]** |
| *Bacillus sp.* | **[27]** |
| *Escherichia coli* | **[42]** |
| *Microbacterium sp.* | **[57]** |
| *Nostoc ellipsosporum* | **[55]** |
| *Pseudomonas aeruginosa* | **[28]** |
| *Pseudomonas fluorescens* | **[30]** |
| *Pseudomonas putida* | **[27]** |
| *Pseudomonas sp.* | **[43]** |
| (*Pseudomonas*) *Brevundimonas vesicularis* | **[47]** |
| *Rhodanobacter lindaniclasticus* | **[46, 58]** |
| *Sphingobium chinhatense IP26* | **[59]** |
| *Sphingobium indicum B90A* | **[49]** |
| *Sphingobium japonicum UT26* | **[28]** |
| *Sphingobium francense* | **[60]** |
| *Sphingobium quisquiliarum P25* | **[61]** |
| *Sphingobium ummariense RL-3* | **[28]** |
| *Sphingobium sp. SS04-5* | **[62]** |
| *Sphingomonas paucimobilis* | **[44]** |
| *Sphingomonas sp. γ 16-9* | **[38]** |
| *Streptomyces sp. M7* | **[63]** |
| *Xanthomonas sp. ICH12* | **[57]** |
| **Microalgae** | |
| *Chlorella vulgaris* | **[30]** |
| *Chlamydomonas reinhardtii* | **[30]** |
| **Fungi** | |
| *Cyathus bulleri* | **[64]** |
| *Phanerochaete chrysosporium* | **[51]** |
| *Phanerochaete sordida* | **[30]** |
| *Pleurotus eryngii* | **[53]** |
| *Pleurotus florida* | **[53]** |
| *Pleurotus sajor-caju* | **[53]** |
| *Trametes hirsutus* | **[30]** |

### 1.7.2.3 Aerobic degradation of γ-HCH

The aerobic degradation pathway of γ-HCH has been studied in some detail for strain UT26 [26] (Figure 2). It has been suggested that two initial dehydrochlorination reactions produce the putative product 1,3,4,6-tetrachloro-1,4-cyclohexadiene (1,3,4,6-TCDN) via the observed intermediate γpentachlorocyclohexene (γ-PCCH) [65]. Subsequently 2,5-dichloro-2,5-cyclohexadiene-1,4-diol (2,5-DDOL) is generated by two rounds of hydrolytic dechlorinations via a second putative metabolite, 2,4,5-trichloro-2,5-cyclohexadiene-1-ol (2,4,5-DNOL) [66]. 2,5-DDOL is then converted by a dehydrogenation reaction to 2,5-dichlorohydroquinone (2,5-DCHQ) [67]. The formation of 2,5-DCHQ completes what is known as the upstream degradation pathway.

It has been proposed that the major upstream pathway reactions described above are enzymatically catalyzed, but two other, minor products, 1,2,4-trichlorobenzene (1,2,4-TCB) and 2,5-dichlorophenol (2,5-DCP), are produced, presumptively by spontaneous dehydrochlorinations of the two putative metabolites, 1,3,4,6-TCDN and 2,4,5-DNOL . Both 1,2,4-TCB and 2,5-DCP appear to be dead-end products in this strain.

The first step in the subsequent, downstream degradation pathway is a reductive dechlorination of 2,5-DCHQ to chlorohydroquinone (CHQ) [68]. The pathway then bifurcates, with the minor route being a further reductive dechlorination to produce hydroquinone (HQ), which is then ring cleaved to γhydroxymuconic semialdehyde (γHMSA). The major route involves the direct ring cleavage of CHQ to an acylchloride, which is further transformed to maleylacetate (MA) [69]. MA is converted to β-ketoadipate [70] and then to succinyl coenzyme A (CoA) and acetyl-CoA, which are both metabolized in the citric acid cycle [26].

### 1.7.2.4 Enzymes involved in the degradation of γ-HCH

#### *1.7.2.4.1 Dehalogenases*

Dehalogenases (Figure 2) are key enzymes for the degradation of various halogenated compounds. Because γ-HCH has six chlorine atoms per molecule, dechlorination is a very significant step in its degradation. Among these dehalogenases, are LinA, LinB, and LinC [26] (Figure 1).

##### *1.7.2.4.1.1 γ-HCH dehydrochlorinase (LinA)*

LinA catalyzes two steps of dehydrochlorination from γ-HCH to 1,3,4,6-TCDN via (γ-PCCH). Dehydrochlorination by LinA may occur stereoselectively at a trans and diaxial pair of hydrogen and chlorine [26].

#### *1.7.2.4.1.2 Haloalkane dehalogenase (LinB)*

LinB is a haloalkane dehalogenase (EC 3.8.1.5), which belongs to the α/β-hydrolase family, with relatively broad substrate specificity [66, 71-72], and has been the subject of crystallographic [73-76], kinetic [77], mutagenesis [78-79], and computational studies [71, 80]. Haloalkane dehalogenases are key enzymes in the degradation of synthetic haloalkanes that occur as soil pollutants [81].

#### *1.7.2.4.1.3 Dehydrogenase (LinC)*

Less is currently known about the third upstream pathway enzyme, LinC, or any of the downstream pathway proteins. LinC is a 2,5-dichloro-2,5-cyclohexadiene-1,4-diol (2,5-DDOL) dehydrogenase in the short-chain alcohol dehydrogenase family [67, 82]. *linC* genes have been recovered from several HCH-degrading sphingomonads [36, 60, 67, 83-84], *Pseudomonas aeruginosa* ITRC-5 (161) and *Microbacterium sp.* ITRC1 [57]. These genes are highly convergent (98% amino acid identities).

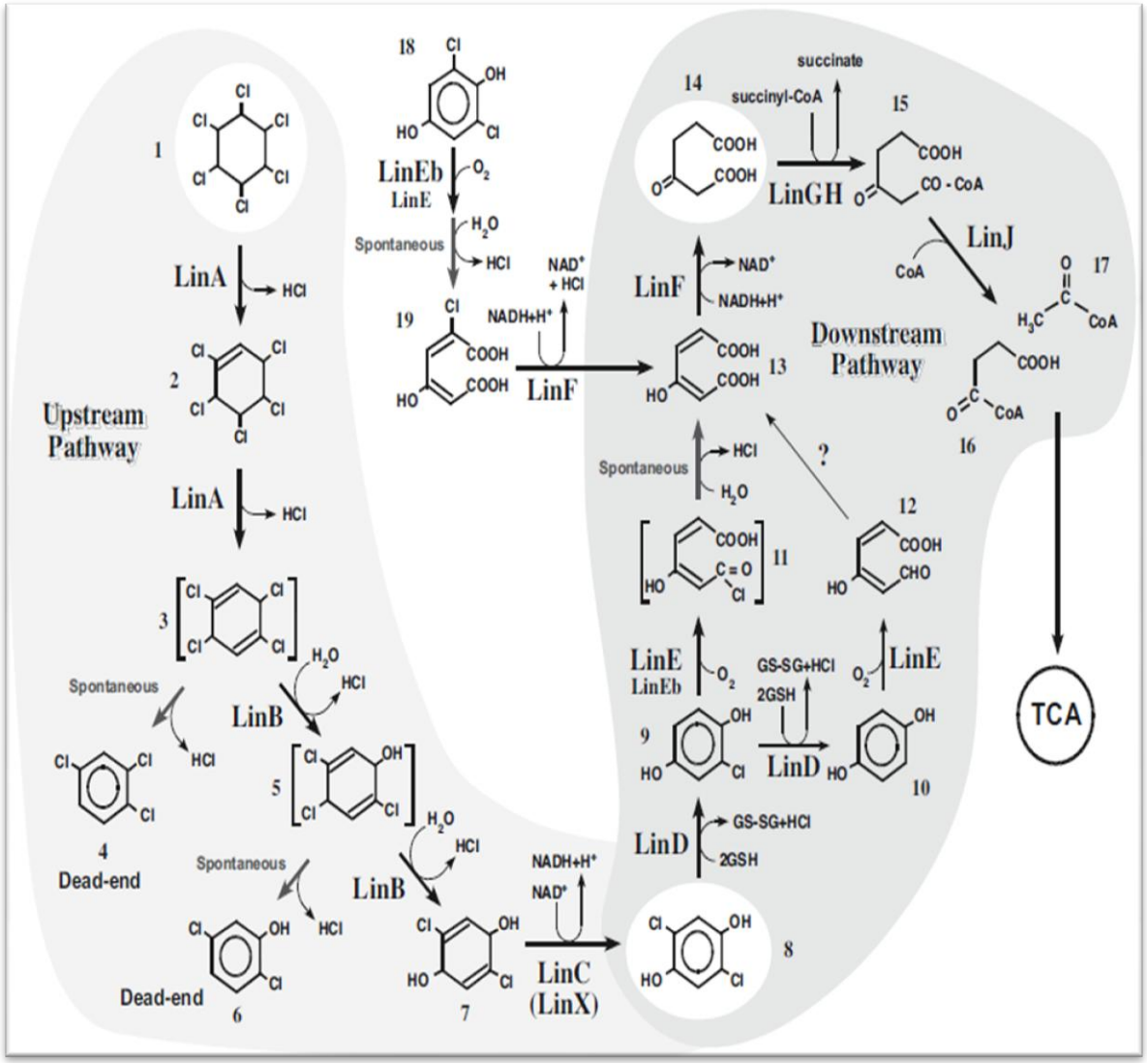


**Figure 2: Proposed degradation pathways of γ-HCH in *Sphingomonas japonicum* UT26. Compounds: 1 γ-Hexachlorocyclohexane (γ-HCH), 2 pentachlorocyclohexene (γ-PCCH), 3 1,3,4,6-tetrachloro-1,4-cyclohexadiene (1,4-TCDN), 4 1,2,4-trichlorobenzene (1,2,4-TCB), 5 2,4,5-trichloro- 2,5-cyclohexadiene-1-ol (2,4,5-DNOL), 6 2,5-dichlorophenol (2,5- DCP), 7 2,5-dichloro-2,5-cyclohexadiene-1,4 diol (2,5-DDOL), 8 2,5-dichlorohydroquinone (2,5-DCHQ), 9 chlorohydroquinone (CHQ), 10 hydroquinone (HQ), 11 MA acylchloride, 12 γ-hydroxymuconic semialdehyde, 13 maleylacetate (MA; 2-maleylacetate, 4-oxohex-2- enedioate), 14 β-ketoadipate (3 oxoadipate), 15 3-oxoadipyl-CoA, 16 succinyl-CoA, 17 acetyl-CoA, 18 2,6-dichlorohydroquinone (2,6- DCHQ), and 19 2-chloromaleylacetate (2-CMA). TCA, citrate/tricarboxylic acid cycle; GSH, glutathione (reduced form); GS-SG, glutathione (oxidized form). Square brackets show unstable compounds that have yet to be detected. Both LinE and LinEb have the degradation activities of CHQ and 2,6-DCHQ, but LinE and LinEb are mainly involved in the degradation of CHQ and 2,6-CHQ, respectively, in UT26 [70]. The light and dark shaded areas indicate upstream and downstream pathways, respectively.**

## 1.8 Flame retardants (FR)

Flame retardants are used to protect the public from accidental fires, by reducing the flammability of combustible materials such as plastics rubbers, textiles and synthetic polymers. The most important group of flame retardants is the brominated flame retardants (BFRs), which contain a diversity of chemicals [85]. Common applications of FR chemicals include the plastic housings of electronic appliances and in printed circuit boards as well as in upholstery and construction materials [86].

### 1.8.1 Brominated flame retardants (BFRs)

Extensive use of brominated flame retardants (BFRs) as additives to plastics, electronics and textiles has led to rising levels in the environment, with a doubling time in wildlife and humans of 5–10 years. The BFRs consist of hydrophobic polybrominated molecules with carbon backbones (Figure 3), e.g. diphenyl ethers (PBDEs), biphenyls (PBBs) and cyclic hydrocarbons (e.g. hexabromocyclododecane, HBCDD). Many BFRs bioaccumulate and may cause adverse health effects in humans and wildlife, similar to those caused by POPs e.g. PCBs and dibenzo-p-dioxins. Microbial degradation and photooxidation are suspected to affect the environmental exposure and toxicity of PBDEs, yet there are limited data regarding the extent of degradative processes in the environment [87].

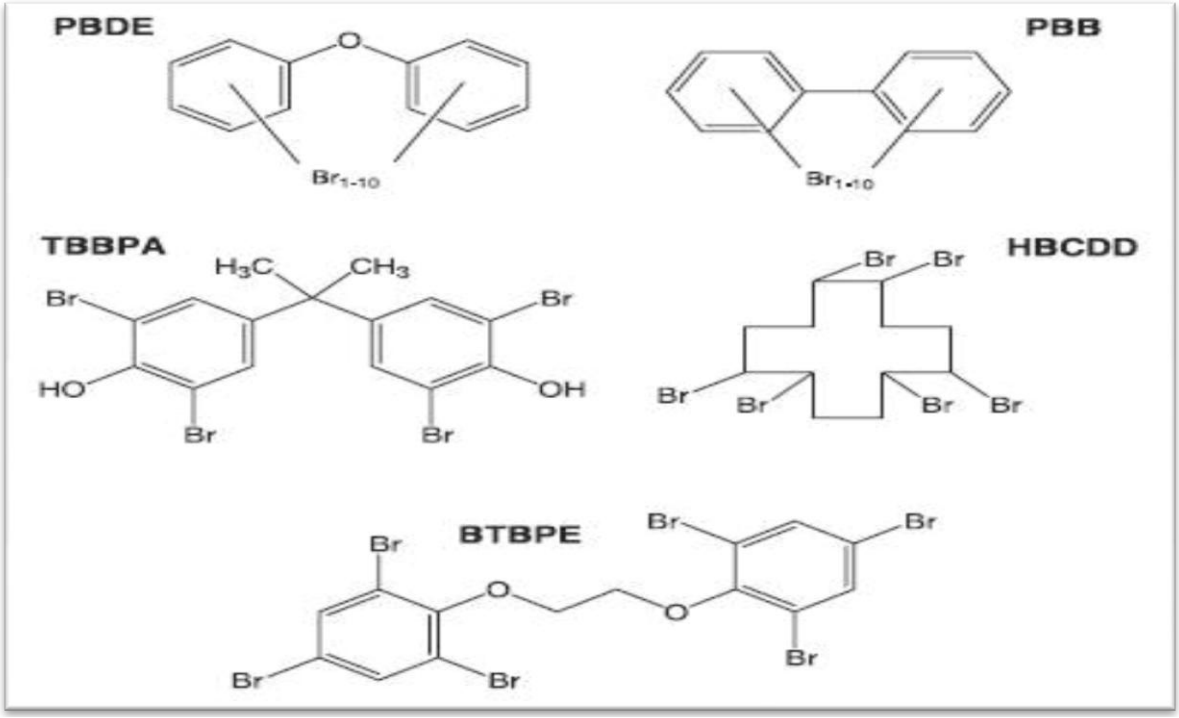


**Figure 3: Structural formulas of common chemicals applied as flame retardants. PBDE, polybrominated diphenyl ethers; PBB, polybrominated biphenyls; TBBPA, tetrabromobisphenol A; HBCDD, hexabromocyclododecane; BTBPE, 1,2-bis(2,4,6-tribromophenoxy) ethane [87].**

Brominated flame retardants are POPs and are the most widely used flame retardants because of their efficiency and low production costs [88]. BFRs are produced via direct bromination of organic molecules or via addition of bromine to alkenes [89]. The major brominated flame retardants used worldwide are tetrabromobisphenol A (TBBPA), hexabromocyclododecane (HBCD), and polybromodiphenyl ethers (PBDEs), [88]. These compounds can enter the environment locally via waste waters of industrial facilities, through volatilization, leaching and combustion. Flame retardants have been found in air, water, soils and sediments far from where they are produced or used [88, 90-91], again providing evidence of the wide dispersal of toxic synthetic organic compounds in the environment. These compounds have been attracting social concern regarding environmental pollution and human exposure for the last two decades [92].

### 1.8.2 Types of compounds

Today, there are more than 175 chemicals classified as flame retardants. The four major groups are inorganic, halogenated organic, organophosphorus and nitrogen-based flame retardants which account for 50%, 25%, 20% and >5% of the annual production, respectively [89]. BFRs are divided into three subgroups depending on the mode of incorporation of these compounds into the polymers: brominated monomers, reactive and additive. A brominated monomer such as brominated styrene or brominated butadiene is used in the production of brominated polymers, which are then blended with nonhalogenated polymers or introduced into the feed mixture prior to polymerization, resulting in a polymer containing both brominated and nonbrominated monomers. Reactive flame retardants, such as tetrabromobisphenol A (TBBPA), are chemically bonded into the plastics. Additive flame retardants, which include PBDEs and hexabromocylododecane (HBCDD) are simply blended with the polymers, and are more likely to leach out of the products [89].

### 1.8.3 Sources of emission of BFRs into the environment

The most obvious sources of emission of BFRs into the environment are effluents from factories producing BFRs, flame-retarded polymers, and plastic products, such as electrical appliances. Other possible sources of emissions into the environment are municipal, hospital, or hazardous waste incinerators, facilities recycling plastics and metals from electronic devices, final disposal sites, and accidental fires. In addition, electronic equipment, such as television sets and computers containing BFRs, may also be sources of emissions of BFRs and PBDDs/DFs into the environment, especially into indoor air [85]. Many BFRs

have vapor pressures (VP) too low to be found in the gas phase at ambient temperatures [93] so BFRs transport tin the atmosphere may be governed by movement of particles [94-95].

### 1.8.4 Polybrominated diphenyl ethers (PBDEs)

PBDEs are widely used as flame retardants in polymers for textiles, electronics, and home furnishings. As a result, PBDEs have been widely detected in biotic and abiotic matrices including sediments, air, water, fish, marine mammals, human plasma, and human milk [96-100]. The levels of PBDEs in the environment have increased rapidly in recent years [92], presumably due to the increasing commercial use of PBDEs [101]. PBDEs have migrated in large quantities from industrial products to the environment and to human body and, furthermore, their concentrations have increased exponentially, as indicated by a meta-analysis of the published PBDE concentration data [102].

The physical, chemical and biological properties of brominated diphenyl ether (BDE) congeners strongly depend on the bromine substitution pattern, similar to those of other polyhalogenated aromatic compounds such as polychlorinated biphenyls (PCBs), polychlorodibenzo-p-dioxins (PCDDs), polychlorodibenzofurans (PCDFs), and polybrominated dibenzo-p-dioxins/di-benzofurans (PBDD/DFs) [103]. However, the toxicity of PBDEs and its origin is still not well understood. Some BDE congeners were shown to have weak or moderate dioxin-like activities or binding affinities to human estrogen receptors [104-105]. In addition, hydroxyl metabolites of PBDEs were found to have strong binding affinity with the thyroxine transporting protein, transthyretin [106]. PBDD/DFs exhibit the similar toxicity as their chlorinated analogues, PCDD/DFs, and are produced during incineration of materials containing brominated flame retardants [104, 107].

### 1.8.5 Classes of PBDEs

The family of PBDEs consists of 209 possible substances, which are called congeners (PBDE = C12H10−xBrxO (x = 1, 2.....10 = m + n)) (Figure 4). Congeners include dibromodiphenyl ethers, tribromodiphenyl ethers, tetrabromodiphenyl ethers, pentabromodiphenyl ethers, hexabromodiphenyl ethers, heptabromodiphenyl ethers, octabromodiphenyl ethers, nonabromodiphenyl ether, and decabromodiphenyl ether. In the United States, PBDEs are marketed with trade names: DE-60F, DE-61, DE-62, and DE-71 applied to pentaBDE mixtures; DE-79 applied to octaBDE mixtures; DE 83R and Saytex 102E applied to decaBDE mixtures. The available commercial PBDE products are not single compounds or even single congeners but rather a mixture of congeners.

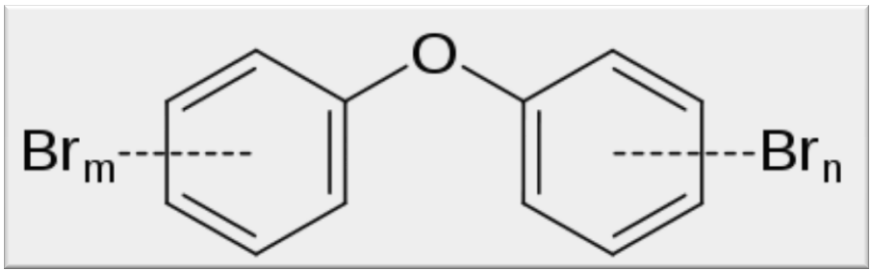


**Figure 4: Chemical structure of PBDEs [99]**

### 1.8.6 Lower brominated PBDEs

These species average 1-5 bromine atoms per molecule and are regarded as more dangerous because they more bioaccumulate efficiently. Lower-brominated PBDEs have been known to affect hormone levels in the thyroid gland. Studies have linked them to reproductive and neurological risks at certain concentration levels.

### 1.8.7 Higher brominated PBDEs

These species average more than 5 bromine atoms per molecule. The commercial mixture, named pentabromodiphenyl ether, contains the pentabromo derivative predominantly (50-62%), however the mixture also contains tetrabromides (24-38%) and hexabromides (4-8%), as well as traces of the tribromides (0-1%). In similar manner, commercial octabromodiphenyl ether is a mixture of homologs: hexa-, hepta-, octa-, nona-, and decabromides.

### 1.8.8 Health and environmental concerns

PBDEs have very low solubility in water (ng/L to µg/L) and are lipophilic thus they readily accumulate in fatty tissues of humans and animals. Although PBDEs have low acute toxicity, they are proven endocrine disruptors that destroy thyroid hormone balance and cause developmental problems [108]. Among the PBDE congeners, penta-BDEs are reportedly being the most toxic, causing developmental toxicity at concentrations starting at 0.8 mg/kg body weight [109] while octa-BDEs are teratogens [96] and deca-BDE is classified as a possible human carcinogen [108]. Because of their ubiquitous use, lipophilicity and inert characteristics, PBDEs have been detected in environmental air, soil, and water samples, as well as in fish and animal tissues. Recently, PBDEs have been detected in human blood serum and breast milk at concentrations that are doubling every five years [92].

Data on the toxicology of the PBDE flame retardants is limited. The main findings published so far are changes in liver weight accompanied by histological alterations in animals given relatively large doses [110].

### 1.8.9 4, 4′-dibromodiphenyl ether (BDE15)

4,4′-Dibromodiphenyl ether (4,4′-DBDE) (Figure 5) is the lowest halogenated commercial congener belonging to this class of compounds of environmental concern [111].

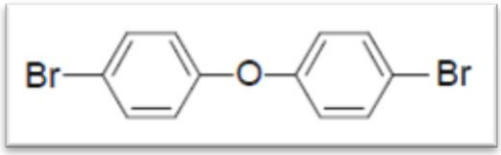


**Figure 5: Structure of BDE15 [112].**

#### 1.8.9.1 Degradation of BDE15

PBDEs have been shown to be anaerobically and aerobically transformed by microorganisms. Recent work on anaerobic biodegradation has shown that PBDEs are debrominated to less brominated congeners by a variety of anaerobic dehalogenating bacteria [108, 113-114]. However, currently very little is known about aerobic biotransformation of PBDEs. In the early 1990s, Schmidt and colleagues isolated two *Sphingomonas sp*. strains capable of breaking down mono- and di- BDE congeners. *Sphingomonas sp.* SS3 (Figure 6) was capable of transforming and growing on 4-bromodiphenyl ether while strain SS33 transformed 4,4′-dibromodiphenyl ether but was not able to use it as a growth substrate [111, 115]. Several transformation products were identified, including 4-bromophenol, 4-bromocatechol, and bromide. More recently, additional *Sphingomonas* species have been shown to aerobically break down a number of mono-, di-, and tri-BDEs. *Sphingomonas sp.* PH-07, which grows on diphenyl ether, was shown to transform but not to grow on 4-bromo-, 2,4-dibromo-, 4,4′-dibromo, and 2,4,4′-tribromodiphenyl ethers [116].

Up to now, most research has dealt with degradation of diphenyl ethers by bacteria [111, 115, 117]. Only a few reports exist on the transformation of these compounds by fungi [118]. The white-rot fungi *Trametes versicolor* (Figure 7) was shown to convert 4-bromodiphenyl ether to its hydroxylated analog [114]. There are also naturally occuring halogenated diphenyl ether derivatives, which are synthesized mainly by fungi and marine organisms [119-120].

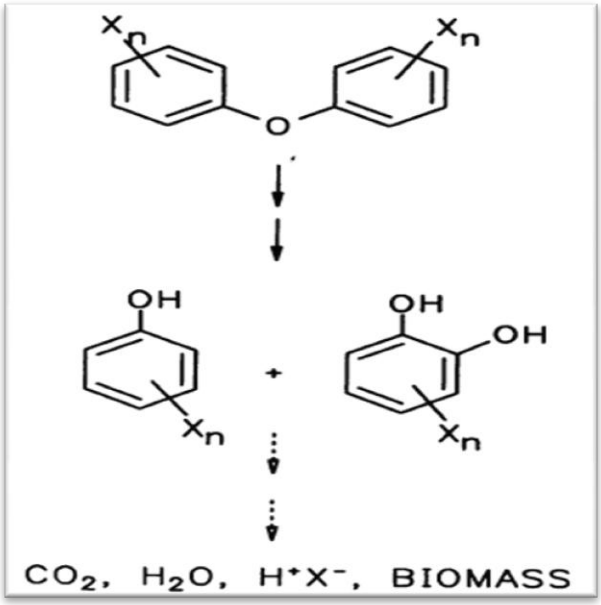


**Figure 6: Proposed pathway for the degradation and/or transformation of dihalogenated diphenyl ethers by *Sphingomonas sp*. strain SS33. Abbreviations: x, F, Cl, or Br; n, 0, 1, or 2 [111].**

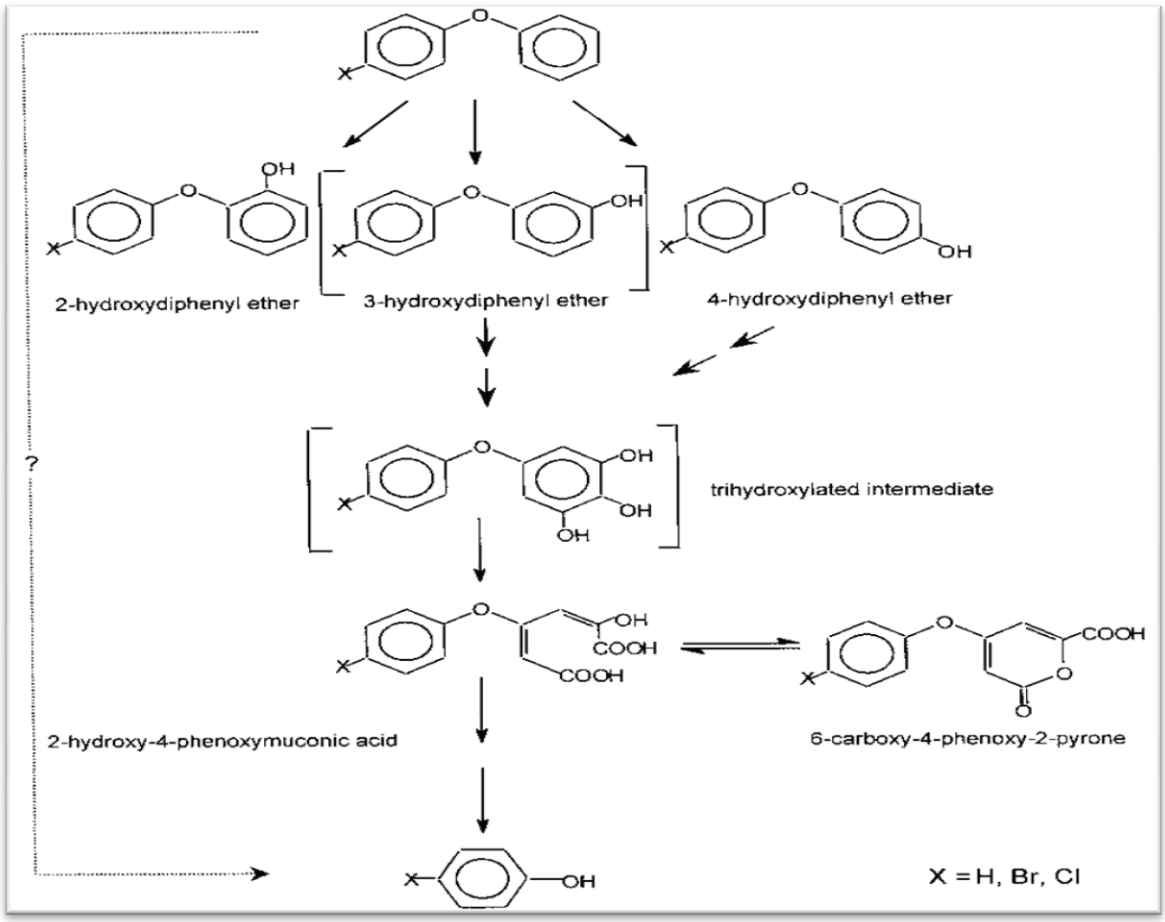


**Figure 7: Proposed pathway for the degradation of diphenyl ethers by *Trametes versicolor* [118].**

## 1.9 Biofilm as microbial life style

A biofilm is an aggregate of microorganisms in which cells are stuck to each other and/or to a surface. These adherent cells are embedded within a self-produced matrix of extracellular polymeric substance (EPS). Biofilm EPS, which is also referred to as "slime," is a polymeric jumble of extracellular DNA, proteins, and polysaccharides. Biofilms may form on living or non-living surfaces, and represent a prevalent mode of microbial life in natural, industrial and hospital settings [121]. The microbial cells growing in a biofilm are physiologically distinct from planktonic cells of the same organism, which, by contrast, are single-cells that may float or swim in a liquid medium.

Microbes form a biofilm in response to many factors, which may include cellular recognition of specific or non-specific attachment sites on a surface, nutritional cues, or in some cases, by exposure of planktonic cells to sub-inhibitory concentrations of antibiotics [122-123]. When a cell switches to the biofilm mode of growth, it undergoes a phenotypic shift in behavior in which large suites of genes are differentially regulated [124].

### 1.9.1 Biofilm Properties

Biofilms are usually found on solid substrates submerged in or exposed to some aqueous solution, although they can form as floating mats on liquid surfaces and also on the surface of leaves, particularly in high humidity climates. Given sufficient resources for growth, a biofilm will quickly grow to be macroscopic. Biofilms can contain many different types of microorganism, e.g. bacteria, archaea, protozoa, fungi and algae; each group performing specialized metabolic functions. However, some organisms will form monospecies films under certain conditions.

Researchers from the Helmholtz Center for Infection Research have investigated the strategies used by biofilms. They discovered that biofilm bacteria apply chemical weapons in order to defend themselves against disinfectants and antibiotics, phagocytes and our immune system. Dr. Kjelleberg began a detailed investigation in order to find why phagocytes cannot annihilate the biofilm bacteria. He analyzed marine bacteria, which defend themselves against amoebae, the behavior of which copies the behavior of phagocytes. The amoebae behave in the sea just like the immune cells in the human body: they search for and feed on the bacteria. When bacteria are alone and separated in the water, they become an easy catch for the attackers. However, when they attach to a surface and join other bacteria, the amoebae cannot assault them [125]. The researcher stated that biofilms may be seen as a source of new

bioactive agents. When bacteria are organized in biofilms, they produce effective substances which individual bacteria are unable to produce alone.

### 1.9.2 Biofilm formation

Formation of a biofilm begins with the attachment of free-floating microorganisms to a surface. These first colonists adhere to the surface initially through weak, reversible van der Waals forces. If the colonists are not immediately separated from the surface, they can anchor themselves more permanently using cell adhesion structures such as pili.

The first colonists facilitate the arrival of other cells by providing more diverse adhesion sites and beginning to build the matrix that holds the biofilm together. Some species are not able to attach to a surface on their own but are often able to anchor themselves to the matrix or directly to earlier colonists. It is during this colonization that the cells are able to communicate via quorum sensing using products as AHL (N-Acyl homoserine lactones). Once colonization has begun, the biofilm grows through a combination of cell division and recruitment. The final stage of biofilm formation is known as mature biofilm, and is the stage in which the biofilm is established and may only change in shape and size. The development of a biofilm may allow for the aggregated cell colonies to be increasingly antibiotic resistant.

### 1.9.3 Biofilm development

The bacterial biofilm development is widely accepted to take place through a number of steps discovered by microscopic analysis of the biofilm communities over time. As demonstrated in Figure 8, these steps include initial attachment. The cells undergo a reversible attachment via the flagellated pole and an irreversible attachment, in which the cells make a more stable interaction with the surface via its long axis [126-127]. The adhesion organelles such as: flagella, type IV pili and CupA fimbriae have been shown to be essential for initial attachment of the bacteria to the surfaces and are required for the biofilm maturation [128-130]. Subsequently, the attached bacteria aggregate, grow and proliferate to form microcolonies. Within the microcolonies the bacteria lose the flagella and start to produce alginate and the extracellular matrix, which consists of several biopolymers including proteins, polysaccharides, and nucleic acids. This matrix plays a crucial role in the structural development of the biofilms [131]. The microcolonies continue to grow and form the mature biofilm, in which mushroom-like colonies separated by water-filled channels are developed, followed by detachment during which bacteria actively leave the biofilm.

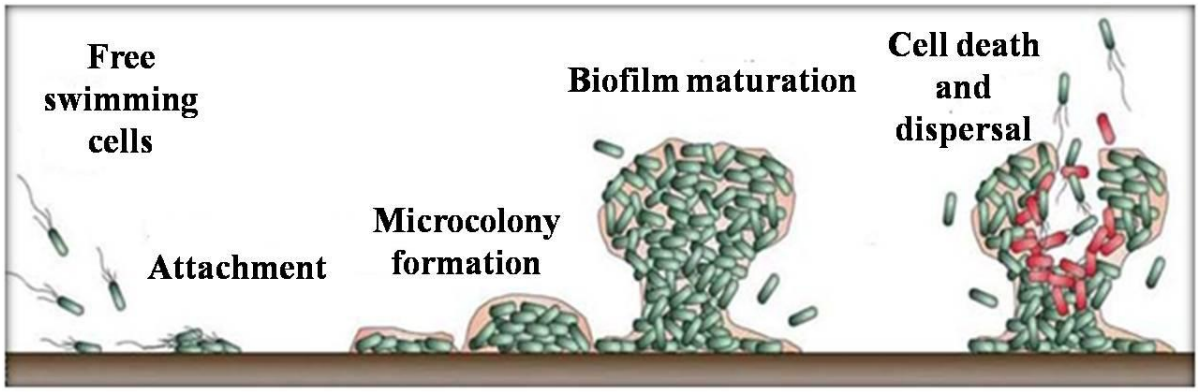


**Figure 8: Stages of the biofilm development. Swimming bacteria attach to an abiotic surface, the attached bacteria aggregate and form microcolonies. Subsequently, they lose the flagella and start to produce the extracellular matrix. In mature biofilms mushroom like structures are separated by water-filled channels. Finally, the biofilm is dispersed by death of subpopulations of cells and detachment of planktonic bacterial cells from the biofilm [127].**

**Factors affecting adhesion are** the nature and type of surface/environment, the surface shape/homogeneity, the charge/lack of surface charges, hydrophobicity and hydrodynamics/flow characteristics. **Factors affecting biofilm growth are** rate-limiting nutrient penetration (culture and environment-dependant), nature of anaerobic and aerobic areas within the biofilm and heterogeneous versus homogeneous populations.

### 1.9.4 Biofilm dispersal

Dispersal of cells from the biofilm colony is an essential stage of the biofilm lifecycle. Dispersal enables biofilms to spread and colonize new surfaces. Enzymes that degrade the biofilm extracellular matrix, such as dispersin B and deoxyribonuclease, may play a role in biofilm dispersal [132-133]. Biofilm matrix degrading enzymes may be useful as anti-biofilm agents [134-135]. Recent evidence has shown that a fatty acid messenger, cis-2-decenoic acid, is capable of inducing dispersion and inhibiting growth of biofilm colonies. Secreted by *Pseudomonas aeruginosa*, this compound induces dispersion in several species of bacteria and the yeast *Candida albicans* [136].

### 1.9.5 Extracellular matrix

The biofilm is held together and protected by a matrix of excreted polymeric compounds called EPS. EPS is an abbreviation for either extracellular polymeric substance or exopolysaccharide. This matrix protects the cells within it and facilitates communication among them through biochemical signals. Some biofilms have been found to contain water channels that help distribute nutrients and signalling molecules. This matrix is strong enough that under certain conditions, biofilms can become fossilized. Bacteria living in a biofilm usually have significantly different properties from free-floating bacteria of the same species,

as the dense and protected environment of the film allows them to cooperate and interact in various ways. One benefit of this environment is increased resistance to detergents and antibiotics, as the dense extracellular matrix and the outer layer of cells protect the interior of the community. In some cases antibiotic resistance can be 1000 fold increased [137].

The concept that biofilms are more resistant to antimicrobials is not completely accurate. For instance the biofilm form of *Pseudomonas aeruginosa* has no greater resistance to antimicrobials, when compared to stationary phase planktonic cells. Although, when the biofilm is compared to logarithmic phase planktonic cells, the biofilm does have greater resistance to antimicrobials. This resistance to antibiotics in both stationary phase cells and biofilms may be due to the presence of persister cells [138].

### 1.9.6 Biodegradation by biofilm communities

Biodegradation is a process whereby microbial communities contribute extensively to the attenuation, mineralization and transport of organic (carbon-based compounds) contaminants in the environment. The development of biofilms by microbial communities is often a key factor contributing to the overall efficiency of these processes. Bacterial biofilms are also able to accumulate inorganic chemicals (compounds of metals such as mercury, copper and aluminium), through various mechanisms. This offers a potential method of removing toxic metals from waste sites [139]. The potential of bioremediation (remediation using biological processes) as an alternative to physical and chemical remediation strategies has resulted in a significant amount of research effort on degradative biofilms. Much emphasis has been placed on the degradation of xenobiotic compounds (organic compounds that are foreign to the organisms) such as chlorophenols and chlorobenzoates. The knowledge gained through these studies has also contributed to an improved understanding of processes involved in the degradation of naturally occurring molecules as well as nutrient cycling (carbon cycle, nutrient cycle, etc.) in general. Biofilms have industrially been used, e. g. for bioremediation of hazardous materials and waste sites, biofilteration of industrial waste water or biofilteration of industrial waste water.

Hydrophobic compounds like crude oil, tar, or soot are also an extreme environment because they are usually difficult to degrade because of their reduced bioavailability due to their low solubility in water. Nevertheless, a number of microbial communities have been characterized many of them specialized in the degradation of some of the chemical compounds of these mixtures. Crude oil has been released to the surface in large amounts both by natural processes and by accidents, e. g in oil spills. To get access to the substrate

many bacteria form biofilms at the water-oil interface where they probably could produce biosurfactants to solubilize the oil to bring it into their cells [140]. It was even reported that microorganisms could be active in the degradation of asphalt [141-142].

There is ample evidence that microbial interactions are important for the functioning of microbial communities, especially when challenged with complicated substrates. Two key properties of degradative biofilms are: (1) the spatial organization of cells and (2) the establishment of a stable microenvironment through the production of EPS. These characteristics promote the assemblage of a larger and more diverse genetic pool in a confined microniche, thereby expanding the range of substrates that can be degraded.

## 1.10 Methods to study microbial diversity

### 1.10.1 Important methods for microbial community analysis

Microbial diversity was assessed traditionally by plate counts with distinct selective media and direct viable counts. This method is usually inexpensive and often fast. However there are some limitations, such as, selection of growth media and conditions, and the impossibility to culture a large number of bacterial and fungal with the present techniques. Additionally, plate growth favors bacterial strains which grow faster. All these limitations may influence the correct analysis of the diversity [143]. Another method known as *Biolog* generate a profile from the ability of the microbial community to use specific substrates as sole carbon source. The generated profile is compared to a data bank giving important information of the functional activity of the community and has been used, for example, to assess metabolic biodiversity in contaminated sites [144]. A further method, which is not dependent of cultivable organisms, is based on the groupings of fatty acids. Major taxonomic groups may be differentiate in a community by use of fatty acid methyl ester (FAME), which can be extracted directly from soil samples, afterward methlylated and then analysed by gas chromatography, and has successfully been used to analyse the microbial diversity soil bacterial population [145].

The three methods presented above are biochemical based methods, now the most common methods based on molecular techniques, beside the later described SSCP, will be presented. An additional method similar to SSCP and very popular for microbial diversity studies is the *Denaturating Gradient Gel Electrophoresis* (DGGE) and *Temperature Gradient Gel Electrophoresis* (TGGE), such as for SSCP these techniques were originally developed to detect point mutations in DNA sequences. These methods are based on the use of amplicons from general primers, where the 5`-end of the forward primer contains a 35-40 base pair GC

clamp to ensure the double strand necessary in this method. By increasing concentration of denaturants the separation of the double strands will occur based on their melting behavior. In 1993 Muyzer et *al.* expanded the use of DGGE to analyse microbial communities [146] and since then many studies have been published [147-148].

*Restriction fragment length polymorphism* (RFLP), also known as *amplified ribosomal DNA restriction analysis* (ARDRA) is also based on the DNA polymorphism. In this method the PCR amplified rDNA is digested by a 4-base cutting restriction enzyme, generating different fragments length which is detected using agarose or non-denaturating polyacrylamide gel electrophoresis [149]. *Terminal restriction fragment length polymorphism* (T-RFLP) follows the same principle of RFLP, excepted that one primer is fluorescent labelled permitting the detection of only one labelled terminal restriction, therefore simplify the banding pattern [149]. *Ribosomal intergenic spacer analysis* (RISA) and *automated ribosomal intergenic spacer* (ARISA) use similar principle as RFLP and T-RFLP provides ribosomal-based fingerprinting of microbial communities. In RISA and ARISA a region between the 16S and 23S ribosomal unit is amplified by PCR and separated on a denaturating gel polyacrylamide, and they are especially interesting for differentiation of bacterial strains and closely related species [150].

### 1.10.2 Fatty acids as biomarkers

A fatty acid is a carboxylic acid with a long usually unbranched aliphatic tail (chain), which is either saturated or unsaturated. Most naturally occurring fatty acids have a chain of an even number of carbon atoms, from 4 to 28. Unsaturated fatty acids have one or more double bonds. The two carbon chains that are bound next to either side of the double bond can occur in a *cis* or *trans* configuration. A *cis* configuration means that adjacent hydrogen atoms are on the same side of the double bond. A *trans* configuration, by contrast, means that the next two hydrogen atoms are bound to *opposite* sides of the double bond. Saturated fatty acids are long-chain carboxylic acids that usually have between 12 and 24 carbon atoms and have no double bonds. Several different systems of nomenclature are used for fatty acids. *n*−*x* (*n* minus *x*; also ω−*x* or omega-*x*) nomenclature both provide names for individual compounds and classifies them by their likely biosynthetic properties in animals. A double bond is located on the $x^{th}$ carbon–carbon bond, counting from the terminal methyl carbon (designated as *n* or ω) toward the carbonyl carbon. For example, α-linolenic acid is classified as a *n*−3 or omega-3 fatty acid, and so it is likely to share a biosynthetic pathway with other compounds of this type. The ω−*x*, omega-*x*, or "omega" notation is common in popular

nutritional literature. The most studied fatty acid biosynthetic pathways are *n*−3 and *n*−6, which are hypothesized to decrease or increase, respectively, inflammation [151].

Biomarkers in microbiology are specific molecules which are used to characterize particular organisms. Those can be any kind of molecule indicating the existence of living microbes. Bacterial fatty acids are shown in many studies to deliver a useful tool in the phylogenetic and taxonomic analysis of microbial communities [152-154] and represent one of the major modules of cellular components.

In bacterial cells, fatty acids can be found primarily in the cell membranes as phospholipids. Membrane fatty acids can be divided into two major groups according to their biosynthetic relationships. The straight-chain fatty acid family counts for the first group, which includes palmitic, stearic, hexadecenoic, octadecenoic, 10-methylhexadecenoic, and 2- or 3- hydroxy fatty acids. These fatty acids occur most commonly in bacteria. They are synthesised from acetyl coenzyme A (acetyl-CoA) as the primer and malonyl-CoA as the chain extender, followed, in some cases, by a modification of the fatty acid products. The second family is the branched-chain fatty acid family, which includes iso-, anteiso-, and ω-alicyclic fatty acids with or without a substitution (unsaturation and hydroxylation). The occurrence of these fatty acids in bacteria is not nearly as common as that of the straight-chain fatty acid family, but is still very significant [155].

Analysis of cellular fatty acid composition is now used routinely to characterize, differentiate, and identify genera, species, and strains of bacteria [156-158]. Taxa are distinguishable by the fatty acids produced and their relative concentrations. Fungi produce fewer different fatty acids than bacteria do [159], and in the past, fatty acids have been considered to have little taxonomic value for this group of organisms. However, recent work has shown that cellular fatty acid profiles can be used to differentiate and identify genera, species, and strains of yeasts and yeast-like organisms [160-161].

Characteristic fatty acids for bacteria are those with a chain length of C12-C19. Unsaturated fatty acids of this chain length are in general allocated to Gram negative bacteria. Branched fatty acids with a chain length of C14-C16 for example indicate the presence of Gram positive bacteria, while saturated fatty acids with the chain length of C16-C19 can be allocated to sulphate-reducing and other anaerobic bacteria [162].

The most common and abundant fatty acids extracted from dikaryotic fungi were 16:0, 18:0, 18:1(cis 9), and 18:2(cis 9, 12), which often made up greater than 95% of the total fatty acid content [159].

In the Eubacteria and Eucaryotes cellular fatty acids have a number of functions. They are esterified with glycerol which carries a phosphate ester or sugar moieties at its terminal end. To the phosphate group a number of different head groups are attached which form the body of the phospholipids. These phospholipids are organized in a bilayer in the cell membrane protecting the cell against the environment. Some polar lipids carry sugar moieties instead of the phosphate head group, the glycolipids, which are usually found at the outside of the cell mediating cell contact or cell-cell communication. The functional distinction between phospho- and glycolipids is blurred in Caulobacteriales where glycolipids seem to be able to replace many of the phospholipids in the cell wall. Furthermore, fatty acids bound to glycerol alone as triglycerols are storage compounds. Fatty acids can also be found in bacteria as bound lipids, e.g. in lipoproteins and in the lipopolysaccharides. All fatty acids in the cells in whatever form they occur are called cellular fatty acids. Their composition is often characteristic for a number of taxa and used for their identification [162-163].

The formation and metabolism of fatty acids is a critical function of the cell, however, little is known about the kinetics of their formation. It has been reported that phospholipids show high turnover rates and that they are rapidly degraded by phospholipases after the death of the cell [164-165] qualifying them for valuable markers for living biomass in environmental samples [166].

### 1.10.3 Single-Strand Conformation Polymorphism (SSCP)

Single-Strand Conformation Polymorphism was originally described to detect mutations and aberrations, and even mobility shift of a single base can be observed in human genomic DNA [167]. The technique is based on differences caused by their folded secondary structure, therefore the migration pattern of PCR amplicons as single-strand fragments in acrylamide gel electrophoresis are different. The single-strand fragment is generated by the digestion of the phosphorylated strands (from phosphorylated primer) by an exonuclease enzyme.

Schwieger and Tebbe [168] developed a new approach for the SSCP technique to analyse microbial diversity in soil samples. Afterwards several works have been applied SSCP as a technique to detect microbial diversity in different kind of samples, such as in raw-milk cheeses [169], bee guts [170], soil fungal communities in natural forest [171], in BTEX (Benzene, Toluene, Ethyle Benzene, Xylene) contaminated soils [172], maize rhizospheres [173], anaerobic digestors [174] and biofilms [142].

## 1.10.4 Microscopy methods to analyze biofilm structures

### 1.10.4.1 Alternative microscopic methods to analyse biofilms

Modern microscopic techniques other than CLSM have been used to analyse biofilms, such as transmission electron microscopy (TEM), which is an imaging technique whereby a beam of electrons is focused onto a specimen, was used in combination with high-pressure freeze-substitution to analyse natural structures of *Pseudomonas aeruginosa* PAO1 biofilms and their integration with the surrounding EPS, which is composed of polymeric and particulate substances [175]. Atomic force microscopy (AFM), which operates by measuring attractive or repulsive forces between a tip and the sample, was used to investigate the adhesion of *E. coli* in modified surfaces [176]. Biofilms formation on intraocular lenses were monitored by scanning electron microscopy (SEM) [177]; in this technique a beam of electrons in a vacuum is collimated by electromagnetic condensor lenses, focused by an objective lens, and scanned across the surface of the sample.

### 1.10.4.2 Confocal Laser Scaninig Microscopy (CLSM)

The main instrument to study biofilm structures is the CLSM. CLSM is an optical microscopy technique that is based on conventional wide-field fluorescence microscopy and offers the observation of thin optical sections in thick, intact fluorescent specimens. Basically, CLSM is a conventional microscope equipped with a laser light source, a laser scanning head, an automatic focusing stage and connected to a PC. A point light source is imaged on the object plane and the emitted fluorescence light is detected by a photomultiplier. On a computer screen the point is displayed as pixel and by scanning the object point by point, line by line optical sections are recorded. CLSM allows the construction of 3D images, due to its ability to perform optical sectioning; thicker samples can be imaged and reconstructed.

## 1.11 Aim of the work

The River Nile and the Mediterranean Sea in Egypt are polluted areas because they receive the major part of the Egyptian Nile Delta Governorates mixed wastewater where are chemical factories. On the fringe of the Egyptian Nile Delta lay five Delta lakes. The Delta lakes are connected to the River Nile distributaries by either canals or drainage ditches and several lakes exchange water with the Mediterranean Sea as well.

The most dangerous pollutants described in the collected samples from Nile Delta lakes, Mediterranean and Red Sea were polycyclic aromatic hydrocarbons (PAHs), pesticides (e.g hexachlorocyclohexane isomers (HCHs), cyclodienes and dichlorodiphenyltrichloroethane (DDT)), polychlorinated biphenyls (PCBs) and heavy metals. The average concentration of pesticides recorded in some marketable fish in Egypt was 20-211 ng/g of wet weight. The concentrations of PCBs in composite sediment samples from three Nile Delta lakes in Egypt ranged from 18 to 71 ng/g. The concentrations of PCBs in mussel samples collected from Mediterranean Sea ranged from 8 to 437 ng/g of wet weight. The concentration of pesticides in mussel samples collected from Mediterranean Sea ranged from 62 to 2232 ng/g of wet weight [178-181].

Soil and sediments of canals, drainage ditches and several lakes accumulate both natural and industrial wastes and can provide a diversity of microorganisms able to grow on these pollutants. The soil/sediment samples of drainages of different factories (food production, detergents, edible oils & soap production, plastics, paper mills, electronic articles, tannery), sewage from cities, Egyptian Mediterranean Sea coast and drainage of some agricultural lands were collected from five Egyptian Nile Delta Governorates (Alexandria, Gharbia, Kafr El-Sheikh, Monufia and Qalyubia).

The objective of this study was to determine the diversity of bacteria and fungi able to metabolize and grow on γ-HCH as an example of organochlorine pesticides and on BDE as an example of polybrominated biphenyls using classical microbiological and analytical methods and characterization of the most tolerant one by FAME profile. In addition to isolation and identification of the most active bacteria and fungi for γ-HCH and BDE, the present work also aimed to study by SSCP gel profiling the microbial biofilm communities which colonized γ-HCH and BDE droplets using polluted soil and sediment samples as inoccula and investigate whether these microbial communities differ from those isolated by classical microbiological methods. This was further supported by characterizing the structures of these microbial communities by CLSM.

# 2 Materials

## 2.1 Instruments

| | |
|---|---|
| 96-well plate shaker & incubator | Titramax 1000, Incubator 1000, Heidolph |
| Autoclave | Bioclav 32-2-3, KSG Sterilisator GmbH, Olching, Germany |
| Balances | 1501; Extend, Sartorius |
| Centrifuges | 5415 R, Eppendorf, Hamburg, Germany; RC 5C, Sorvall, ThermoScientific, Thermofisher; Multifuge1 S-R, Heraeus, ThermoScientific |
| Clean bench | HSP 15, Heraeus, ThermoScientific |
| Cooling thermostat | Ecoline RE 104, Lauda |
| Confocal laser scanning microscopy | TCS SP5, Leica, Heidelberg, Germany |
| Evaporator | TR-L 288, Liebisch |
| Gas chromatography (GC) | 7683 Series Injector, Agilent; 6890N Network GC System, Agilent Technologies |
| Horizontal electrophoresis system | 2010-001 Macrophor Electrophoresis Unit, LKB Bromma, Bromma, Sweden |
| Magnetic stirrer | M20/1, Framo-Gerätetechnick |
| Multi-well plate reader | µQuant, Synergy™ 4, Bio-TEK |
| pH-Meter | WTW pH 325, Biochem Laborbedarf, Weilburg, Germany |
| Photometer | BioPhotometer, Eppendorf, Hamburg, Germany |
| Pipettes | Research 0.5-10 µl/10-100µl/20-200 µl/100-1000 µl, Eppendorf |
| Scanner | HP Scanjet G4050 |
| Shaker | Duomx 1030, Heidolph |
| Shaker incubator | Certomat® BS-1, Sartorius Stedim Biotech |
| Spectrophotometer | NanoDrop 2000c, PeqLab Biotechnologie GmbH, Erlangen, Germany |
| Speed-vac | Concentrator 5301, Eppendorf, Hamburg, Germany |

| | |
|---|---|
| Thermocycler | Mastercycler, Eppendorf, Hamburg, Germany |
| Thermomixer | Compact, Eppendorf, Hamburg, Germany |
| Tissue & cell homogenizer | FastPrep® -24, MPBiomedicals, Eschwege, Germany |
| Vertical electrophoresis system | Perfect Blue Dual Gel System Twin L, PeqLab, Erlangen, Germany |
| Vortexmixer | IKA® MS 3 basic; Scientifica |
| Water purification | water purification system Milli-Q Academic A10, Millipore |

## 2.2 Chemicals & reagents

The test compounds γ-hexachlorocyclohexane (γ-HCH) and 4, 4`-bromodiphenylether (BDE) were purchased from Sigma-Aldrich (Steinheim, Germany). The chemicals used in the current study were supplied by Sigma-Aldrich, Merck (Darmstadt, Germany), Fluka (Buchs, Switzerland) and Roth (Karlsruhe, Germany).

Lambda exonuclease and Lambda exonuclease buffer were purchased from New England Biolabs (Schwalbach, Germany); the primers were from Invitrogen (Karlsruhe, Germany) and the reagents for PCR (Taq polymerase, buffer, dNTP's & $MgCl_2$) were supplied by Qiagen (Hilden, Germany). The cell proliferation reagent (WST-1) was purchased from Roche Diagnostics GmbH, Roche Applied Science (Mannheim, Germany).

## 2.3 DNA markers

| | Company |
|---|---|
| **1Kb DNA Ladder** | GeneRuler™, Fermentas |
| **DNA Molecular Weight III (0.12-21.2 Kbp)** | Roche Applied Science, Mannheim, Germany |

## 2.4 Staining solutions

| | Company |
|---|---|
| **DAPI dihydrochloride Nucleic Acid Stain** | Molecular Probes, Invitrogen, Karlsruhe, Germany |
| **FilmTracer™ SYPRO® Ruby Biofilm Matrix Stain** | Molecular Probes, Invitrogen, Karlsruhe, Germany |
| **Nile Red Stain** | Sigma, St. Louis, MO |

## 2.5 Kits

| | Company |
|---|---|
| **DyeEx™ 2.0 96 Plate (1) Spin Kit** | Qiagen, Hilden, Germany |
| **Fast-DNA® Spin for Soil Kit** | Q-Biogen, MP Biomedicals, Heidelberg, Germany |
| **Live/Dead® BacLight™ bacterial viability kit** | Molecular Probes, Invitrogen, Karlsruhe, Germany |
| **MiniElute™ Spin Columns Kit** | Qiagen, Hilden, Germany |
| **NucleoSEQ Columns Kit** | Macherey Nagel, Düren, Germany |
| **PCR Clean-up Gel extraction kit Nucleospin Extract II** | Macherey Nagel, Düren, Germany |
| **Qiagen II Agarose Gel Extraction Kit** | Qiagen, Hilden, Germany |

# 2.6 Media, buffers & solutions

## 2.6.1 Minimal growth medium (M9)

| | |
|---|---|
| Mineral-buffer solution | 100 ml |
| Magnesium solution | 0.67 ml |
| Iron-EDTA solution | 4 ml |
| Iron-EDTA solution | 1.33 ml |
| distilled water | 1000 ml |

(Sterile filtered, pH 7.0±0.2)

**Mineral-buffer solution**

| | |
|---|---|
| $Na_2HPO_4 .2\ H_2O$ | 87.78 ml |
| $KH_2PO_4$ | 30 g |
| $(NH_4)_2SO_4$ | 12.37 g |
| distilled water | 1000 ml |

(Autoclaved)

**Magnesium solution**

| | |
|---|---|
| $Mg_2SO_4 .7\ H_2O$ | 246.48 g |
| distilled water | 1000 ml |

(Autoclaved)

**Iron-EDTA solution**

| | |
|---|---|
| $Fe_2SO_4 .7\ H_2O$ | 3.20 g |
| EDTA | 12.37 g |
| distilled water | 1000 ml |

(Autoclaved)

**Trace elements solution**

| | |
|---|---|
| MgO | 10.75 g |
| $Fe_2SO_4 .7\ H_2O$ | 4.5 g |
| $CaCO_3$ | 2.0 g |
| $ZnSO_4 .7\ H_2O$ | 1.44 g |
| $MnSO_4 .2\ H_2O$ | 0.87 g |
| $CoSO_4 .7\ H_2O$ | 0.28 g |
| $CuSO_4 .5\ H_2O$ | 0.25 g |
| $H_3BO_3 .7\ H_2O$ | 0.06 g |
| Conc. HCl | 51.3 ml |
| distilled water | 1000 ml |

(Autoclaved)

## 2.6.2 Basic medium (M269)

| | |
|---|---|
| $(NH_4)_2SO_4$ | 2 g |
| KCl | 100 mg |
| $K_2HPO_4$ | 500 mg |
| $MgSO_4.7H_2O$ | 500 mg |
| distilled water | 1000 ml |

(Autoclaved, pH 7.0)

## 2.6.3 Basic Czapek-DOX medium

| | |
|---|---|
| $NaNO_3$ | 3 g |
| $K_2HPO_4$ | 1 g |
| $MgSO_4.7H_2O$ | 0.5 g |
| KCl | 0.5 g |
| $FeSO_4.7H_2O$ | 0.01 g |
| distilled water | 1000 ml |

(Autoclaved, pH 6.8±0.2)

## 2.6.4 LB-medium (Luria Bertani medium)

| | |
|---|---|
| Tryptone | 10 g |
| Yeast extract | 5 g |
| NaCl | 5 g |
| distilled water | 1000 ml |

(Autoclaved, pH 7.0)

## 2.6.5 R2A medium

| | |
|---|---|
| Yeast extract | 0.5 g |
| Proteose peptone NO. 3 | 0.5 g |
| Casamini acids | 0.5 g |
| Dextrose | 0.5 g |
| Soluble starch | 0.5 g |
| Sodium pyruvate | 0.3 g |
| $K_2HPO_4$ | 0.3 g |
| $MgSO_4$ | 0.05 g |
| distilled water | 1000 ml |

(Autoclaved, pH 7.2±0.2)

## 2.6.6 PDA (Potato-Dextrose-Agar) medium

| | |
|---|---|
| Potato starch (from infusion)* | 4 g |
| Dextrose | 20 g |
| distilled water | 1000 ml |

*Approximates 200 g of infusion from potatoes

(Autoclaved, pH 7.2±0.2)

*Solid medium was prepared by adding of 15 g/L of agar to the medium.

## 2.6.7 TE buffer (Tris-EDTA-muffer)

| | | |
|---|---|---|
| Tris-HCl (2-amino-2-(hydroxymethyl)-1,3-propanediol HCl, 1M, pH 8.0) | (12.114 g / 100 ml distilled water) | 5 ml |
| EDTA (ethylenedinitrilotetraacetic acid, 0.5M, pH 8.0) | (18.6 g / 100 ml distilled water) | 1 ml |
| distilled water | | 500 ml |

(Autoclaved, pH 7.0)

## 2.6.8 TBE buffer (Tris-Borate-EDTA-buffer) (10X)

| | |
|---|---|
| Tris base | 108 g |
| Boric acid | 55 g |
| $Na_2EDTA.2H_2O$ | 8.3 g |
| distilled water | 1000 ml |

(Autoclaved, pH 8.0)

## 2.6.9 SSCP loading buffer

| | |
|---|---|
| Formamide | 47.5% |
| NaOH | 5 mM |
| Bromophenol blue | 0.12% |
| Xylene cyanol | 0.12% |
| (Autoclaved) | |

## 2.6.10 SSCP elution buffer

| | |
|---|---|
| Tris buffer | 10 mM |
| KCl | 5 mM |
| $MgCl_2.6H_2O$ | 1.5 mM |
| TritonX-100 (pH 9.0) | 0.1% |
| (Autoclaved) | |

## 2.6.11 PBS (Phosphate buffered saline) (10X)

| | |
|---|---|
| $NaH_2PO_4$ | 0.54 g |
| $Na_2HPO_4$ | 0.85 g |
| NaCl | 8.75 g |
| distilled water | 1000 ml |
| (Autoclaved, pH 7.0) | |

## 2.6.12 PFA solution (paraformaldehyde) (4%)

| | |
|---|---|
| PFA (10%) | 4 ml |
| PBS | 100 ml |

## 2.6.13 Solutions for the preparation of Fatty Acid Methyl Esters (FAMEs)

**Solution 1**

| | |
|---|---|
| Methanol | 100 ml |
| 15% NaOH (w/v) | 100 ml |

**Solution 2**

| | |
|---|---|
| Methanol | 100 ml |
| 37% HCl | 20 ml |

**Solution 3**

| | |
|---|---|
| Hexane | 100 ml |
| Tetra-butyl ethyl ether | 100 ml |

**Solution 4**

| | |
|---|---|
| NaOH | 0.5 M |

## 2.7 Primers

| Primer | Sequence |
|---|---|
| 16F27 | 5`-AGAGTTTGATCMTGGCTCAG-3` |
| 16R1492 | 5`-TACGGYTACCTTGTTACGACTT-3` |
| 16R1087 | 5`-ACTGGCGGACGGGTGAGTAA-3` |
| 16F945 | 5`-TACGGYTACCTTGTTACGACTT-3` |
| 16R518 | 5`-AGAGTTTGATCMTGGCTCAG-3` |
| 16F357 | 5`-CCGCTTGTGCGGGCCCCCGTC-3` |
| 16FCOM1 | 5`-CAGCAGCCGCCGTAATAC-3` |
| 16RCOM2-Ph | 5`-P-CCGTCAATTCCTTTGAGTTT-3` |
| 18FITS1 | 5`-CTTGGTCATTTAGAGGAAGTAA-3` |
| 18RITS4 | 5`-TCCTCCGCTTATTGATATGC-3` |
| 18FNS7 | 5`-GAGGCAATAACAGGTCTGTGATGC-3` |
| 18RNS8-Ph | 5`-P-TCCGCAGGTTCACCTACGGA-3` |

## 2.8 Software

- Microsoft®Office 2007
- Gen5 1.06 (BioTek)
- Adobe® Photoshop®Professional 7
- Adobe®Acrobat®Professional 7
- Endnote X3.0.1(Thomson)
- Sequencher™ 4.8 (Gene Codes Corporation, Ann Arbor, USA)
- BioEdit 7.0.5.3
- MEGA version 4
- ClustalW (EMBL, Hinxton, UK)
- GIMP 2.6
- Leica confocal software, version 2.5, Build 1347d

# 3 Experimental methods

## 3.1 Collection of soil/sediment samples

A total of twelve soil/sediment samples (approx. 50 g) were collected from Egypt at different locations, as listed in Table 2 and shown in Figure 9, around factories which produce chemicals, insecticides, and pesticides. The samples were collected in plastic bags, homogenized and stored at 4°C until use [182].

**Table 2: List of locations of samples used in the study**

| Locations number | Governorate | No. of sites |
|---|---|---|
| 1 | Alexandria | 4 |
| 2 | Kafr El-Sheikh | 1 |
| 3 | Gharbia | 1 |
| 4 | Qalyubia | 2 |
| 5 | Monufia | 4 |


**Figure 9: Maps showing the sampling locations in Egypt**

## 3.2 Isolation and purification of the γ-HCH & BDE-degrading bacteria and fungi

One gram of soil was incubated in 250 ml Erlenmeyer flasks containing 100 ml of M9 medium with γ-HCH or BDE (2 mM) as the sole source of carbon and energy. After one month of cultivation at 30°C and shaking on a rotary shaker operated at 150 rpm, bacteria and fungi were isolated from the soil through serial dilutions in PBS buffer. One hundred microliters of the dilution were spread onto M269 minimal medium (for bacteria) and basic Czapek-DOX medium (for fungi) agar plates supplemented with crystals of γ-HCH or BDE in the lid of the plate.

After 7 days of incubation, colonies were picked up and transferred to new plates by repeated subculturing and streaking on R2A medium or LB (for bacteria) and PDA medium (for fungi) agar plates until pure cultures were obtained.

## 3.3 Stock cultures

For stock cultures a loop of a pure culture was added to 750 µl sterile LB or R2A medium-depending on the isolate and PDA medium for bacteria and fungi, respectively in a 2 ml cryo-vial and incubated for one day and 3 days for bacteria and fungi, respectively at 30°C. Then 500 µl sterile glycerol was added, the vial was mixed by vortexing and frozen at -20°C.

## 3.4 Sequencing of bacterial 16S and fungal 18S rRNA genes

### 3.4.1 Genomic DNA extraction

A colony of strains was picked up and resuspended in 50 µl TE-buffer and kept for 15 min at 96°C in a heating block. The suspension was centrifuged for 1 min at 15.700 x g to pellet the cell debris. The DNA-containing supernatant was utilized for the following polymerase chain reaction (PCR). Alternatively, in case of a negative result, the bacterial and fungal DNA were extracted by employing the FastDNA® Spin Kit for Soil by following the supplier's instructions. Yield of genomic DNA was measured in a NanoDrop spectrophotometer by measuring the absorbance at 260 nm. Purity was determined by calculating the ratio of absorbance at 260 nm to absorbance at 280 nm. A pure DNA has an $A_{260}/A_{280}$ ratio of 1.7 - 1.9.

### 3.4.2 Amplification of the DNA by Polymerase Chain Reaction (PCR)

The extracted DNA was amplified by PCR [183], which is a method that enables the exponential augment of particular sequences of the DNA by enzymatic replication. Those were appointed by using specific sets of primer pairs which enabled the amplification of a special region of the DNA template. The primers, short oligonucleotides, bind at specific regions coding for the 16S ribosomal RNA gene (16S rRNA) or 18S rRNA of the denaturated bacterial and fungal DNA template, respectively. The polymerase enables the synthesis of the new complementary DNA strand to the primers by the accumulation of free desoxynucleosidtriphosphates (dNTP's). The PCR

reactions were performed in a thermocycler at a total volume of 50 µl using the temperature programs as described in Table 3, Table 4, Table 5, and Table 6.

**Table 3: Composition of the 16S rRNA PCR reaction**

| Volume (µl) | |
|---|---|
| 1 | Forward primer 16F27 |
| 1 | Reverse primer 16R1492 |
| 2 | dNTP's |
| 5 | 10 x Taq-Buffer |
| 39.5 | $ddH_2O$ |
| 1 | Template |
| 0.5 | Taq-Polymerase |
| 50 | PCR reaction |

**Table 4: Temperature program for the 16S rRNA PCR**

| Temperature (°C) | | Time | |
|---|---|---|---|
| 94 | Initial denaturation | 3 min | |
| 94 | Denaturation | 40 sec | 30 cycles |
| 60 | Annealing | 1 min | |
| 72 | Elongation | 1.5 min | |
| 72 | Final elongation | 5 min | |

**Table 5: Composition of the 18S rRNA PCR reaction**

| Volume (µl) | |
|---|---|
| 2 | Forward primer ITS1 |
| 2 | Reverse primer ITS4 |
| 1 | dNTP's |
| 2 | $MgCl_2$ |
| 5 | 10 x Taq-buffer |
| 35.5 | $ddH_2O$ |
| 2 | Template |
| 0.5 | Taq-polymerase |
| 50 | PCR reaction |

**Table 6: Temperature program for the 18S rRNA PCR**

| Temperature(°C) | | Time | |
|---|---|---|---|
| 94 | Initial denaturation | 5 min | |
| 94 | Denaturation | 40 sec | 35 cycles |
| 55 | Annealing | 45 sec | |
| 72 | Elongation | 1.5 min | |
| 72 | Final elongation | 7 min | |

### 3.4.3 Gel electrophoresis

The size of DNA fragments was determined by electrophoresis on 1.5 % agarose gels. The necessary amount of agarose was dissolved in 1X TBE buffer. The samples were loaded onto the gel and the electrophoresis was performed at 100 Volt $cm^{-1}$ in 1X TBE buffer. DNA was visualized by soaking in a dilute solution of ethidium bromide.

After separation on agarose gels, the DNA fragments of interest were excised from the gel by a lancet, weighted and treated by the Qiagen II Agarose Gel Extraction Kit. The extraction was performed according to the suggested protocol of the provider. The PCR products were purified by employing the PCR Clean-up Gel extraction Kit Nucleospin Extract II by implementing the manufacturer's instructions.

### 3.4.4 Sequencing reaction

The 16S and 18S rRNA genes were sequenced to enable a phylogenetic analysis of the bacterial and fungal strains. This was performed by employing the classical chain-termination or Sanger method which requires a single-stranded DNA template, a DNA primer, a DNA polymerase, fluorescence labelled nucleotides and modified nucleotides that terminate DNA strand elongation. The DNA sample is divided into four separate sequencing reactions, containing the four standard deoxynucleosidtriphosphates (dATP, dGTP, dCTP and dTTP) and the DNA polymerase. For each reaction one of the four fluorescence labeled dideoxynucleosidtriphosphates (ddATP, ddGTP, ddCTP, or ddTTP) is added. These ddNTP's are the chain-terminating nucleotides, lacking a 3`-OH group required for the formation of a phosphodiester bond between two nucleotides during DNA strand elongation. Incorporation of a ddNTP into the elongation DNA strand therefore terminates DNA strand extension, resulting in various DNA fragments of varying length. The dideoxynucleotides are added at a lower concentration than the standard deoxynucleotides to allow strand elongation sufficient for sequence analysis. The sequencing reactions were performed in a thermocycler at a total volume of 10 µl by using the temperature program as described in Table 7, Table 8, and Table 9.

**Table 7: Composition of the sequencing reaction for 16S rRNA PCR product**

| **Volume (µl)** | |
|---|---|
| 2 | BigDye RR Mix (Applied Biosystems, Darmstadt) |
| 1 | BigDye Buffer (Applied Biosystems, Darmstadt) |
| 2.5 | $ddH_2O$ |
| 0.5 | R1087 |
| 0.5 | F945 |
| 0.5 | R518 |
| 0.5 | F357 |
| 4 | Purified PCR product |
| 10 | PCR reaction |

**Table 8: Composition of the sequencing reaction for 18S rRNA PCR product**

| Volume (µl) | |
|---|---|
| 2 | BigDye RR Mix |
| 1 | BigDye Buffer |
| 2.5 | $ddH_2O$ |
| 0.5 | FITS1 |
| 0.5 | RITS4 |
| 4 | Purified PCR product |
| 10 | PCR reaction |

**Table 9: Temperature program of the sequencing reaction for 16S & 18S rRNA PCR product**

| Temperature (°C) | | Time | |
|---|---|---|---|
| 96 | Initial denaturation | 1 min | |
| 96 | Denaturation | 30 sec | 25 cycles |
| 60 | Annealing | 10 sec | |
| 60 | Elongation | 4 min | |
| 72 | Final elongation | 5 min | |

The sequencing reaction products were purified by employing the DyeEx 2.0 Spin Kit by implementing the specifications which are provided by the supplier's manual. The purified sequencing reaction products were dried in vacuum centrifuge and analyzed using an ABI PRISM BigDye Terminator v1.1 Ready Reaction Cycle Sequencing Kit (Applied Biosystems) and employing an ABI 3130xl Genetic Analyser (Applied Biosystems, Darmstadt).

### 3.4.5 Homology analyses

The gene sequences were annotated using the Sequencher™ 4.8 Software. DNA similarity searches were performed using the BlastN program and the databases of EMBL and GenBank from the National Center for Biotechnology Information website (NCBI) http://blast.ncbi.nlm.nih.gov/Blast.cgi?PROGRAM=blastn&BLAST_PROGRAMS=megaBlast&PAGE_TYPE=BlastSearch&SHOW_DEFAULTS=on&LINK_LOC=blasthome and http://rdp.cme.msu.edu/seqmatch/seqmatch_intro.jsp. For filtration and manipulation (reverse complement) of DNA, the following web site was used: http://www.bioinformatics.org/sms/index.html.

Phylogenetic and molecular evolutionary analysis for 16S and 18S rRNA gene nucleotide sequences were conducted for sequence alignments using the computer programs ClustalW [184] and BioEdit 7.0.5.3 (Hall *et al.*, 1999) and implemented in MEGA software version 4 [185].

Phylogenetic trees were constructed using the Neighbor-Joining (N-J) method algorithm [186]. Distances were generated using the Kimura Matrix, and the tree stability was supported through Bootstrap analysis (1000 replications) according to Junca and Pieper [172].

## 3.5 Selection of the best bacterial and fungal strains for degradation

### 3.5.1 Liquid cultures for inoculation

Bacterial and fungal strains from frozen stock cultures were streaked on R2A or LB and PDA agar plates, respectively and incubated at 30°C until the formation of the colony was visible. Single colonies were used for inoculation of liquid cultures.

### 3.5.2 Bacterial inoculum preparation

Single colony was inoculated in liquid culture (LB or R2A medium). The culture was incubated overnight at 30°C with orbital shaking at 150 rpm. A volume of 300 µl of the culture showing $OD_{600}$ = 0.5 - 0.7 was transferred into the liquid culture (M269) which contain 2 mM of compounds (γ-HCH or BDE) to be tested. This culture was incubated at the same conditions.

### 3.5.3 Fungal inoculum preparation

Inocula were prepared by transferring 7 days old conidia grown on PDA slopes into 5 ml sterile $dH_2O$. Each slant was shaken vigorously for one min., and then added to 95 ml sterile water and few drops of Tween-80 for homogeneity. This spore suspension contains about $10^5$ - $10^7$ spores / ml. Two hundred microliters of spore suspension of each species was inoculated into Czapek-DOX broth medium with 2 mM of halogenated compounds (γ-HCH or BDE) and incubated at 28 ± 2°C in a rotary shaker (150 rev/min).

### 3.5.4 An absorbance-based cell viability assay using high absorptivity, Water-soluble Tetrazolium salts (WST-1)

Quantitation of tissue culture cells has been the hallmark for the determination of efficacy of agents that either promote or inhibit cell growth. While cells grown in suspension can be counted directly, most tissue cultures are grown in monolayer culture, which requires dispersal using proteolytic agents such as trypsin prior to quantitation. Dispersed cells can be directly quantitated both manually with the use of a microscope and a hemocytometer or in an automated cell counter. These methods are slow and labor intensive, requiring individual samples to be quantitated individually. There are a number of different indirect methodologies to quantitate cell number with large numbers of samples using microplates. Simple total protein and nucleic acid assays that indirectly provide information regarding cell number or more specifically changes in cell number are based on the concept that cells on average have a constant amount of these polymers. However, these assays do not necessarily provide information regarding the viability of the cells in question and several "live cell" assays have been developed. Tetrazolium salts are reduced enzymatically to produce colored formazan dyes. One of the first and most notable of these salts is (3-(4,5-Dimethylthiazol-2-yl)-2,5-diphenyltetrazolium bromide) MTT, which produces a colored insoluble product that has to be solublized with ethanol. Improvements of the tetrazolium substrates have produced compounds that have water soluble products; the first of which is WST-1. This compound has a maximal absorbance wavelength of 438 nm. Further improvements in the tetrazolium salts have improved both reactivity and molar absorbtivity, along with decreasing toxicity. NADH (nicotineamido adenine dinucleotide reduced form) and NADPH (nicotineamido adenine dinucleotide phosphate reduced form) are generated from $NAD^+$ or $NADP^+$ by the reaction of dehydrogenase enzymes and their substrates, such as lactate dehydrogenase and lactic acid respectively. Therefore, the tetrazolium salt is utilized for the determination of the dehydrogenase activity or a substrate of the dehydrogenase [187].

The bacterial and fungal cell density was quantified by measuring the viability of the cells using WST-1 reagent, starting at 0 incubation time. One hundred and sixty microliters of culture was incubated with 20 µl of WST-1 in a 96-well plate for 30 min with shaking at 650 rpm and at 30°C. The absorbance was measured at λ of 450 nm.

## 3.6 Analytical methods

### 3.6.1 Preparation of Fatty Acid Methyl Esters (FAMEs)

For the saponification of the bacterial fatty acids 40 mg wet cells were resuspended in 1 ml of solution 1 in a 4 ml glass vial and securely sealed with a Teflon lined cap. The suspension was boiled for 1h at 100°C in a heating block. Then the solution was cooled to room temperature.

To methylate the saponified fatty acids 1.8 ml of solution 2 was added followed by another heating step at 80°C for 10 min. The reaction was quickly stored on ice until cooled. For the extraction of the fatty acid methyl esters (FAMEs) from the aqueous phase, 0.9 ml of solution 3 was added. After vigorous vortexing for 30 seconds, the upper organic phase was transferred to a new 4 ml vial. This extraction step was performed three times. To prevent contamination from the organic phase during gas chromatography analysis, 3 ml of basic solution 4 were added. After vortexing again for 30 seconds the organic phase was transferred to a 2 ml crimp top vial. The solvent was evaporated by a gentle stream of nitrogen. For the gas chromatographic analysis FAMEs were resuspended in n-octane containing internal standard n-alkanes $C_{24}H_{50}$ and $C_{16}H_{34}$.

### 3.6.2 Gas Chromatography (GC)

The extracted FAMEs were analysed by employing an Agilent 6890N gas chromatograph equipped with a 5% -PhenylMethylpolysiloxan Optima 5 capillary column (50 m length; 0.32 mm inner diameter; 0.25 µm film thickness and a Flame Ionisation Detector (FID). Hydrogen served as the carrier gas. For FAMEs analysis the injector temperature was set to 250°C and the detector temperature was 300°C. The oven program for the FAMEs analysis was 100°C for 2 minutes, subsequently increasing the temperature to 290°C at 4°C $min^{-1}$. The heating steps are followed by an isothermal period of 10 minutes.

## 3.7 Methodological approaches to survey the microbial biofilm diversity

### 3.7.1 Biofilm microcosms

About five grams of homogenised soil/sediment sample were placed in a 100 ml stoppered glass vessel and 80 ml of sterile tap water were added (Figure 10). Six parallel microcosms per soil sample and per compound were prepared, resulting in 144 microcosms in total. Twenty mg of each tested compound were dissolved in 1 ml of dichloromethane (DCM). Droplets of 25 µl of each tested compounds were placed on sterile Permanox™(Nunc, USA) plastic slides (100 x 20 mm) and the DCM was allowed to evaporate. Permanox™ is a polyester which does not react with DCM. One slide, loaded with 8 droplets of each compound, was placed in each microcosm, sides with droplets facing the water surface of a reservoir. The microcosms were maintained at room temperature.

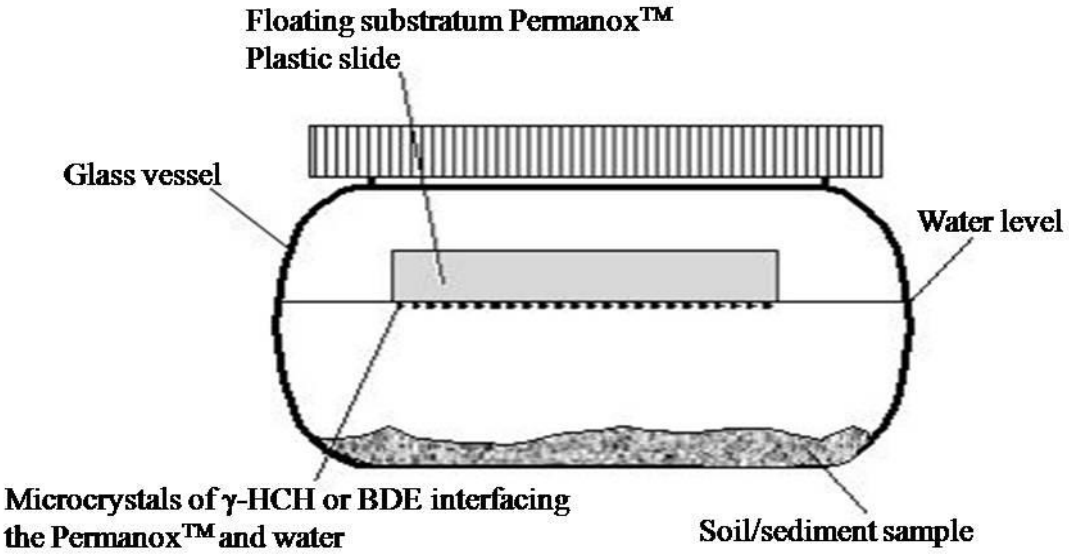


**Figure 10: Scheme of the microcosm used to grow biofilm.**

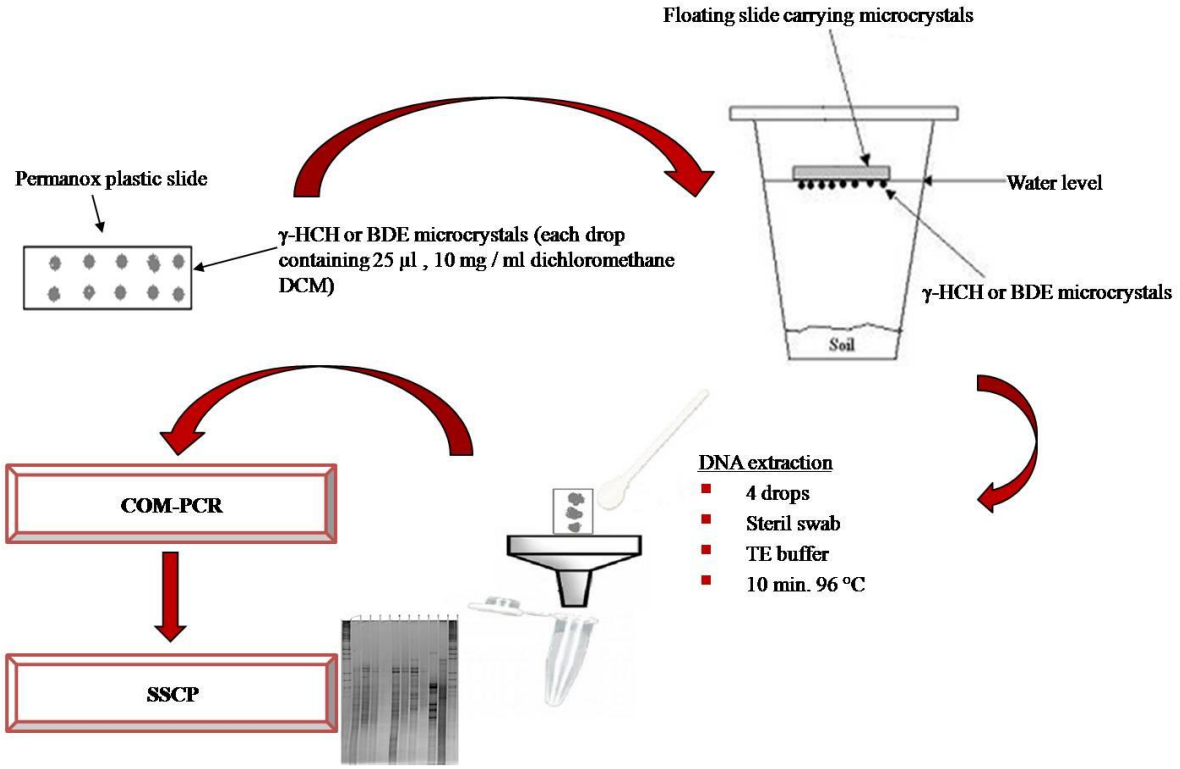


**Figure 11: Schematic protocol of methodological approaches to survey microbial biofilm diversity.**

## 3.7.2 Extraction and amplification of the DNA

The biofilm communities were harvested weekly with a sterile cotton swap from 4 γ-HCH or BDE droplets, transferred to columns provided in the commercially available FastDNA® SPIN® Kit for Soil, and the total DNA was extracted according to the manufacturer's instructions.

Partial bacterial 16S rRNA gene sequences were amplified using the primers COM1F (binds to the positions 519 to 536 of *E. coli*) and COM2-phosphorylated (binds to the positions 907 to 926 and containing a 5`-terminal phosphate group), as described in [168]. These primers amplify a region of the DNA that code for 16S ribosomal RNA (rRNA), a gene of about 1520 nucleotides that is widely used for the analysis of the phylogeny of bacteria. 16S rRNA are extremely well conserved molecules in overall structure and a significant component of the cellular mass [188], where they exhibit 9 small variable regions which allow species differentiation, thus identification.

Partial fungal 18S rRNA gene sequences were amplified using the primers NS7F (binds to the positions 1185 to 1207) and NS8-phosphorylated (binds to the positions 1508 to 1527 and containing a 5`-terminal phosphate group), as described by (Peters *et al*., 2000) [189]. The PCR reactions were performed in a thermocycler in a total volume of 50 µl, as shown in Table 10, Table 11, Table 12 and Table 13.

**Table 10: Composition of the COM-PCR reaction**

| **Volume (µl)** | |
|---|---|
| 2 | Forward primer Com1 |
| 2 | Reverse primer Com2-Ph |
| 1 | dNTP's |
| 2 | $MgCl_2$ |
| 5 | 10 x Taq-buffer |
| 35.5 | $ddH_2O$ |
| 2 | Template |
| 0.5 | Hot star Taq-polymerase |
| 50 | PCR reaction |

**Table 11: Temperature program for the COM-PCR**

| **Temperature (°C)** | | **Time** | |
|---|---|---|---|
| 95 | Initial denaturation | 15 min | |
| 94 | Denaturation | 40 sec | 30 cycles |
| 50 | Annealing | 40 sec | |
| 72 | Elongation | 1 min | |
| 72 | Final elongation | 10 min | |

**Table 12: Composition of the NS-PCR reaction**

| Volume (µl) | |
|---|---|
| 2 | Forward primer NS7 |
| 2 | Reverse primer NS8-Ph |
| 1 | dNTP's |
| 2 | $MgCl_2$ |
| 5 | 10 x Taq-buffer |
| 35.5 | $ddH_2O$ |
| 2 | Template |
| 0.5 | Hot star Taq-polymerase |
| 50 | PCR reaction |

**Table 13: Temperature program for the NS-PCR**

| Temperature (°C) | | Time | |
|---|---|---|---|
| 94 | Initial denaturation | 3 min | |
| 94 | Denaturation | 60 sec | 35 cycles |
| 50 | Annealing | 60 sec | |
| 72 | Elongation | 70 sec | |
| 72 | Final elongation | 5 min | |

The PCR products obtained from the sequence reaction were purified with the PCR Clean-up Gel extraction Kit Nucleospin Extract II by following the manufacturer's instructions.

### 3.7.3 SSCP fingerprint & sequencing analysis of the microbial community

Single Stranded Conformation Polymorphism (SSCP) is a technique for genetic profiling of microbial communities based on PCR-amplified signature genes. It is an important technique to evaluate natural viability between microbial communities, i.e., in response to environmental changes. It is a culture-independent method that contributes to both the fast differentiation and identification of microorganisms, even for those microorganisms which have not yet been cultured in the laboratory [190].

The phosphorylated strand of PCR product from the reaction with COM and NS primers were digested with 2.5 µl lambda exonuclease buffer and with 2.5 µl lambda exonuclease for 1 hour at 37°C and 700 rpm in a mixer. This enzyme removes the phosphorylated strand, resulting in a single strand DNA product and further purified with MiniElute Kit by following the manufacturer's instructions. The amount of DNA was measured by a NanoDrop spectrophotometer and 100 ng of DNA was dried in a vacuum centrifuge at 30°C for about 20 minutes. The DNA was then resuspended in 4 µl denaturating SSCP loading buffer. Three DNA markers were prepared; each one had 3 µl SSCP loading

buffer and 1 µl DNA marker. All samples and two markers were heated at 96°C for 2.5 minutes, then cooled down quickly in a water-ice bath at least for 3 minutes and then subjected to SSCP in a polyacrylamide gel [168].

The gel consisted of 9 ml MDE TM gel (2-fold concentrated solution Acrylamide, BMA Lonza, Rockland, USA); 3 ml 10X TBE buffer; 18 ml bidistilled water; 120 µl 10% ammonium persulfate (APS) and 12 µl N,N,N`,N`tetraethylmethylendiamine (TEMED, Amresco, Solon, Ohio, USA).

Before pouring the gel, two glass plates (thermo-glass-plate and glass-gel-plate) were washed with detergent, water and cleaned with absolute ethanol. The glass-gel-plate was then coated with a solution of 3 ml (100 %) ethanol; 30 µl of acetic acid and 30 µl of Bind-silane (GE Healthcare Bio-Science AB, Uppsala, Sweden). The other glass plate was treated with 1 ml of Repel-silane ES (Amersham Bio-Science, Uppsala, Sweden). After 10 minutes, both plates were gently cleaned with absolute ethanol and dried for 10 minutes. Spacers (0.4 mm) were placed between the plates and secured with clamps. The gel was poured between the plates and allowed to polymerize for 2.5-3 hours.

The SSCP chamber was filled with 1X TBE and the apparatus was connected to a cooling water system adjusted to 20°C. The 8 µl samples and 4 µl markers were loaded into the gel pockets and it was run at 400 V for 16 hours. Afterward, the gels were silver stained according to [191] as described in Table 14.

The single bands obtained in the SSCP gel were excised from the gel and DNA was extracted with 50 µl of SSCP elution buffer at 96°C, 700 rpm mixer for 15 minutes. Extracts were centrifuged at 15.700 x g for 1 minute and the DNA in the supernatant fluid was used for amplification using PCR with the same primers described above. The PCR-product was purified by MiniElute Kit for the sequence reaction.

The purified PCR-product was sequenced using the same primers, cleaned with the DyeEx™ Spin Kit and then the sequence analyzed as described before.

**Table 14: Siver-Staining of SSCP gel procedure**

| Step | Quantity | Composition | Time |
|---|---|---|---|
| 1. Fixation: | 500 ml | 10% acetic acid<br>[50 ml acetic acid] | 30 minutes |
| 2. Washing: | 500 ml | Milli-Q-$H_2O$ | 3x5 minutes |
| 3. Silver staining: | 500 ml | 0.1% silver nitrate (w/v)<br>[0.5 g silver nitrate<br>+ 500 µl formaldehyde] | 30 minutes |
| 4. Washing: | 500 ml | Milli-Q-$H_2O$ | 20 seconds |
| 5. Development: | 500 ml | 2.5% $Na_2CO_3$<br>[(12.5 g $Na_2CO_3$<br>+ 500 µl formaldehyde<br>+ 500 µl Na-thiosulphate (2%)<br>(1g/50ml)] | 2-5 minutes |
| 6. Stop: | 500 ml | 2% Glycine, 0.5% EDTA-$Na_2$<br>[10 g Glycine & 2.5 g EDTA-$Na_2$] | 10 minutes |
| 7. Impregnation: | 500 ml | 10% Glycerol<br>[57 ml Glycerol] | 10 minutes |

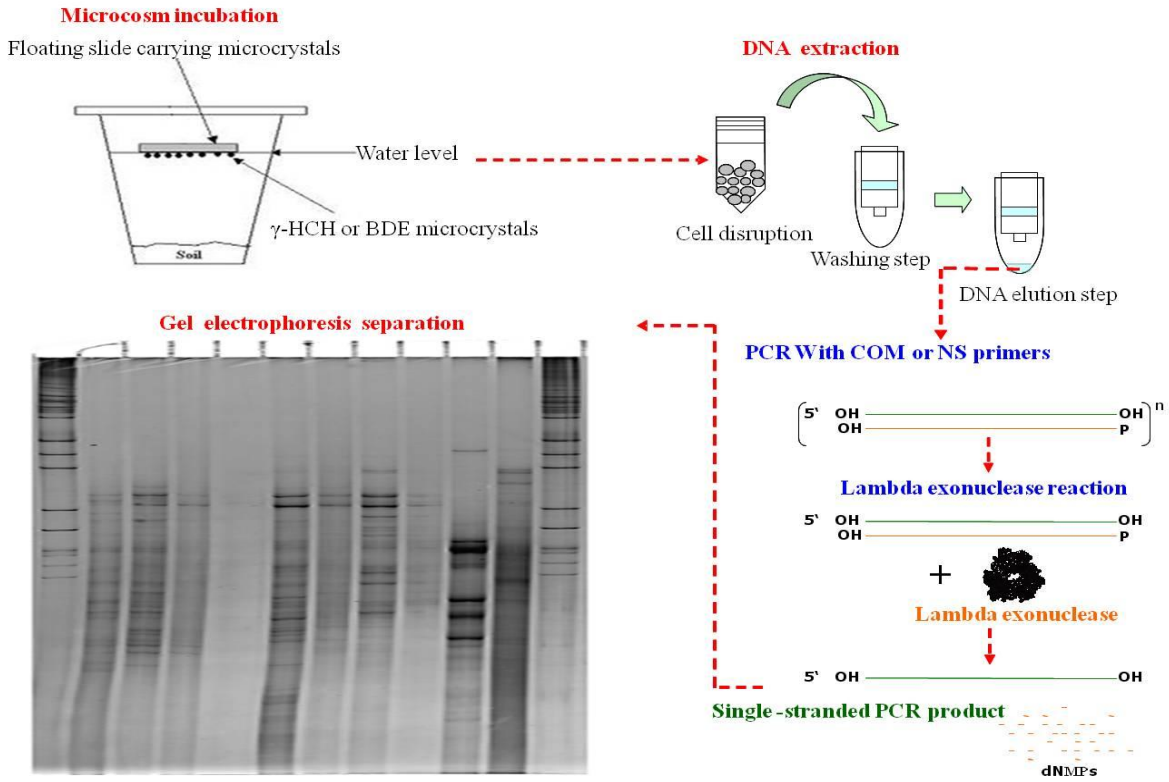


**Figure 12: Schematic protocol of SSCP gel preparation using biofilm sample for microbial diversity analysis.**

## 3.8 Microscopy methods to analyze the biofilm structures

### 3.8.1 Biofilm staining

The biofilms on the slides were stained for proteins with SYPRO® applied as described by the manufacturer. The working solution was applied directly to the biofilms and incubated for 30 minutes then the samples were washed by deionized $H_2O$.

The droplets on the slides were stained for hydrophobic compounds with Nile Red. For this purpose a stock solution of 2 mg Nile Red in 1 ml acetone-water (1:1 vol/vol) was diluted 1:1000 in demineralized water. After staining for 15 minutes, the sample was carefully rinsed twice and counterstained using a nucleic acid-specific stain (DAPI). DAPI stain was used as stock solution 10 mg/ 2ml of deionized water, then diluted to 300 nM in PBS (21 µl from stock solution were completed to 1ml with PBS), incubated for 1-5 minutes, the sample was rinsed several times in PBS.

Cells in biofilms were stained with the BacLight™ kit and applied as described by the manufacturer. Live cells stained green while damaged or dead cells stained red. The staining solution contained 5 ml deionized water and 5 µl each of the two components SYTO9 and propidium iodide. This working solution was applied directly to the biofilms and incubated at

the room temperature for 15 minutes. All samples were incubated in the dark and examined immediately after staining using confocal laser scanning microscope.

### 3.8.2 Confocal Laser Scanning Microscopy (CLSM)

Confocal laser scanning microscopy (CLSM) was performed using the model TCS SP attached to an upright microscope. The instrument was controlled by Leica Confocal software. The system was equipped with three visible lasers: an Ar laser (458, 476, 488, and 514 nm), a laser iodide (561 nm), and a He-Ne laser (633 nm). The spectrophotometer feature allowed flexible and optimal adjustment of sliders on the detector side.

The following settings were used for excitation and recording of emission signals (ex/em), respectively: SYPRO (280 and 450/610 nm), Nile Red (488 and 550/700 nm), DAPI (358/461 nm), SYTO9 (488/500 nm) and propidium iodide (490/635 nm). Biofilm samples were observed 10x 0.3-numerical aperture (NA), 20x0.5-NA, and 63x0.9-NA water-immersible lenses.

**Table 15: Summarize for biofilm staining procedure**

| Staining solution | Dilution | Incubation time (in the dark) | Washing (rinsed by) |
|---|---|---|---|
| SYPRO | applied directly | 30 min. | $dH_2O$ |
| BacLight kit (2X/5 ml deionized $H_2O$) | 500 µl + 500 µl $dH_2O$ | 15 min. | $dH_2O$ |
| Nile Red (2 mg / 1 ml acetone-water) diluted to 1/1000 | 10 µl + 495 µl $dH_2O$ + 495 µl acetone | 15 min. | $dH_2O$ |
| DAPI (10 mg /2 ml PBS) | 21 µl + 979 µl PBS | 1-5 min. | PBS |

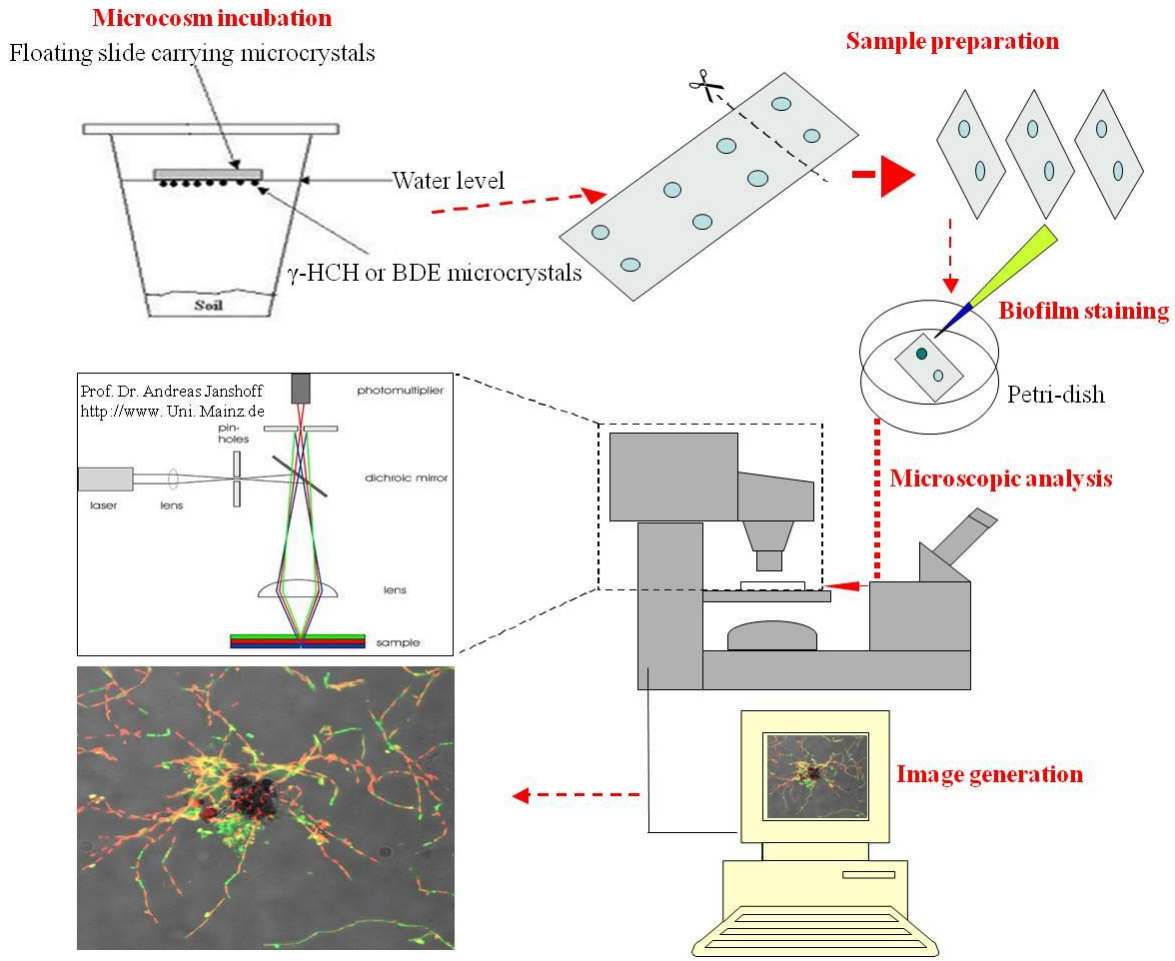


**Figure 13: Schematic procedures for microscopic analysis of biofilm using CLSM.**

# 4 Results

## 4.1 Phylogeny and characteristics of bacterial and fungal isolates from Egyptian localities that were able to grow in the presence of γ-HCH

### 4.1.1 Bacteria

#### 4.1.1.1 Phylogeny of bacterial isolates

The sequence of the 16S ribosomal RNA genes of the isolated strains from the several localities, compared to the database of the National Centre for Biotechnology Information (NCBI), revealed the bacterial communities able to grow in the presence of γ-HCH as a nutrient. The Alexandria samples showed a community which was mainly composed of the genera *Acetobacter, Achromobacter, Agromyces, Bacillus, Brucella, Microbacterium, Ochrobactrum, Pseudomonas, Rhodococcus and Starkeya.* The community members showed a homology towards the bacterial strains as shown in Table 16. The phylogenetic tree showed the diversity and the bacterial relationship of these isolates (Figure 14) while the bacterial community of the Monufia samples was very rich with different bacterial members (Table 17). The phylogenetic tree of Monufia samples listed the main classes which were found in this sample such as Firmicutes, Alphaproteobacteria, Gammaproteobacteria, Betaproteobacteria and Actinobacteria (Figure 15).

**Table 16: Sequence homology of the 16S rRNA gene of the bacterial isolates from the Alexandria samples with isolates from public data bases**

| Isolate | Size (bp) | Closely related bacteria | Accession number | Homology (%) |
|---|---|---|---|---|
| **Alexandria1.1** | 1196 | *Pseudomonas sp.* | AB284047 | 99 |
| **Alexandria 1.2** | 1218 | *Achromobacter xylosoxidans* | FJ796451 | 98 |
| **Alexandria 1.3** | 934 | *Pseudomonas sp.* | DQ453830 | 99 |
| **Alexandria 2.1** | 1429 | *Acetobacter pasteurianus* | FM178866 | 95 |
| **Alexandria 2.4** | 1482 | *Achromobacter piechaudii* | EU239469 | 74 |
| **Alexandria 2.5** | 1504 | *Pseudomonas sp.* | WAB1666 | 97 |
| **Alexandria 2.6** | 1458 | *Pseudomonas panipatensis* | EF424401 | 99 |
| **Alexandria 3.1** | 1485 | *Rhodococcus sp.* | AY822615 | 99 |
| **Alexandria 3.2** | 1505 | *Ochrobactrum anthropi* | AF526518 | 98 |
| **Alexandria 3.3** | 1455 | *Brucella sp.* | AY331581 | 99 |
| **Alexandria 3.4** | 1495 | *Pseudomonas sp.* | FJ375383 | 95 |
| **Alexandria 3.5** | 1486 | *Microbacterium sp.* | GQ495641 | 99 |
| **Alexandria 4.1** | 1200 | *Bacillus sp.* | FJ607361 | 98 |
| **Alexandria 4.2** | 1607 | *Starkeya sp.* | FJ555530 | 99 |
| **Alexandria 4.3** | 1516 | *Agromyces sp.* | FM209088 | 98 |
| **Alexandria 4.4** | 1270 | *Pseudomonas stutzeri* | U65012 | 96 |

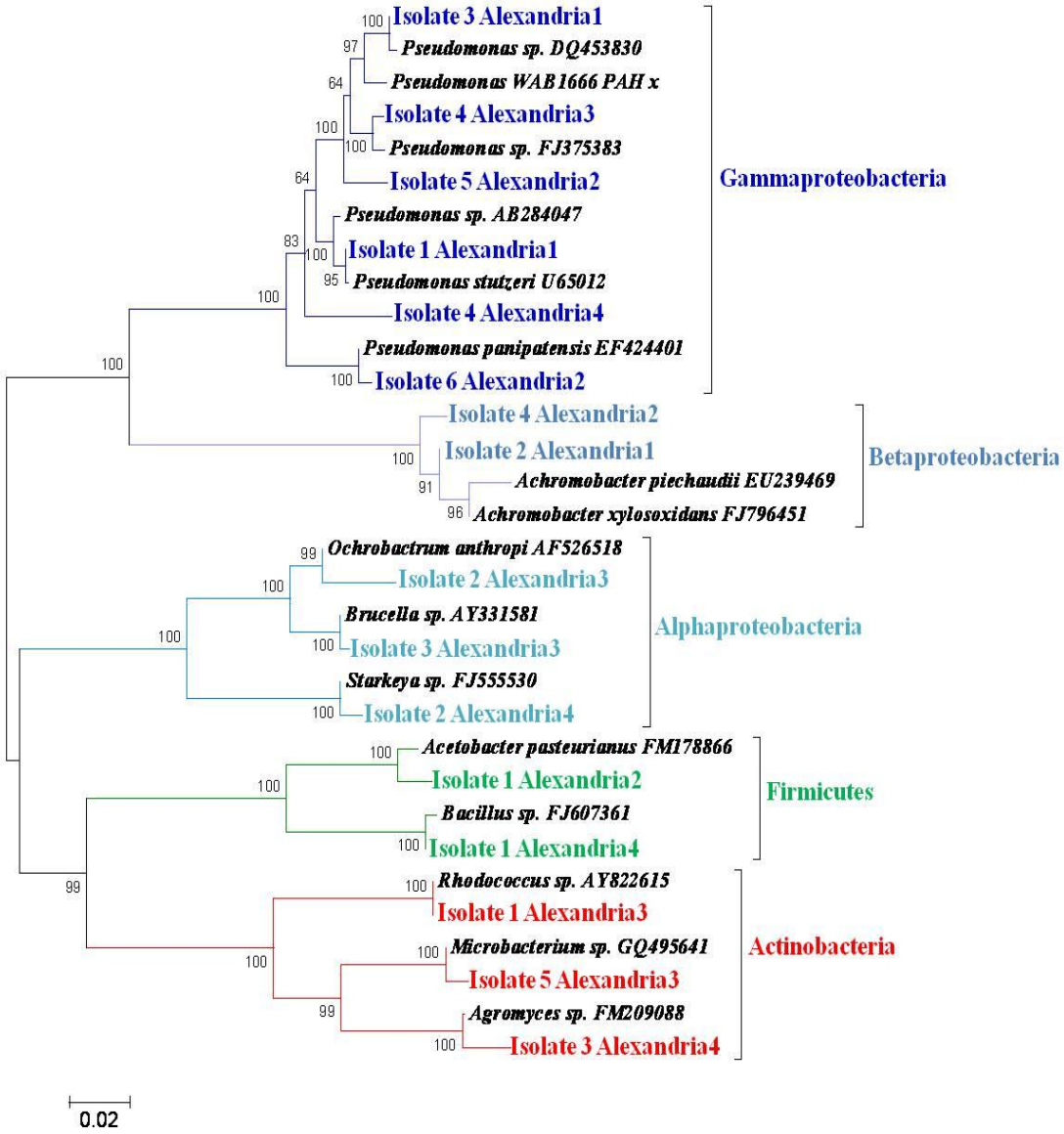


**Figure 14: Phylogeny of bacterial isolates from the Alexandria samples that were able to grow on γ-HCH. Multiple alignments of the sequences corresponding to the 16S rRNA of the studied isolates were carried out followed by neighbor joining clustering. Bootstrap values expressed as percentages of 1000 replications. Bar represents 2% sequence dissimilarity.**

**Table 17: Sequence homology of the 16S rRNA gene of the bacterial isolates from the Monufia samples**

| Isolate | Size (bp) | Closely related bacteria | Accession number | Homology (%) |
|---|---|---|---|---|
| **Monufia1.1** | 1008 | *Bacillus licheniformis* | X68416 | 98 |
| **Monufia1.2** | 1239 | *Pseudomonas stutzeri* | CP000304 | 94 |
| **Monufia1.3** | 1274 | *Bacillus licheniformis* | X68416 | 98 |
| **Monufia1.4** | 1170 | *Bacillus thuringiensis* | FJ772020 | 99 |
| **Monufia1.5** | 837 | *Bacillus licheniformis* | X68416 | 97 |
| **Monufia1.6** | 977 | *Bacillus licheniformis* | X68416 | 98 |
| **Monufia1.7** | 1212 | *Bacillus simplex* | AJ439078 | 98 |
| **Monufia1.8** | 1179 | *Bacillus pumilus* | AY876287 | 99 |
| **Monufia1.9** | 1235 | *Bacillus megaterium* | HM047741 | 99 |
| **Monufia1.10** | 1053 | *Bacillus altitudinis* | AJ831842 | 99 |
| **Monufia1.11** | 1272 | *Bacillus megaterium* | HM047741 | 99 |
| **Monufia1.12** | 1176 | *Cupriavidus oxalaticus* | EU024156 | 98 |
| **Monufia1.13** | 1429 | *Brevundimonas sp.* | FJ544245 | 98 |
| **Monufia1.14** | 1149 | *Pseudomonas stutzeri* | CP000304 | 96 |
| **Monufia2.1** | 1460 | *Novosphingobium sp.* | EU440981 | 99 |
| **Monufia2.2** | 1491 | *Rhodococcus ruber* | AY247275 | 98 |
| **Monufia2.3** | 1460 | *Bacillus sp.* | DQ416793 | 98 |
| **Monufia2.5** | 1519 | *Bacillus circulans* | X60613 | 99 |
| **Monufia2.6** | 1520 | *Bacillus sp.* | DQ298267 | 99 |
| **Monufia2.8** | 1569 | *Oceanobacillus picturae* | AJ315060 | 94 |
| **Monufia2.10** | 1509 | *Bacillus cibi* | FJ458438 | 99 |
| **Monufia2.12** | 1522 | *Paenibacillus ginsengisoli* | AB245382 | 94 |
| **Monufia2.13** | 1522 | *Bacillus mycoides* | EU221418 | 99 |
| **Monufia2.14** | 1597 | *Bacillus mycoides* | EU221418 | 82 |
| **Monufia3.1** | 2010 | *Bacillus megaterium* | AB366310 | 100 |
| **Monufia3.2** | 1498 | *Bacillus subtilis* | FN393812 | 99 |
| **Monufia3.3** | 1486 | *Bacillus sp.* | AF350926 | 99 |
| **Monufia3.4** | 1974 | *Bacillus flexus* | EU977771 | 99 |
| **Monufia3.5** | 1513 | *Bacillus sp.* | EU384247 | 100 |
| **Monufia3.6** | 1623 | *Bacillus sp.* | DQ223132 | 84 |
| **Monufia3.7** | 1517 | *Bacillus megaterium* | DQ789400 | 100 |
| **Monufia4.1** | 1522 | *Bacillus sp.* | FJ413048 | 99 |
| **Monufia4.2** | 1525 | *Bacillus thuringiensis* | EF210309 | 100 |
| **Monufia4.3** | 1512 | *Bacillus megaterium* | FJ613544 | 99 |
| **Monufia4.4** | 1514 | *Bacillus sp.* | FJ943261 | 99 |
| **Monufia4.5** | 1621 | *Bacillus amyloliquefaciens* | AY651023 | 81 |
| **Monufia4.6** | 1511 | *Bacillus flexus* | EU860182 | 100 |
| **Monufia4.7** | 1519 | *Bacillus sp.* | AB366347 | 99 |

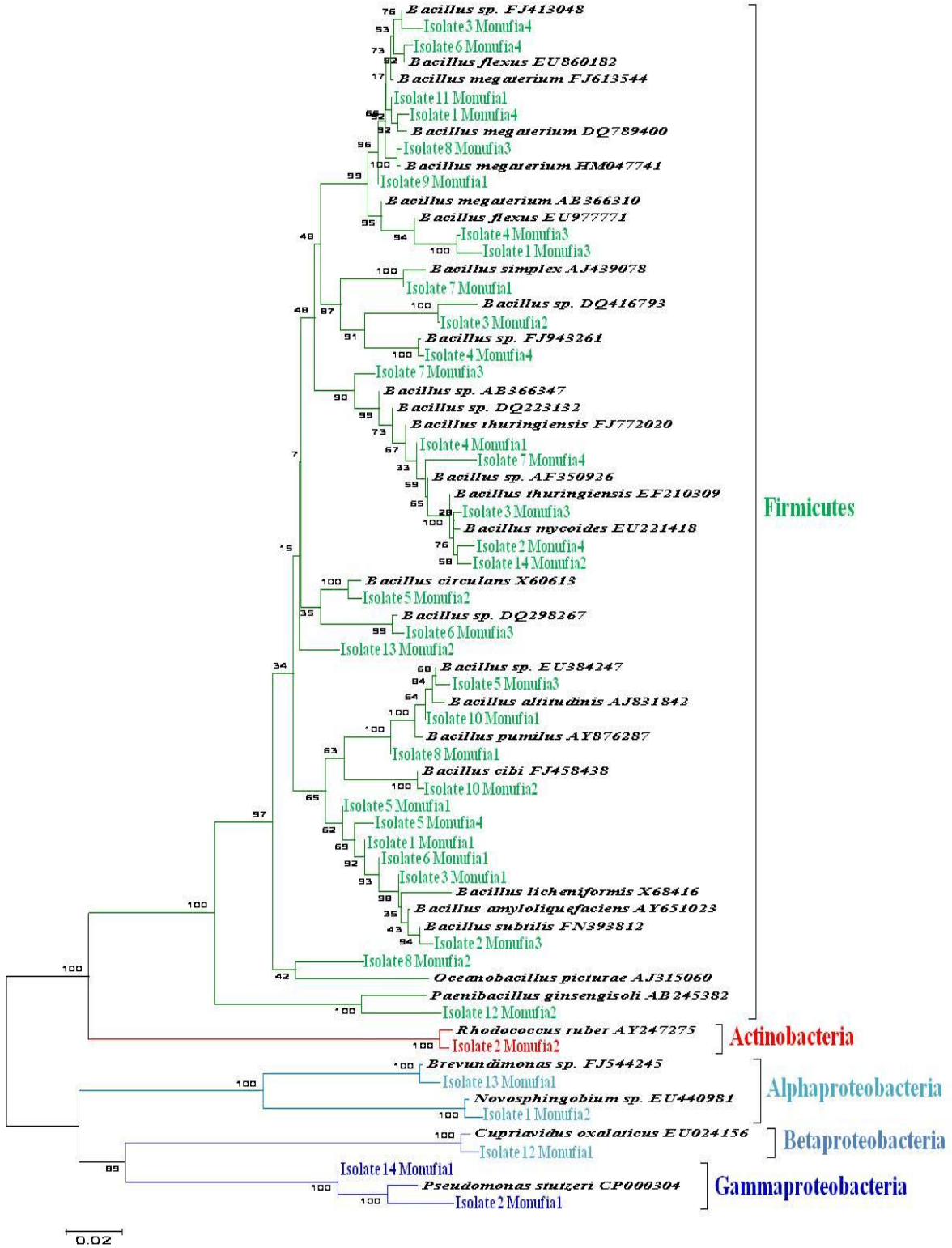


**Figure 15: Phylogeny of bacterial isolates from the Monufia samples that were able to grow on γ-HCH. Multiple alignments of the sequences corresponding to the 16S rRNA of the studied isolates were carried out followed by neighbor joining clustering. Bootstrap values expressed as percentages of 1000 replications. Bar represents 2% sequence dissimilarity.**

It was found that the bacterial strains which were isolated from Gharbia samples were completely different from the previous samples. The community was composed mainly of bacterial strains of the genera *Aquamicrobium, Bacillus, Gordonia, Micromonospora and Rhodococcus* (Table 18). The majority of identified strains were members of Actinobacteria, Alphaproteobacteria and Firmicutes (Figure 16). Only three bacterial strains in Kafr El-Sheikh sample could be identified. *Alcaligenes, Lysobacter and Peseudomonas* were the members of the community (Table 19) and the phylogenetic tree showed that two of these strains belonged to Gammaproteobacteria and the third one was belonging to Betaproteobacteria (Figure 17). From Qalyubia samples, we isolated *Bacillus, Brevundimonas, Frateuria, Luteimonas, Ochrobactrum, Pseudomonas and Rhodococcus* (Table 20). The phylogenetic tree showed the classes of the identified strains (Figure 18).

**Table 18: Sequence homology of the 16S rRNA gene of the bacterial isolates from the Gharbia sample**

| Isolate | Size (bp) | Closely related bacteria | Accession number | Homology (%) |
|---|---|---|---|---|
| **1** | 1493 | *Rhodococcus sp.* | DQ066434 | 99 |
| **2** | 1443 | *Aquamicrobium sp.* | FM210786 | 97 |
| **3** | 1523 | *Bacillus flexus* | FJ641022 | 100 |
| **4** | 1451 | *Aquamicrobium sp.* | FM210786 | 96 |
| **5** | 1497 | *Micromonospora sp.* | EF544146 | 99 |
| **6** | 1394 | *Rhodococcus sp.* | FJ189543 | 98 |
| **7** | 1484 | *Gordonia sp.* | FN561544 | 97 |

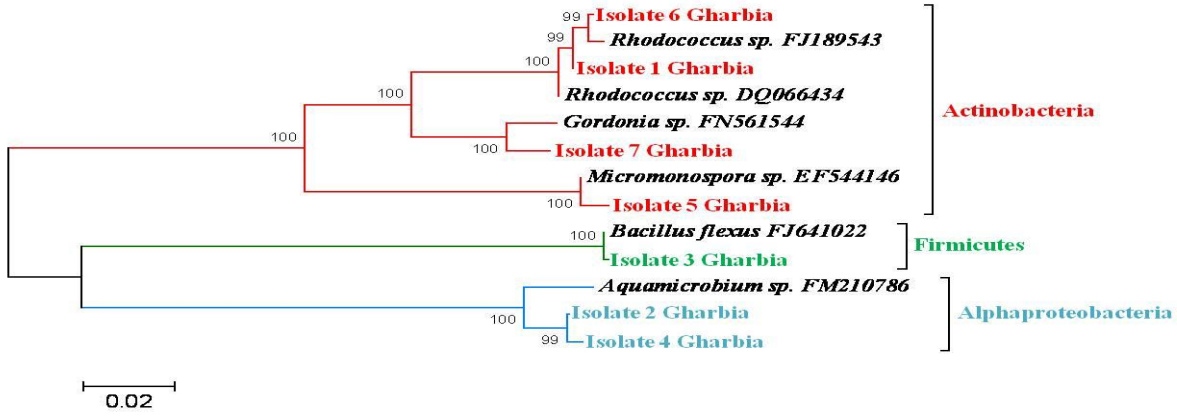


**Figure 16: Phylogeny of bacterial isolates from the Gharbia sample that were able to grow on γ-HCH. Multiple alignments of the sequences corresponding to the 16S rRNA of the studied isolates were carried out followed by neighbor joining clustering. Bootstrap values expressed as percentages of 1000 replications. Bar represents 2% sequence dissimilarity.**

**Table 19: Sequence homology of the 16S rRNA gene of the bacterial isolates from the Kafr El-Sheikh sample**

| Isolate | Size (bp) | Closely related bacteria | Accession number | Homology (%) |
|---|---|---|---|---|
| **1** | 1507 | *Pseudomonas stutzeri* | EU275359 | 100 |
| **2** | 1496 | *Alcaligenes faecalis* | EU075145 | 99 |
| **3** | 1506 | *Lysobacter daejeonensis* | DQ191178 | 99 |


**Figure 17: Phylogeny of bacterial isolates from the Kafr El-Sheikh sample that were able to grow on γ-HCH. Multiple alignments of the sequences corresponding to the 16S rRNA of the studied isolates were carried out followed by neighbor joining clustering. Bootstrap values expressed as percentages of 1000 replications. Bar represents 2% sequence dissimilarity.**

**Table 20: Sequence homology of the 16S rRNA gene of the bacterial isolates from the Qalyubia sample**

| Isolate | Size (bp) | Closely related bacteria | Accession number | Homology (%) |
|---|---|---|---|---|
| **Qalyubia1.1** | 1495 | *Pseudomonas putida* | DQ232745 | 99 |
| **Qalyubia1.2** | 1392 | *Luteimonas mephitis* | AB433628 | 95 |
| **Qalyubia1.3** | 1511 | *Bacillus sp.* | GQ292772 | 99 |
| **Qalyubia1.4** | 1509 | *Bacillus sp.* | GQ292772 | 99 |
| **Qalyubia1.5** | 1422 | *Brevundimonas diminuta* | AB167225 | 99 |
| **Qalyubia1.6** | 1511 | *Frateuria sp.* | DQ419968 | 97 |
| **Qalyubia1.7** | 1514 | *Luteimonas mephitis* | AJ012228 | 98 |
| **Qalyubia1.8** | 1509 | *Luteimonas mephitis* | AJ012228 | 98 |
| **Qalyubia1.9** | 1489 | *Rhodococcus wratislaviensis* | EU043327 | 99 |
| **Qalyubia2.1** | 1154 | *Ochrobactrum sp.* | EU769201 | 93 |
| **Qalyubia2.2** | 1488 | *Rhodococcus sp.* | AY822615 | 99 |

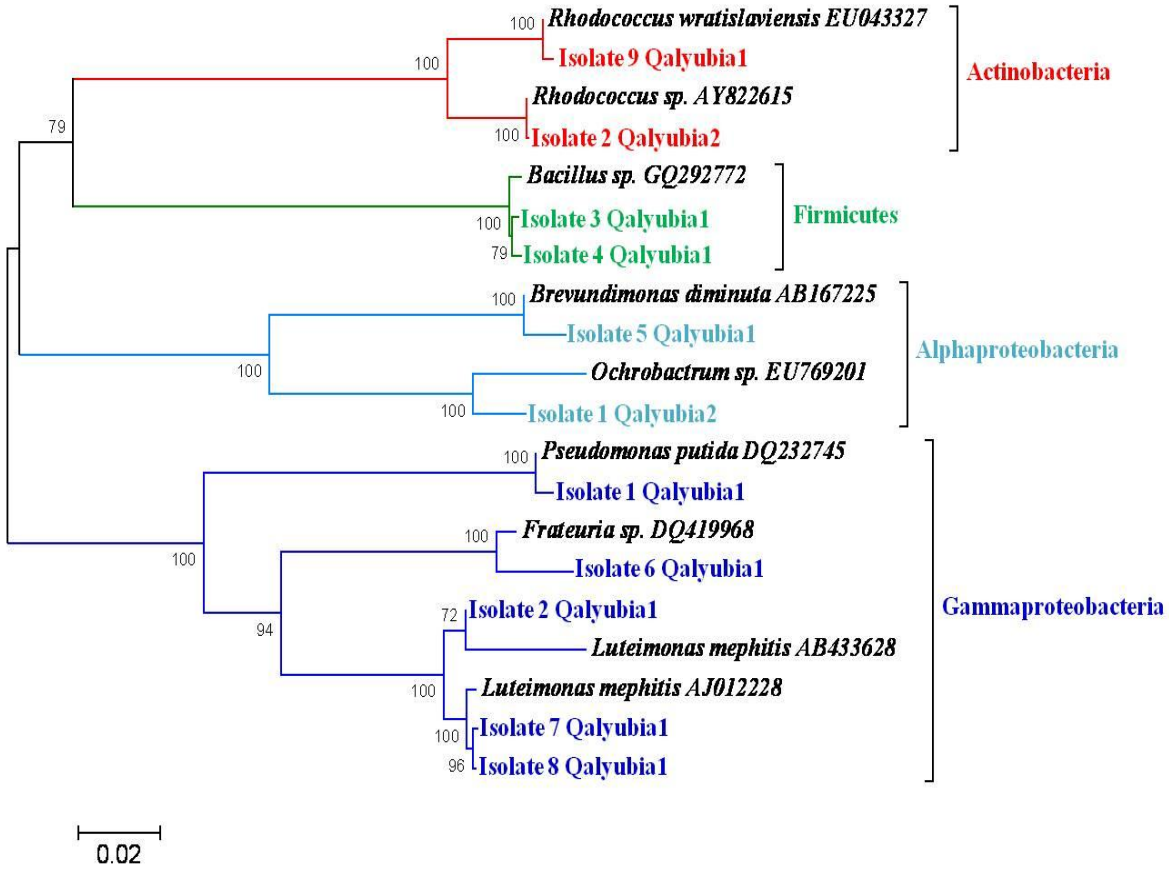


**Figure 18: Phylogeny of bacterial isolates from the Qalyubia sample that were able to grow on γ-HCH. Multiple alignments of the sequences corresponding to the 16S rRNA of the studied isolates were carried out followed by neighbor joining clustering. Bootstrap values expressed as percentages of 1000 replications. Bar represents 2% sequence dissimilarity.**

### 4.1.1.2 Growth of the most tolerant bacterial isolates on γ-HCH

The metabolization and degradation of γ-HCH and bacterial growth was carried out for 15 days at 30°C in shaking flasks. The degradation activity of γ-HCH was determined in the cultural filtrate every day during the cultivation period.

It is clear from Figure 19 that the growth of isolate2.Qalyubia2 was maximal after the 2nd day of cultivation. The growth of isolate3.Alexandria4, isolate7.Monufia4 and isolate4.Gharbia gradually increased with increasing time up to the optimal point at 3rd day of incubation. The growth of isolate3.Kafr El-Sheikh was at the maximum point after the 4th day of cultivation. After that the growth of all isolates gradually decreased over time.

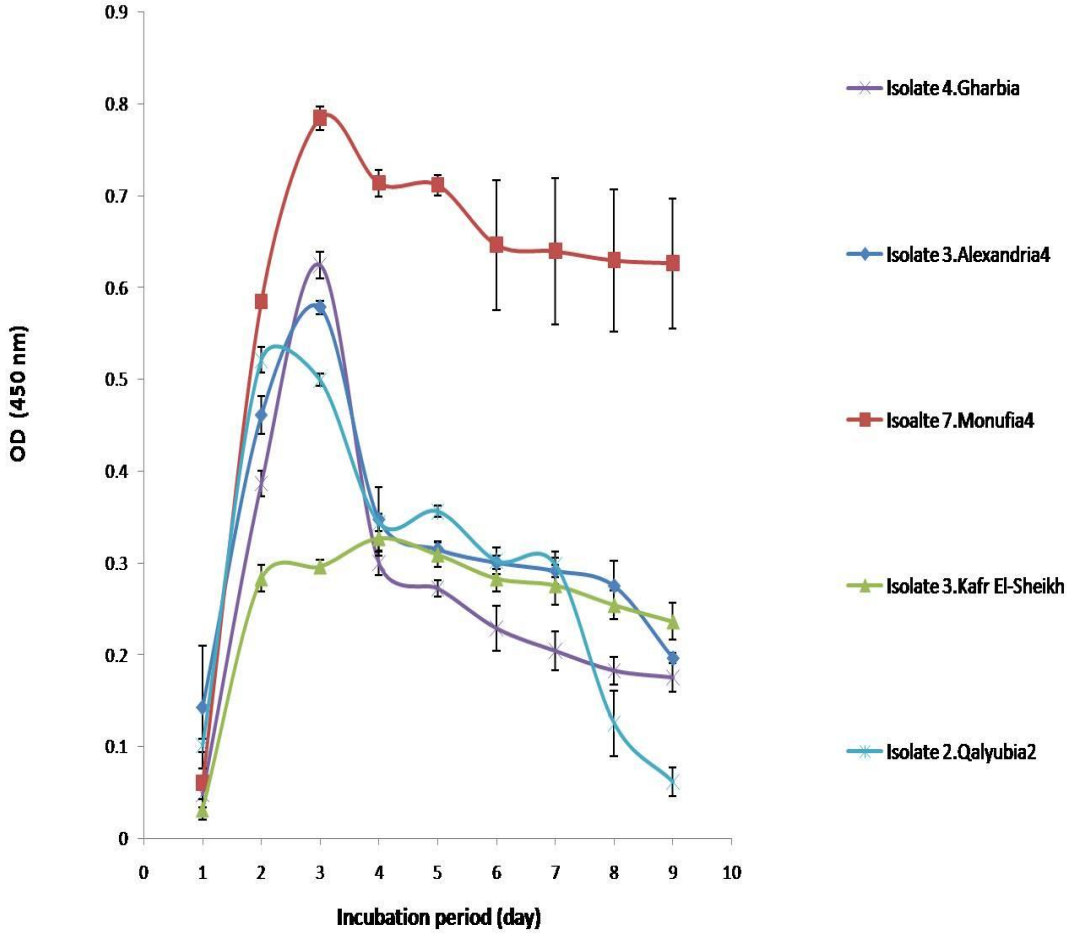


**Figure 19: Growth curves for the most capable bacterial isolates to grow on γ-HCH. The strains isolated from several locations in Egypt were grown in M269 medium containing 2mM γ-HCH. The growth was detected by the change in the absorbance at $\lambda_{max}$=450 nm.**

### 4.1.1.3 Analysis of fatty acids of the most tolerant bacterial isolates grown on γ-HCH

The differences in geometry between saturated and unsaturated fatty acids play an important role in biological processes and in the construction of biological structures such as cell membranes. From Figure 20 and Table 21, it was found that the major cellular fatty acids (>10 % of the total fatty acids) in the most abundant γ-HCH-degrading bacterial isolates were as follow; in Isolate4.Alexandria4 were C16:0, anteiso-C15:0, iso-C16:0, anteiso-C17:0, and C18:1ω9, in Isolate3.Kafr El-Sheikh were iso-C15:0, and anteiso- C17:1ω7, in Isolate2.Qalyubia2 were C16:0, C16:1ω7, C18:1ω9, and unknown fatty acid and in Isolate4.Gharbia were C19:0, and C18:1ω7, in Isolate7.Monufia4 was iso-C15.

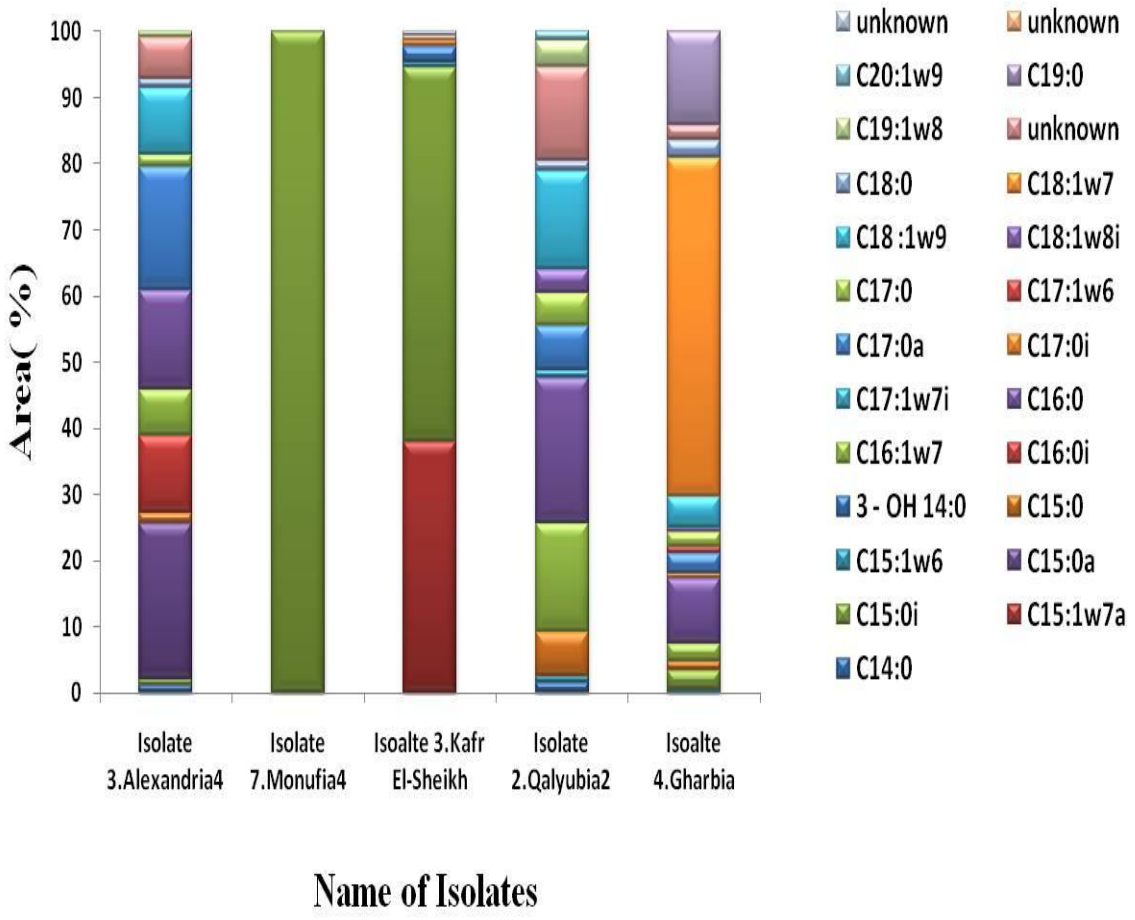


**Figure 20: Percentage of the extracted fatty acids from the most tolerant bacterial isolates for γ-HCH.**

**Table 21: Major cellular fatty acids content (%) of the most tolerant bacterial isolates for γ-HCH. Values are percentage of total fatty acids. -, Not detected.**

| Fatty acid | Isolate4. Alexandria4 | Isolate7. Monufia4 | Isolate3. Kafr el-Sheikh | Isolate2. Qalyubia2 | Isolate4. Gharbia |
|---|---|---|---|---|---|
| **Saturated fatty acids:** | | | | | |
| **$C_{16:0}$** | 15 | - | - | 22 | - |
| **$C_{19:0}$** | - | - | - | - | 14.1 |
| **Branched fatty acids :** | | | | | |
| **iso-$C_{15:0}$** | - | 100 | 56.8 | - | - |
| **anteiso- $C_{15:0}$** | 23.5 | - | - | - | - |
| **iso-$C_{16:0}$** | 11.8 | - | - | - | - |
| **anteiso- $C_{17:0}$** | 18.5 | - | - | - | - |
| **Monounsaturated fatty acids:** | | | | | |
| **anteiso- $C_{17:1\omega7}$** | - | - | 37.9 | - | - |
| **$C_{16:1\omega7}$** | - | - | - | 16.5 | - |
| **$C_{18:1\omega7}$** | - | - | - | - | 51.2 |
| **$C_{18:1\omega9}$** | 10 | - | - | 14.8 | - |
| **Unknwon fatty acid** | - | - | - | 14.2 | - |

### 4.1.1.4 Analysis of bacterial biofilm community compositions developing on γ-HCH droplets

Biofilms developing on the γ-HCH droplets were harvested after different time points (7, 14, 21, 28, 35 and 42 days). DNA was extracted, a segment of the bacterial 16S rRNA gene was amplified by PCR, and the amplicons were analysed on SSCP gels. The main SSCP bands were excised and sequenced.

SSCP community profiling showed highly diverse and distinct bacterial communities for γ-HCH droplets with the biofilm from the soil/sediment samples. Analysis of bacterial biofilm structure from Alexandria location by SSCP (Figure 21) showed huge diversity in the bacterial communities. By comparing the sequences of 11 excised bands, 8 different operational taxonomic units (OTUs) could be identified which were closely related to *Sphingomonas sp., Pseudomonas sp., Pseudomonas fluorescens, Nitrosospira sp., Parvibaculum sp., Methyloversatilis sp., Aquabacterium sp. and Cronobacter sakazakii.*

The phylogenetic tree (Figure 22) presents the closest related genus to each sequence obtained. The majority of the identified OTUs were members of the phylum Alphaproteobacteria followed by Betaproteobacteria and Gammaproteobacteria.

In the Monufia sample (Figure 23), 8 different OTUs were identified from 10 excised bands. These OTUs were closely related to *Sphingomonas sp., Burkholderia sp., Caulobacter sp., Planococcus sp., Ochrobactrum sp., Comamonas sp., Escherichia coli and Cronobacter*

*sakazakii.* The phylogenetic tree (Figure 24) showed that the majority of the identified OTUs were members of the phyla Alphaproteobacteria, Betaproteobacteria, Gammaproteobacteria and Firmicutes.

From the Kafr El-Sheikh, Qalyubia and Gharbia locations (Figure 25), 5 OTUs were identified and they were related to *Cronobacter sakazakii, Sphingomonas sp., Coleochaete pulvinata, Escherichia coli and Burkholderia gladioli.* The OTUs were members of the phyla Gammaproteobacteria followed by Alphaproteobacteria, Betaproteobacteria and Cyanobacteria (Figure 26).

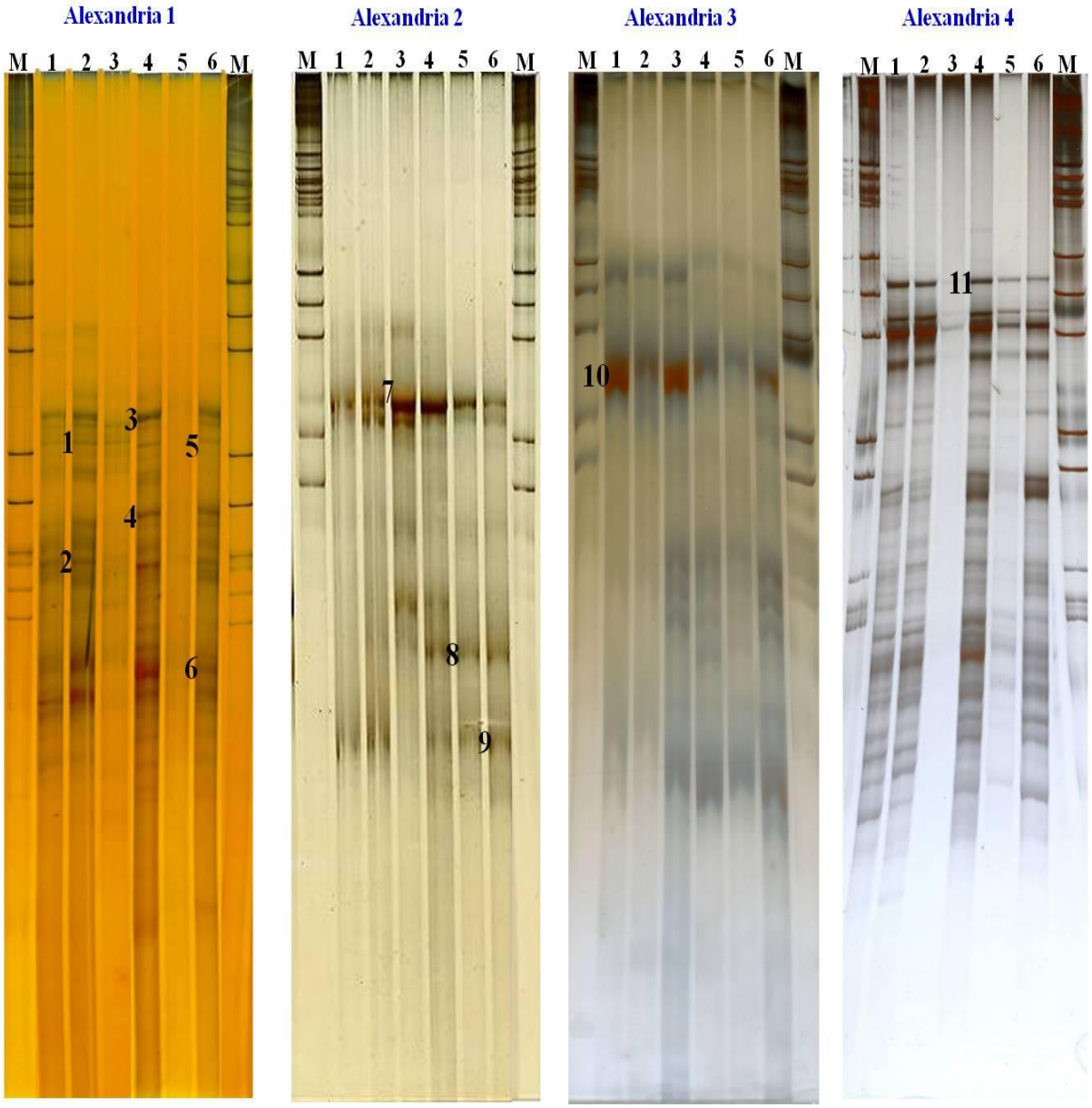


**Figure 21: SSCP fingerprints of PCR amplicons of partial 16S rRNA gene sequences of DNA extracted from γ-HCH biofilm of the Alexandria samples. Numbers on top of the gel correspond to sampling time in weeks and M corresponds to the lane of the marker. Marked bands have been excised, sequenced and compared with sequences of described species (Table 22).**

**Table 22: Phylogenetic assignment of sequences of prominent bands visualized on SSCP gel profiles of bacterial biofilm communities from the Alexandria samples**

| SSCP bands | Size (bp) | Cultured closest match | Accession number | Identity (%) |
|---|---|---|---|---|
| **Alexandria1.1** | 299 | *Sphingomonas sp.* | AF227857 | 93 |
| **Alexandria 1.2** | 330 | *Pseudomonas sp.* | AY321977 | 97 |
| **Alexandria 1.3** | 334 | *Pseudomonas fluorescens* | EU048319 | 91 |
| **Alexandria 1.4** | 409 | *Nitrosospira sp.* | AJ298729 | 99 |
| **Alexandria 1.5** | 271 | *Sphingomonas sp.* | DQ339627 | 99 |
| **Alexandria 1.6** | 323 | *Parvibaculum sp.* | DQ337073 | 96 |
| **Alexandria 2.7** | 388 | *Methyloversatilis sp.* | DQ337076 | 95 |
| **Alexandria 2.8** | 394 | *Sphingomonas sp.* | DQ166180 | 97 |
| **Alexandria 2.9** | 372 | *Sphingomonas sp.* | DQ173037 | 97 |
| **Alexandria 3.10** | 319 | *Aquabacterium sp.* | AY928247 | 84 |
| **Alexandria 4.11** | 368 | *Cronobactersakazakii* | GU227653 | 96 |

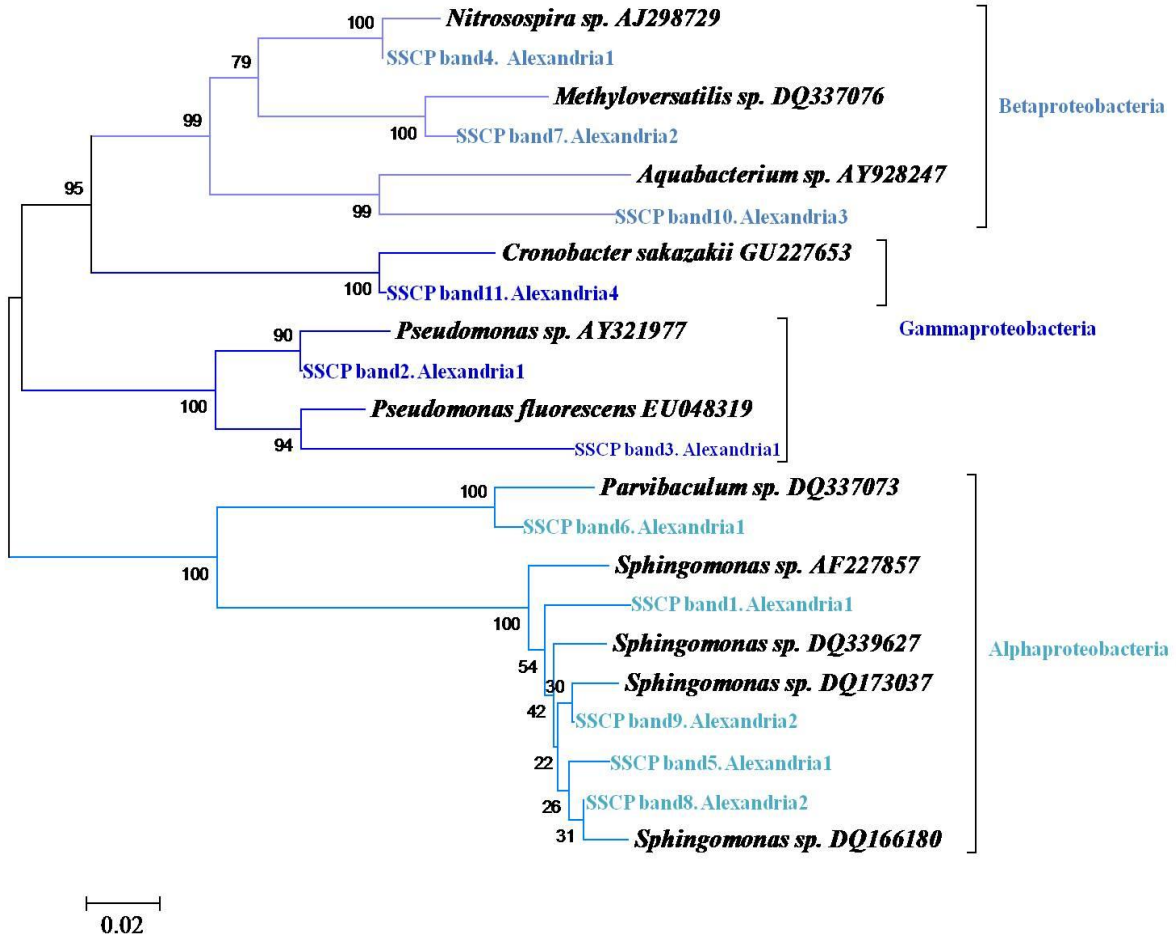


**Figure 22: Phylogenetic tree based on neighbor joining clustering after multiple alignments of the partial 16S rRNA gene sequences of the SSCP bands excised from γ-HCH droplet biofilms from the Alexandria samples. Bootstrap values expressed as percentages of 1000 replications. Bar represents 0.02 substitutions per nucleotide position.**

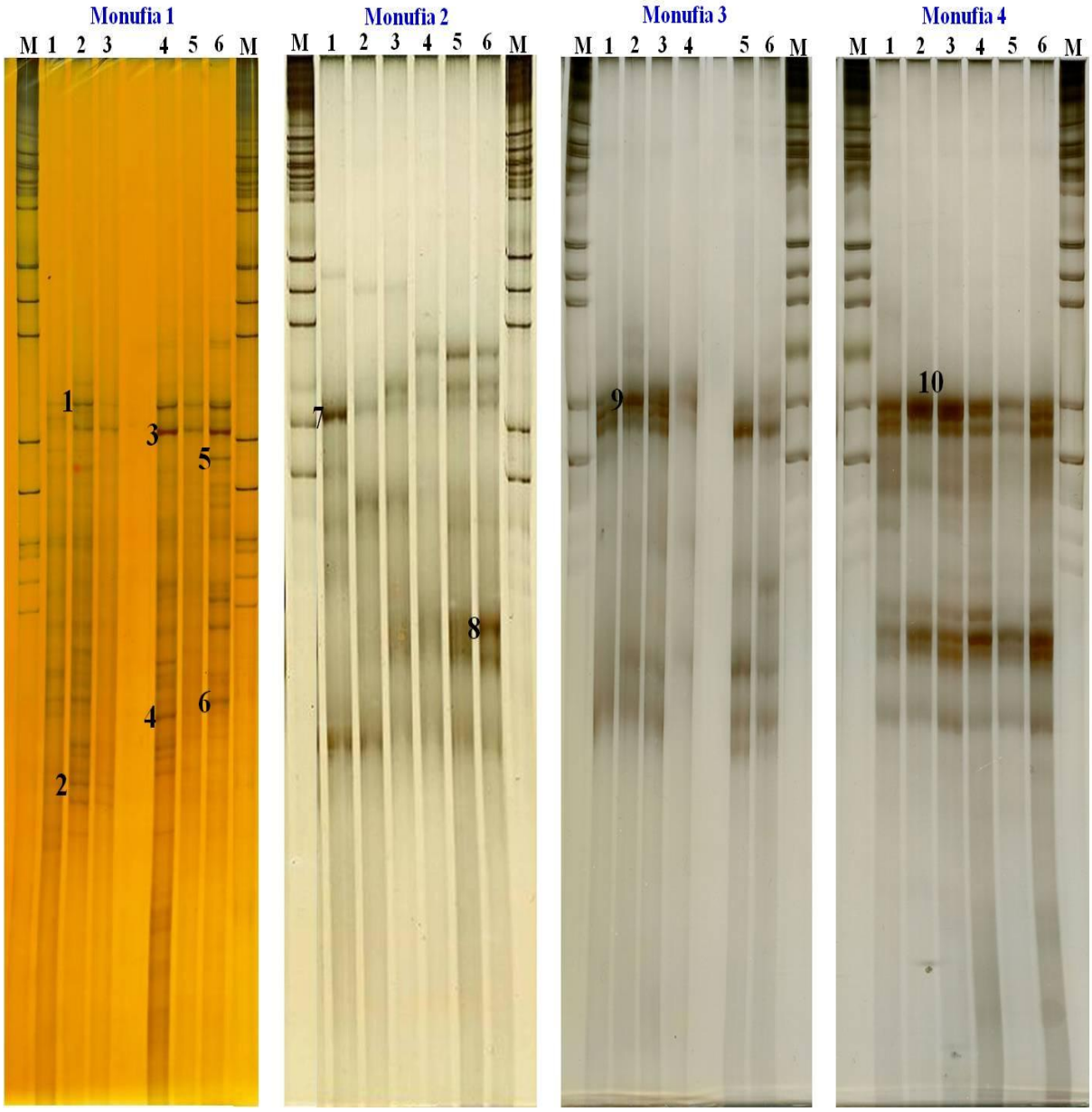


**Figure 23: Composition of γ-HCH bacterial biofilm communities obtained from the Monufia soil samples analysed by 16S rRNA gene based community fingerprint (SSCP). Numbers on top of the gel correspond to sampling time in weeks and M corresponds to the lane of the marker. Marked bands have been excised, sequenced and compared with sequences of described species (Table 23).**

**Table 23: Identification of the main bands of the SSCP gel profiles of bacterial biofilm communities from the Monufia samples by comparison with 16S rRNA gene sequences from public databases**

| SSCP bands | Size (bp) | Cultured closest match | Accession number | Identity (%) |
|---|---|---|---|---|
| **Monufia1.1** | 360 | *Sphingomonas sp.* | DQ166180 | 100 |
| **Monufia1.2** | 385 | *Sphingomonas sp.* | FJ192182 | 96 |
| **Monufia1.3** | 360 | *Burkholderia sp.* | DQ264474 | 99 |
| **Monufia1.4** | 306 | *Caulobacter sp.* | DQ984595 | 91 |
| **Monufia1.5** | 164 | *Planococcus sp.* | AM260556 | 76 |
| **Monufia1.6** | 337 | *Ochrobactrum sp.* | EU876660 | 98 |
| **Monufia2.7** | 357 | *Comamonas sp.* | EU804005 | 86 |
| **Monufia2.8** | 364 | *Sphingomonas sp.* | FN421940 | 94 |
| **Monufia3.9** | 357 | *Cronobacter sakazakii* | GU252268 | 94 |
| **Monufia4.10** | 413 | *Escherichia coli* | GU329913 | 93 |

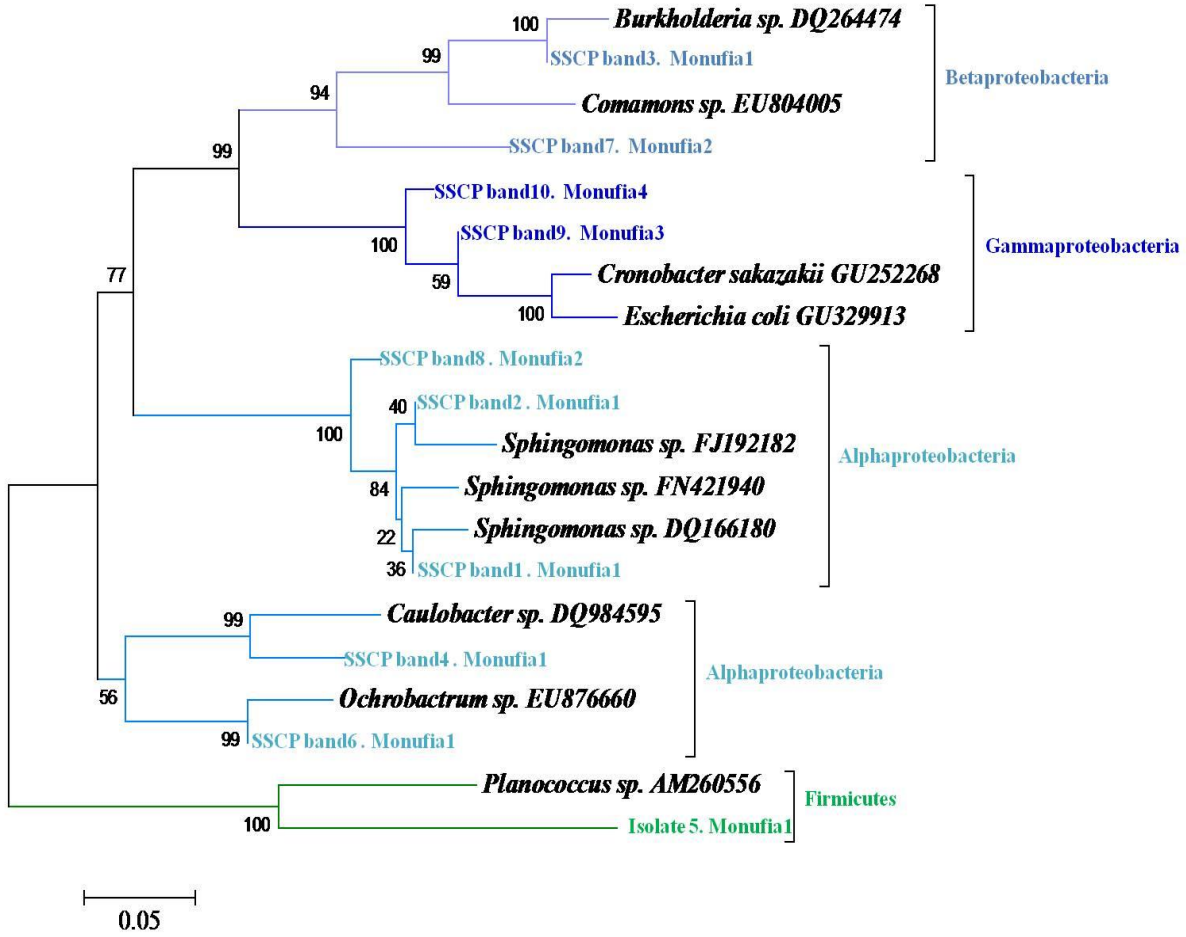


**Figure 24: Phylogenetic tree based on neighbor joining clustering after multiple alignments of the partial 16S rRNA gene sequences of the SSCP bands excised from γ-HCH droplet biofilms from the Monufia samples. Bootstrap values expressed as percentages of 1000 replications. Bar represents 0.05 substitutions per nucleotide position.**

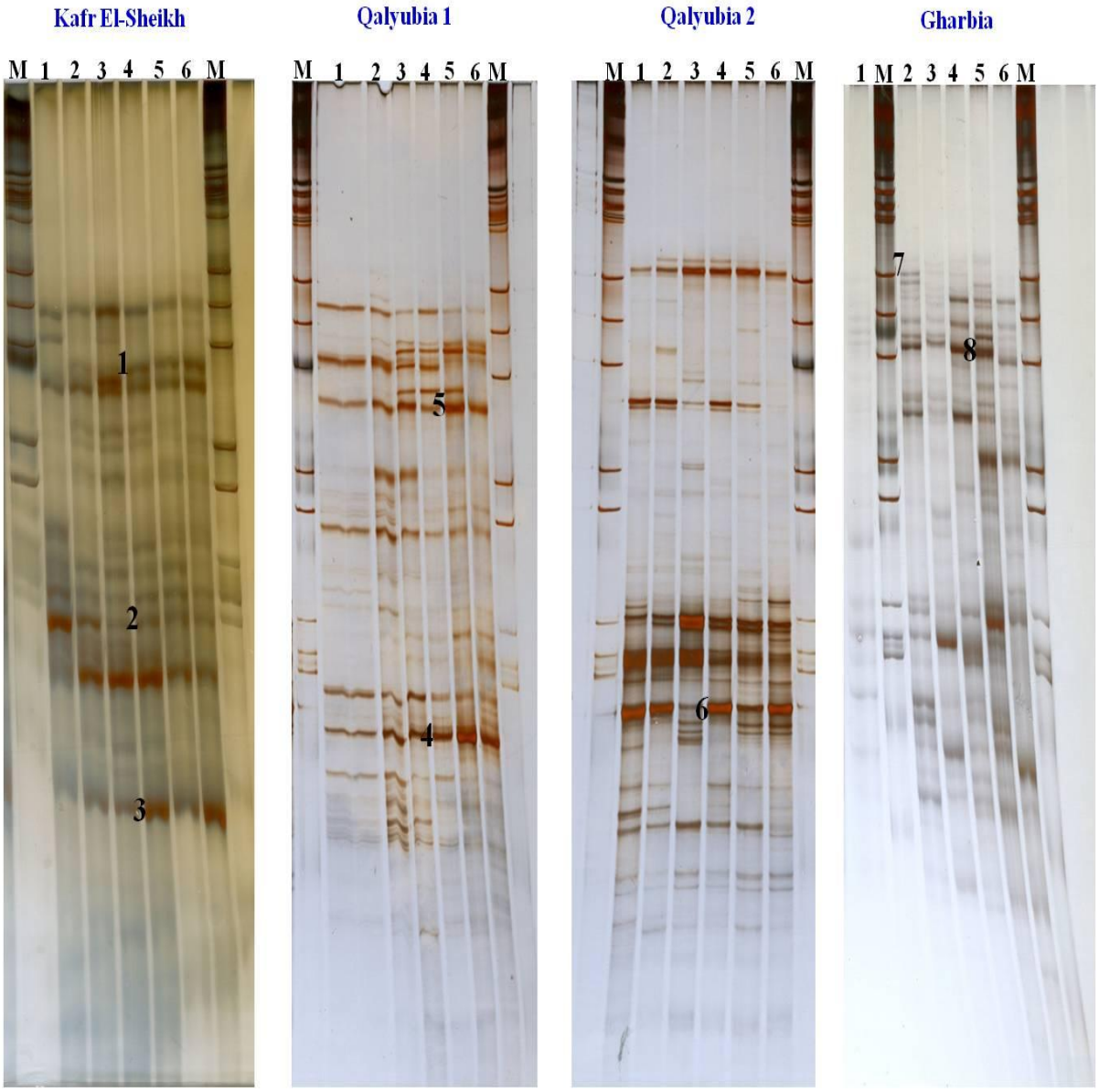


**Figure 25: Composition of γ-HCH bacterial biofilm communities obtained from the Kafr El-Sheikh, Qalyubia and Gharbia soil samples analysed by 16S rRNA gene based community fingerprint (SSCP). Numbers on top of the gel correspond to sampling time in weeks and M corresponds to the lane of the marker. Marked bands have been excised, sequenced and compared with sequences of described species (Table 24).**

**Table 24: Identification of the main bands of the SSCP gel profiles of bacterial biofilm communities from the Kafr El-Sheikh, Qalyubia and Gharbia samples by comparison with 16S rRNA gene sequences from public databases**

| SSCP bands | Size (bp) | Cultured closest match | Accession number | Identity (%) |
|---|---|---|---|---|
| **Kafr El-Sheikh.1** | 408 | *Cronobacter sakazakii* | GU252237 | 92 |
| **Kafr El-Sheikh.2** | 390 | *Cronobacter sakazakii* | GU252237 | 90 |
| **Kafr El-Sheikh.3** | 341 | *Sphingomonas sp.* | EU131000 | 90 |
| **Qalyubia1.3** | 403 | *Cronobacter sp.* | FJ489840 | 92 |
| **Qalyubia1.4** | 386 | *Coleochaete pulvinata* | AF497785 | 83 |
| **Qalyubia2.5** | 372 | *Escherichia coli* | GU329913 | 90 |
| **Gharbia.6** | 303 | *Escherichia coli* | HQ873730 | 95 |
| **Gharbia.7** | 372 | *Burkholderia gladioli* | S55001 | 90 |

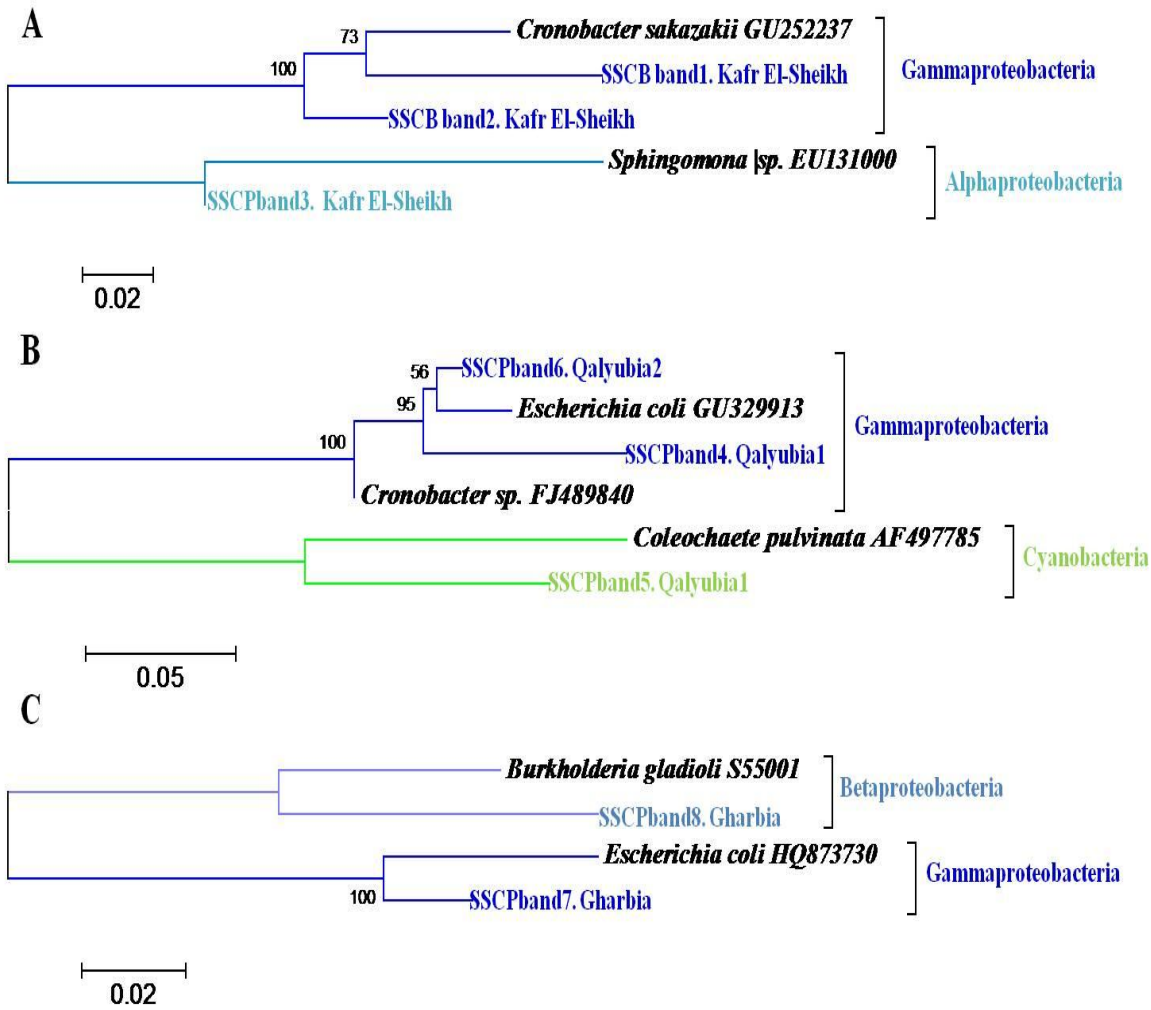


**Figure 26: Phylogenetic trees based on neighbor joining clustering after multiple alignment of the partial 16S rRNA gene sequences of the SSCP bands excised from γ-HCH droplet biofilms from A) the Kafr El-Sheikh, B) Qalyubia C) the Gharbia samples. Bootstrap values expressed as percentages of 1000 replications. Bar represents 0.02 and 0.05 substitutions per nucleotide position.**

## 4.1.2 Fungi

### 4.1.2.1 Phylogeny of fungal isolates

Because a huge diversity of the bacterial strains was found which were able to use γ-HCH as a nutrient, it was also examined whether fungi would be able to degrade it. The 18S ribosomal RNA gene was used as an eukaryotic marker for fungi. The sequence analysis of the 18S ribosomal RNA was compared to the database at NCBI. The genera *Penicillium, Scedosporium and Talaromyces* were found in the Alexandria samples (Table 25). The phylogenetic tree depicted the classes of theses fungal strains. The fungal strains were members of Eurotiomycetes and Sordariomycetes (Figure 27).

**Table 25: Sequence homology of the 18S rRNA gene of the fungal isolates from the Alexandria samples**

| Isolate | Size (bp) | Closely related fungi | Accession number | Homology(%) |
|---|---|---|---|---|
| **Alexandria1.5** | 491 | *Penicillium commune* | HM366606 | 99 |
| **Alexandria2.3** | 329 | *Talaromyces sp.* | GU973739 | 89 |
| **Alexandria3.1** | 543 | *Scedosporium apiospermum* | AJ888396 | 96 |
| **Alexandria3.3** | 520 | *Pseudallescheria ellipsoidea* | AJ888427 | 72 |
| **Alexandria4.1** | 624 | *Penicillium griseofulvum* | GQ305305 | 99 |
| **Alexandria4.4** | 1059 | *Talaromyces sp.* | DQ123599 | 99 |

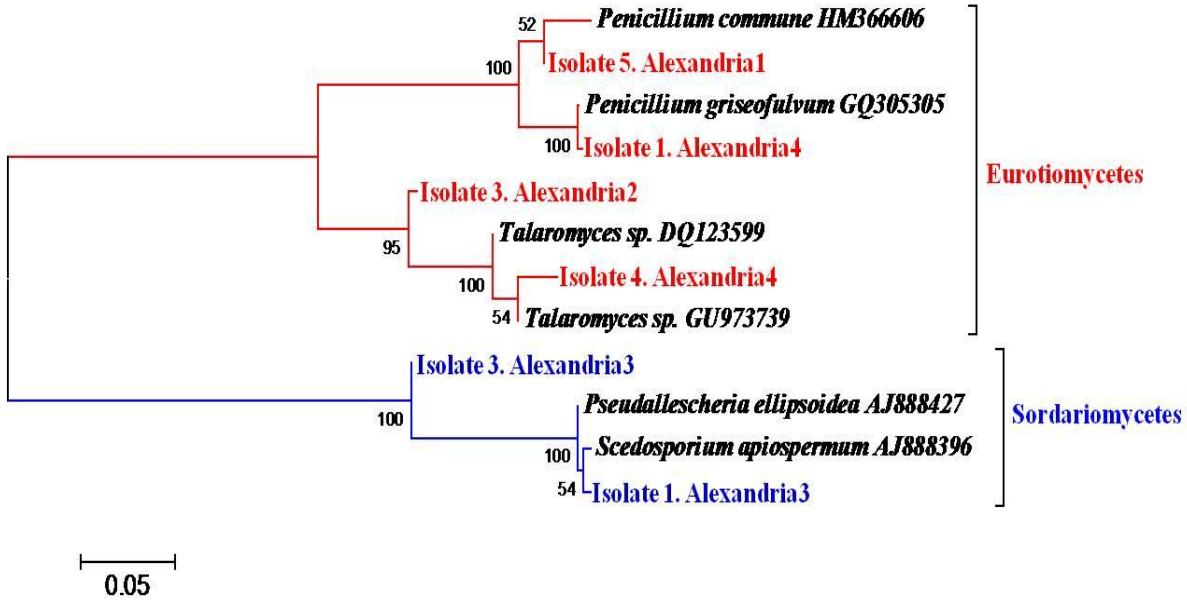


**Figure 27: Phylogeny of fungal isolates from the Alexandria samples that were able to grow on γ-HCH. Multiple alignments of the sequences corresponding to the 18S rRNA gene of the studied isolates were carried out followed by neighbor joining clustering. Bootstrap values expressed as percentages of 1000 replications. Bar represents 0.05 substitutions per nucleotide position.**

Similar to the bacterial community observed in the Monufia samples, it was found that this site is rich with strains of fungal genera such as *Aspergillus, Dichotomomyces, Eurotium, Mortierella, Paecilomyces, Penicillium, Talaromyces and Thielavia* (Table 26). It was revealed from the phylogenetic tree that most of the strains were members of Eurotiomycetes and the rest are members of Sordariomycetes or Zygomycetes (Figure 28).

**Table 26: Sequence homology of the 18S rRNA gene of the fungal isolates from the Monufia samples**

| Isolate | Size (bp) | Closely related fungi | Accession number | Homolgy (%) |
|---|---|---|---|---|
| **Monufia1.2** | 100 | *Penicillium chrysogenum* | EU664454 | 481 |
| **Monufia1.4** | 100 | *Penicillium commune* | FJ499454 | 508 |
| **Monufia1.5** | 96 | *Thielavia hyalocarpa* | EF192179 | 333 |
| **Monufia1.7** | 98 | *Aspergillus terreus* | AF078897 | 403 |
| **Monufia2.3** | 93 | *Penicillium pinophilum* | FJ515906 | 558 |
| **Monufia2.5** | 92 | *Dichotomomyces cejpii* | EF669956 | 379 |
| **Monufia2.8** | 97 | *Paecilomyces tenuis* | EU816415 | 499 |
| **Monufia2.9** | 99 | *Eurotium rubrum* | AF455528 | 500 |
| **Monufia3.1** | 99 | *Penicillium dipodomyicola* | AY371616 | 525 |
| **Monufia3.2** | 99 | *Penicillium dipodomyicola* | AY371616 | 527 |
| **Monufia3.3** | 66 | *Mortierella gamsii* | DQ093723 | 588 |
| **Monufia3.5** | 98 | *Talaromyces trachyspermus* | EU888919 | 539 |
| **Monufia3.6** | 95 | *Penicillium raperi* | AF033433 | 556 |
| **Monufia4.1** | 97 | *Talaromyces trachyspermus* | AB176609 | 539 |
| **Monufia4.2** | 98 | *Aspergillus terreus* | FJ037754 | 494 |
| **Monufia4.3** | 97 | *Eurotium rubrum* | HM145962 | 470 |
| **Monufia4.4** | 82 | *Talaromyces unicus* | AB176637 | 477 |
| **Monufia4.5** | 96 | *Aspergillus fumigatus* | HQ589141 | 327 |

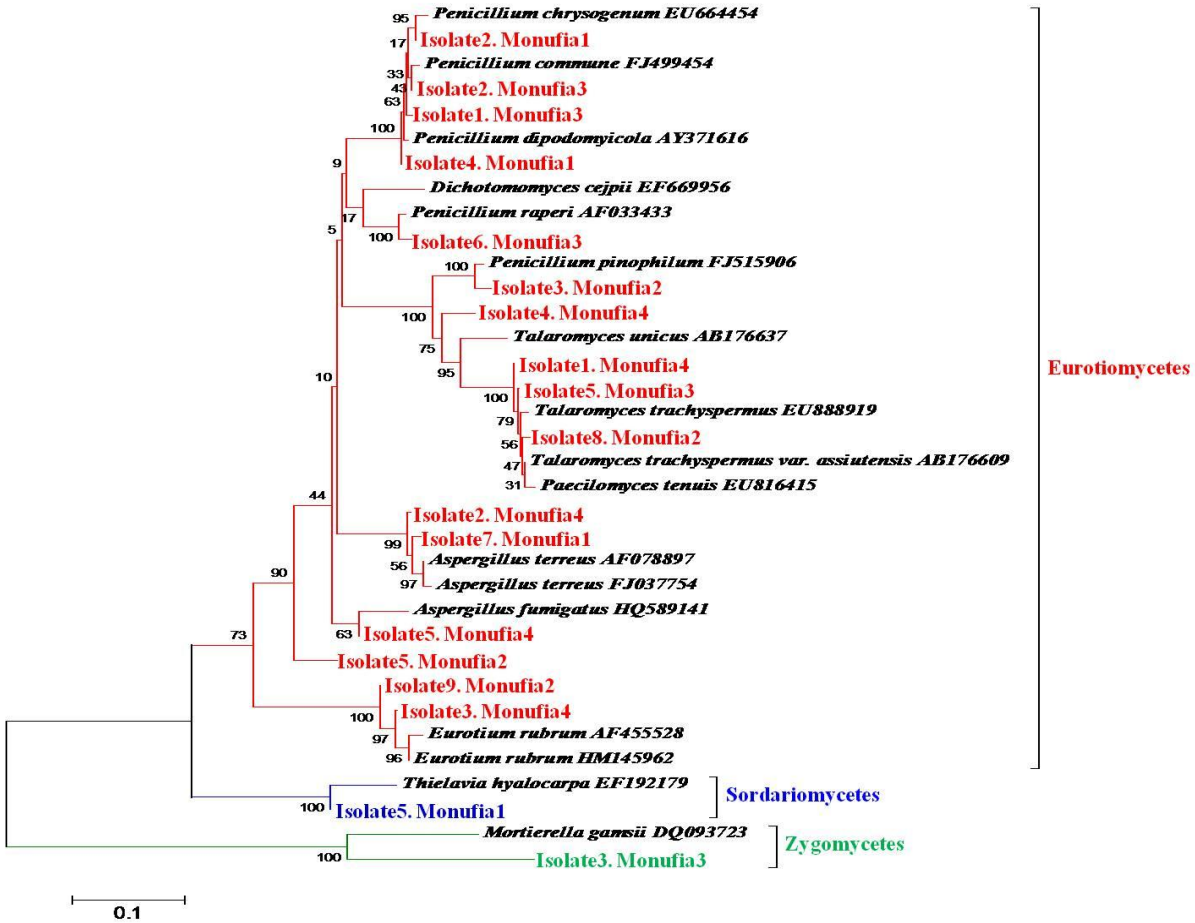


**Figure 28: Phylogeny of fungal isolates from the Monufia samples that were able to grow on γ-HCH. Multiple alignments of the sequences corresponding to the 18S rRNA gene of the studied isolates were carried out followed by neighbor joining clustering. Bootstrap values expressed as percentages of 1000 replications. Bar represents 0.1 substitutions per nucleotide position.**

The fungal community composition of the Gharbia site was that of the genera *Mortierella, Penicillium, Talaromyces* and *Zopfiella* (Table 27). These strains were members of the same classes as in the Mounifa samples. Two of the identified strains were members of the Eurotiomycetes. The other two strains were members of Sordariomycetes or Zygomycetes (Figure 29).

Only three fungal strains were found in the Kafr El-Sheikh sample. The community members were species of *Dichotomomyces, Gymnascella,* and *Pseudallescheria* (Table 28). Two of these strains belonged to the Eurotiomycetes class and the third one belonged to the class Sordariomycetes (Figure 30).

We found that the fungal community composition in the Qalyubia samples has a different composition of genera. The community was composed of fungal strains of the genera *Cylindrocarpon, Monascus, Paecilomyces, Penicillium, Pseudallescheria, Pycnidiophora,*

*Scedosporium*, *Talaromyces* and *Thielavia* (Table 29). The phylogenetic tree showed the involvement of a new class in the γ-HCH degradation because the majority of the identified strains were members of the Eurotiomycetes followed by Sordariomycetes and one strain of the class Dothideomycetes was detected (Figure 31).

**Table 27: Sequence homology of the 18S rRNA gene of the fungal isolates from the Gharbia sample**

| Isolate | Size (bp) | Closely related fungi | Accession number | Homology (%) |
|---|---|---|---|---|
| **2** | 569 | *Zopfiella latipes* | FJ175158 | 96 |
| **3** | 592 | *Penicillium griseofulvum* | GQ305305 | 97 |
| **5** | 724 | *Mortierella sp.* | AJ541798 | 96 |
| **9** | 1045 | *Talaromyces trachyspermus* | EU076917 | 99 |

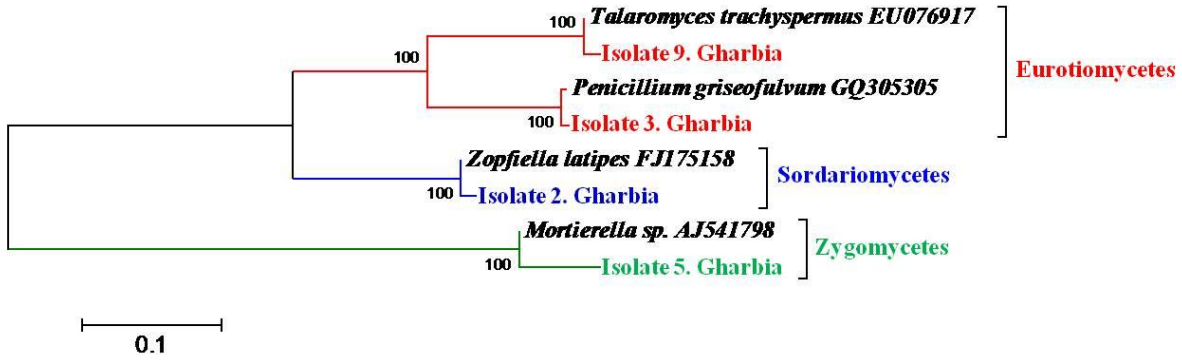


**Figure 29: Phylogeny of fungal isolates from the Gharbia sample that were able to grow on γ-HCH. Multiple alignments of the sequences corresponding to the 18S rRNA of the studied isolates were carried out followed by neighbor joining clustering. Bootstrap values expressed as percentages of 1000 replications. Bar represents 0.1 substitutions per nucleotide position.**

**Table 28: Sequence homology of the 18S rRNA gene of the fungal isolates from the Kafr El-Sheikh sample**

| Isolate | Size (bp) | Closely related fungi | Accession number | Homology (%) |
|---|---|---|---|---|
| **1** | 520 | *Dichotomomyces cejpii* | EF669956 | 96 |
| **2** | 501 | *Pseudallescheria boydii* | FJ713064 | 90 |
| **3** | 549 | *Gymnascella hyalinospora* | AF129853 | 98 |
| **4** | 533 | *Pseudallescheria boydii* | EU332872 | 100 |

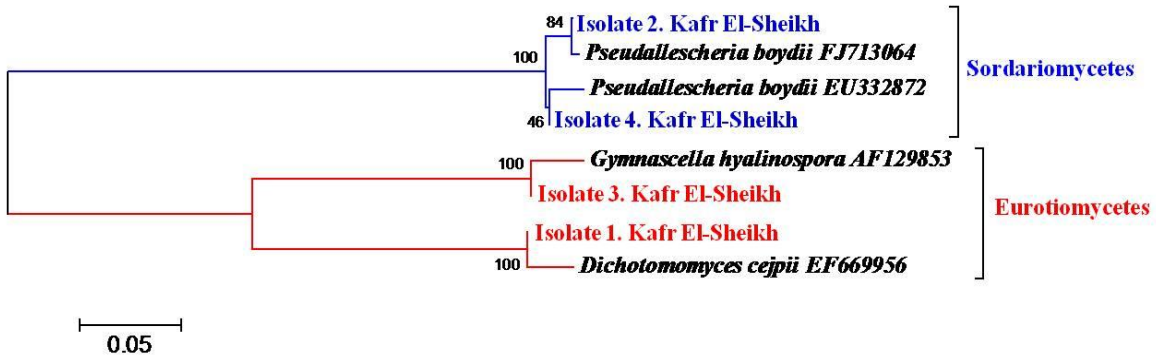


**Figure 30: Phylogeny of fungal isolates from the Kafr El-Sheikh sample that were able to grow on γ-HCH. Multiple alignments of the sequences corresponding to the 18S rRNA of the studied isolates were carried out followed by neighbor joining clustering. Bootstrap values expressed as percentages of 1000 replications. Bar represents 0.05 substitutions per nucleotide position.**

**Table 29: Sequence homology of the 18S rRNA gene of the fungal isolates from the Qalyubia sample**

| Isolate | Size (bp) | Closely related fungi | Accession number | Homology (%) |
|---|---|---|---|---|
| **Qalyubia1.1** | 571 | *Paecilomyces sp.* | AM262343 | 100 |
| **Qalyubia1.2** | 625 | *Penicillium griseofulvum* | GQ305305 | 99 |
| **Qalyubia1.3** | 619 | *Pseudallescheria boydii* | EU781833 | 99 |
| **Qalyubia1.4** | 605 | *Thielavia sp.* | EU620136 | 97 |
| **Qalyubia1.5** | 583 | *Pycnidiophora aurantiaca* | AY943057 | 99 |
| **Qalyubia1.7** | 591 | *Penicillium sp.* | GQ120993 | 98 |
| **Qalyubia1.8** | 627 | *Cylindrocarpon sp.* | EF601608 | 100 |
| **Qalyubia1.9** | 609 | *Thielavia sp.* | GU055740 | 90 |
| **Qalyubia1.10** | 620 | *Talaromyces helicus* | AF033396 | 90 |
| **Qalyubia1.12** | 654 | *Scedosporium apiospermum* | AB489081 | 99 |
| **Qalyubia1.13** | 620 | *Monascus ruber* | AY498572 | 100 |
| **Qalyubia1.15** | 601 | *Penicillium chrysogenum* | DQ249212 | 98 |
| **Qalyubia1.16** | 1033 | *Talaromyces sp.* | DQ123599 | 99 |
| **Qalyubia1.17** | 618 | *Talaromyces helicus* | AB176623 | 99 |
| **Qalyubia1.18** | 607 | *Penicillium sp.* | GU566279 | 98 |
| **Qalyubia2.1** | 656 | *Pseudallescheria boydii* | GU180097 | 100 |
| **Qalyubia2.4** | 1037 | *Paecilomyces tenuis* | EU004812 | 94 |

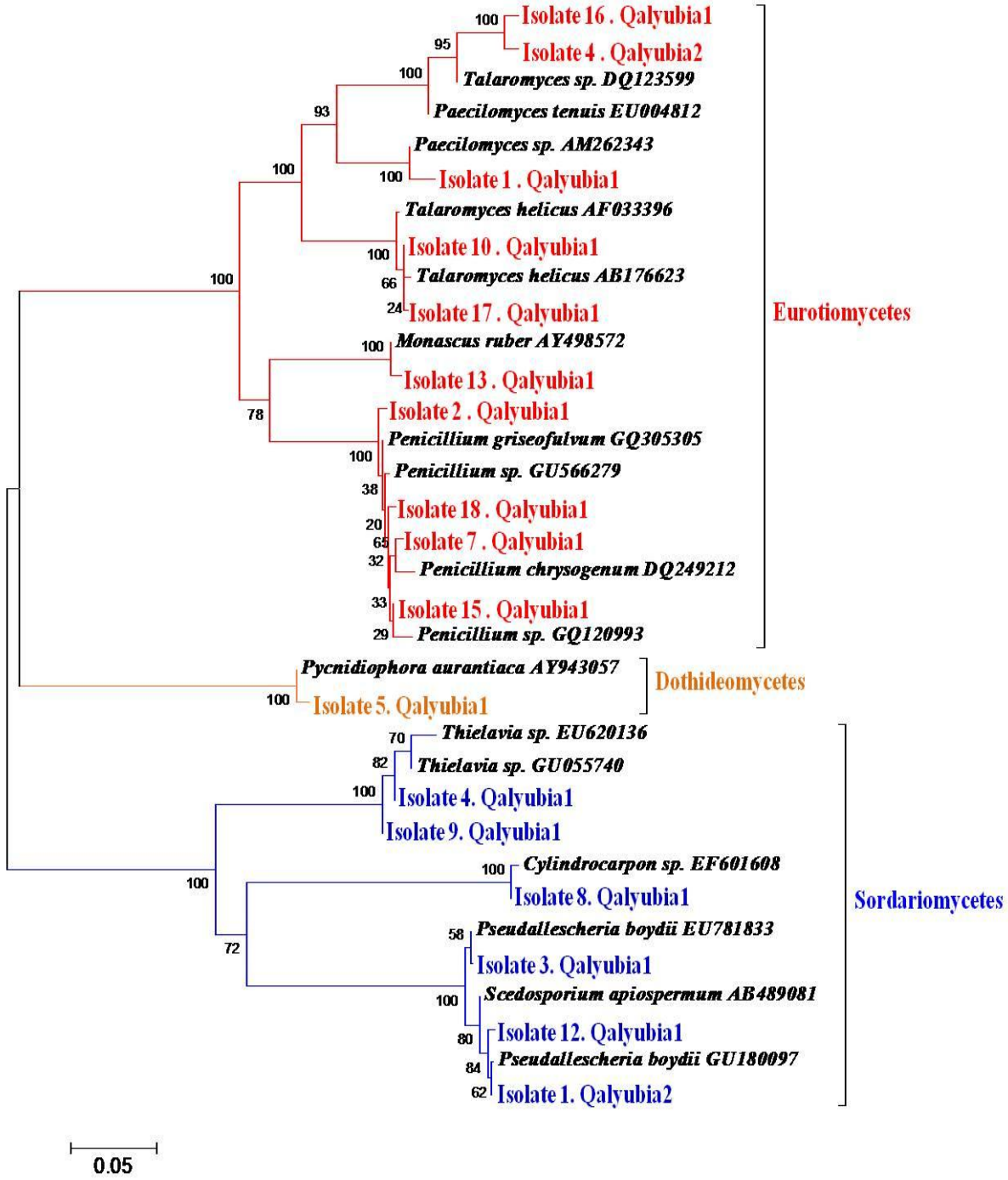


**Figure 31: Phylogeny of fungal isolates from the Qalyubia sample that were able to grow on γ-HCH. Multiple alignments of the sequences corresponding to the 18S rRNA of the studied isolates were carried out followed by neighbor joining clustering. Bootstrap values expressed as percentages of 1000 replications. Bar represents 0.05 substitutions per nucleotide position.**

### 4.1.2.2 Growth of the most tolerant fungal isolates on γ-HCH

The metabolization and degradation of γ-HCH and fungal growth was carried out for 30 days at 30°C in shaking flasks. The growth on γ-HCH was determined in the cultural filtrate every 3 days during the cultivation period.

It is clear from Figure 32 that, the growth of isolate10.Qalyubia1 and isolate9.Gharbia were at the maximum point after the 9$^{th}$ day of shake flasks cultivation. The growth of isolate1.Qalyubia2, isolate1.Kafr El-Sheikh and isolate2.Monufia1 gradually increased with increasing time up to the optimal point at the 12$^{th}$ day of incubation. The growth of isolate1.Alexandria4 was at the maximum point after the 15$^{th}$ day of cultivation. Then the growth of all isolates decreased gradually over time.

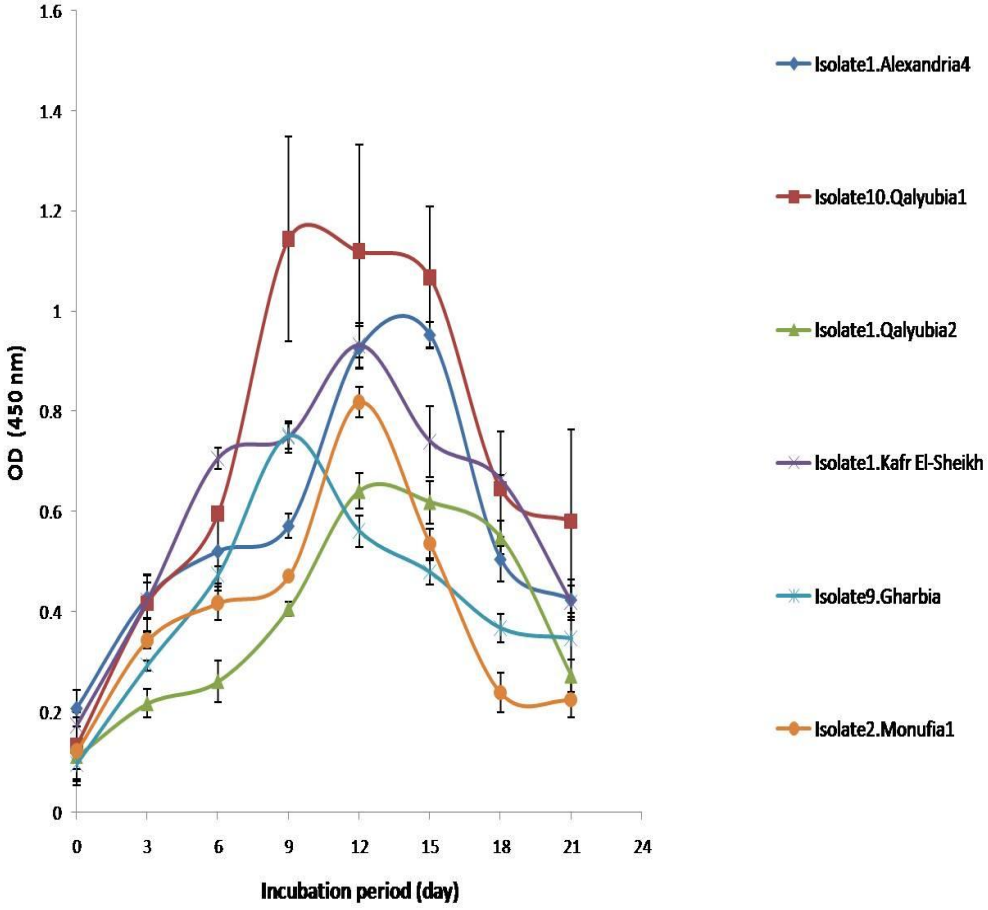


**Figure 32: Growth curves for the most capable fungal isolates to grow on γ-HCH. The strains isolated from several locations in Egypt were grown in basal DOX medium containing 2 mM γ-HCH. The growth was detected by the change in the absorbance at $\lambda_{max}$=450 nm.**

### 4.1.2.3 Analysis of fatty acids of the most tolerant fungal isolates grown on γ-HCH

From Figure 33 and Table 30, it was found that the major cellular fatty acids (>10 % of the total fatty acids) in the most abundant fungal isolates for γ-HCH were C16:0, C18:2ω6,9, and C18:1ω9.

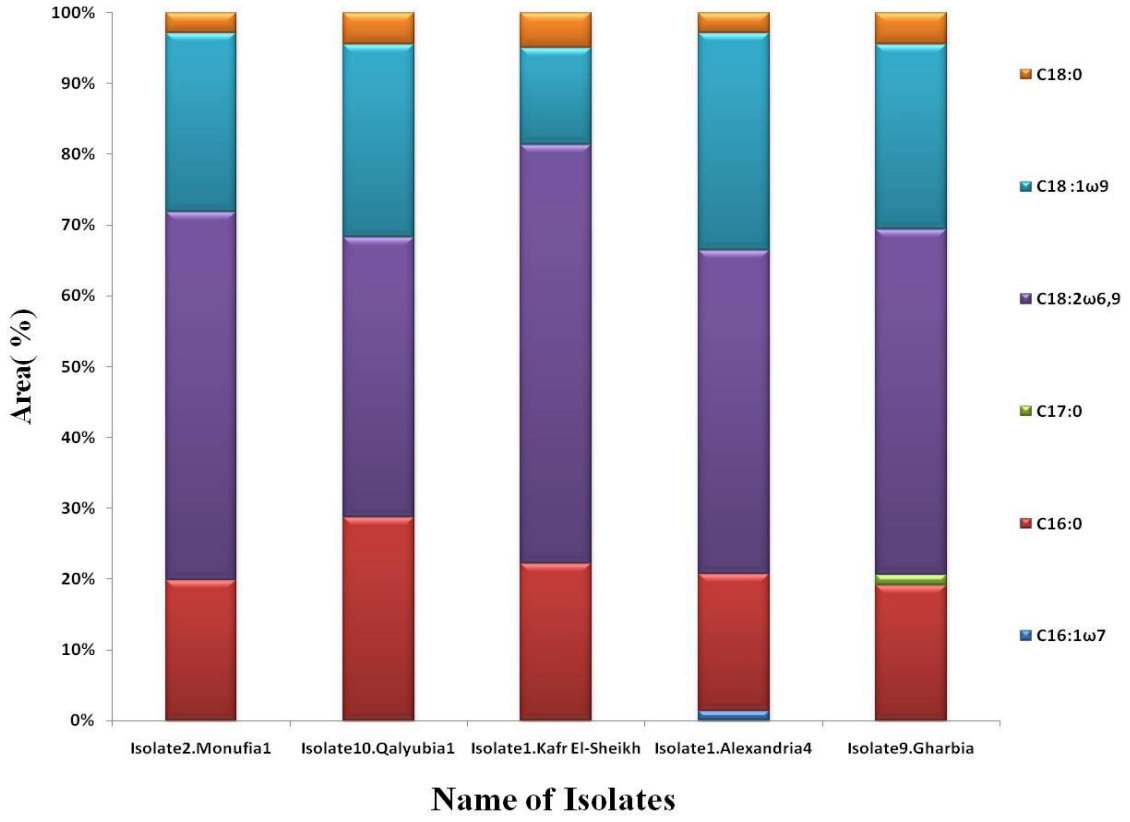


**Figure 33: Percentage of the extracted fatty acids from the most tolerant fungal isolates for γ-HCH.**

**Table 30: Major cellular fatty acids content (%) of the most tolerant fungal isolates for γ-HCH. Values are percentage of total fatty acids. -, Not detected.**

| Fatty acid | Isolate1. Alexandria4 | Isolate2. Monufia1 | Isolate1. Kafr el-Sheikh | Isolate10. Qalyubia1 | Isolate9. Gharbia |
|---|---|---|---|---|---|
| **Saturated fatty acids:** | | | | | |
| $C_{16:0}$ | 19.4 | 19.8 | 22.2 | 28.7 | 19.1 |
| $C_{17:0}$ | - | - | - | - | 1.5 |
| $C_{18:0}$ | 2.9 | 2.9 | 4.9 | 4.4 | 4.4 |
| **Monounsaturated fatty acids:** | | | | | |
| $C_{16:1\omega7}$ | 1.3 | - | - | - | - |
| $C_{18:2\omega6,9}$ | 45.7 | 52.1 | 59.2 | 39.6 | 48.8 |
| $C_{18:1\omega9}$ | 30.7 | 25.2 | 13.7 | 27.2 | 26.1 |

### 4.1.2.4 Analysis of fungal biofilm community composition developing on γ-HCH droplets

SSCP community profiling (Figure 34) showed highly distinct and diverse fungal communities. By comparing the sequences of 12 excised bands, 2 different operational taxonomic units (OTUs) could be identified which were closely related to: *Penicillium sp.* and *Penicillium expansum.*

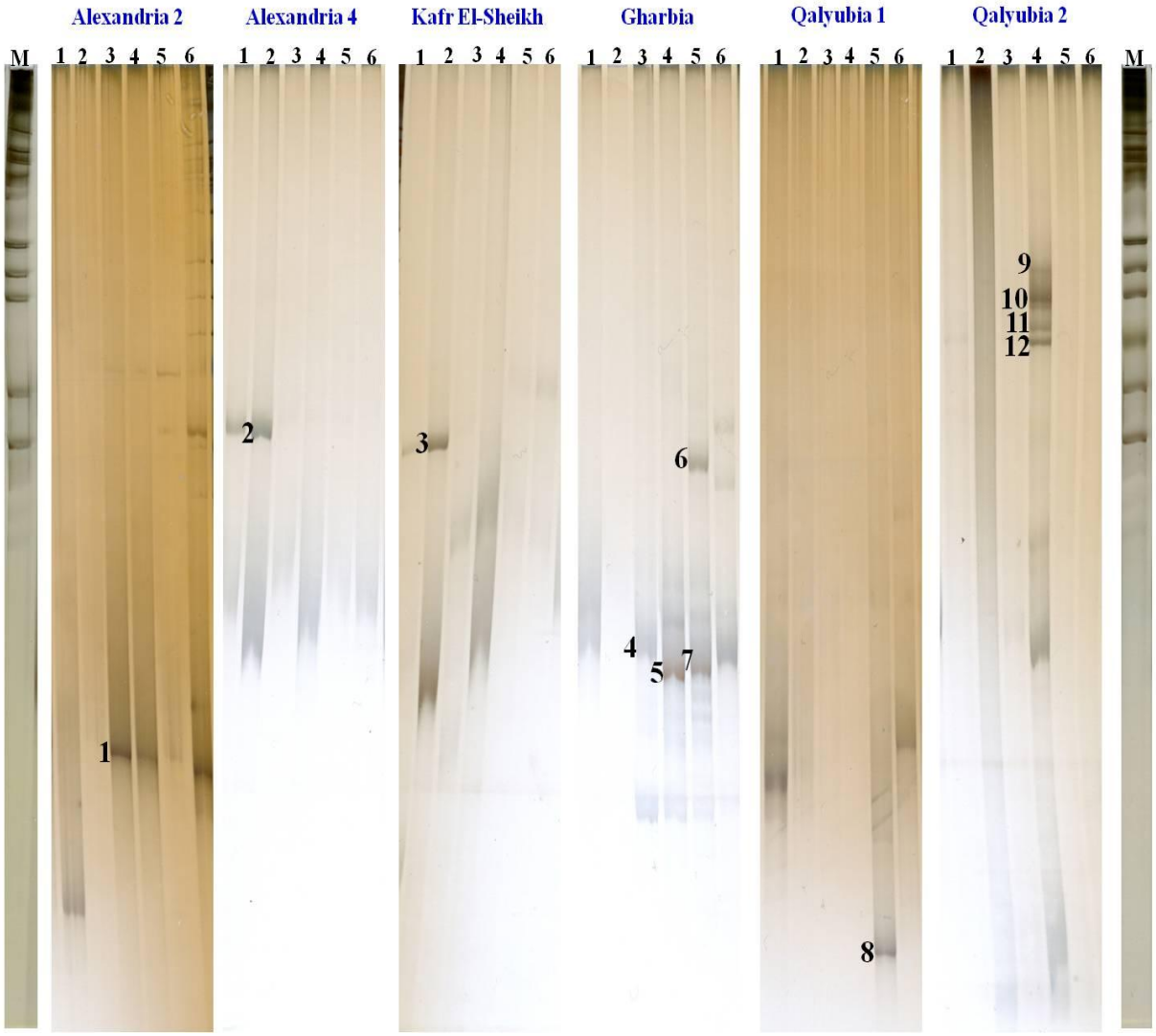


**Figure 34: Composition of γ-HCH fungal biofilm communities obtained from the Alexandria, Kafr El-Sheikh, Gharbia and the Qalyubia soil samples analysed by 18S rRNA gene based community fingerprint (SSCP). Numbers on top of the gel correspond to sampling time in weeks and M corresponds to the lane of the marker. Marked bands have been excised, sequenced and compared with sequences of described species.**

The following phylogenetic tree (Figure 35) presents the closest related genus from each sequence obtained. The identified OTUs were members of the class Eurotiomycetes.

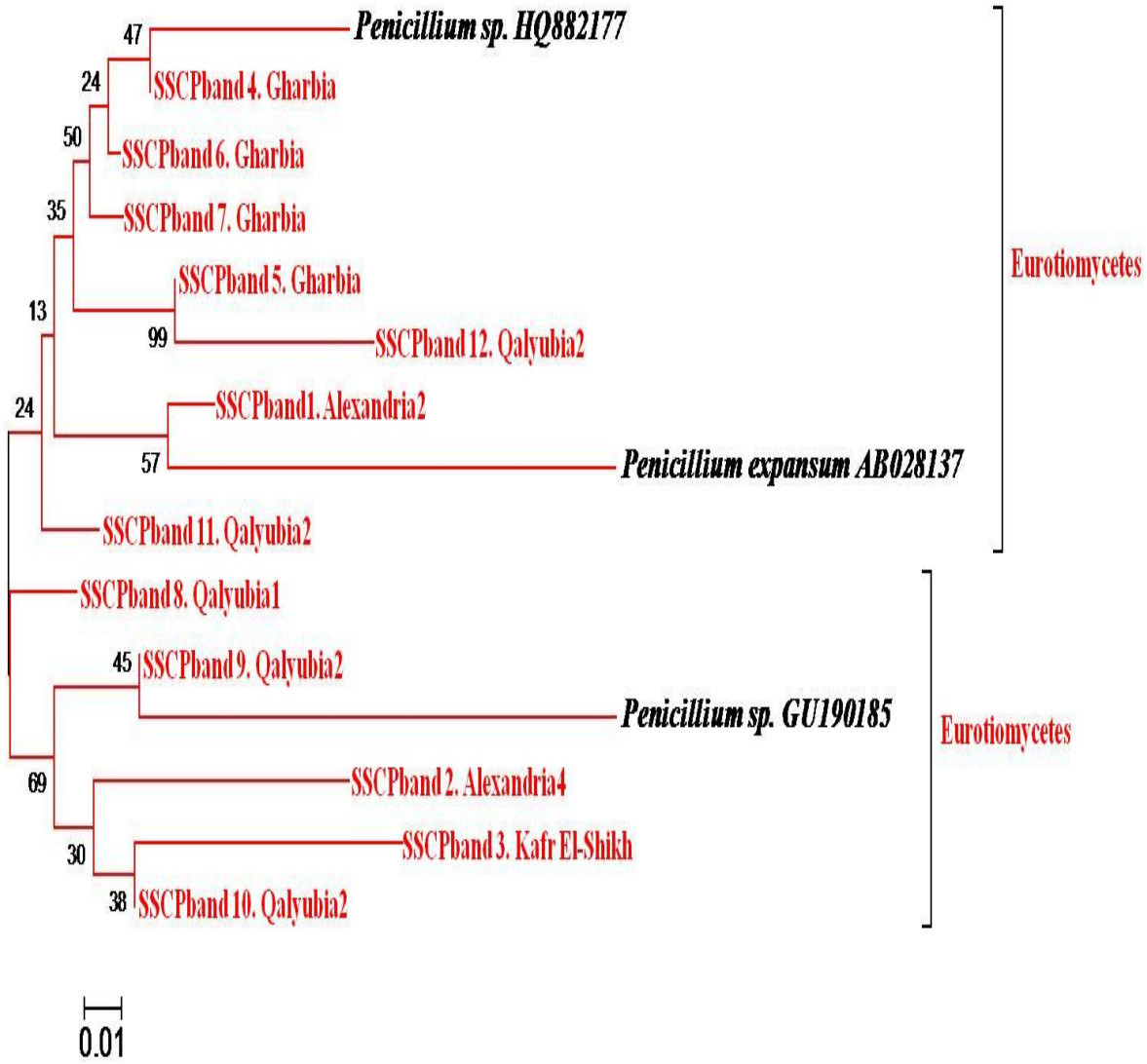


**Figure 35: Phylogenetic tree based on neighbor joining clustering after multiple alignment of the partial 18S rRNA gene sequences of the SSCP bands excised from γ-HCH droplet biofilms from the Alexandria, Kafr El-Sheikh, Gharbia and the Qalyubia samples. Bootstrap values expressed as percentages of 1000 replications. Bar represents 0.01 substitutions per nucleotide position.**

# 4.2 Phylogeny and characteristics of bacterial and fungal isolates from Egyptian localities that were able to grow on BDE

## 4.2.1 Bacteria

### 4.2.1.1 Phylogeny of bacterial isolates

The isolates of the Alexandria site were bacterial strains of the genera *Alcaligenes, Arthrobacter, Brevundimonas, Dokdonella, Isoptericola, Microbacterium, Nitratireductor, Promicromonospora, Pseudomonas, Pseudoxanthomonas and Sphingomonas.* They showed homologies towards the bacterial strains shown in Table 31. The diversity as well as the bacterial relationship is depicted in the phylogenetic tree (Figure 36). The majority of the identified strains were members of the Gammaproteobacteria followed by Alphaproteobacteria and Actinobacteria. Also one strain of the class Betaproteobacteria was isolated.

**Table 31: Sequence homology of the 16S rRNA gene of the bacterial isolates from the Alexandria samples**

| Isolate | Size (bp) | Closely related bacteria | Accession number | Homology (%) |
|---|---|---|---|---|
| **Alexanria1.1** | 1482 | *Promicromonospora sp.* | GU574151 | 99 |
| **Alexanria1.2** | 1509 | *Pseudomonas sp.* | DQ910404 | 99 |
| **Alexanria1.3** | 1499 | *Microbacterium sp.* | EU419939 | 99 |
| **Alexanria1.4** | 1365 | *Brevundimonas sp.* | EU584506 | 95 |
| **Alexanria1.5** | 1487 | *Alcaligenes faecalis* | EU075145 | 99 |
| **Alexanria2.1** | 1498 | *Arthrobacter oxydans* | EU086792 | 99 |
| **Alexanria2.2** | 1492 | *Arthrobacter sp.* | AF197051 | 99 |
| **Alexanria2.3** | 1492 | *Arthrobacter oxydans* | EU086792 | 99 |
| **Alexanria2.4** | 1514 | *Pseudoxanthomonas sp.* | AY576705 | 99 |
| **Alexanria2.5** | 1518 | *Pseudoxanthomonas mexicana* | AY124375 | 100 |
| **Alexanria3.1** | 1452 | *Sphingomonas sp.* | GU479372 | 100 |
| **Alexanria3.2** | 1509 | *Dokdonella koreensis* | EF589679 | 99 |
| **Alexanria3.3** | 1513 | *Dokdonella koreensis* | EF589679 | 99 |
| **Alexanria3.4** | 1457 | *Sphingopyxis sp.* | DQ413171 | 99 |
| **Alexanria3.5** | 1428 | *Brevundimonas sp.* | FJ529023 | 99 |
| **Alexanria3.6** | 1517 | *Stenotrophomonas acidaminiphila* | FJ544377 | 100 |
| **Alexanria4.1** | 1489 | *Isoptericola sp.* | EU910875 | 99 |
| **Alexanria4.2** | 1601 | *Nitratireductor sp.* | DQ659453 | 98 |

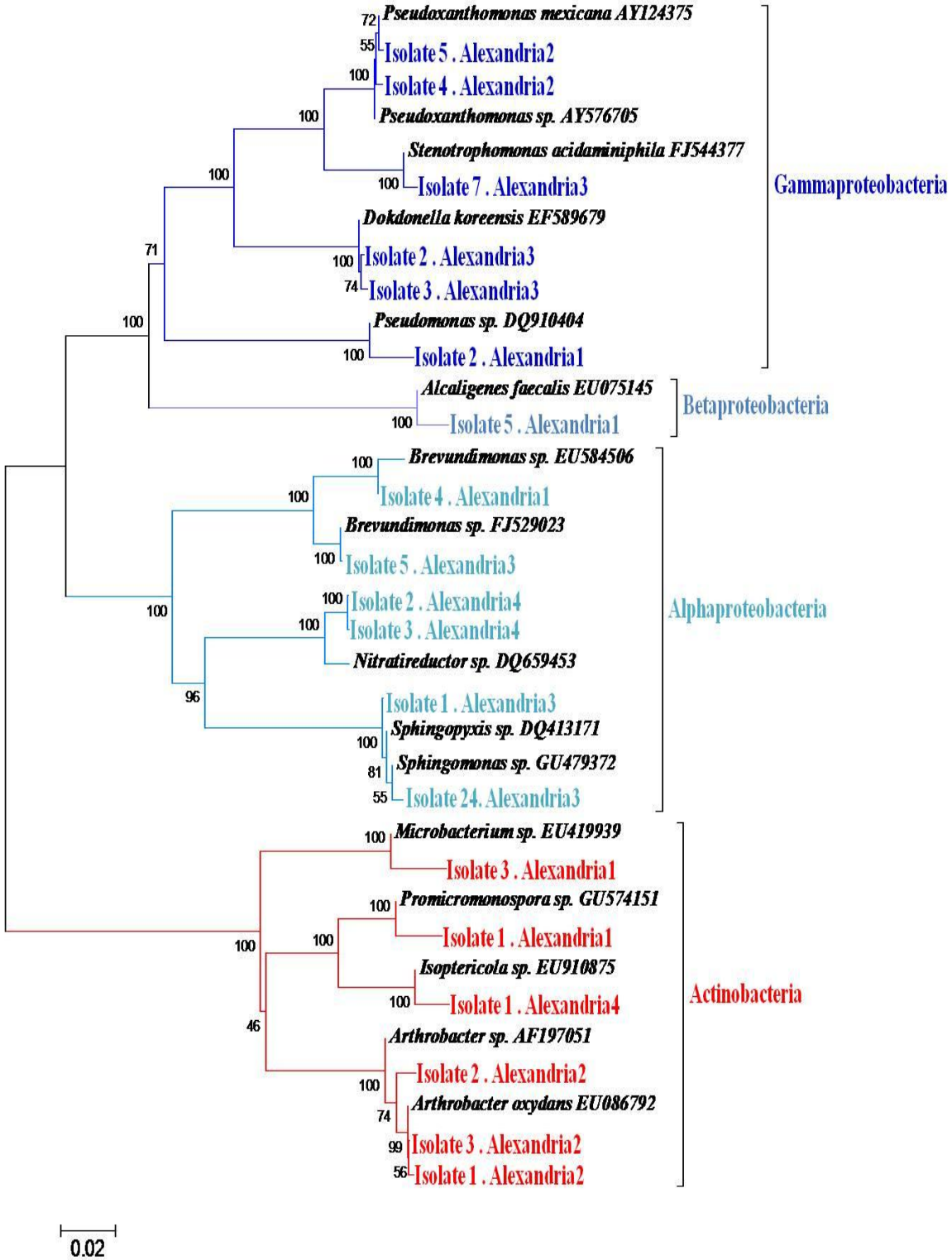


**Figure 36: Phylogeny of bacterial isolates from the Alexandria samples that were able to grow on BDE. Multiple alignments of the sequences corresponding to the 16S rRNA of the studied isolates were carried out followed by neighbor joining clustering. Bootstrap values expressed as percentages of 1000 replications. Bar represents 2% sequence dissimilarity.**

In the Monufia site, the community was composed mainly of bacterial strains of the genera *Agrococcus, Bacillus, Alcaligenes, Castellaniella, Devosia, Dokdonella, Ensifer, Frateuria, Gordonia, Micromonospora, Paenibacillus, Pseudaminobacter, Pusillimonas, Rhodanobacter, Rhodococcus Staphylococcus, and Thauera* (Table 32). The phylogenetic tree showed that the majority of the isolates were members of Firmicutes and Actinobacteria followed by Gammaproteobacteria, Betaproteobacteria and Alphaproteobacteria (Figure 37).

**Table 32: Sequence homology of the 16S rRNA gene of the bacterial isolates from the Monufia samples**

| Isolate | Size (bp) | Closely related bacteria | Accession number | Homology (%) |
|---|---|---|---|---|
| **Monufia1.1** | 1494 | *Rhodococcus sp.* | AF103733 | 99 |
| **Monufia1.2** | 1512 | *Paenibacillus turicensis* | AF378697 | 94 |
| **Monufia1.3** | 1508 | *Thauera sp.* | EF205257 | 88 |
| **Monufia1.4** | 1501 | *Agromyces sp.* | AF479332 | 98 |
| **Monufia1.5** | 1499 | *Paenibacillus chinjuensis* | AF164345 | 94 |
| **Monufia1.6** | 1503 | *Agromyces neolithicus* | AY507128 | 97 |
| **Monufia1.7** | 1485 | *Rhodococcus sp.* | GQ174491 | 99 |
| **Monufia1.8** | 1485 | *Micromonospora pattaloongensis* | EU274359 | 99 |
| **Monufia1.9** | 1507 | *Dokdonella sp.* | EU685334 | 98 |
| **Monufia1.10** | 1499 | *Agrococcus sp.* | EU374908 | 94 |
| **Monufia1.11** | 1520 | *Paenibacillus amylolyticus* | AM062689 | 98 |
| **Monufia1.13** | 1446 | *Ensifer meliloti* | EU849576 | 99 |
| **Monufia1.14** | 1491 | *Rhodococcus sp.* | GQ174491 | 80 |
| **Monufia1.15** | 1510 | *Streptomyces clavuligerus* | EU146061 | 98 |
| **Monufia2.1** | 1491 | *Alcaligenes sp.* | FJ984330 | 99 |
| **Monufia2.2** | 1507 | *Bacillus sp.* | GQ302985 | 99 |
| **Monufia2.3** | 2180 | *Frateuria sp.* | AY495959 | 72 |
| **Monufia2.4** | 1503 | *Rhodanobacter lindaniclasticus* | AB245366 | 99 |
| **Monufia2.5** | 1969 | *Castellaniella sp.* | AF150694 | 97 |
| **Monufia2.6** | 2003 | *Bacillus sp.* | GQ302985 | 99 |
| **Monufia3.1** | 1457 | *Devosia sp.* | EF540511 | 95 |
| **Monufia3.2** | 2013 | *Bacillus niacini* | FJ772024 | 99 |
| **Monufia3.3** | 1490 | *Rhodococcus sp.* | AB376627 | 76 |
| **Monufia3.4** | 1487 | *Rhodococcus sp.* | AB376627 | 99 |
| **Monufia3.5** | 1987 | *Pusillimonas terrae* | DQ466075 | 98 |
| **Monufia3.6** | 2021 | *Bacillus sp.* | AM411969 | 99 |
| **Monufia3.7** | 1516 | *Bacillus firmus* | EF032672 | 98 |
| **Monufia3.8** | 1670 | *Rhodococcus equi* | AJ272473 | 94 |
| **Monufia3.9** | 1457 | *Pseudaminobacter defluvii* | D32248 | 98 |
| **Monufia3.10** | 1522 | *Bacillus firmus* | EF032672 | 99 |
| **Monufia3.11** | 1489 | *Rhodococcus sp.* | AF103733 | 99 |
| **Monufia3.12** | 1511 | *Paenibacillus sp.* | AJ345018 | 98 |
| **Monufia4.1** | 1514 | *Staphylococcus epidermidis* | HM058991 | 100 |
| **Monufia4.2** | 1490 | *Gordonia amicalis* | GQ848235 | 100 |
| **Monufia4.3** | 1518 | *Rhodanobacter sp.* | FN430654 | 99 |

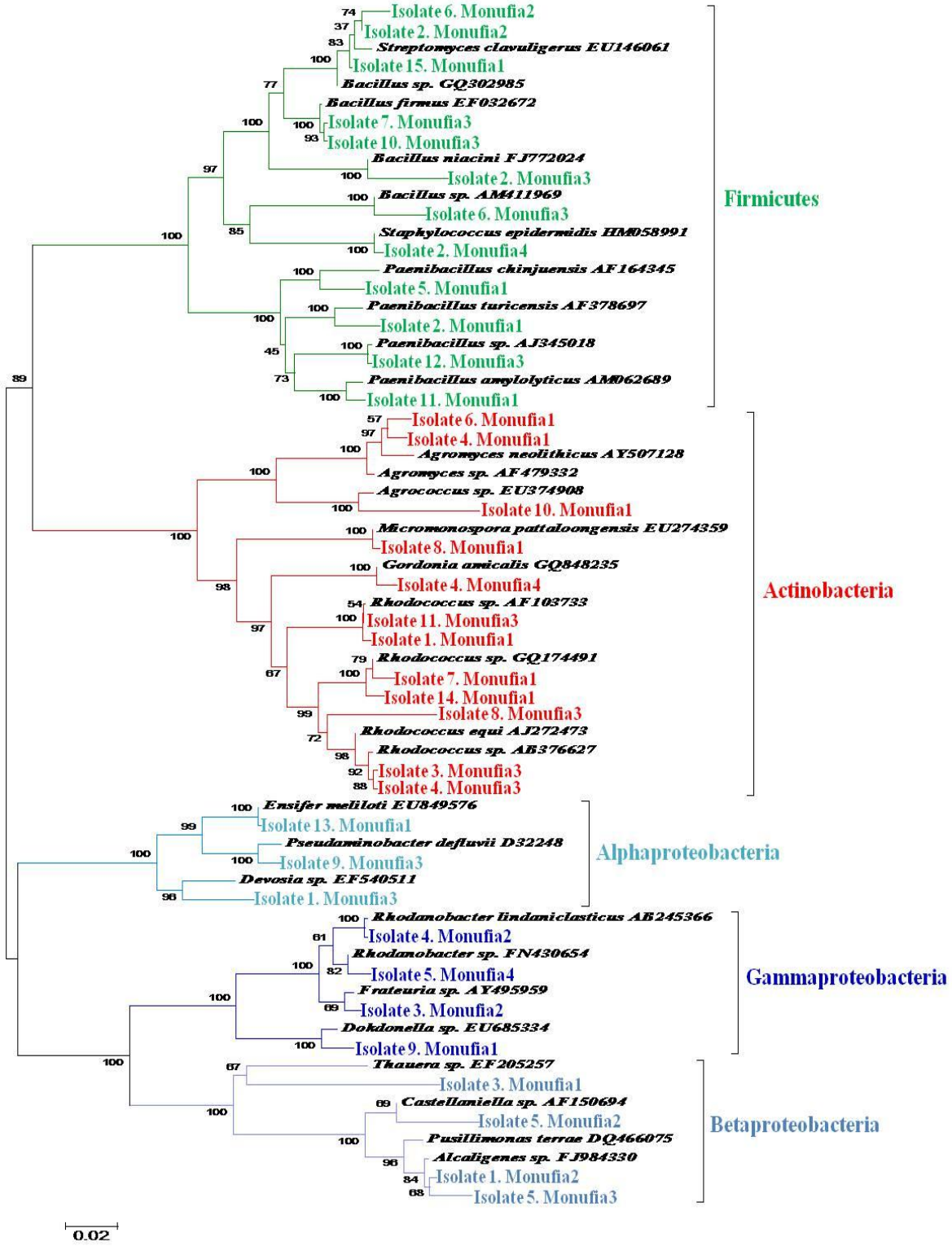


**Figure 37: Phylogeny of bacterial isolates from the Monufia samples that were able to grow on BDE. Multiple alignments of the sequences corresponding to the 16S rRNA of the studied isolates were carried out followed by neighbor joining clustering. Bootstrap values expressed as percentages of 1000 replications. Bar represents 2% sequence dissimilarity.**

The community at the Gharbia or Kafr El-Sheikh sites was poor and composed of bacterial strains of the genera *Aquamicrobium, Nocardia, and Rhodococcus* (Table 33) or *Luteimonas, and Rhodococcus* (Table 34), respectively. The phylogenetic tree depicted that the bacterial strains were members of Actinobacteria, Alphaproteobacteria and Gammaproteobacteria (Figure 38 and Figure 39).

At the Qalyubia site most of the members in the community were found to be similar to the Alexandia site for example the genera *Bacillus, Brucella, Castellaniella, Frateuria, Ochrobactrum, andRhodanobacter* (Table 35). These strains belonged to the Gammaproteobacteria, Betaproteobacteria, Alphaproteobacteria and Firmicutes.

**Table 33: Sequence homology of the 16S rRNA gene of the bacterial isolates from the Gharbia sample**

| Isolate | Size (bp) | Closely related bacteria | Accession number | Homology (%) |
|---|---|---|---|---|
| **1** | 1490 | *Nocardia sp.* | EF538720 | 100 |
| **2** | 1489 | *Rhodococcus erythropolis* | AM905947 | 100 |
| **3** | 1454 | *Aquamicrobium sp.* | FM210786 | 97 |

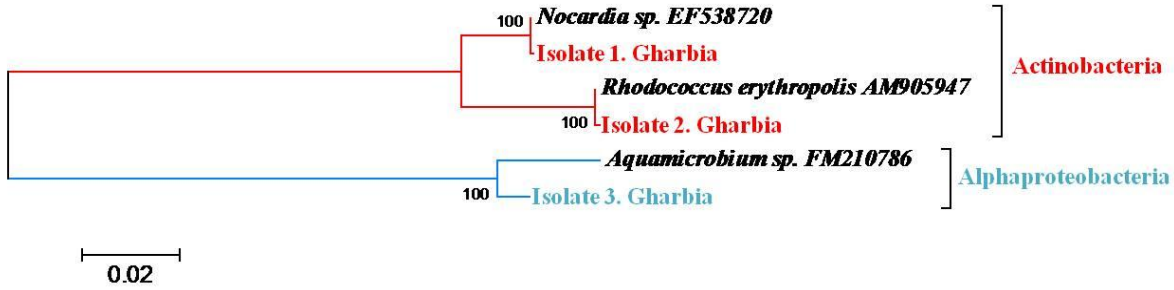


**Figure 38: Phylogeny of bacterial isolates from the Gharbia sample that were able to grow on BDE. Multiple alignments of the sequences corresponding to the 16S rRNA of the studied isolates were carried out followed by neighbor joining clustering. Bootstrap values expressed as percentages of 1000 replications. Bar represents 2% sequence dissimilarity.**

**Table 34: Sequence homology of the 16S rRNA gene of the bacterial isolates from the Kafr El-Sheikh sample**

| Isolate | Size (bp) | Closely related bacteria | Accession number | Homology (%) |
|---|---|---|---|---|
| **1** | 1481 | *Rhodococcus erythropolis.* | AP008957 | 99 |
| **2** | 1521 | *Luteimonas mephitis.* | NR_025304 | 99 |
| **3** | 1613 | *Luteimonas mephitis.* | NR_025304 | 84 |

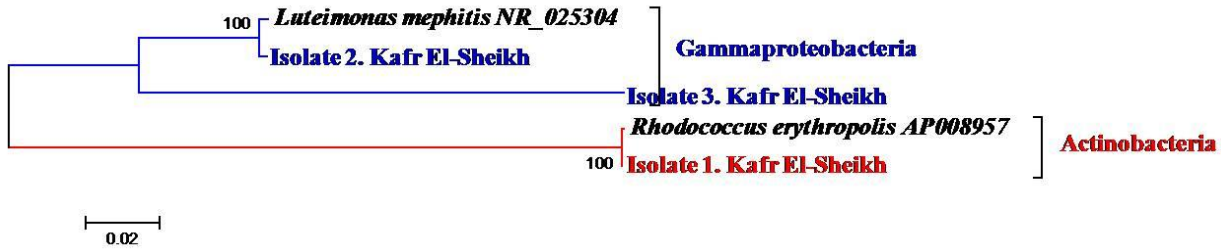


**Figure 39: Phylogeny of bacterial isolates from the Kafr El-Sheikh sample that were able to grow on BDE. Multiple alignments of the sequences corresponding to the 16S rRNA of the studied isolates were carried out followed by neighbor joining clustering. Bootstrap values expressed as percentages of 1000 replications. Bar represents 2% sequence dissimilarity.**

**Table 35: Sequence homology of the 16S rRNA gene of the bacterial isolates from the Qalyubia sample**

| Isolate | Size (bp) | Closely related bacteria | Accession number | Homology (%) |
|---|---|---|---|---|
| **Qalyubia1.2** | 1518 | *Castellaniella ginsengisoli* | EU873313 | 98 |
| **Qalyubia1.3** | 1514 | *Castellaniella sp.* | EF175377 | 98 |
| **Qalyubia1.4** | 1518 | *Bacillus sp.* | AM411965 | 99 |
| **Qalyubia1.5** | 1520 | *Bacillus sp.* | AM411965 | 99 |
| **Qalyubia1.6** | 2202 | *Frateuria sp.* | AY495959 | 72 |
| **Qalyubia1.7** | 1990 | *Rhodanobacter sp.* | FJ851443 | 98 |
| **Qalyubia1.8** | 1505 | *Rhodanobacter lindaniclasticus* | AB245366 | 99 |
| **Qalyubia 2.1** | 597 | *Ochrobactrum sp.* | EF219049 | 97 |

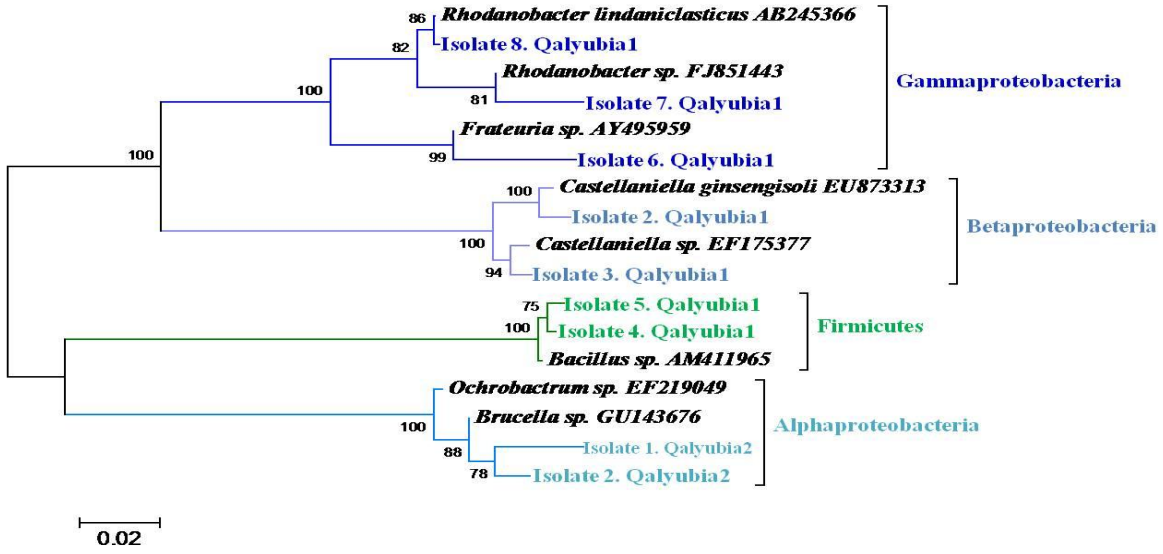


**Figure 40: Phylogeny of bacterial isolates from Qalyubia sample that were able to grow on BDE. Multiple alignments of the sequences corresponding to the 16S rRNA of the studied isolates were carried out followed by neighbor joining clustering. Bootstrap values expressed as percentages of 1000 replications. Bar represents 2% sequence dissimilarity.**

### 4.2.1.2 Growth of the most tolerant bacterial isolates on BDE

The metabolization and degradation of BDE and bacterial growth was carried out for 15 days at 30°C in shaking flasks. The degradation activity of BDE was determined in the cultural filtrate every day during the cultivation period.

It is clear from Figure 41 that, the growth of isolate8.Qalyubia1 was at the maximum point after the 2nd day of shake flasks cultivation. The growth of isolate2.Monufia2 was at the maximum point after the 4th day of cultivation. The growth of isolate1.Gharbia, and isolate1.Kafr El-Sheikh gradually increased with increasing time up to the optimal point the 6th day of incubation. The growth of isolate5.Alexandria3 was at the maximum point after the 7th day of cultivation. Then the growth of all isolates decreased gradually over time.

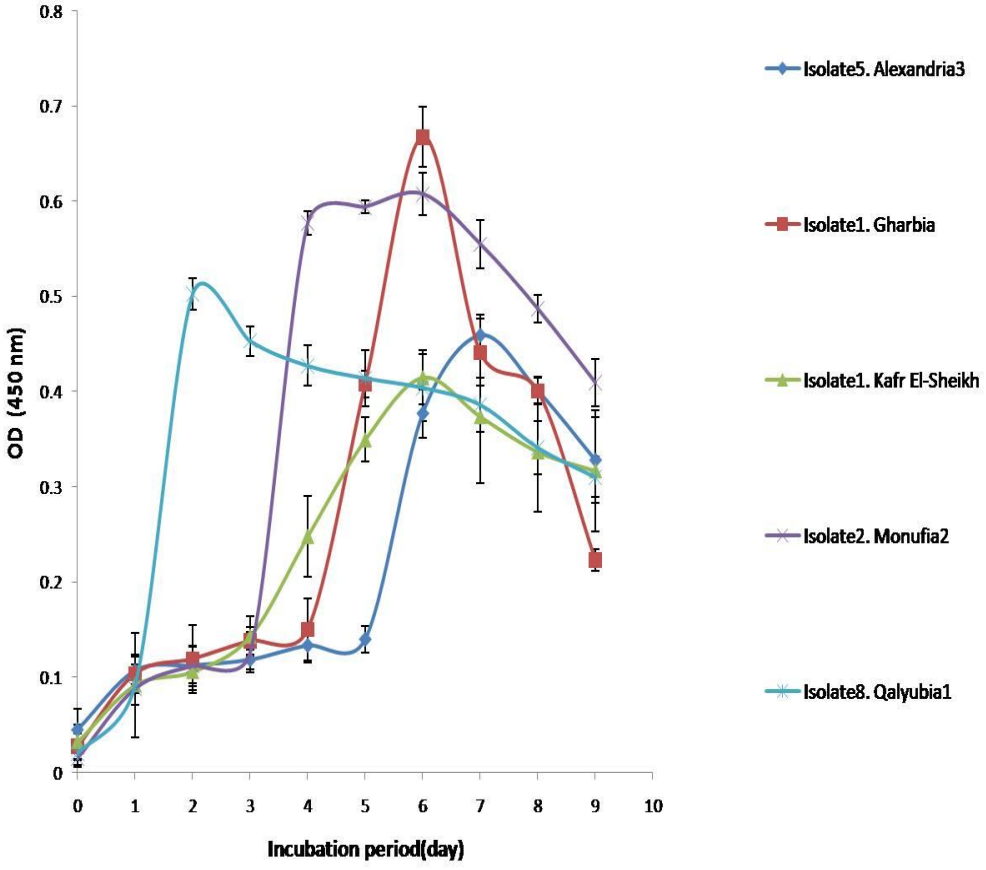


**Figure 41: Growth curves for the most capable bacterial isolates to grow on BDE. The strains isolated from several locations in Egypt were grown in M269 medium containing 2mM BDE. The growth was detected by the change in the absorbance at $\lambda_{max}$=450 nm.**

### 4.2.1.3 Analysis of fatty acids of the most active bacterial isolates grown on BDE

From Figure 42 and Table 36 it could be seen that the major cellular fatty acids (>10 % of the total fatty acids) in the best BDE-degrading bacterial isolates were C16:0, 10Me- C18:0, C18:1ω9, and C16:1ω7 in Isolate1.Gharbia, 10Me- C18:0, C16:0, and C16:1ω7 in Isolate1.Kafr El-Sheikh, iso-C15:0, C20:1ω9, and anteiso-C15:0 in Isolate2.Monufia2 and C18:1ω12, C19:0, and C18:0 in Isolate5.Alexandria3. In Isolate8.Qalyubia1, the major cellular fatty acid was anteiso-C15:0.

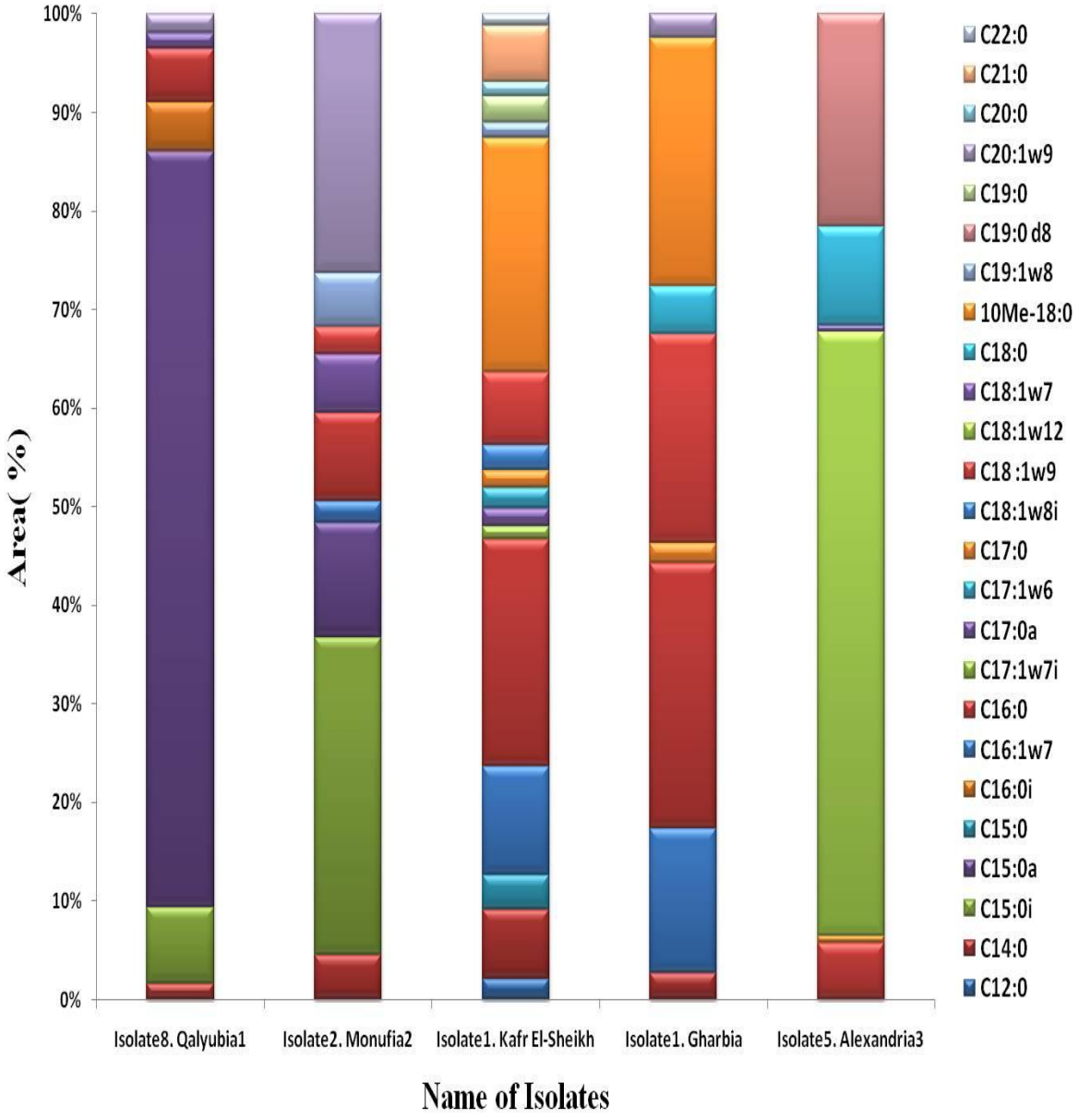


**Figure 42: Percentage of the extracted fatty acids from the best BDE degrading bacterial isolates.**

**Table 36: Major cellular fatty acids content (%) of the best BDR degrading bacterial isolates. Values are percentage of total fatty acids. -, not detected.**

| Fatty acid | Isolate8. Qalyubia1 | Isolate2. Monufia2 | Isolate1. Kafr el-Sheikh | Isolate1. Gharbia | Isolate1. Alexandria3 |
|---|---|---|---|---|---|
| **Saturated fatty acids:** | | | | | |
| $C_{12:0}$ | - | - | 2.1 | - | - |
| $C_{14:0}$ | 1.7 | 4.6 | 7 | 2.7 | - |
| $C_{15:0}$ | - | - | 3.5 | - | - |
| $C_{16:0}$ | 5.5 | 8.9 | 23 | 26.9 | 5.7 |
| $C_{17:0}$ | - | - | 1.7 | 2 | 0.8 |
| $C_{18:0}$ | - | - | - | 5 | 10.1 |
| $C_{19:0}$ | - | - | 2.7 | - | 21.5 |
| $C_{20:0}$ | - | - | 1.5 | - | - |
| $C_{21:0}$ | - | - | 5.8 | - | - |
| $C_{22:0}$ | - | - | 1.2 | - | - |
| **Branched fatty acids:** | | | | | |
| iso-$C_{15:0}$ | 7.7 | 32.1 | - | - | - |
| anteiso- $C_{15:0}$ | 76.7 | 11.7 | - | - | - |
| iso-$C_{16:0}$ | 5 | - | - | - | - |
| anteiso- $C_{17:0}$ | 1.6 | 6 | 1.8 | - | - |
| 10Me- $C_{18:0}$ | - | - | 32.8 | 25.1 | - |
| **Monounsaturated fatty acids:** | | | | | |
| $C_{16:1\omega7}$ | - | 2.2 | 11 | 14.7 | - |
| iso- $C_{17:1\omega7}$ | - | - | 1.3 | - | - |
| $C_{17:1\omega6}$ | - | - | 2.1 | - | - |
| $C_{18:1\omega12}$ | - | - | - | - | 61.2 |
| $C_{18:1\omega9}$ | - | 2.8 | 7.4 | 21.2 | - |
| iso-$C_{18:1\omega8}$ | - | - | 2.5 | - | - |
| $C_{18:1\omega8}$ | - | 5.4 | - | - | - |
| $C_{18:1\omega7}$ | - | - | - | - | 0.7 |
| $C_{19:1\omega8}$ | - | - | 1.5 | - | - |
| $C_{20:1\omega9}$ | 1.9 | 26.3 | - | 2.4 | - |

#### 4.2.1.4 Analysis of bacterial biofilm community composition developing on BDE droplets

Biofilms developing on the BDE droplets were set up as in γ-HCH. The biofilm community was analyzed by SSCP. The Alexandria sample (Figure 43) showed a huge bacterial diversity where 26 different OTUs from 31 excised bands were identified and closely related to *Aquabacterium sp., Pseudonocardia sp., Methyloversatilis sp., Hydrogenophaga sp., Methylibium sp., Halomonas desiderata, Thalassobaculum sp., Caulobacter sp., Aeromicrobium sp., Pseudomonas sp., Limnobacter sp., Sphingopyxis sp., Brevundimonas sp., Acidovorax sp., Hyphomicrobium sp., Pseudomonas fluorescens, Haliea sp., Parvibaculum sp., Crenothrix polyspora, Thioploca sp., Rhodoferax sp., Denitratisoma sp., Oleomonas sp., Phenylobacterium sp., Lentzea sp., and Klebsiella oxytoca* (Table 37).

Figure 44 and Figure 45 show the phylogenetic trees identifying the majority of the identified OTUs as members of the class Alphaproteobacteria followed by Betaproteobacteria, Gammaproteobacteria and Actinobacteria.

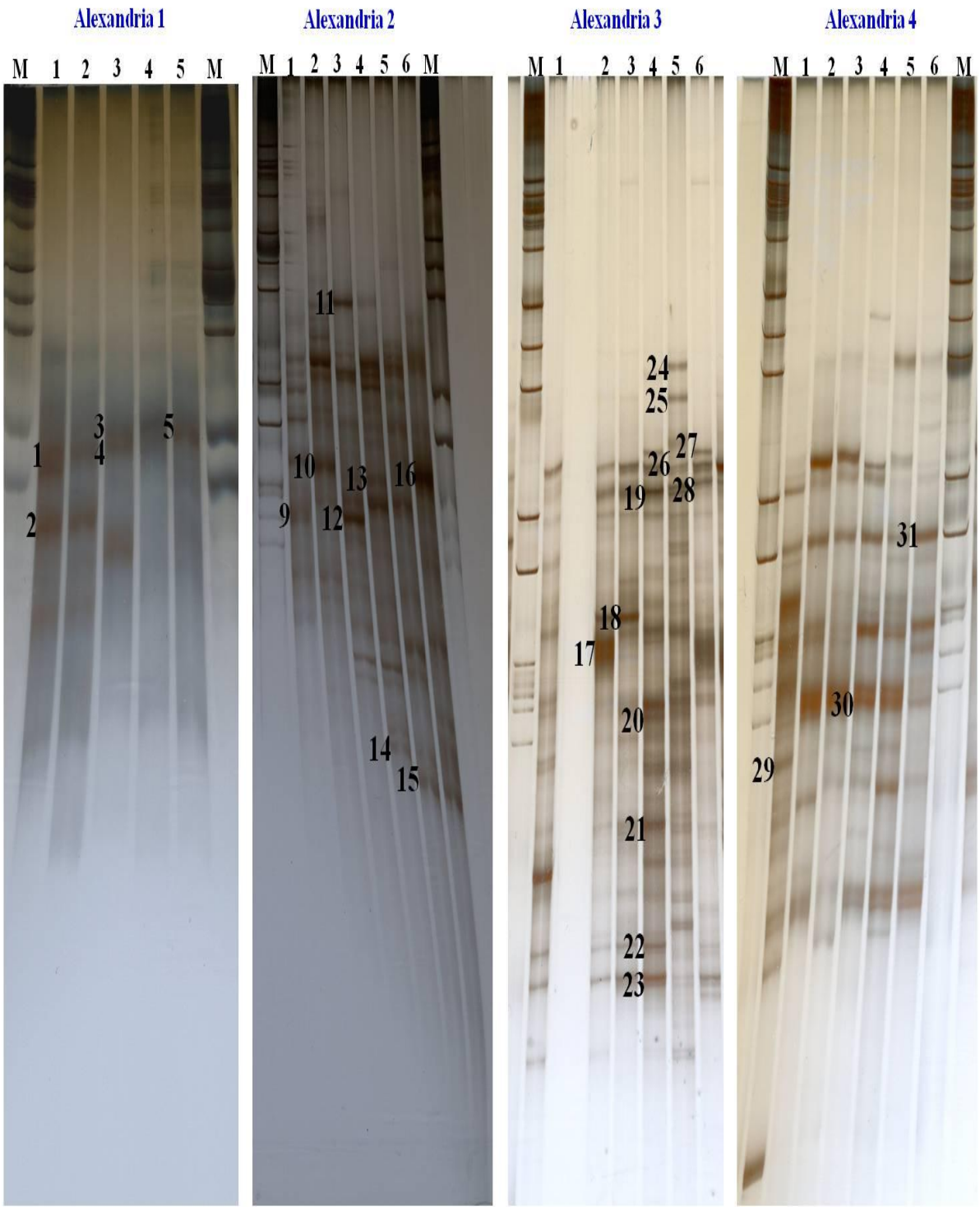


**Figure 43: SSCP fingerprints of PCR products of partial 16S rRNA gene amplicons of DNA extracted from BDE biofilm of the Alexandria samples. Numbers on top of the gel correspond to sampling time in weeks and M corresponds to the lane of the marker. Marked bands have been excised, sequenced and compared with sequences of described species (Table 37).**

**Table 37: Phylogenetic assignment of sequences of prominent bands visualized on SSCP gel profiles of bacterial biofilm communities from the Alexandria samples**

| SSCP bands | Size (bp) | Cultured closest match | Accession number | Identity (%) |
|---|---|---|---|---|
| **Alexandria1.1** | 407 | *Aquabacterium sp.* | HQ178858 | 98 |
| **Alexandria 1.2** | 412 | *Pseudonocardia sp.* | JF049435 | 98 |
| **Alexandria 1.3** | 364 | *Methyloversatilis sp.* | HQ682050 | 98 |
| **Alexandria 1.4** | 384 | *Hydrogenophaga sp.* | AM950239 | 97 |
| **Alexandria 1.5** | 340 | *Methylibium sp.* | GQ453183 | 98 |
| **Alexandria 1.6** | 371 | *Halomonas desiderata* | GU112956 | 86 |
| **Alexandria 1.7** | 409 | *Thalassobaculum sp.* | AM936707 | 99 |
| **Alexandria 1.8** | 389 | *Caulobacter sp.* | JF190399 | 94 |
| **Alexandria 2.9** | 273 | *Aeromicrobium sp.* | JF180769 | 80 |
| **Alexandria 2.10** | 276 | *Pseudomonas sp.* | EU781745 | 90 |
| **Alexandria 2.11** | 373 | *Limnobacter sp.* | EU639708 | 95 |
| **Alexandria 2.12** | 413 | *Pseudomonas sp.* | HM770945 | 98 |
| **Alexandria 2.13** | 377 | *Caulobacter sp.* | CU927822 | 95 |
| **Alexandria 2.14** | 361 | *Sphingopyxis sp.* | HM186258 | 96 |
| **Alexandria 2.15** | 377 | *Brevundimonas sp.* | EU789983 | 98 |
| **Alexandria 2.16** | 391 | *Acidovorax sp.* | GU271859 | 97 |
| **Alexandria 3.17** | 394 | *Hyphomicrobium sp.* | AM936463 | 96 |
| **Alexandria 3.18** | 376 | *Pseudomonas fluorescens* | EF428995 | 91 |
| **Alexandria 3.19** | 344 | *Hydrogenophaga sp.* | JF042202 | 93 |
| **Alexandria 3.20** | 354 | *Haliea sp.* | FR683596 | 92 |
| **Alexandria 3.21** | 374 | *Parvibaculum sp.* | EU375046 | 94 |
| **Alexandria 3.22** | 377 | *Crenothrix polyspora* | EF192250 | 85 |
| **Alexandria 3.23** | 344 | *Caulobacter sp.* | AM940947 | 98 |
| **Alexandria 3.24** | 409 | *Thioploca sp.* | AB472269 | 92 |
| **Alexandria 3.25** | 373 | *Rhodoferax sp.* | HM856516 | 96 |
| **Alexandria 3.26** | 350 | *Denitratisoma sp.* | DQ663910 | 97 |
| **Alexandria 3.27** | 396 | *Oleomonas sp.* | FJ377393 | 96 |
| **Alexandria 3.28** | 383 | *Phenylobacterium sp.* | AB512185 | 97 |
| **Alexandria 4.29** | 358 | *Parvibaculum sp.* | EU167984 | 89 |
| **Alexandria 4.30** | 388 | *Lentzea sp.* | HQ857654 | 97 |
| **Alexandria 4.31** | 410 | *Klebsiella oxytoca* | EU993529 | 94 |

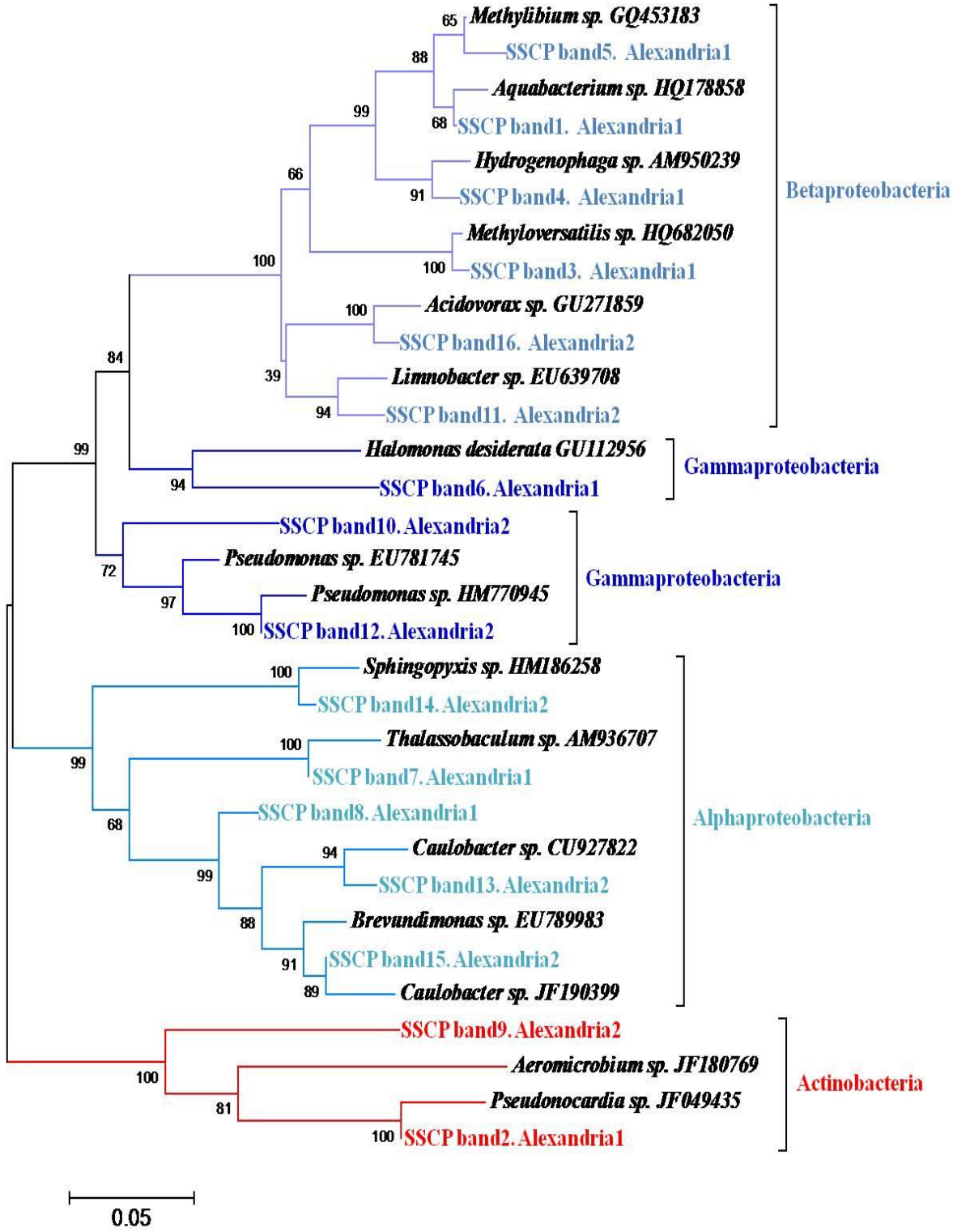


**Figure 44: Phylogenetic tree based on neighbor joining clustering after multiple alignment of the partial 16S rRNA gene sequences of the SSCP bands excised from BDE droplet biofilms from the Alexandria samples. Bootstrap values expressed as percentages of 1000 replications. Bar represents 0.05 substitutions per nucleotide position.**

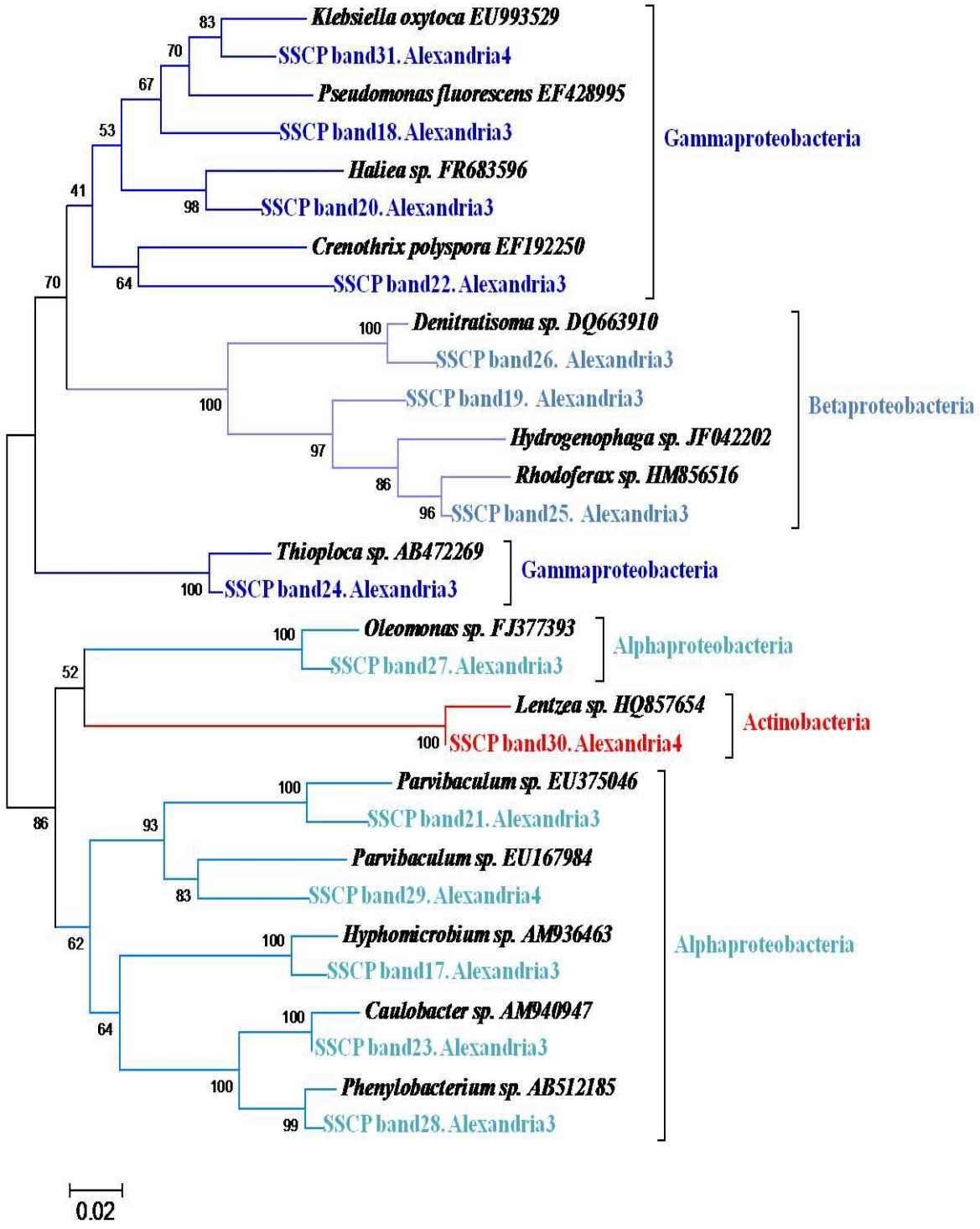


**Figure 45: Phylogenetic tree based on neighbor joining clustering after multiple alignment of the partial 16S rRNA gene sequences of the SSCP bands excised from BDE droplet biofilms from the Alexandria samples. Bootstrap values expressed as percentages of 1000 replications. Bar represents 0.02 substitutions per nucleotide position.**

SSCP community profiling of the Monufia sample (Figure 46) showed moderate diversity in bacterial communities. 8 different OTUs were identified and were closely related to: *Methyloversatilis sp., Caulobacter sp., Pseudomonas sp., Solimonas sp., Halomonas salifodinae, Alcanivorax sp., Haliea sp., and Halomonas salina* (Table 38). The OTUs belonged to the class of Alphaproteobacteria followed by Betaproteobacteria, Gammaproteobacteria and Firmicutes (Figure 47).

SSCP community profiling of the Kafr El-Sheikh, Qalyubia and Gharbbia samples (Figure 48) showed huge diversities in their bacterial communities. By comparing the sequences of 24 excised bands, 21 different operational taxonomic units (OTUs) could be identified which were closely related to: *Halomonas sp., Phenylobacterium sp., Methylibium sp., Methyloversatilis sp., Burkholderia sp., Caulobacter sp., Caulobacter sp., Thiobacter sp., Hydrocarboniphaga sp., Aquabacterium sp., Bradyrhizobium sp., Pseudonocardia sp., Solimonas sp., Hyphomicrobium sp., Thioalkalivibrio sp., Haliscomenobacter sp., Parvibaculum sp., Halomonas maura, Herbaspirillum sp., Rhodococcus sp., Novosphingobium sp., and Pseudomonas sp.*

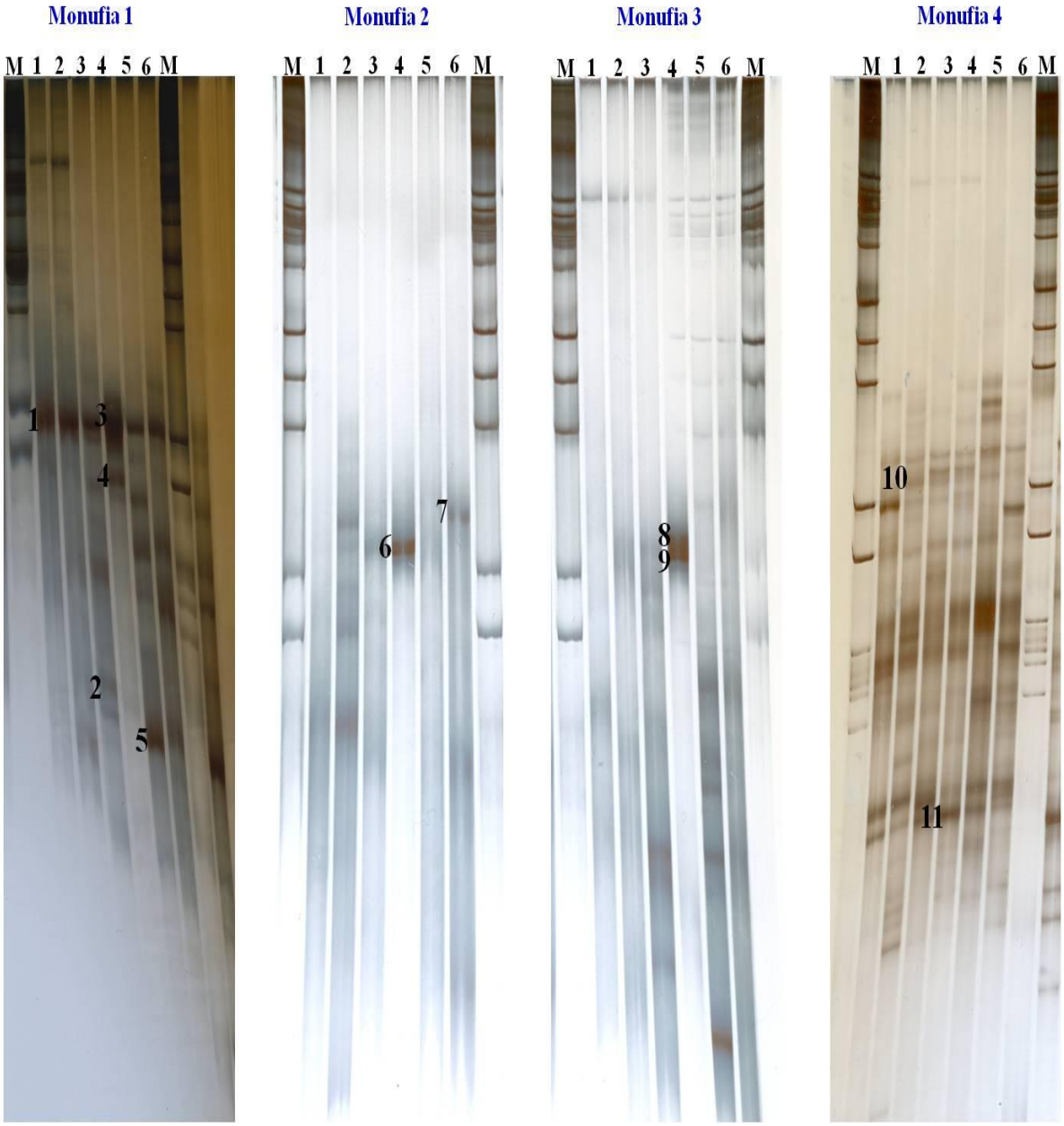


**Figure 46: Composition of BDE bacterial biofilm communities obtained from the Monufia soil samples analysed by 16S rRNA gene based community fingerprint (SSCP). Numbers on top of the gel correspond to sampling time in weeks and M corresponds to the lane of the marker. Marked bands have been excised, sequenced and compared with sequences of described species (Table 38).**

**Table 38: Identification of the main bands of the SSCP gel profiles of bacterial biofilm communities from the Monufia samples by excision, sequencing and comparison with 16S rRNA gene sequence from public databases**

| SSCP bands | Size (bp) | Cultured closest match | Accession number | Identity (%) |
|---|---|---|---|---|
| **Monufia1.1** | 373 | *Methyloversatilis sp.* | HQ397478 | 98 |
| **Monufia1.2** | 375 | *Caulobacter sp.* | DQ165172 | 94 |
| **Monufia1.3** | 409 | *Pseudomonas sp.* | GQ339183 | 99 |
| **Monufia1.4** | 409 | *Pseudomonas sp.* | HQ674994 | 99 |
| **Monufia1.5** | 384 | *Solimonas sp.* | GQ009439 | 96 |
| **Monufia2.6** | 408 | *Pseudomonas sp.* | FJ569777 | 99 |
| **Monufia2.7** | 374 | *Halomonas salifodinae* | GU001905 | 92 |
| **Monufia3.8** | 238 | *Pseudomonas sp.* | GQ853514 | 92 |
| **Monufia3.9** | 409 | *Alcanivorax sp.* | GQ412856 | 92 |
| **Monufia4.10** | 410 | *Haliea sp.* | AY958898 | 78 |
| **Monufia4.11** | 366 | *Halomonas salina* | GU001907 | 93 |

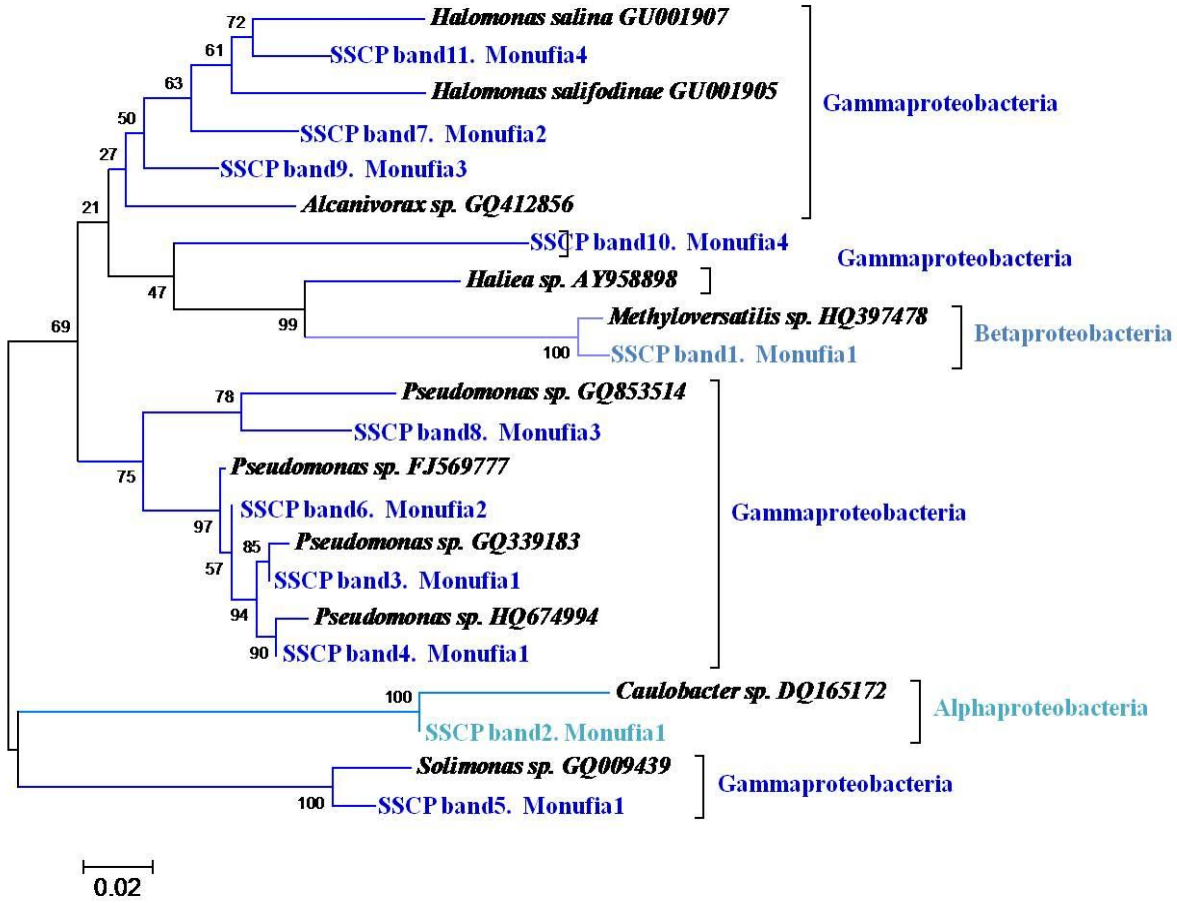


**Figure 47: Phylogenetic tree based on neighbor joining clustering after multiple alignment of the partial 16S rRNA gene sequences of the SSCP bands excised from BDE droplet biofilms from the Monufia samples. Bootstrap values expressed as percentages of 1000 replications. Bar represents 0.02 substitutions per nucleotide position.**

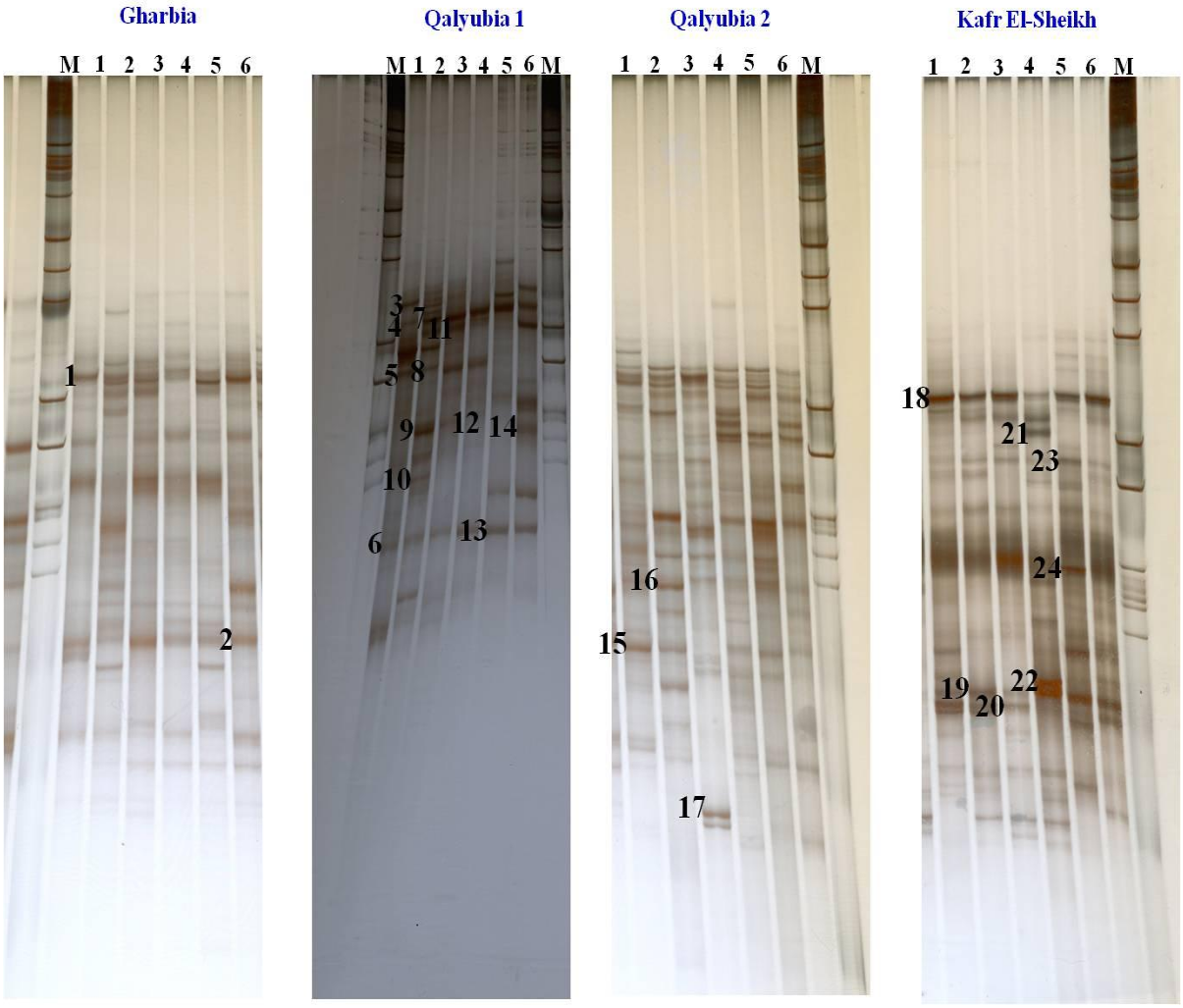


**Figure 48: Composition of γ-HCH bacterial biofilm communities obtained from the Kafr El-Sheikh, Qalyubia and Gharbia soil samples analysed by 16S rRNA gene based community fingerprint (SSCP). Numbers on top of the gel correspond to sampling time in weeks and M corresponds to the lane of the marker. Marked bands have been excised, sequenced and compared with 16S rDNA sequences of described species (Table 39).**

**Table 39: Identification of the main bands of the SSCP gel profiles of bacterial biofilm communities from the Kafr El-Sheikh, Qalyubia and Gharbia samples by comparison of the sequences of the bands with 16S rRNA gene sequence from public databases**

| SSCP bands | Size (bp) | Cultured closest match | Accession number | Identity (%) |
|---|---|---|---|---|
| **Gharbia.1** | 333 | *Halomonas sp.* | HM854275 | 96 |
| **Gharbia.2** | 363 | *Phenylobacterium sp.* | GU568986 | 98 |
| **Qalyubia1.3** | 409 | *Methylibium sp.* | EU267840 | 99 |
| **Qalyubia1.4** | 392 | *Methyloversatilis sp.* | HQ397478 | 99 |
| **Qalyubia1.5** | 365 | *Burkholderia sp.* | GU205728 | 94 |
| **Qalyubia1.6** | 411 | *Caulobacter sp.* | DQ263435 | 96 |
| **Qalyubia1.7** | 367 | *Phenylobacterium sp.* | AM411917 | 95 |
| **Qalyubia1.8** | 370 | *Thiobacter sp.* | EF643413 | 95 |
| **Qalyubia1.9** | 409 | *Hydrocarboniphaga sp.* | EU723429 | 100 |
| **Qalyubia1.10** | 409 | *Bradyrhizobium sp.* | FJ802297 | 98 |
| **Qalyubia1.11** | 407 | *Aquabacterium sp.* | JF019295 | 100 |
| **Qalyubia1.12** | 414 | *Pseudonocardiasp.* | JF049435 | 98 |
| **Qalyubia1.13** | 383 | *Solimonas sp.* | EU808164 | 98 |
| **Qalyubia1.14** | 409 | *Hyphomicrobium sp.* | FJ439830 | 99 |
| **Qalyubia2.15** | 364 | *Solimonas sp.* | FJ444727 | 93 |
| **Qalyubia2.16** | 386 | *Thioalkalivibrio sp.* | DQ001673 | 97 |
| **Qalyubia2.17** | 373 | *Haliscomenobacter sp.* | HM241111 | 94 |
| **Kafr El-Sheikh.18** | 411 | *Methyloversatilis sp.* | HQ397478 | 99 |
| **Kafr El-Sheikh.19** | 395 | *Parvibaculum sp.* | FJ439100 | 96 |
| **Kafr El-Sheikh.20** | 392 | *Halomonas maura* | FN257741 | 92 |
| **Kafr El-Sheikh.21** | 374 | *Herbaspirillum sp.* | AB608680 | 97 |
| **Kafr El-Sheikh.22** | 411 | *Rhodococcus sp.* | JF272213 | 99 |
| **Kafr El-Sheikh.23** | 400 | *Novosphingobium sp.* | FJ674974 | 97 |
| **Kafr El-Sheikh.24** | 390 | *Pseudomonas sp.* | AB583907 | 94 |

The following phylogenetic trees (Figure 49, Figure 50 and Figure 51) present the closest related genera for each obtained sequence. The majority of the identified OTUs were members of the class Gammaproteobacteria followed by Alphaproteobacteria, Betaproteobacteria and Actinobacteria. One strain of the class Sphingobacteria was detected.

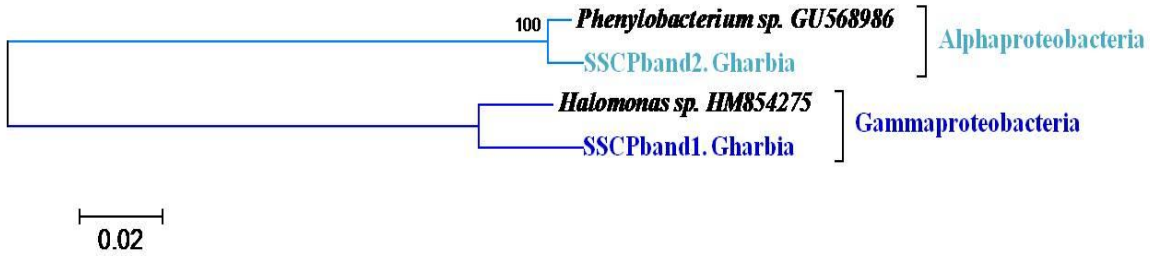


**Figure 49: Phylogenetic trees based on neighbor joining clustering after multiple alignment of the partial 16S rRNA gene sequences of the SSCP bands excised from BDE droplet biofilms from the Gharbia sample. Bootstrap values expressed as percentages of 1000 replications. Bar represents 0.02 substitutions per nucleotide position.**

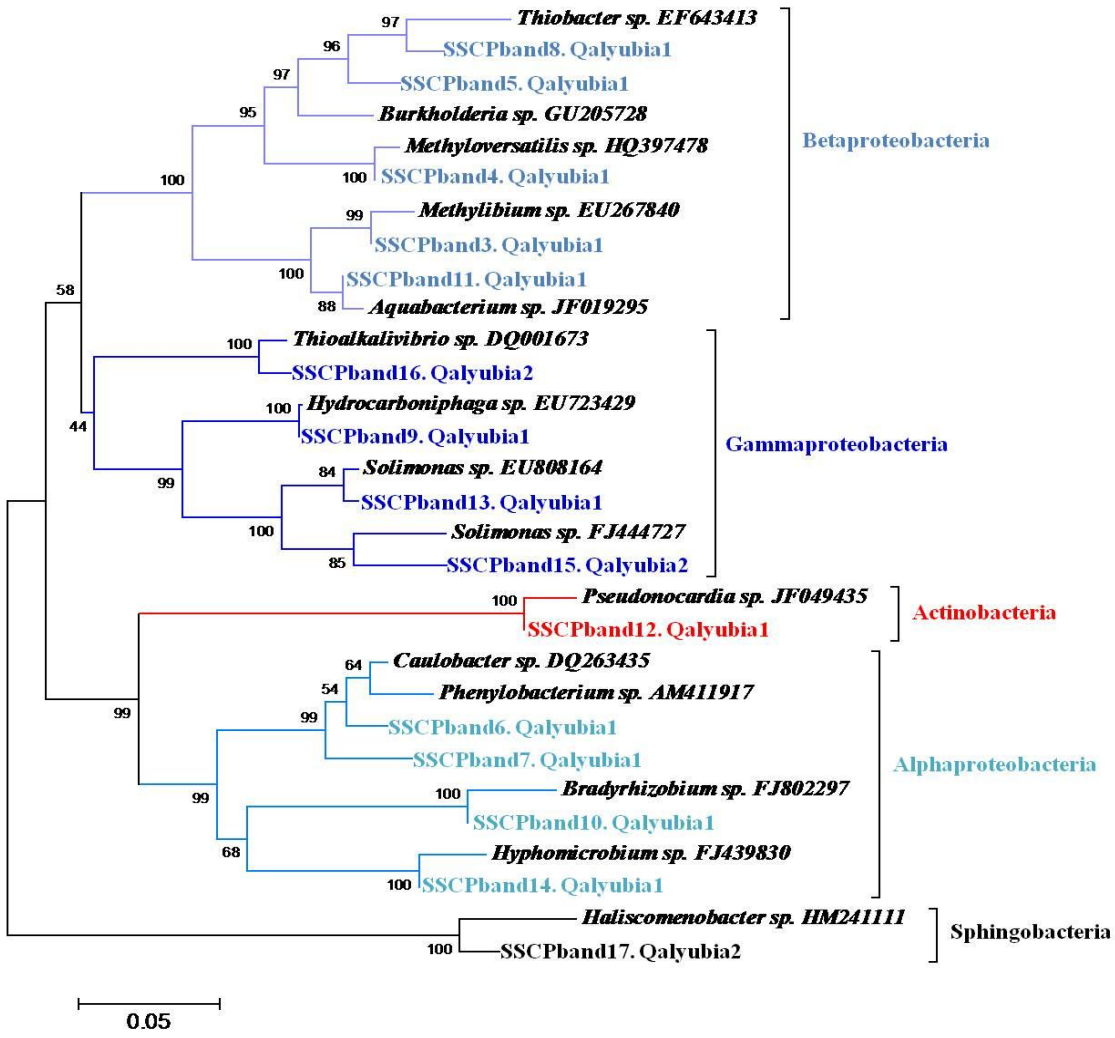


**Figure 50: Phylogenetic trees based on neighbor joining clustering after multiple alignment of the partial 16S rRNA gene sequences of the SSCP bands excised from BDE droplet biofilms from the Qalyubia samples. Bootstrap values expressed as percentages of 1000 replications. Bar represents 0.05 substitutions per nucleotide position.**

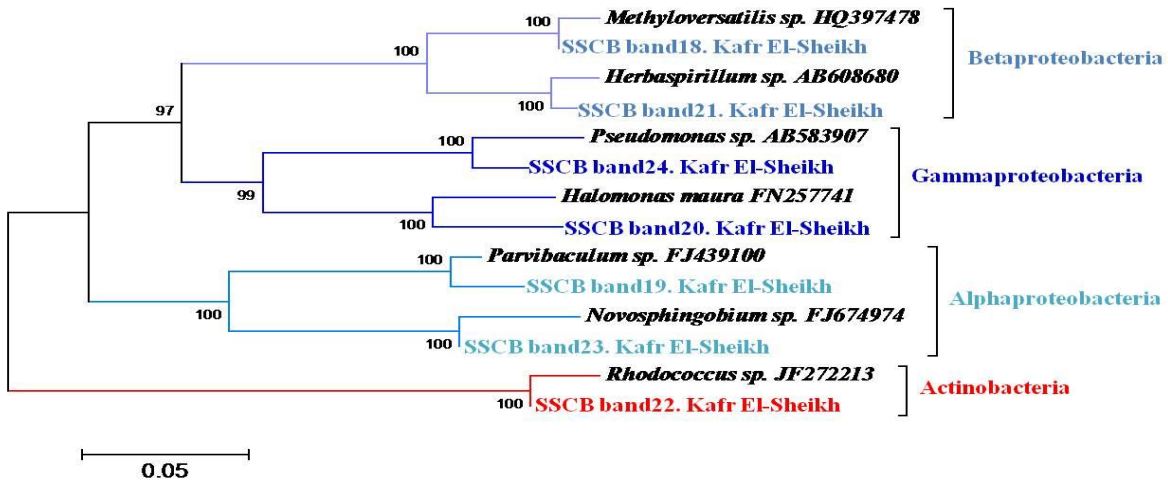


**Figure 51: Phylogenetic trees based on neighbor joining clustering after multiple alignment of the partial 16S rRNA gene sequences of the SSCP bands excised from BDE droplet biofilms from the Kafr El-Sheikh sample. Bootstrap values expressed as percentages of 1000 replications. Bar represents 0.05 substitutions per nucleotide position.**

## 4.2.2 Fungi

### 4.2.2.1 Phylogeny of fungal isolates growing on BDE

Because very little is known on fungi using BDE fungi were also isolated beside bacteria from the different samples. The sequence analysis for the isolates which were able to degrade BDE was done as mentioned in γ-HCH degradation. From the Alexandria site, the sequence analysis showed that the community was composed of fungal strains of the genera *Chrysosporium, Eurotium, Penicillium, Pseudallescheria, and Talaromyces* (Table 40). It was found from the phylogenetic tree that the majority of the identified strains were members of the Eurotiomycetes followed by Sordariomycetes (Figure 52).

**Table 40: Sequence homology of the 18S rRNA gene of the fungal isolates from the Alexandria samples**

| Isolate | Size (bp) | Closely related fungi | Accession number | Homology (%) |
|---|---|---|---|---|
| **Alexandria1.2** | 636 | *Penicillium sp.* | AJ279476 | 98 |
| **Alexandria1.6** | 591 | *Penicillium polonicum* | GU566221 | 98 |
| **Alexandria1.7** | 621 | *Penicillium crustosum* | X82361 | 99 |
| **Alexandria 2.2** | 1042 | *Talaromyces trachyspermus* | EU076917 | 99 |
| **Alexandria 2.3** | 621 | *Talaromyces helicus* | AB176621 | 99 |
| **Alexandria 2.4** | 588 | *Penicillium sp.* | HM535373 | 98 |
| **Alexandria 2.5** | 621 | *Talaromyces stipitatus* | AB176630 | 100 |
| **Alexandria 2.11** | 647 | *Chrysosporium articulatum* | GQ376097 | 98 |
| **Alexandria 3.2** | 652 | *Pseudallescheria boydii* | EF639871 | 97 |
| **Alexandria 3.3** | 589 | *Talaromyces helicus* | FJ430759 | 99 |
| **Alexandria 4.1** | 593 | *Eurotium sp.* | GU721877 | 100 |
| **Alexandria 4.2** | 688 | *Penicillium griseofulvum* | GQ305305 | 97 |

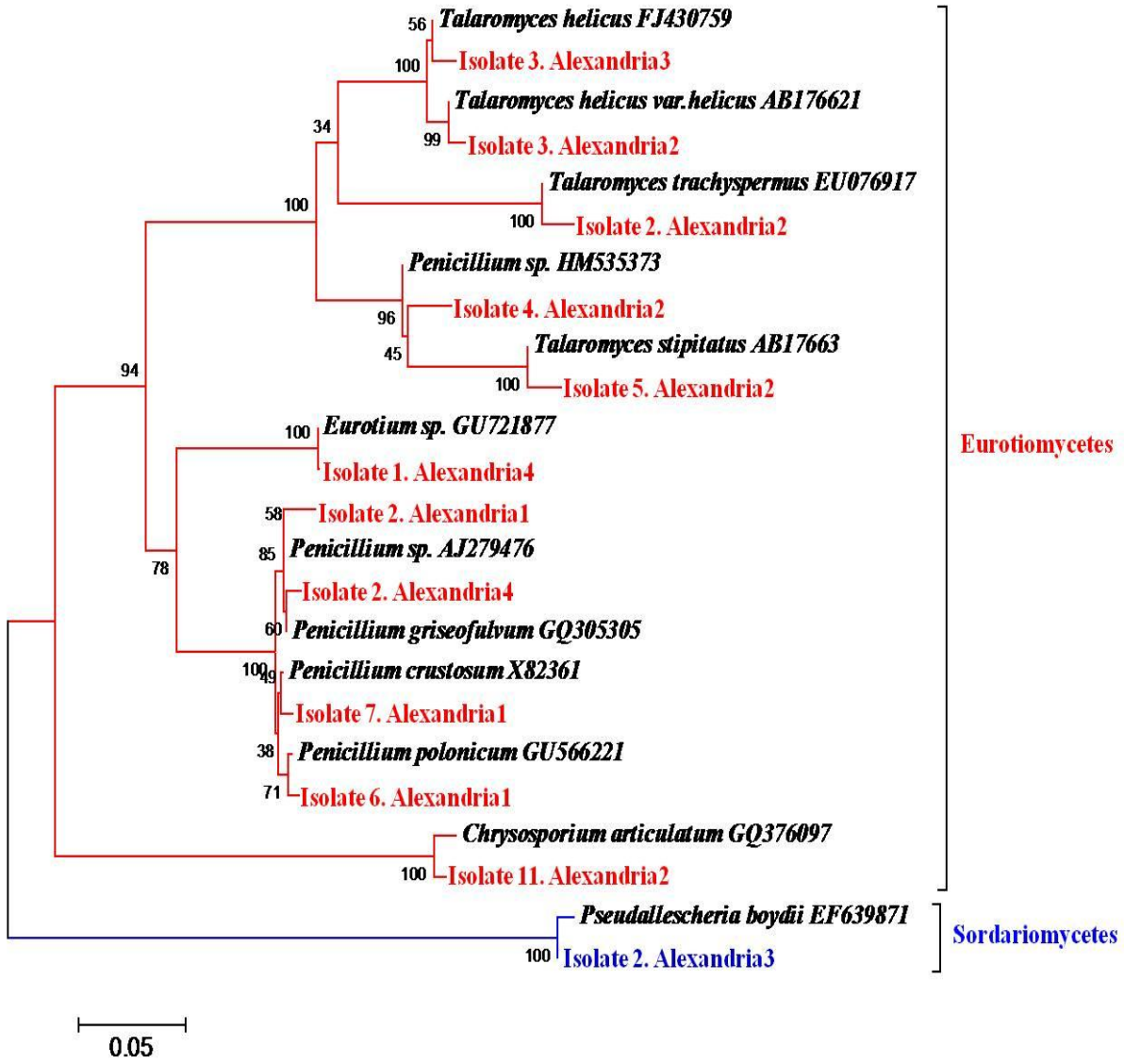


**Figure 52: Phylogeny of fungal isolates from the Alexandria samples that were able to grow on BDE. Multiple alignments of the sequences corresponding to the 18S rRNA of the studied isolates were carried out followed by neighbor joining clustering. Bootstrap values expressed as percentages of 1000 replications. Bar represents 0.05 substitutions per nucleotide position.**

The analysis of the fungal community from the Monufia site revealed that the fungal isolates were of the genera *Eurotium, Penicillium, Pycnidiophora, TalaromycesThielavia, and Westerdykella* (Table 41). The identified strains were members of the Eurotiomycetes, Sordariomycetes and Dothideomycetes (Figure 53).

**Table 41: Sequence homology of the 18S rRNA genes of the fungal isolates from the Monufia samples**

| Isolate | Size (bp) | Closely related fungi | Accession number | Homology (%) |
|---|---|---|---|---|
| **Monufia1.3** | 583 | *Penicillium griseofulvum* | GQ305305 | 98 |
| **Monufia1.4** | 619 | *Penicillium marneffei* | HM595497 | 98 |
| **Monufia2.1** | 1000 | *Talaromyces flavus* | AY532416 | 99 |
| **Monufia2.2** | 584 | *Pycnidiophora aurantiaca* | AY943057 | 99 |
| **Monufia2.5** | 612 | *Talaromyces stipitatus* | AB176630 | 100 |
| **Monufia2.11** | 579 | *Westerdykella globosa* | AY943046 | 98 |
| **Monufia3.1** | 590 | *Eurotium sp.* | GQ999231 | 97 |
| **Monufia3.2** | 569 | *Penicillium sp.* | EU680525 | 95 |
| **Monufia3.5** | 600 | *Thielavia sp.* | GU055740 | 91 |
| **Monufia3.6** | 586 | *Penicillium chrysogenum* | DQ249212 | 96 |
| **Monufia3.7** | 1030 | *Talaromyces trachyspermus* | EU076917 | 99 |
| **Monufia4.2** | 556 | *Talaromyces trachyspermus* | EU076917 | 96 |
| **Monufia4.7** | 558 | *Talaromyces trachyspermus* | EU076917 | 98 |

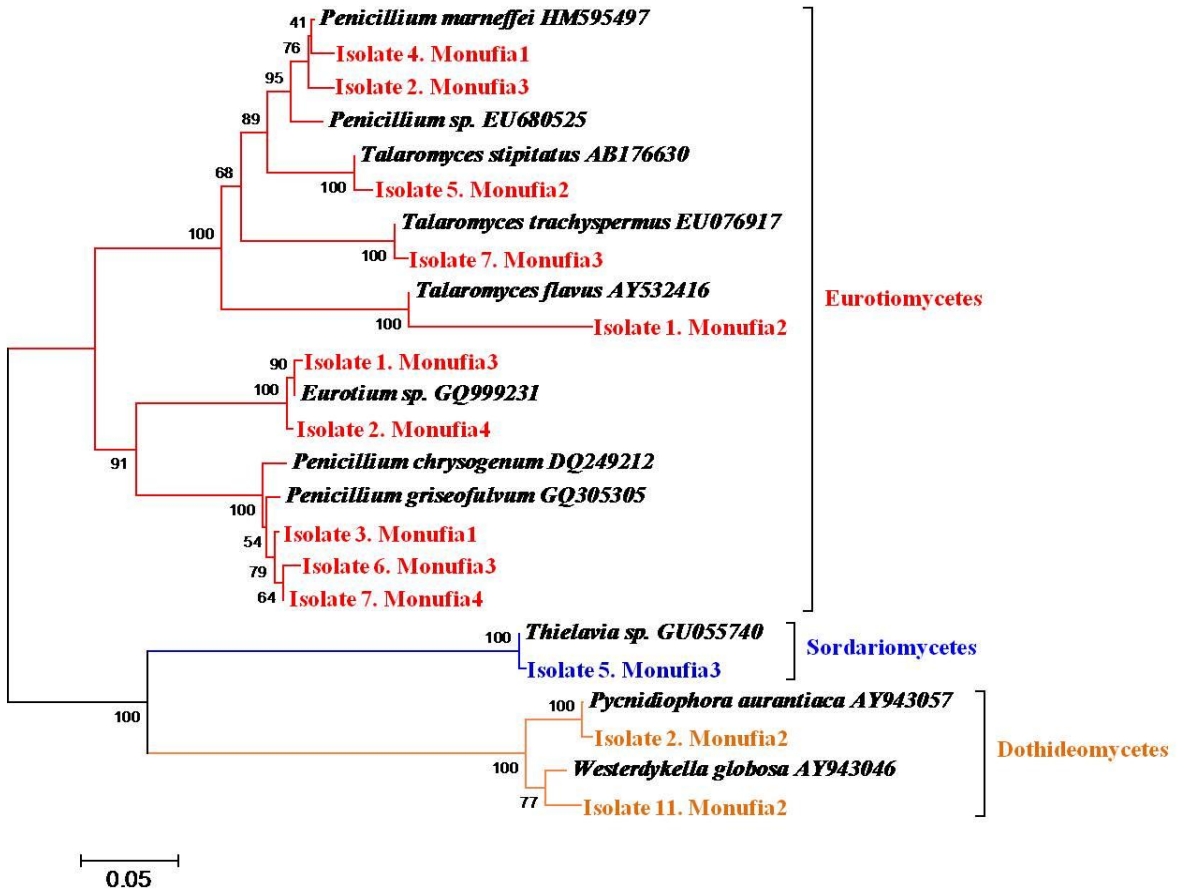


**Figure 53: Phylogeny of fungal isolates from the Monufia samples that were able to grow on BDE. Multiple alignments of the sequences corresponding to the 18S rRNA of the studied isolates were carried out followed by neighbor joining clustering. Bootstrap values expressed as percentages of 1000 replications. Bar represents 0.05 substitutions per nucleotide position.**

Again it was found that the community at the Gharbia site was not rich with isolates that were able to use BDE as a nutrient. The community was composed of fungal strains of the genera *Penicillium, and Scedosporium* (Table 42) and which are members of Eurotiomycetes and Sordariomycetes respectively (Figure 54).

**Table 42: Sequence homology of the 18S rRNA gene of the fungal isolates from the Gharbia sample**

| Isolate | Size (bp) | Closely related fungi | Accession number | Homology (%) |
|---|---|---|---|---|
| **1** | 610 | *Scedosporium dehoogii* | AJ888419 | 98 |
| **4** | 591 | *Penicillium sp.* | FJ647576 | 99 |

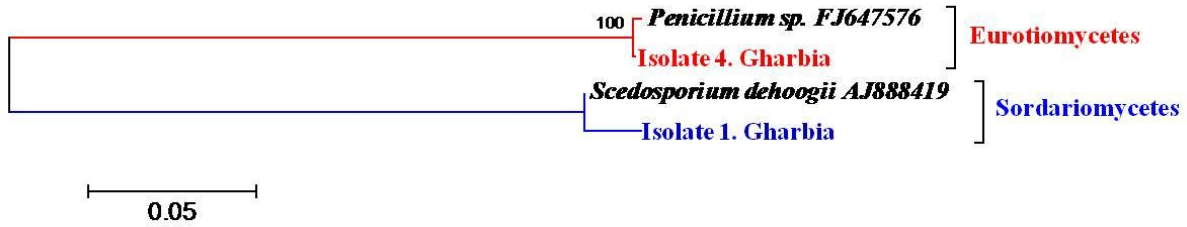


**Figure 54: Phylogeny of fungal isolates from the Gharbia sample that were able to grow on BDE. Multiple alignments of the sequences corresponding to the 18S rRNA of the studied isolates were carried out followed by neighbor joining clustering. Bootstrap values expressed as percentages of 1000 replications. Bar represents 0.05 substitutions per nucleotide position.**

A moderate diversity of the fungal isolates was found both in the Kafr El-Sheikh and the Qalybia samples. The communities were composed of fungal strains of the genera *Gymnascella, Gymnoascus, Penicillium, Talaromyces and Westerdykella* (Table 43) or *Penicillium and Pseudallescheria* (Table 44), respectively. These strains were members either of the Eurotiomycetes, Dothideomycetes (Figure 55) or the Sordariomycetes (Figure 56).

**Table 43: Sequence homology of the 18S rRNA gene of the fungal isolates from the Kafr El-Sheikh sample**

| Isolate | Size (bp) | Closely related fungi | Accession number | Homology (%) |
|---|---|---|---|---|
| **1** | 584 | *Westerdykella dispersa* | DQ468030 | 98 |
| **2** | 660 | *Gymnascella aurantiaca* | HM991264 | 99 |
| **3** | 629 | *Gymnoascus hyalinosporus* | AJ315826 | 99 |
| **4** | 1025 | *Talaromyces sp.* | GU973739 | 98 |
| **5** | 596 | *Penicillium sp.* | EU670718 | 99 |

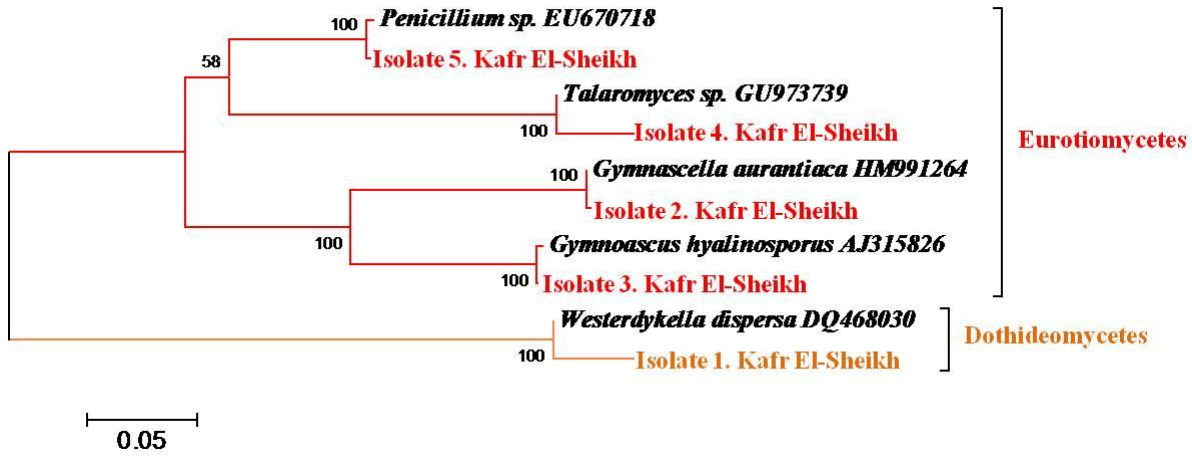


**Figure 55: Phylogeny of fungal isolates from the Kafr El-Sheikh sample that were able to grow on BDE. Multiple alignments of the sequences corresponding to the 18S rRNA of the studied isolates were carried out followed by neighbor joining clustering. Bootstrap values expressed as percentages of 1000 replications. Bar represents 0.05 substitutions per nucleotide position.**

**Table 44: Sequence homology of the 18S rRNA gene of the fungal isolates from the Qalyubia sample**

| Isolate | Size (bp) | Closely related fungi | Accession number | Homology (%) |
|---|---|---|---|---|
| **Qalyubia1.1** | 584 | *Penicillium marneffei* | HM595497 | 94 |
| **Qalyubia1.2** | 1006 | *Penicillium sp.* | EU639449 | 97 |
| **Qalyubia2.2** | 605 | *Pseudallescheria boydii* | GU566237 | 98 |

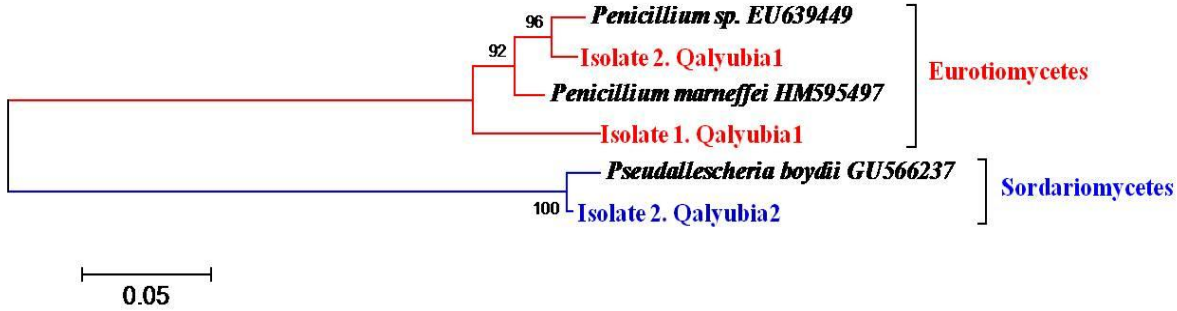


**Figure 56: Phylogeny of fungal isolates from the Qalyubia sample that were able to grow on BDE. Multiple alignments of the sequences corresponding to the 18S rRNA of the studied isolates were carried out followed by neighbor joining clustering. Bootstrap values expressed as percentages of 1000 replications. Bar represents 0.05 substitutions per nucleotide position.**

### 4.2.2.2 Growth on BDE of the most active fungal isolates

The metabolization and degradation of BDE by fungi was carried out for 30 days at 30°C in shaking flasks. Samples were taken every 3 days during the cultivation period.

Figure 57 showed that the growth of isolate6.Alexandria1, isolate1.Monufia2, and isolate4.Gharbia were at the maximum point after the 12$^{th}$ day of cultivation while the growth of isolate2.Qalyubia2 and isolate1.Kafr El-Sheikh gradually increased with increasing time up to the optimal point the 18$^{th}$ day of incubation. Then the growth of all isolates decreased gradually over time.

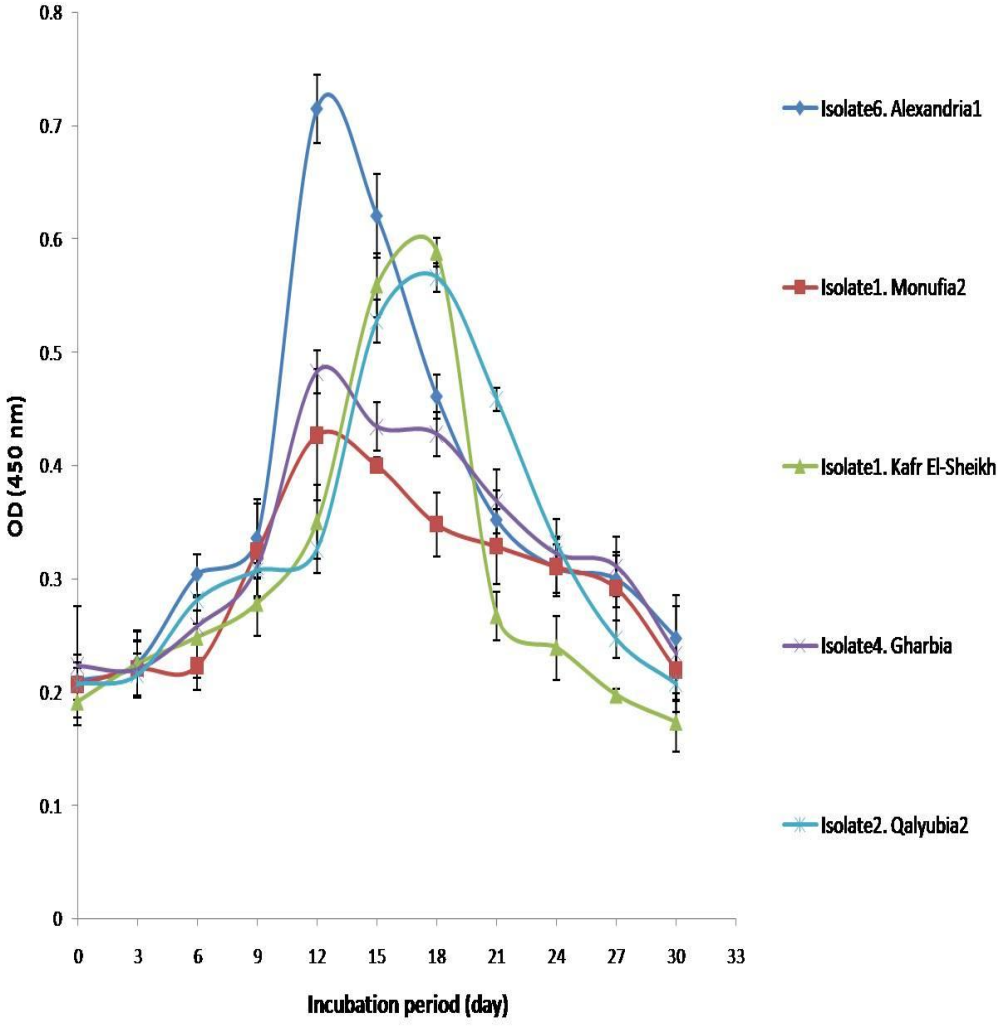


**Figure 57: Growth curves for the most capable fungal isolates to grow on BDE. The strains isolated from several locations in Egypt were grown in basal DOX medium containing 2mM BDE. The growth was determined by the change in the absorbance at $\lambda_{max}$=450 nm.**

### 4.2.2.3 Analysis of fatty acids of the most active fungal isolates for BDE degradation

From Figure 58 and Table 45, it was found that the major cellular fatty acids (>10 % of the total fatty acids) in the most abundant BDE-degrading fungal isolates were C16:0, C18:2ω6,9, and C18:1ω9.

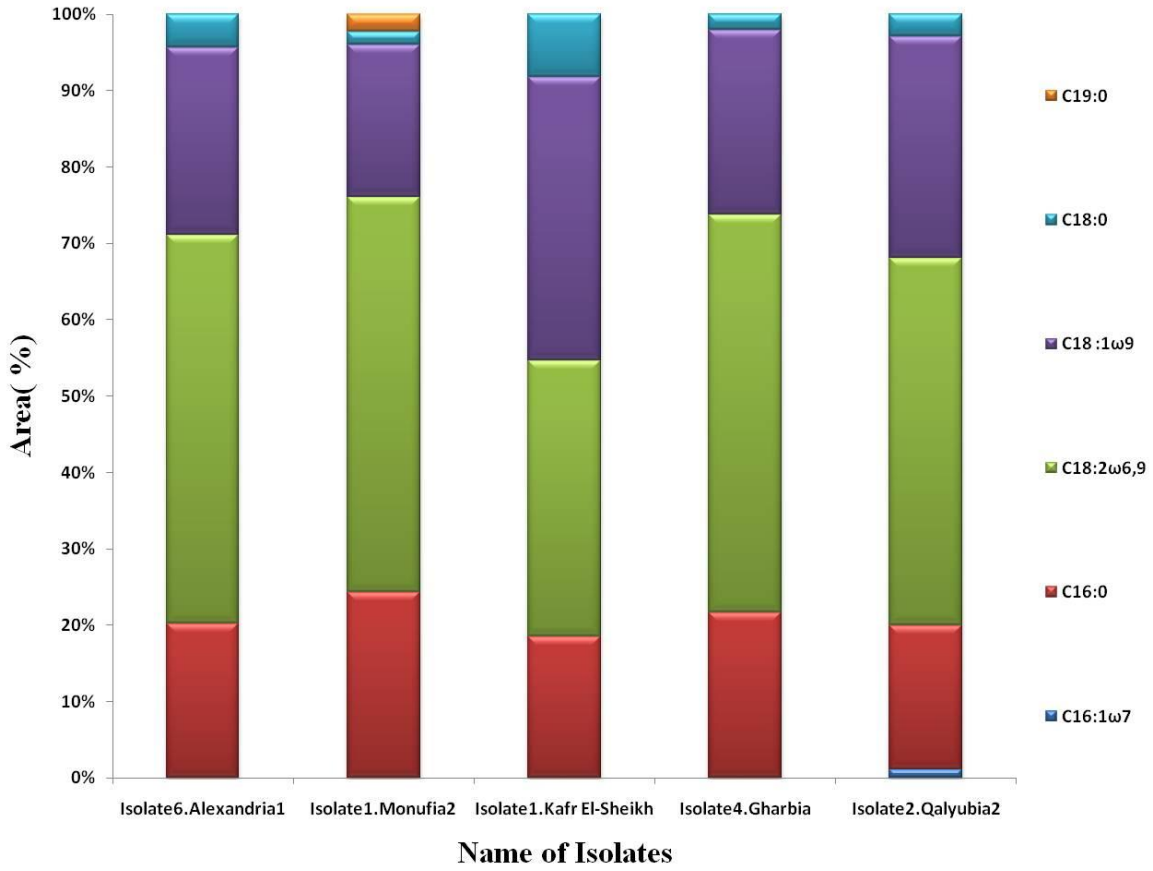


**Figure 58: Percentage of the total fatty acids for the most active fungal isolates grown on BDE.**

**Table 45: Major cellular fatty acids content (%) of the most active fungal isolates for BDE degradation. Values are percentage of total fatty acids. -, not detected.**

| Fatty acid | Isolate6. Alexandria1 | Isolate1. Monufia2 | Isolate1. Kafr el-Sheikh | Isolate4. Gharbia | Isolate2. Qalyubia2 |
|---|---|---|---|---|---|
| **Saturated fatty acids:** | | | | | |
| $C_{16:0}$ | 20.2 | 24.3 | 18.5 | 21.6 | 18.9 |
| $C_{18:0}$ | - | - | - | - | 1.5 |
| $C_{19:0}$ | 4.3 | 1.7 | 8.2 | 2.1 | 2.9 |
| **Monounsaturated fatty acids:** | | | | | |
| $C_{16:1\omega7}$ | - | - | - | - | 1.1 |
| $C_{18:2\omega6,9}$ | 50.9 | 51.8 | 36.2 | 52.1 | 48 |
| $C_{18:1\omega9}$ | 24.6 | 20 | 37.1 | 24.1 | 29 |

### 4.2.2.4 Analysis of fungal biofilm communities composition grown on BDE droplets

Figure 59 and Figure 60 showed the SSCP of fungi in the biofilm communities. By comparing the sequences of 9 excised bands, 5 different OTUs could be identified which were closely related to *Blastomyces dermatitidis, Penicillium chrysogenum, Penicillium requeforti, Penicillium sp. and Thelebolus microsporus.* The phylogenetic tree (Figure 61) presents the closest related genera of each sequence obtained. The identified OTUs were members of the class Eurotiomycetes and Leotiomycetes.

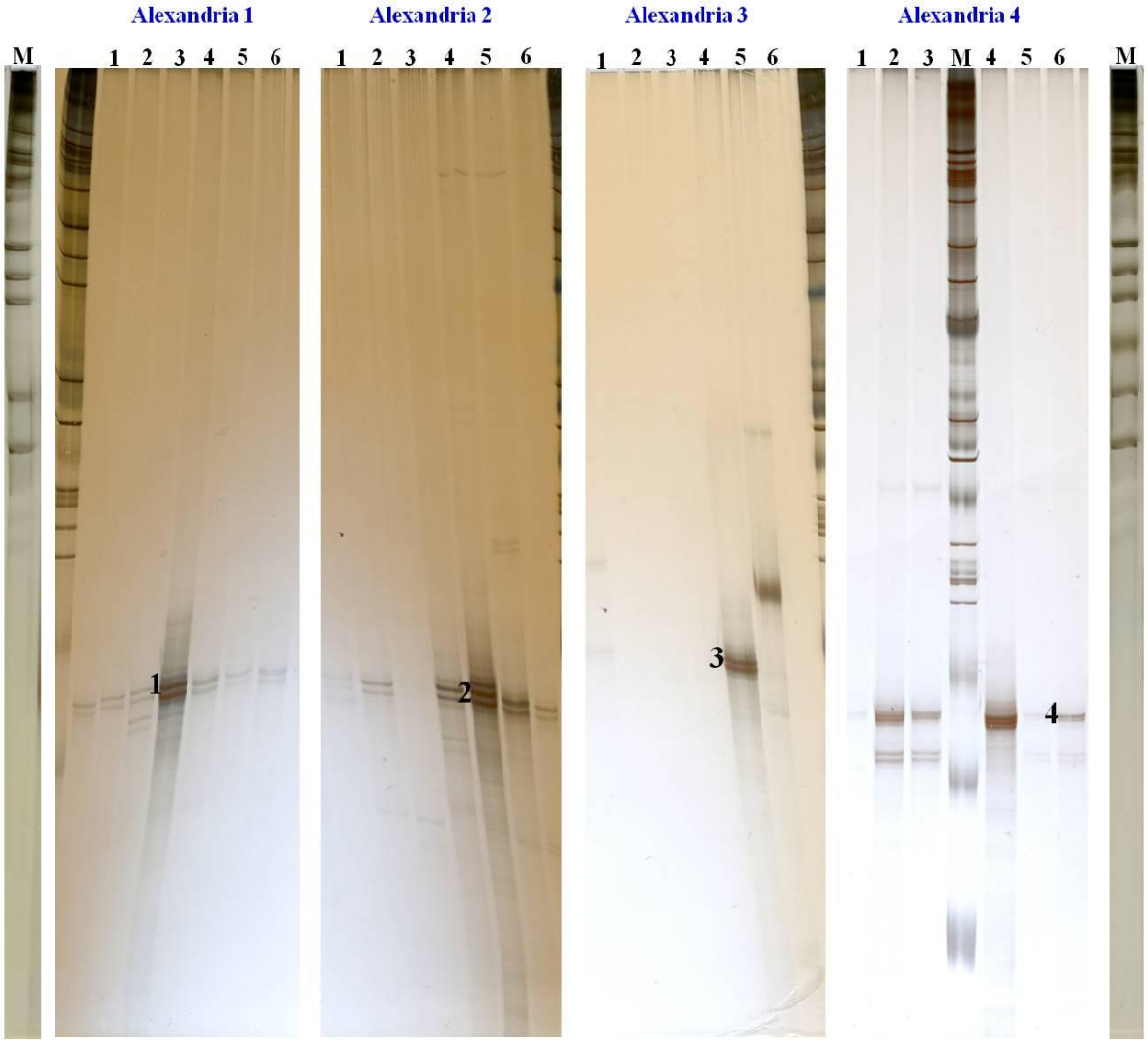


**Figure 59: Composition of BDE fungal biofilm communities obtained from the Alexandria soil samples analysed by 18S rRNA gene based community fingerprinting (SSCP). Numbers on top of the gel correspond to sampling time in weeks and M corresponds to the lane of the marker. Marked bands have been excised, sequenced and compared with sequences of described species.**

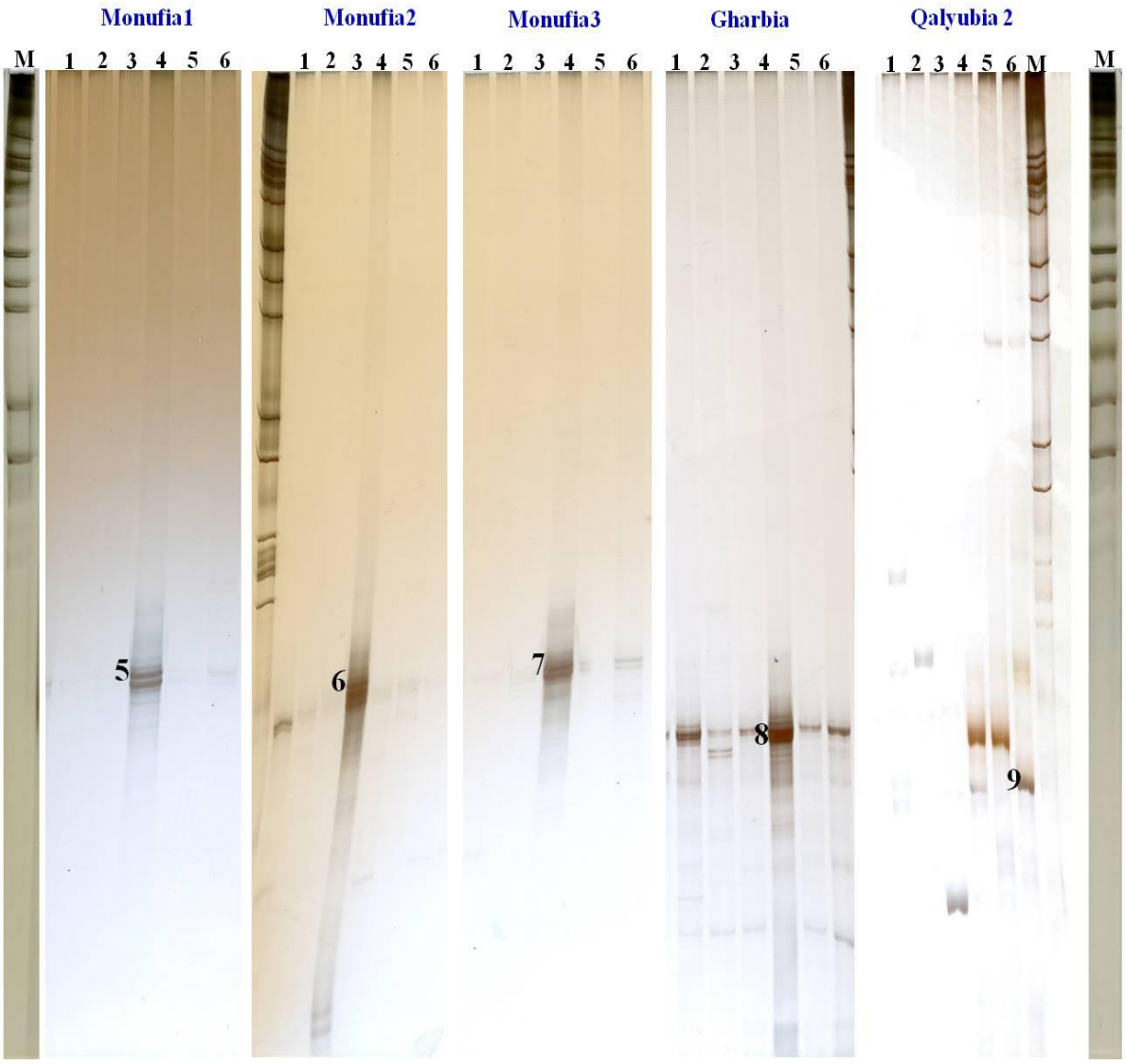


**Figure 60: Composition of BDE fungal biofilm communities obtained from the Monufia, Gharbia and Qalyubia soil samples analysed by 18S rRNA gene based community fingerprint (SSCP). Numbers on top of the gel correspond to sampling time in weeks and M corresponds to the lane of the marker. Marked bands have been excised, sequenced and compared with sequences of described species.**

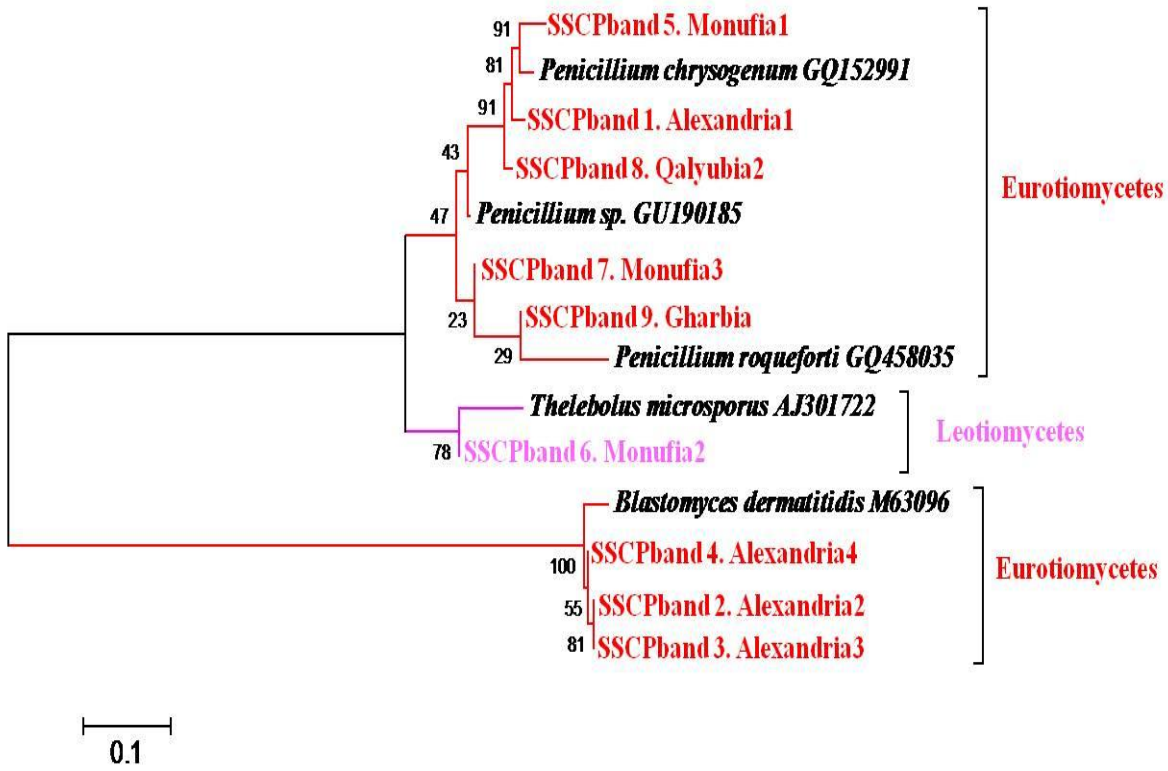


**Figure 61: Phylogenetic tree based on neighbor joining clustering after multiple alignment of the partial 18S rRNA gene sequences of the SSCP bands excised from BDE droplet biofilms from Alexandria, Monufia, Gharbia and Qalyubia samples. Bootstrap values expressed as percentages of 1000 replications. Bar represents 0.1 substitutions per nucleotide position.**

## 4.3 Structure of the biofilm changes along the pollution gradient

Microbial communities organized in biofilms show a multitude of interactions, including carbon sharing [192], interspecies communication [193], and steep physicochemical gradients [121] and are very well protected against environmental stress factors such as toxic compounds, water stress, or grazing [194].

To take advantage of the special conditions in biofilms, soil and sediment samples were taken to grow biofilm communities on the pollutants. The biofilm was monitored by CLSM over 42 days using Nile red to stain hydrophobic areas and Live/Dead for the bacteria to examine the structure of biofilms along the pollution gradient. To show the position of the droplet, the hydrophobic dye Nile Red was used and, interestingly, this dye stained also some aggregates of bacteria indicating hydrophobic cell surfaces. Contrary to the droplets of BDE the crystals of HCH, although also hydrophobic, could not be stained with Nile Red. The biofilm originating from soil sample was also treated with Live/Dead stain to determine the rate of live to damaged cells. However, in this case it was not possible to decide whether red stained cells were damaged or had hydrophobic surfaces, due to the possibility of staining cells with hydrophobic surfaces simultaneously with Nile Red.

Figure 62 depicts the formation and development of the biofilm on the γ-HCH crystals showing the spatial progress of the biofilm on them. After 7 days (Figure 62 A) of incubation a biofilm was detected on the Permanox™ slide close to the crystals but only few cells were observed on the crystals directly. Subsequently, after 14 days (Figure 62 B) a substantial biofilm accumulation on the margins of the pollutant was observed. Further, after 14 days the number of live cells was higher than those of the defective cells. After 21 days (Figure 62 C) the biofilm showed the highest number of species and large microbial aggregates encircling the microcrystals of γ-HCH. Twenty-eight days (Figure 62 D) after incubation, the bacterial population on the Permanox™ substratum was somewhat reduced and the crystals started to break up. The 35 and 42 days old biofilms revealed the dominance of damaged cells and the complete disappearance of the γ-HCH crystals. It can be assumed that the red stain seen in these pictures are caused not oly by damaged bacterial cells but also by cells with hydrophobic surfaces and/or nanocrystals of the pollutants (Figure 62 E and F).

Figure 63 depicts the formation and development of the biofilm on the droplets of BDE showing again the spatial progress of the biofilm on them. After 7 days (Figure 63 A) of

incubation a biofilm was detected on the Permanox™ slide loosely surrounding the droplets but only few cells were observed on the droplets. Subsequently, after 14 days (Figure 63 B) a substantial biofilm accumulation on Permanox slide concentrating around the margins of the droplets was observed. After 14 days the number of live cells was still higher than those of the defective cells. After 21 days (Figure 63 C) the biofilm showed the highest number of species and started to colonize the droplets as evident from the presence of yellow aggregates caused by the superposition of the green stain of the bacteria and the red stain of BDE. Twenty-eight days (Figure 63 D) after incubation, the bacterial population on the Permanox™ substratum started to decrease but increased on the droplets. The 35 and 42 days old biofilm revealed the dominance of damaged cells and hardly any live cells could be seen. The number of microorganisms is also considerably decreasing and the droplets seem to break up into much smaller droplets (Figure 63 E and F).

The biofilm developing from polluted soils displayed a pronounced pattern of maturation. The first step was the colonization of the Permanox substratum, while the pollutants were hardly populated. When a certain density of bacteria was reached on the Permanox slide, the pollutants were colonized, but afterwards the number of damaged cells increased sharply accompanied by dramatic increase in crystal or droplet degradation. Finally, the aggregates of pollutants almost disappeared and almost all cells were damaged. One reason could be metabolites inhibiting or damaging cells in the biofilm leading to a higher ratio of damaged to living cells [142].

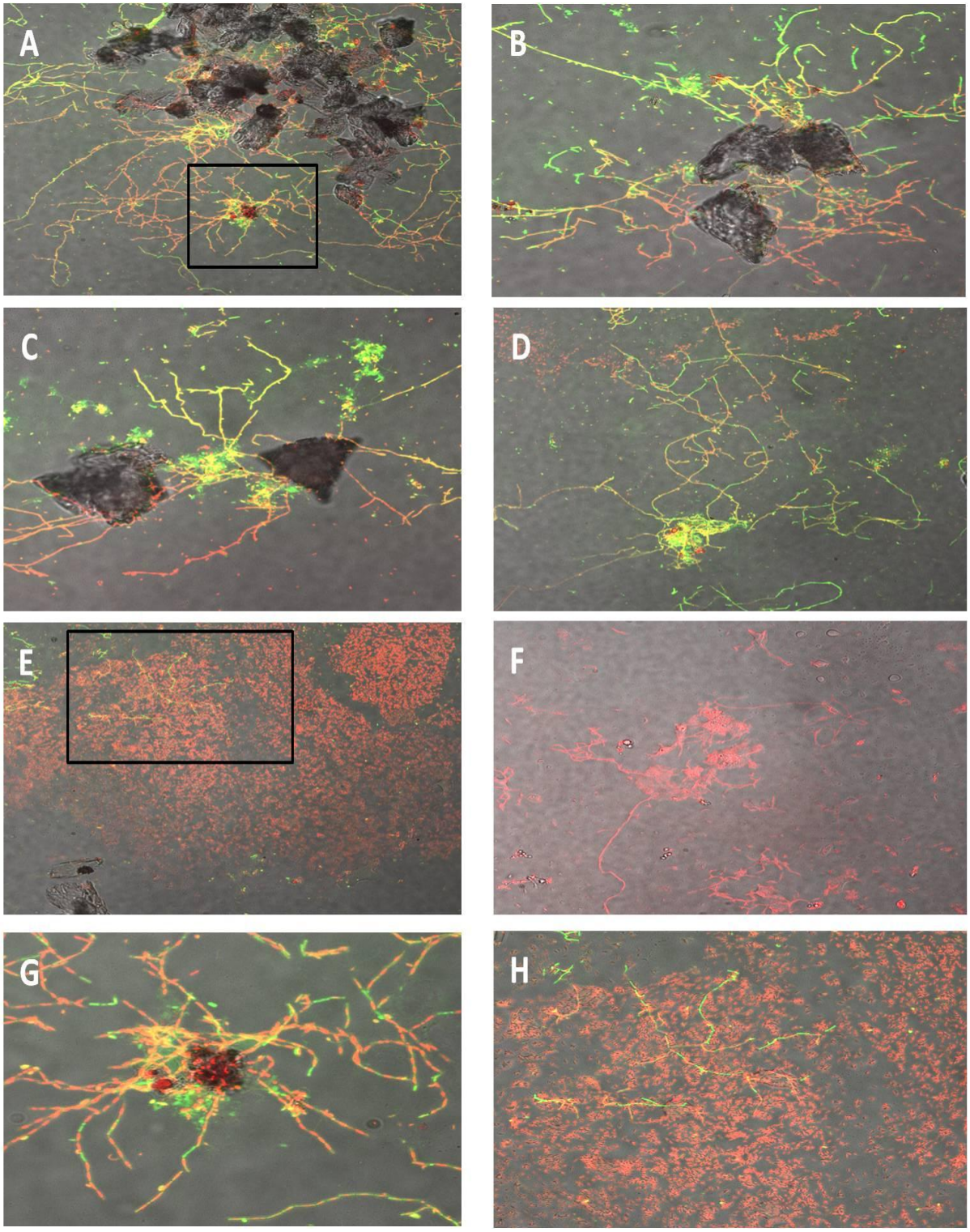


**Figure 62: Biofilm development after 7, 14, 21, 28, 35 and 42 days (A, B, C, D and F). γ-HCH biofilm stained with LIVE (= green)/ DEAD (= red) and Nile red (γ-HCH droplets) is shown as XY and grid size = 20 µm. G and H were magnified part from A and E, respectively and grid size = 40 µm.**

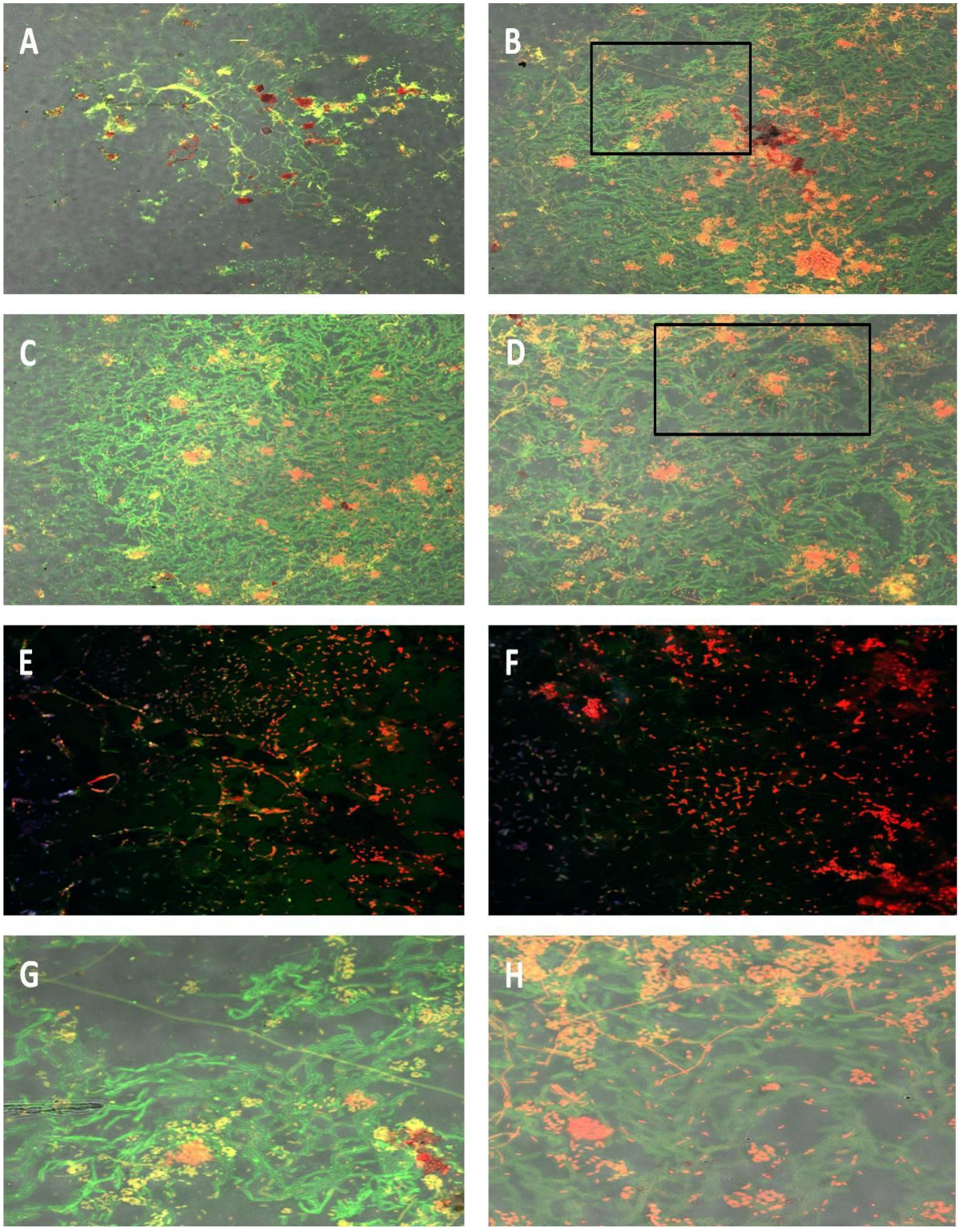


**Figure 63: Biofilm development after 7, 14, 21, 28, 35 and 42 days (A, B, C, D and F). BDE biofilm stained with LIVE (= green)/ DEAD (= red) and Nile red (BDE droplets) is shown as XY and grid size = 20 µm. G and H were magnified part from B and D, respectively and grid size = 40 µm**

# 5 Discussion

γ-HCH or lindane, one of the most commonly used pesticides, has been mainly used in agriculture; this pesticide is known to be highly toxic and persistent, causing serious water and soil contamination and intensive scientific studies in HCH detoxification were conducted due to health and environmental concerns [63]. Many countries continue to use lindane and residues of HCH isomers persist in the environment and bioaccumulate at various levels of the food chain, thus, becoming a threat to human health [24]. To eliminate these contaminants from the environment, attempts have been made to isolate lindane-utilizing native microorganisms and improve their utilizing ability.

In the present study, 75 different bacterial and 49 different fungal species were isolated from several soil/sediment samples from Egyptian locations. Bacteria recorded in this investigation were classified into 3 phyla: Proteobacteria, Firmicutes and Actinobacteria according to their frequency of occurrence and diversity. The phylum with the highest frequency was Proteobacteria which contained 19 different species which were closely related to: *Achromobacter piechaudii, A. xylosoxidans, Alcaligenes faecalis, Aquamicrobium sp., Brevundimonas diminuta, B. sp., Brucella sp., Cupriavidus oxalaticus, Frateuria sp., Luteimonas mephitis, Lysobacter daejeonensis, Novosphingobium sp., Ochrobactrum anthropi, O. sp., Pseudomonas panipatensis, P. putida, P. sp., P. stutzeri* and *Starkeya sp.*. The phylum with moderate frequency and diversity phylum was Firmicutes which contained 16 different species which were mainly related to: *Acetobacter pasteurianus, Bacillus altitudinis, B. amyloliquefaciens, B. cibi, B. circulans, B. flexus, B. licheniformis, B. megaterium, B. mycoides, B. pumilus, B. simplex, B. sp. subtilis, B. thuringiensis, Oceanobacillus picturae* and *Paenibacillus ginsengisoli*. The low diversity phylum was Actinobacteria which contained 7 different species which were closely related to: *Agromyces sp., Gordonia sp., Microbacterium sp., Micromonospora sp., Rhodococcus ruber, R. sp.* and *R. wratislaviensis*. The highest number of bacterial isolates was obtained from samples collected from the Monufia location.

*Bacillus*, *Pseudomonas* and *Rhodococcus* were the most frequent and diverse genera and their species have been reported frequently to grow on γ-HCH. The study presented here enlarges the number of genera and species able to use HCH offering novel possibilities in using bacteria in HCH degradation. To achieve this however genetic characterizations of these isolates are required in order to optimize the metabolic capabilities of these strains.

Not all of the isolated bacterial and fungal species from soil/sediment samples had good growth in the presence of γ-HCH. Screening or selection of the most suitable bacterial and fungal species was dependent on the growth rate on the medium containing γ-HCH. The results of the present study (Figure 19) revealed that the most active bacterial isolates were isolate2.Qalyubia2, isolate3.Alexandria4, isolate7.Monufia4, isolate4.Gharbia and isolate3.Kafr El-Sheikh which were closely related to: *Rhodococcus sp., Agromyces sp., Bacillus sp., Aquamicrobium sp.* and *Lysobacter daejeonensis*, respectively. The species found here as the best HCH degraders are different to the ones usually used to study HCH degradation. Sahu *et al.* studied the degradation of γ-HCH by a *Pseudomonas sp.* isolated from sugarcane rhizosphere soil. The authors demonstrated the almost complete disappearance of the pesticide within 24 h of incubation with a concomitant release of $Cl^-$ almost in stoechiometric amounts [49]. Lindane was totally consumed within 72 h by a consortium of bacteria isolated from a river sediment and 6 mol of $Cl^-$ was generated from 1 mol of lindane during bacterial growth [63]. Further work is needed to characterize the degradation pathways and the optimal conditions for HCH degradation for any of the above isolates.

In most studies on the degradation of HCH fungi have been ignored. To close this gap not only bacteria but also fungi have been isolated in this study as HCH-degraders. Fungi identified in this study and able to metabolize γ-HCH can be mainly divided into 4 classes: Eurotiomycetes, Sordariomycetes, Zygomycetes and Dothideomycetes. The class of highest diversity was Eurotiomycetes which contained 20 different species which were closely related to: *Aspergillus terreus, A. fumigates, Dichotomomyces cepjpii, Eurotium rubrum, Gymnascella hyalinospora, Monascus ruber, Paecilomyces sp., P. tenuis, Penicillium chrysogenum, P. commune, P. dipodomyicola, P. griseofulvum, P. pinophilum, P. raperi, P. sp., Talaromyces helices, T. sp., T. trachyspermus, P. trachyspermus var. assiutensis* and *T. unicus*. The class with moderate frequency was Sordariomycetes which contained 7 different species which were closely related to: *Cylindrocarbon sp., Pseudallascheria boydii, P. ellipsoida, Scedosporium apiospermum, Thielavia hyalocarpa, T. sp.* and *Zopfiella latipes*. The low diversity classes were Zygomycetes and Dothideomycetes which contained two species *Mortierella gamsii* and *M. sp.*, and one species *Pycnidiophora aurantiaca*, respectively.*Penicillium, Talaromyces* and *Pseudallascheria* were the most diverse genera and the highest number of fungal isolates was obtained from samples collected at the Qalyubia location. These isolates increased the known range of fungi using HCH considerable because only a few fungal strains have been shown before to be able to

degrade HCH isomers [24]. The ability of several white-rot fungi to degrade lindane was tested by Arisoy [53]. The white-rot fungi causing white-rot of wood have recently become the object of increasing attention by scientists working in the hazardous waste field. These fungi normally grow on decaying wood and forest litter, and appear to be unique among microorganisms in that they can rapidly depolymerize and mineralize lignin to carbon dioxide [195]. White-rot fungi are also able to degrade a wide variety of environmentally pollutants to carbon dioxide, including a number of chlorinated pollutants such as DDT and lindane [196]. Biodegradation of the pollutants occurs at a high rate only under nutrient limitation and in the presence of cellulose or glucose. In our study most of the fungal isolates were white-rote fungi and we discovered new isolates from this group being able to grow on γ-HCH.

The most abundant fungal isolates (Figure 32) were of isolate10.Qalyubia1, isolate9.Gharbia, isolate1.Qalyubia2, isolate1.Kafr El-Sheikh, isolate2.Monufia1 and isolate1.Alexandria4 which metabolized γ-HCH and gave a good growth in presence of it. They were closely related to: *Talaromyces helicus, Talaromyces trachyspermus, Pseudallescheria boydii, Dichotomomyces cejpii, Penicillium chrysogenum* and *Penicillium griseofulvum*, respectively. As has been already stated in the introduction little has been done to study HCH degradation by fungi and all of these studies were focused on white rot fungi. The fungi found in this present study are different to those studied for HCH degradation so far and broaden the field of fungi useful for bioremediation and degradation of chlorinated organic pollutants.

After isolation and identification of the most tolerant bacteria and fungi for γ-HCH, the objective of the present work was to compare the diversity and activity of the isolates with microbial biofilm communities colonizing γ-HCH crystals. The question was here whether these microbial communities differ from those isolated through classical microbiological methods. Using SSCP gel profiling it was possible to analyse the biofilm community indicating that bacteria and fungi are better adapted to the conditions of the biofilms in the microcosms and consequently, were more successful in colonizing the slides with γ-HCH crystals. For all samples it was possible to grow biofilms on the HCH crystals and the individual biofilm communities different considerably between the different sites. This underlines that different communities are able to do HCH degradation and that probably conditions specific for the site controls community composition as has been shown before in the case of PCB degradation [197]. The comparative community analysis of the biofilms allowed the identification of the taxa performing the dechlorination. The members of the individual biofilm communities turned out to be different

from those isolated through classical microbiological methods from the same soil samples. From bacterial biofilm communities 38 OTUs were identified and classified into the 3 phyla Proteobacteria, Firmicutes and Cyanobacteria. The phylum Proteobacteria contained 15 different OTUs which were closely related to *Aquabacterium sp., Burkholderia gladioli, B. sp., Caulobacter sp., Comamonas sp., Coronobacter sakazakii, C. sp., Escherichia coli, Methyloversatilis sp., Nitrosospira sp., Ochrobactrum sp., Pravibaculum sp., Pseudomonas fluorescens, P. sp.* and *Sphingomonas sp.* The phyla Firmicutes and Cyanobacteria contained one OTU for each which was mainly related to: *Planococcus sp.* and *Coleochaete pulvinata,* respectively. *Sphingomonas, Coronobacter, Pseudomonas* and *Burkholderia* were the most frequent and diverse genera. The bacterial biofilm from the contaminated soils Alexandria and Monufia possessed the highest diversity.

This is an interesting finding because most of the HCH-degrading aerobic bacterial strains reported until now are gram-negative and members of the family Sphingomonadaceae. A few other HCH-degrading isolates such as *Rhodanobacter lindaniclasiticus* and *Xanthomonas sp.* were also reported. Only very few gram-positive strains such as *Microbacterium sp.* and *Bacillus sp.* have been shown to degrade HCH [24]. Previous studies have shown before that the individual strains do not act isolated from the other community members but have strong interactions with each orther [198]. A simple comparison of the isolates with the activity of the biofilm communities is therefore not possible. Furthermore, the experience in our laboratory is that a mere combination of the isolates is not possible to gain activities and robustness comparable to the one observed in the biofilms. Probably modern day techniques as meta-genome sequencing or stable isotope analyses are required to get a much deeper understanding of HCH degradation in biofilms communities. Nevertheless biofilm communities certainly have advantages in *in situ* bioremediations due to their robustness and resilience.

The results of our study revealed diverse microbial communities in the Egyptian soil/sediment samples which were able to colonize γ-HCH crystals. Generally, the bacterial biofilms in the $2^{nd}$ and $3^{rd}$ weeks were more prominent and diverse, but remained relatively constant in the $4^{th}$ week and no new significant bands appeared. In the 5 and 6 weeks old biofilms, most of the microbial communities disappeared. Fungi were only minor components in any of the biofilm communities grown on HCH crystals. The fungal biofilm communities detected by SSCP had very low diversity compared with the bacterial ones, with *Penicillium* as the only genus and strains closely related to *Penicillium expansum* and *P. sp.* In the case of the

temporal dynamics of the fungal species in the biofilms, the fungal communities appeared only in the 4$^{th}$ week and then disappeared in the following weeks pointing to a minor role of fungi in the degradation of HCH at least in these biofilm communities.

It was interesting to compare the results on HCH-degrading communities with biofilm communities grown from the same soil samples but on another substrate and here BDE was chosen. In recent years there has been interest in using polyhalogenated diphenyl ethers as chemicals to replace the polyhalogenated biphenyls formerly utilized as flame retardants. 4,4'-Dibromodiphenyl ether (4,4'-DBDE) is the lowest halogenated commercial congener belonging to this class of compounds of environmental concern [111]. To eliminate these contaminants from the environment, attempts have been made in our laboratory to isolate BDE15-utilizing native microorganisms and improve their utilizing ability.

From the enrichment culture after one month, bacterial and fungal strains that can utilize BDE15 as sole source of carbon and energy were isolated and identified. In the present study a broad diversity of microorganisms were detected: 68 different bacterial and 35 different fungal species were isolated from several soil/sediment samples from Egyptian locations. Bacteria recorded in this investigation were classified into 3 phyla: Proteobacteria, Actinobacteria and Firmicutes according to their frequency of occurrence and diversity. The phylum of highest frequency was Proteobacteria which contained 24 different species which were closely related to: *Alcaligenes faecalis, A. sp., Aquamicrobium sp., Brevundimonas sp., Castellaniella ginsengisoli, C. sp., Devosia sp., Dokdonella koreensis, Ensifer meliloti, Frateuria sp., Luteimonas mephitis, Nitratireductor sp., Ochrobactrum sp., Pseudaminobacter deflvii, Pseudomonas sp., Pseudoxanthomonas mexicana, P. sp., Pusillimonas terrae, Rhodanobacter lindaniclasticus, Rh. sp., Sphingomonas sp., Sphingopyxis sp., Stenotrophomonas acidaminiphila* and *Thauera sp*. The phylum of moderate frequency and diversity was Actinobacteria which contained 13 different species which were mainly related to Agrococcus *sp*., *Agromyces neolithicus, A. sp., Arthrobacter oxydans, A. sp., Gordonia amicalis, Isoptericola sp., Microbacterium sp., Micromonospora pattaloongensis, Nocardia sp., Promicromonospora sp., Rhodococcus equi, R. erythropolis* and *R. sp.* The lowest diversity was found in Firmicutes which contained 9 different species closely related to: *Bacillus firmus, B. niacin, B. sp., Paenibacillus amylolyticus, P. chinjuensis, P. sp., P. turicensis, Staphylococcus epidermidis and Streptomyces clavuligerus*. The highest diversity of bacterial isolates was observed in samples collected from the Monufia

location. *Rhodococcus, Bacillus*, *Paenibacillus,* and *Rhodanobacter* were the most frequent and diverse genera and their species have frequently reported to grow on BDE.

Again the diversity found in the isolates is broader than what was known so far. The ability of the polychlorinated biphenyl (PCB) degrading bacteria *Rhodococcus jostii* RHA1, *Burkholderia xenovorans* LB400, *Rhodococcus sp.* RR1 and the ether-degrading *Pseudonocardia dioxanivorans* CB1190 to utilize and transform mono- to hexa-BDEs have been reported [114]. However, no attempts were made in our study to test any of the isolates on their ability to use different congeners of BDE or any mixtures or congeners of PCB.

It has been assumed that microbial degradation of PBDEs will be low and/or only under aerobic conditions. It has also been suggested that combinations of anaerobic and aerobic microbial processing may possess the ability to fully degrade PBDEs [112]. To test this, Vonderheid [199] examined the diversity of sewage microbial communities and their ability to degrade BDEs under both anaerobic and aerobic conditions. In this study microorganisms from a sewage biosolid reactor were isolated, cultured and tested for the capability to degrade BDE. Generally, isolates fell into 3 main genera; *Aeromonas*, *Xanthomonas* and *Pseudomonas*. The application of biofilms offers the possibility to create anaerobic niches within an aerobically grown biofilm [200]. This has been shown for the degradation of PCB but it is highly likely that it also applies for the degradation BDEs.

As expected not all of the isolated bacterial and fungal species from soil/sediment samples displayed good growth on of BDE. The results in the present study (Figure 41) revealed that the most active bacterial isolates were Isolate8.Qalyubia1, isolate2.Monufia2, isolate1.Gharbia, isolate1.Kafr El-Sheikh and isolate5.Alexandria3 which were closely related to: *Rhodanobacter lindaniclasticus, Bacillus sp., Nocardia sp., Rhodococcus sp.* and *Brevundimonas sp.*, respectively.

On the basis of the evidence provided so far, both anaerobic and aerobic microorganisms can initiate debromination of BDEs in the laboratory, but apparently aerobic bacteria are faster (i.e. days/weeks) compared to anaerobic bacteria (months/year). Under aerobic conditions, *Sphingomonas sp.* had been reported to utilize BDEs as sole carbon and energy source. Within 6 days, the initial amount of 1 g/L BDEs was completely utilized, and the highest cell density was reached with a culture turbidity of 1.2 at $OD_{578}$ [116].

Fungi identified in this study and able to metabolize BDE were mainly divided into 3 classes: Eurotiomycetes, Sordariomycetes and Dothideomycetes. The class of highest diversity

was Eurotiomycetes which contained 14 different species which were closely related to: *Chrysosporium articulatum, Eurotium sp., Gymnascella aurantiaca, Gymnoascus hyalinospora, Penicillium chrysogenum, P. crustosum, P. griseofulvum, P. marneffei, P. polonicum, P. sp., Talaromyces flavus, T. helices, T. stipitatus* and *T. trachyspermus.* A class of moderate frequency was Sordariomycetes which contained 3 different species which were closely related to: *Pseudallascheria boydii, Scedosporium dehoogii* and *Thielavia sp.* The lowest diversity class was Dothideomycetes which contained three species: *Pycnidiophora aurantiaca, Westerdykella dispersa* and *W. globosa*. *Penicillium* and *Talaromyces* were found to be the most diverse genera and the highest number of fungal isolates could be obtained from samples collected from the Monufia and Alexandria locations. The most abundant fungal isolates (Figure 57) were of isolate 6.Alexandria1, isolate1.Monufia2, isolate4.Gharbia, isolate2.Qalyubia2 and isolate1.Kafr El-Sheikh which metabolized BDE and showed good growth on it. They were closely related to: *Penicillium polonicum, Talaromyces flavus, Penicillium sp., Pseudallescheria boydii,* and *Westerdykella dispersa*, respectively.

The pollutant degradation by white-rot fungi is due to the role of ligninolytic enzymes including manganese peroxidases, lignin peroxidases and laccases. In contrast to what is known about some polycyclic aromatic hydrocarbons [201-204] little or no information exists concerning their abilities for the degradation of biarylic compounds like polychlorinated biphenyls, diphenyl ethers or dibenzo-p-dioxins [51, 205]. Obviously, in addition to the action of extracellular ligninolytic enzymes, intracellular processes also seem to be of importance for the biotransformation of these compounds by white-rot fungi [206-207].

As for the degradation of HCH the objective of the present work was to compare the BDE degrading isolates with the microorganims in microbial biofilm communities colonizing BDE droplets. By SSCP gel profiling it was possible to determine the composition of the biofilm communities demonstrating that bacteria and fungi were different from those isolated from the same soil sample. The comparative community analysis of the biofilms allowed the tentative identification of the taxa performing the debromination. In the bacterial biofilm communities we identified 66 OTUs grouped into 3 phyla: Proteobacteria, Actinobacteria and Sphingobacteria according to their diversity.

The phylum Proteobacteria was present with 36 different OTUs which were closely related to: *Acidovorax sp.,Alcanivorax sp, Aquabacteria sp., Bradyrhizobium sp., Brevundimonas sp., Burkholderia sp., Caulobacter sp., Crenothrix polyspora, Denitratisoma sp., Haliea sp.,*

*Halomonas desiderata, H. maura, H. salifodinae, H. salina, H. sp., Herbaspirillum sp., Hydrogenophaga sp., Hyphomicrobium sp., Klebsiella oxytoca, Limnobacter sp., Methylibium sp., Methyloversatilis sp., Novosphingobium sp., Oleomonas sp., Pravibaculum sp., Pseudomonas fluorescens, P. sp., Phenylobacterium sp., Rhodococcus sp., Rhodoferax sp., Solimonas sp., Sphingopyxis sp., Thalassobaculum sp., Thialkalivibrio sp., Thiobacter sp.* and *Thioploca sp.*. The 3 OTUs were members of the phylum Actinobacteria most closely related to: *Aeromicrobium sp., Lentzea sp.* and *Pseudonocardia sp.* The phylum Sphingobacteria contained one OTU which was closely related to *Haliscomenobacter sp. Pseudomonas, Caulobacter, Halomonas,* and *Methyloversatilis* were the most frequent and diverse genera in the biofilms. The bacterial biofilm communities from contaminated soils of the Alexandria and Qalyubia possessed the highest diversity.

The fungal biofilm communities had very low diversity compared with bacterial biofilm and were closely related to *Blastomyces dermatitidis*, *Penicillium chrysogenum* and *P. roqueforti* (class Eurotiomycetes) and *Thelebolus microspores* (class Leotiomycetes).

Evidence of rapid degradation of BDEs has been presented by Zhou *et al*. [208], who evaluated the ability of white rot fungi to degrade BDEs in a liquid culture media and the effect of Tween-80 and β-cyclodextrin on the degradation of BDEs by white-rot fungi. The results showed that test systems with only white-rot fungi added showed a decrease of 42% in the amount of BDEs over 10 days in the test system compared to the sterile controls. Tween 80 was found to enhance BDEs degradation at an appropriate concentration (maximum degradation 96.5% over 10 days). Cyclodextrin was also shown to enhance BDEs degradation (maximum degradation of 78.4% over 10 days). Such a fast degradation has not been found in any of the microcosm experiments shown here. However, no attempt has been made to optimize or even enhance the degradation because this would have been outside of the scope of the presented study.

It is interesting to compare the results from the biofilm architecture over time both between the HCH and the BDE biofilm communities and the ones reported for PCB degrading biofilms. The HCH crystals were never heavily colonized by bacteria, instead they were surrounded by bacteria probably took advantage of the diffusion gradient of HCH dissolving in water. An astonishing phenomenon is the fragmentation and dissolution of the HCH microcrystals at the end of the experiment not seen before in any of these microcosms. Contrary to HCH the biofilm communities colonize after two weeks BDE as has also been seen in the case

of PCB. For BDE again we could see a fragmentation of the droplets probably caused by bacterial invasion, action of biosurfactants or other still unknown mechanisms. For all three substrates damage of the bacterial cell wall can be seen after 4 weeks probably caused by the hydrophobic nature of the substrates and/or the formation of toxic intermediates formed during biodegradation. The damaged cells however are not dead but still showed metabolic activities and many contributions have been made concerning the distinction between damaged and dead bacterial cells [209]. This has been reported in the case of PCB but for the results presented here one has to keep in mind that a co-staining with Nile Red has been used which may obscure the results due to staining of lipophilic particles/membranes.

Microcosms are closer to the situation in the field than isolate microorganisms, however, they are still not the same than the situation *in situ*. Although it is highly probable that biofilm communities are indeed the metabolic entities in soil doing most of the degradation of organic matter including pollutants many more interactions play a role in the performance of microorganisms. One of them is the symbiotic relationship between fungi and plant roots, known as arbuscular mycorrhizas. These mycorrhizas are ubiquitous and may facilitate metabolism of substances such as polycyclic aromatic hydrocarbons in the soil. This effect was considered to be due to the mycorrhiza-associated microflora, since the microbial community structure had an altered phospholipid fatty acid profile [210]. The current work is therefore only a step forward in understanding the role of different microorganism and their communities in the degradation of HCH and BDE. The findings presented here strongly support the use of biofilm communities in *in situ* bioremediations.

# 6 Conclusion

γ-Hexachlorocyclohexane (γ-HCH) and 4,4`-diphenylether (BDE) are extensively in use in the tropical countries and in some developed countries. They are highly halogenated pollutants that persist in the environment for a long time and the residues have been reported from water, vegetables and food commodities. They have been banned in many countries because of its toxicity, mutagenicity and carcinogenicity to humans. These compounds are very difficult for bacteria and fungi to degrade. However, bacteria and fungi can cooperate within a community making the degradation process easier. The purpose of this work was to determine the extent of the microbial potential for the degradation of γ-HCH and BDE in soils. This study demonstrated the huge diversity of bacteria and fungi from 12 soil samples collected around chemicals and pesticide producing factories from Egypt. From γ-HCH and BDE enrichment cultures, all samples yielded broad biodiversities as revealed by the analyses of the16S rRNA genes for bacteria and 18S rRNA genes for fungi.

In the present study, 75 different bacterial and 49 different fungal species were isolated from several soil/sediment samples which are able to metabolize and grow on γ-HCH. The highest count of bacteria was observed on samples collected from the Monufia location. *Bacillus*, *Pseudomonas* and *Rhodococcus* were the most frequent and diverse genera and their species have frequently reported to grow on γ-HCH. *Penicillium*, *Talaromyces* and *Pseudallascheria* were the most diverse genera and the highest count of fungi was observed on samples collected from the Qalyubia location. The best degrading bacterial isolates were *Rhodococcus sp.* isolate2.Qalyubia2, *Agromyces sp.* isolate3.Alexandria4, *Bacillus sp.* isolate7.Monufia4, *Aquamicrobium sp.* isolate4.Gharbia and *Lysobacter daejeonensis* isolate3.Kafr El-Sheikh. The most abundant fungal isolates were *Talaromyces helicus* isolate10.Qalyubia1, *Talaromyces trachyspermus* isolate9.Gharbia, *Pseudallescheria boydii* isolate1.Qalyubia2, *Dichotomomyces cejpii* isolate1.Kafr El-Sheikh, *Penicillium chrysogenum* isolate2.Monufia1 and *Penicillium griseofulvum* isolate1.Alexandria4 which metabolized γ-HCH and showed good growth in its presence.

Also, 68 different bacterial and 35 different fungal species were isolated from several soil/sediment samples which were able to metabolize and grow on BDE. The highest diversity of bacteria was observed in samples collected from the Monufia location. *Rhodococcus, Bacillus*, *Paenibacillus*, and *Rhodanobacter* were the most frequent and diverse genera and their species

have frequently reported to grow on BDE. For the fungal isolates *Penicillium* and *Talaromyces* were found to be the most diverse genera and the highest number of fungi was observed in samples collected from the Monufia and Alexandria locations. The most active bacterial isolates were *Rhodanobacter lindaniclasticus* Isolate8.Qalyubia1, *Bacillus sp,* isolate2.Monufia2, *Nocardia sp.* isolate1.Gharbia, *Rhodococcus sp.* isolate1.Kafr El-Sheikh and *Brevundimonas sp.* isolate5.Alexandria3. The most abundant fungal isolates were *Penicillium polonicum* isolate 6.Alexandria1, *Talaromyces flavus* isolate1.Monufia2, *Penicillium sp.* isolate4.Gharbia, *Pseudallescheria boydii* isolate2.Qalyubia2 and *Westerdykella dispersa* isolate1.Kafr El-Sheikh which metabolized BDE and grew well with it.

These isolates were compared with biofilm communities grown from the same soil and sediment samples using γ-HCH microcrystals and BDE droplets as substrates. The experiments were done in microcosms and the biofilm communities were monitored by SSCP profiling. The microorganisms detected in the biofilm communities were different from those isolated through classical microbiological methods inoculated with the same soil sample.

All soil samples yielded biofilms on γ-HCH & BDE and SSCP analysis of the biofilms revealed rather diverse bacterial and fungal communities. From γ-HCH-bacterial biofilm communities, we identified 38 OTUs. The bacterial biofilm from the contaminated soils Alexandria and Monufia possessed the highest diversity. *Sphingomonas, Coronobacter, Pseudomonas* and *Burkholderia* were the most frequent and diverse genera. The fungal biofilm communities had very low diversity compared with the bacterial ones and were closely related to *Penicillium expansum* and *P. sp*. Doing the same experiments with BDE instead of γ-HCH yielded different microbes. In BDE-bacterial biofilm communities, we identified 66 OTUs, *Pseudomonas, Caulobacter, Halomonas,* and *Methyloversatilis* were the most frequent and diverse genera. The bacterial biofilm from contaminated soils Alexandria and Qalyubia possessed the highest diversity. The fungal biofilm communities had low diversity compared with the bacteria in the biofilm. The main fungal members of the biofilms were closely related to *Blastomyces dermatitidis*, *Penicillium chrysogenum* and *P. roqueforti* and *Thelebolus microspores.*

The structural biofilm development was monitored by Confocal Laser Scanning Microscope (CLSM) using Nile Red to stain the substrate and any lipophilic areas in the biofilm and Bac Light Kit, for LIVE (green)/DEAD (red) bacteria. The formation and development of the biofilm on the microcrystals showed the spatial progress of the biofilm around them. However,

contrary to the biofilm development described for PCB droplets [142] the biofilm communities did not colonize the HCH crystals. Instead the microbes accumulated around these crystals and finally dissolved them. The structural dynamic of the BDE-degrading biofilm communities followed closer the model described for the PCB droplets but at the end of the experiments was again first fragmentation and finally dissolution of the entire droplets. Both for HCH and BDE and similar to the observation made for PCB droplets the majority of microbes showed cell wall damages at the end of the experiments.

From the soil samples, a huge diversity of species was obtained and most isolates were able to metabolize and grow on γ-HCH and BDE and use them as sole source of carbon. New γ-HCH- and BDE-degrading isolates have been identified and characterized phylogenetically and by FAME profile. Bacteria and fungi in microbial communities play different roles and together they are able to form biofilm communities using γ-HCH and BDE as a carbon source: (a functional diversity cooperation). The method applied was very effective in selecting communities of γ-HCH and DFE degraders, which could metabolize its microcrystals or droplets. Despite some members of the communities disappeared over time, the most abundant members (identified through SSCP bands) tend to remain over time. The method used proved to be a good method to follow the dynamics of biofilm communities composed by uncultured bacteria and fungi. The insights gained from this study on the diversity of HCH and BDE degraders and their dynamics in the biofilm communities will help to optimize *in situ* bioremediations using biofilm communities.

# 7 References


[1] McGuinness, M. and D. Dowling, (**2009)** "Plant-associated bacterial degradation of toxic organic compounds in soil." *Int J Environ Res Public Health,* **6** (8): pp. 2226-2247.

[2] Burkhard, L.P. and M.T. Lukasewycz, (**2008)** "Toxicity equivalency values for polychlorinated biphenyl mixtures." *Environ Toxicol Chem,* **27** (3): pp. 529-534.

[3] Ortiz, X., L. Carabellido, M. Marti, R. Marti, X. Tomas, and J. Diaz-Ferrero, (**2010)** "Elimination of persistent organic pollutants from fish oil with solid adsorbents." *Chemosphere,* **82** (9): pp. 1301-1307.

[4] Kelly, B.C., M.G. Ikonomou, J.D. Blair, A.E. Morin, and F.A. Gobas, (**2007)** "Food web-specific biomagnification of persistent organic pollutants." *Science,* **317** (5835): pp. 236-239.

[5] White, J.C., (**2010)** "Inheritance of p,p'-DDE phytoextraction ability in hybridized *Cucurbita pepo* cultivars." *Environ Sci Technol,* **44** (13): pp. 5165-5169.

[6] Walters, D.M., K.M. Fritz, B.R. Johnson, J.M. Lazorchak, and F.H. McCormick, (**2008)** "Influence of trophic position and spatial location on polychlorinated biphenyl (PCB) bioaccumulation in a stream food web." *Environ Sci Technol,* **42** (7): pp. 2316-2322.

[7] Helm, P.A., S.B. Gewurtz, D.M. Whittle, C.H. Marvin, A.T. Fisk, and G.T. Tomy, (**2008)** "Occurrence and biomagnification of polychlorinated naphthalenes and non- and mono-ortho PCBs in Lake Ontario sediment and biota." *Environ Sci Technol,* **42** (4): pp. 1024-1031.

[8] Marti, M., X. Ortiz, M. Gasser, R. Marti, M.J. Montana, and J. Diaz-Ferrero, (**2010)** "Persistent organic pollutants (PCDD/Fs, dioxin-like PCBs, marker PCBs, and PBDEs) in health supplements on the Spanish market." *Chemosphere,* **78** (10): pp. 1256-1262.

[9] Pozo, K., T. Harner, S.C. Lee, R.K. Sinha, B. Sengupta, M. Loewen, V. Geethalakshmi, K. Kannan, and V. Volpi, (**2011)** "Assessing seasonal and spatial trends of persistent organic pollutants (POPs) in Indian agricultural regions using PUF disk passive air samplers." *Environ Pollut,* **159** (2): pp. 646-653.

[10] Elfes, C.T., G.R. Vanblaricom, D. Boyd, J. Calambokidis, P.J. Clapham, R.W. Pearce, J. Robbins, J.C. Salinas, J.M. Straley, P.R. Wade, and M.M. Krahn, (**2010)** "Geographic variation of persistent organic pollutant levels in humpback whale (*Megaptera novaeangliae*) feeding areas of the North Pacific and North Atlantic." *Environ Toxicol Chem,* **29** (4): pp. 824-834.

[11] Chiou, C.T., L.J. Peters, and V.H. Freed, (**1979)** "A physical concept of soil-water equilibria for nonionic organic compounds." *Science,* **206** (4420): pp. 831-832.

[12] Murano, H., T. Otani, N. Seike, and M. Sakai, (**2010)** "Dieldrin uptake and translocation in plants growing in hydroponic medium." *Environ Toxicol Chem,* **29** (1): pp. 142-148.

[13] Collins, C., M. Fryer, and A. Grosso, (**2006)** "Plant uptake of non ionic organic chemicals." *Environ Sci Technol,* **40** (1): pp. 45-52.

[14] Sverdrup, L.E., T. Nielsen, and P.H. Krogh, (**2002)** "Soil ecotoxicity of polycyclic aromatic hydrocarbons in relation to soil sorption, lipophilicity, and water solubility." *Environ Sci Technol,* **36** (11): pp. 2429-2435.

[15] Lunney, A.I., B.A. Zeeb, and K.J. Reimer, (**2004)** "Uptake of weathered DDT in vascular plants: potential for phytoremediation." *Environ Sci Technol,* **38** (22): pp. 6147-6154.

[16] Mattina, M.J., W. Iannucci-Berger, and L. Dykas, (**2000)** "Chlordane uptake and its translocation in food crops." *J Agric Food Chem,* **48** (5): pp. 1909-1915.

[17] Dachs, J., R. Lohmann, W.A. Ockenden, L. Mejanelle, S.J. Eisenreich, and K.C. Jones, (**2002)** "Oceanic biogeochemical controls on global dynamics of persistent organic pollutants." *Environ Sci Technol,* **36** (20): pp. 4229-4237.

[18] Echeveste, P., J. Dachs, N. Berrojalbiz, and S. Agusti, (**2010)** "Decrease in the abundance and viability of oceanic phytoplankton due to trace levels of complex mixtures of organic pollutants." *Chemosphere,* **81** (2): pp. 161-168.

[19] Lohmann, R., K. Breivik, J. Dachs, and D. Muir, (**2007)** "Global fate of POPs: current and future research directions." *Environ Pollut,* **150** (1): pp. 150-165.

[20] Carmichael, S.L., A.H. Herring, A. Sjodin, R. Jones, L. Needham, C. Ma, K. Ding, and G.M. Shaw, (**2010)** "Hypospadias and halogenated organic pollutant levels in maternal mid-pregnancy serum samples." *Chemosphere,* **80** (6): pp. 641-646.

[21] Valeron, P.F., J.J. Pestano, O.P. Luzardo, M.L. Zumbado, M. Almeida, and L.D. Boada, (**2009)** "Differential effects exerted on human mammary epithelial cells by environmentally relevant organochlorine pesticides either individually or in combination." *Chem Biol Interact,* **180** (3): pp. 485-491.

[22] Shi, Y.Q., Y.P. Wang, Y. Song, H.W. Li, C.J. Liu, Z.G. Wu, and K.D. Yang, (**2010)** "p,p'-DDE induces testicular apoptosis in prepubertal rats via the Fas/FasL pathway." *Toxicol Lett,* **193** (1): pp. 79-85.

[23] Johri, A.K., M. Dua, D. Tuteja, R. Saxena, D.M. Saxena, and R. Lal, (**1996)** "Genetic manipulations of microorganisms for the degradation of hexachlorocyclohexane." *FEMS Microbiol Rev,* **19** (2): pp. 69-84.

[24] Elcey, C.D. and A.A. Kunhi, (**2010)** "Substantially enhanced degradation of hexachlorocyclohexane isomers by a microbial consortium on acclimation." *J Agric Food Chem,* **58** (2): pp. 1046-1054.

[25] Li, Y.F., M.T. Scholtz, and B.J. Van Heyst, (**2003)** "Global gridded emission inventories of beta-hexachlorocyclohexane." *Environ Sci Technol,* **37** (16): pp. 3493-3498.

[26] Nagata, Y., R. Endo, M. Ito, Y. Ohtsubo, and M. Tsuda, (**2007)** "Aerobic degradation of lindane (gamma-hexachlorocyclohexane) in bacteria and its biochemical and molecular basis." *Appl Microbiol Biotechnol,* **76** (4): pp. 741-752.

[27] Phillips, T.M., A.G. Seech, H. Lee, and J.T. Trevors, (**2005)** "Biodegradation of hexachlorocyclohexane (HCH) by microorganisms." *Biodegradation,* **16** (4): pp. 363-392.

[28] Lal, R., G. Pandey, P. Sharma, K. Kumari, S. Malhotra, R. Pandey, V. Raina, H.P. Kohler, C. Holliger, C. Jackson, and J.G. Oakeshott, (**2010)** "Biochemistry of microbial

degradation of hexachlorocyclohexane and prospects for bioremediation." *Microbiol Mol Biol Rev,* **74** (1): pp. 58-80.

[29] Weber, R., C. Gaus, M. Tysklind, P. Johnston, M. Forter, H. Hollert, E. Heinisch, I. Holoubek, M. Lloyd-Smith, S. Masunaga, P. Moccarelli, D. Santillo, N. Seike, R. Symons, J.P. Torres, M. Verta, G. Varbelow, J. Vijgen, A. Watson, P. Costner, J. Woelz, P. Wycisk, and M. Zennegg, (**2008)** "Dioxin- and POP-contaminated sites--contemporary and future relevance and challenges: overview on background, aims and scope of the series." *Environ Sci Pollut Res Int,* **15** (5): pp. 363-393.

[30] Singh, B.K., R.C. Kuhad, A. Singh, K.K. Tripathi, and P.K. Ghosh, (**2000)** "Microbial degradation of the pesticide lindane (gamma-hexachlorocyclohexane)." *Adv Appl Microbiol,* **47**: pp. 269-298.

[31] Barros, S.B., K. Simizu, and V.B. Junqueira, (**1991)** "Liver lipid peroxidation-related parameters after short-term administration of hexachlorocyclohexane isomers to rats." *Toxicol Lett,* **56** (1-2): pp. 137-144.

[32] Carlson, L.A. and B. Kolmodin-Hedman, (**1972)** "Hyper- -lipoproteinemia in men exposed to chlorinated hydrocarbon pesticides." *Acta Med Scand,* **192** (1-2): pp. 29-32.

[33] Carrero, I., M.D. Fernandez-Moreno, M.A. Perez-Albarsanz, and J.C. Prieto, (**1989)** "Lindane effect upon the vasoactive intestinal peptide receptor/effector system in rat enterocytes." *Biochem Biophys Res Commun,* **159** (3): pp. 1391-1396.

[34] Magour, S., H. Maser, and I. Steffen, (**1984)** "Effect of lindane on synaptosomal $Na^+/K^+$-ATPase in relation to its subcellular distribution in the brain." *Acta Pharmacol Toxicol (Copenh),* **54** (4): pp. 299-303.

[35] Hothem, R.L. and S.G. Zador, (**1995)** "Environmental contaminants in eggs of California least terns (*Sterna antillarum browni*)." *Bull Environ Contam Toxicol,* **55** (5): pp. 658-665.

[36] Boltner, D., S. Moreno-Morillas, and J.L. Ramos, (**2005)** "16S rDNA phylogeny and distribution of lin genes in novel hexachlorocyclohexane-degrading *Sphingomonas* strains." *Environ Microbiol,* **7** (9): pp. 1329-1338.

[37] Lal, R., C. Dogra, S. Malhotra, P. Sharma, and R. Pal, (**2006)** "Diversity, distribution and divergence of lin genes in hexachlorocyclohexane-degrading sphingomonads." *Trends Biotechnol,* **24** (3): pp. 121-130.

[38] Mohn, W.W., B. Mertens, J.D. Neufeld, W. Verstraete, and V. de Lorenzo, (**2006)** "Distribution and phylogeny of hexachlorocyclohexane-degrading bacteria in soils from Spain." *Environ Microbiol,* **8** (1): pp. 60-68.

[39] Heritage, A.D. and I.C. Rae, (**1977)** "Identification of intermediates formed during the degradation of hexachlorocyclohexanes by *Clostridium sphenoides*." *Appl Environ Microbiol,* **33** (6): pp. 1295-1297.

[40] Ohisa, N., M. Yamaguchi, and N. Kurihara, (**1980)** "Lindane degradation by cell-free extracts of *Clostridium rectum*." *Arch Microbiol,* **125** (3): pp. 221-225.

[41] Jagnow, G., K. Haider, and P.C. Ellwardt, (**1977)** "Anaerobic dechlorination and degradation of hexachlorocyclohexane isomers by anaerobic and facultative anaerobic bacteria." *Arch Microbiol,* **115** (3): pp. 285-292.

[42] Francis, A.J., R.J. Spanggord, and G.I. Ouchi, (**1975)** "Degradation of lindane by *Escherichia coli*." *Appl Microbiol,* **29** (4): pp. 567-568.

[43] Nawab, A., A. Aleem, and A. Malik, (**2003)** "Determination of organochlorine pesticides in agricultural soil with special reference to gamma-HCH degradation by *Pseudomonas* strains." *Bioresour Technol,* **88** (1): pp. 41-46.

[44] Adhya, T.K., S.K. Apte, K. Raghu, N. Sethunathan, and N.B. Murthy, (**1996)** "Novel polypeptides induced by the insecticide lindane (gamma-hexachlorocyclohexane) are required for its biodegradation by a *Sphingomonas paucimobilis* strain." *Biochem Biophys Res Commun,* **221** (3): pp. 755-761.

[45] Okeke, B.C., T. Siddique, M.C. Arbestain, and W.T. Frankenberger, (**2002)** "Biodegradation of gamma-hexachlorocyclohexane (lindane) and alpha-hexachlorocyclohexane in water and a soil slurry by a *Pandoraea* species." *J Agric Food Chem,* **50** (9): pp. 2548-2555.

[46] Thomas, J.C., F. Berger, M. Jacquier, D. Bernillon, F. Baud-Grasset, N. Truffaut, P. Normand, T.M. Vogel, and P. Simonet, (**1996)** "Isolation and characterization of a novel gamma-hexachlorocyclohexane-degrading bacterium." *J Bacteriol,* **178** (20): pp. 6049-6055.

[47] Bachmann, A., P. Walet, P. Wijnen, W. de Bruin, J.L. Huntjens, W. Roelofsen, and A.J. Zehnder, (**1988)** "Biodegradation of alpha- and beta-hexachlorocyclohexane in a soil slurry under different redox conditions." *Appl Environ Microbiol,* **54** (1): pp. 143-149.

[48] Sahu, S.K., K.K. Patnaik, and N. Sethunathan, (**1992)** "Dehydrochlorination of delta-isomer of hexachlorocyclohexane by a soil bacterium, *Pseudomonas sp*." *Bull Environ Contam Toxicol,* **48** (2): pp. 265-268.

[49] Sahu, S.K., K.K. Patnaik, M. Sharmila, and N. Sethunathan, (**1990)** "Degradation of alpha-, beta-, and gamma-Hexachlorocyclohexane by a soil bacterium under aerobic conditions." *Appl Environ Microbiol,* **56** (11): pp. 3620-3622.

[50] Arisoy, M. and N. Kolankaya, (**1997)** "Biodegradation of Lindane by *Pleurotus sajor-caju* and toxic effects of Lindane and its metabolites on mice." *Bull Environ Contam Toxicol,* **59** (3): pp. 352-359.

[51] Bumpus, J.A., M. Tien, D. Wright, and S.D. Aust, (**1985)** "Oxidation of persistent environmental pollutants by a white rot fungus." *Science,* **228** (4706): pp. 1434-1436.

[52] Kennedy, D.W., S.D. Aust, and J.A. Bumpus, (**1990)** "Comparative biodegradation of alkyl halide insecticides by the white rot fungus, *Phanerochaete chrysosporium* (BKM-F-1767)." *Appl Environ Microbiol,* **56** (8): pp. 2347-2353.

[53] Arisoy, M., (**1998)** "Biodegradation of chlorinated organic compounds by white-Rot fungi." *Bull Environ Contam Toxicol,* **60** (6): pp. 872-876.

[54] Gupta, A., C.P. Kaushik, and A. Kaushik, (**2001)** "Degradation of hexachlorocyclohexane isomers by two strains of *Alcaligenes faecalis* isolated from a contaminated site." *Bull Environ Contam Toxicol,* **66** (6): pp. 794-800.

[55] Kuritz, T. and C.P. Wolk, (**1995)** "Use of filamentous cyanobacteria for biodegradation of organic pollutants." *Appl Environ Microbiol,* **61** (3): pp. 1169.

[56] Datta, J., A.K. Maiti, D.P. Modak, P.K. Chakrabartty, P. Bhattacharyya, and P.K. Ray, (**2000)** "Metabolism of gamma-hexachlorocyclohexane by *Arthrobacter citreus* strain BI-100: Identification of metabolites." *J Gen Appl Microbiol,* **46** (2): pp. 59-67.

[57] Manickam, N., M. Mau, and M. Schlomann, (**2006)** "Characterization of the novel HCH-degrading strain, *Microbacterium sp.* ITRC1." *Appl Microbiol Biotechnol,* **69** (5): pp. 580-588.

[58] Nalin, R., P. Simonet, T.M. Vogel, and P. Normand, (**1999)** "*Rhodanobacter lindaniclasticus* gen. nov., sp. nov., a lindane-degrading bacterium." *Int J Syst Bacteriol,* **49 Pt 1**: pp. 19-23.

[59] Dadhwal, M., S. Jit, H. Kumari, and R. Lal, (**2009)** "*Sphingobium chinhatense sp*. nov., a hexachlorocyclohexane (HCH)-degrading bacterium isolated from an HCH dumpsite." *Int J Syst Evol Microbiol,* **59** (Pt 12): pp. 3140-3144.

[60] Ceremonie, H., H. Boubakri, P. Mavingui, P. Simonet, and T.M. Vogel, (**2006)** "Plasmid-encoded gamma-hexachlorocyclohexane degradation genes and insertion sequences in *Sphingobium francense* (ex-*Sphingomonas paucimobilis* Sp+)." *FEMS Microbiol Lett,* **257** (2): pp. 243-252.

[61] Bala, K., P. Sharma, and R. Lal, (**2010)** "*Sphingobium quisquiliarum sp*. nov., a hexachlorocyclohexane (HCH)-degrading bacterium isolated from an HCH-contaminated soil." *Int J Syst Evol Microbiol,* **60** (Pt 2): pp. 429-433.

[62] Yamamoto, S., S. Otsuka, Y. Murakami, M. Nishiyama, and K. Senoo, (**2009)** "Genetic diversity of gamma-hexachlorocyclohexane-degrading sphingomonads isolated from a single experimental field." *Lett Appl Microbiol,* **49** (4): pp. 472-477.

[63] Benimeli, C.S., G.R. Castro, A.P. Chaile, and M.J. Amoroso, (**2006)** "Lindane removal induction by *Streptomyces sp*. M7." *J Basic Microbiol,* **46** (5): pp. 348-357.

[64] Tekere, M., I. Ncube, J.S. Read, and R. Zvauya, (**2002)** "Biodegradation of the organochlorine pesticide, lindane by a sub-tropical white rot fungus in batch and packed bed bioreactor systems." *Environ Technol,* **23** (2): pp. 199-206.

[65] Imai, R., Y. Nagata, M. Fukuda, M. Takagi, and K. Yano, (**1991)** "Molecular cloning of a *Pseudomonas paucimobilis* gene encoding a 17-kilodalton polypeptide that eliminates HCl molecules from gamma-hexachlorocyclohexane." *J Bacteriol,* **173** (21): pp. 6811-6819.

[66] Nagata, Y., T. Nariya, R. Ohtomo, M. Fukuda, K. Yano, and M. Takagi, (**1993)** "Cloning and sequencing of a dehalogenase gene encoding an enzyme with hydrolase activity involved in the degradation of gamma-hexachlorocyclohexane in *Pseudomonas paucimobilis*." *J Bacteriol,* **175** (20): pp. 6403-6410.

[67] Nagata, Y., R. Ohtomo, K. Miyauchi, M. Fukuda, K. Yano, and M. Takagi, (**1994)** "Cloning and sequencing of a 2,5-dichloro-2,5-cyclohexadiene-1,4-diol dehydrogenase gene involved in the degradation of gamma-hexachlorocyclohexane in *Pseudomonas paucimobilis*." *J Bacteriol,* **176** (11): pp. 3117-3125.

[68] Miyauchi, K., S.K. Suh, Y. Nagata, and M. Takagi, (**1998)** "Cloning and sequencing of a 2,5-dichlorohydroquinone reductive dehalogenase gene whose product is involved in degradation of gamma-hexachlorocyclohexane by *Sphingomonas paucimobilis*." *J Bacteriol,* **180** (6): pp. 1354-1359.

[69] Miyauchi, K., Y. Adachi, Y. Nagata, and M. Takagi, (**1999)** "Cloning and sequencing of a novel meta-cleavage dioxygenase gene whose product is involved in degradation of gamma-hexachlorocyclohexane in *Sphingomonas paucimobilis*." *J Bacteriol,* **181** (21): pp. 6712-6719.

[70] Endo, R., M. Kamakura, K. Miyauchi, M. Fukuda, Y. Ohtsubo, M. Tsuda, and Y. Nagata, (**2005)** "Identification and characterization of genes involved in the downstream degradation pathway of gamma-hexachlorocyclohexane in *Sphingomonas paucimobilis* UT26." *J Bacteriol,* **187** (3): pp. 847-853.

[71] Kmunicek, J., K. Hynkova, T. Jedlicka, Y. Nagata, A. Negri, F. Gago, R.C. Wade, and J. Damborsky, (**2005)** "Quantitative analysis of substrate specificity of haloalkane dehalogenase LinB from Sphingomonas paucimobilis UT26." *Biochemistry,* **44** (9): pp. 3390-3401.

[72] Nagata, Y., K. Miyauchi, J. Damborsky, K. Manova, A. Ansorgova, and M. Takagi, (**1997)** "Purification and characterization of a haloalkane dehalogenase of a new substrate class from a gamma-hexachlorocyclohexane-degrading bacterium, *Sphingomonas paucimobilis* UT26." *Appl Environ Microbiol,* **63** (9): pp. 3707-3710.

[73] Marek, J., J. Vevodova, I.K. Smatanova, Y. Nagata, L.A. Svensson, J. Newman, M. Takagi, and J. Damborsky, (**2000)** "Crystal structure of the haloalkane dehalogenase from *Sphingomonas paucimobilis* UT26." *Biochemistry,* **39** (46): pp. 14082-14086.

[74] Oakley, A.J., M. Klvana, M. Otyepka, Y. Nagata, M.C. Wilce, and J. Damborsky, (**2004)** "Crystal structure of haloalkane dehalogenase LinB from *Sphingomonas paucimobilis* UT26 at 0.95 A resolution: dynamics of catalytic residues." *Biochemistry,* **43** (4): pp. 870-878.

[75] Oakley, A.J., Z. Prokop, M. Bohac, J. Kmunicek, T. Jedlicka, M. Monincova, I. Kuta-Smatanova, Y. Nagata, J. Damborsky, and M.C. Wilce, (**2002)** "Exploring the structure and activity of haloalkane dehalogenase from *Sphingomonas paucimobilis* UT26: evidence for product- and water-mediated inhibition." *Biochemistry,* **41** (15): pp. 4847-4855.

[76] Streltsov, V.A., Z. Prokop, J. Damborsky, Y. Nagata, A. Oakley, and M.C. Wilce, (**2003)** "Haloalkane dehalogenase LinB from *Sphingomonas paucimobilis* UT26: X-ray crystallographic studies of dehalogenation of brominated substrates." *Biochemistry,* **42** (34): pp. 10104-10112.

[77] Prokop, Z., M. Monincova, R. Chaloupkova, M. Klvana, Y. Nagata, D.B. Janssen, and J. Damborsky, (**2003)** "Catalytic mechanism of the maloalkane dehalogenase LinB from *Sphingomonas paucimobilis* UT26." *J Biol Chem,* **278** (46): pp. 45094-45100.

[78] Chaloupkova, R., J. Sykorova, Z. Prokop, A. Jesenska, M. Monincova, M. Pavlova, M. Tsuda, Y. Nagata, and J. Damborsky, (**2003)** "Modification of activity and specificity of haloalkane dehalogenase from *Sphingomonas paucimobilis* UT26 by engineering of its entrance tunnel." *J Biol Chem,* **278** (52): pp. 52622-52628.

[79] Nagata, Y., Z. Prokop, S. Marvanova, J. Sykorova, M. Monincova, M. Tsuda, and J. Damborsky, (**2003)** "Reconstruction of mycobacterial dehalogenase Rv2579 by cumulative mutagenesis of haloalkane dehalogenase LinB." *Appl Environ Microbiol,* **69** (4): pp. 2349-2355.

[80] Damborsky, J., E. Rorije, A. Jesenska, Y. Nagata, G. Klopman, and W.J. Peijnenburg, (**2001)** "Structure-specificity relationships for haloalkane dehalogenases." *Environ Toxicol Chem,* **20** (12): pp. 2681-2689.

[81] Janssen, D.B., (**2004)** "Evolving haloalkane dehalogenases." *Curr Opin Chem Biol,* **8** (2): pp. 150-159.

[82] Persson, B., M. Krook, and H. Jornvall, (**1991)** "Characteristics of short-chain alcohol dehydrogenases and related enzymes." *Eur J Biochem,* **200** (2): pp. 537-543.

[83] Dogra, C., V. Raina, R. Pal, M. Suar, S. Lal, K.H. Gartemann, C. Holliger, J.R. van der Meer, and R. Lal, (**2004)** "Organization of lin genes and IS6100 among different strains of hexachlorocyclohexane-degrading *Sphingomonas paucimobilis*: evidence for horizontal gene transfer." *J Bacteriol,* **186** (8): pp. 2225-2235.

[84] Wu, J., Q. Hong, P. Han, J. He, and S. Li, (**2007)** "A gene linB2 responsible for the conversion of beta-HCH and 2,3,4,5,6-pentachlorocyclohexanol in *Sphingomonas sp*. BHC-A." *Appl Microbiol Biotechnol,* **73** (5): pp. 1097-1105.

[85] Watanabe, I. and S. Sakai, (**2003)** "Environmental release and behavior of brominated flame retardants." *Environ Int,* **29** (6): pp. 665-682.

[86] Sjodin, A., D.G. Patterson, Jr., and A. Bergman, (**2003)** "A review on human exposure to brominated flame retardants--particularly polybrominated diphenyl ethers." *Environ Int,* **29** (6): pp. 829-839.

[87] Holmstrand, H., M. Unger, D. Carrizo, P. Andersson, and O. Gustafsson, (**2010)** "Compound-specific bromine isotope analysis of brominated diphenyl ethers using gas chromatography multiple collector/inductively coupled plasma mass spectrometry." *Rapid Commun Mass Spectrom,* **24** (14): pp. 2135-2142.

[88] Birnbaum, L.S. and D.F. Staskal, (**2004)** "Brominated flame retardants: cause for concern?" *Environ Health Perspect,* **112** (1): pp. 9-17.

[89] Alaee, M., P. Arias, A. Sjodin, and A. Bergman, (**2003)** "An overview of commercially used brominated flame retardants, their applications, their use patterns in different countries/regions and possible modes of release." *Environ Int,* **29** (6): pp. 683-689.

[90] de Wit, C.A., M. Alaee, and D.C. Muir, (**2006)** "Levels and trends of brominated flame retardants in the Arctic." *Chemosphere,* **64** (2): pp. 209-233.

[91] Law, R.J., C.R. Allchin, J. de Boer, A. Covaci, D. Herzke, P. Lepom, S. Morris, J. Tronczynski, and C.A. de Wit, (**2006)** "Levels and trends of brominated flame retardants in the European environment." *Chemosphere,* **64** (2): pp. 187-208.

[92] de Wit, C.A., (**2002)** "An overview of brominated flame retardants in the environment." *Chemosphere,* **46** (5): pp. 583-624.

[93] Hermanson, M.H., E. Isaksson, S. Forsstrom, C. Teixeira, D.C. Muir, V.A. Pohjola, and R.S. van de Wal, (**2010)** "Deposition history of brominated flame retardant compounds in an ice core from Holtedahlfonna, Svalbard, Norway." *Environ Sci Technol,* **44** (19): pp. 7405-7410.

[94] Covaci, A., A.C. Gerecke, R.J. Law, S. Voorspoels, M. Kohler, N.V. Heeb, H. Leslie, C.R. Allchin, and J. De Boer, (**2006)** "Hexabromocyclododecanes (HBCDs) in the environment and humans: a review." *Environ Sci Technol,* **40** (12): pp. 3679-3688.

[95] Gouin, T., G.O. Thomas, C. Chaemfa, T. Harner, D. Mackay, and K.C. Jones, (**2006)** "Concentrations of decabromodiphenyl ether in air from Southern Ontario: implications for particle-bound transport." *Chemosphere,* **64** (2): pp. 256-261.

[96] Darnerud, P.O., G.S. Eriksen, T. Johannesson, P.B. Larsen, and M. Viluksela, (**2001)** "Polybrominated diphenyl ethers: occurrence, dietary exposure, and toxicology." *Environ Health Perspect,* **109 Suppl 1**: pp. 49-68.

[97] Dodder, N.G., B. Strandberg, and R.A. Hites, (**2002)** "Concentrations and spatial variations of polybrominated diphenyl ethers and several organochlorine compounds in fishes from the northeastern United States." *Environ Sci Technol,* **36** (2): pp. 146-151.

[98] Palm, A., I.T. Cousins, D. Mackay, M. Tysklind, C. Metcalfe, and M. Alaee, (**2002)** "Assessing the environmental fate of chemicals of emerging concern: a case study of the polybrominated diphenyl ethers." *Environ Pollut,* **117** (2): pp. 195-213.

[99] Rahman, F., K.H. Langford, M.D. Scrimshaw, and J.N. Lester, (**2001)** "Polybrominated diphenyl ether (PBDE) flame retardants." *Sci Total Environ,* **275** (1-3): pp. 1-17.

[100] Strandberg, B., N.G. Dodder, I. Basu, and R.A. Hites, (**2001)** "Concentrations and spatial variations of polybrominated diphenyl ethers and other organohalogen compounds in Great Lakes air." *Environ Sci Technol,* **35** (6): pp. 1078-1083.

[101] Zhao, Y.Y., F.M. Tao, and E.Y. Zeng, (**2008)** "Theoretical study on the chemical properties of polybrominated diphenyl ethers." *Chemosphere,* **70** (5): pp. 901-907.

[102] Hites, R.A., (**2004)** "Polybrominated diphenyl ethers in the environment and in people: a meta-analysis of concentrations." *Environ Sci Technol,* **38** (4): pp. 945-956.

[103] Safe, S., (**1990)** "Polychlorinated biphenyls (PCBs), dibenzo-p-dioxins (PCDDs), dibenzofurans (PCDFs), and related compounds: environmental and mechanistic considerations which support the development of toxic equivalency factors (TEFs)." *Crit Rev Toxicol,* **21** (1): pp. 51-88.

[104] Behnisch, P.A., K. Hosoe, and S. Sakai, (**2003)** "Brominated dioxin-like compounds: in vitro assessment in comparison to classical dioxin-like compounds and other polyaromatic compounds." *Environ Int,* **29** (6): pp. 861-877.

[105] Meerts, I.A., R.J. Letcher, S. Hoving, G. Marsh, A. Bergman, J.G. Lemmen, B. van der Burg, and A. Brouwer, (**2001)** "In vitro estrogenicity of polybrominated diphenyl ethers, hydroxylated PDBEs, and polybrominated bisphenol A compounds." *Environ Health Perspect,* **109** (4): pp. 399-407.

[106] Meerts, I.A., J.J. van Zanden, E.A. Luijks, I. van Leeuwen-Bol, G. Marsh, E. Jakobsson, A. Bergman, and A. Brouwer, (**2000)** "Potent competitive interactions of some brominated flame retardants and related compounds with human transthyretin *in vitro*." *Toxicol Sci,* **56** (1): pp. 95-104.

[107] Ebert, J. and M. Bahadir, (**2003)** "Formation of PBDD/F from flame-retarded plastic materials under thermal stress." *Environ Int,* **29** (6): pp. 711-716.

[108] He, J., K.R. Robrock, and L. Alvarez-Cohen, (**2006)** "Microbial reductive debromination of polybrominated diphenyl ethers (PBDEs)." *Environ Sci Technol,* **40** (14): pp. 4429-4434.

[109] Eriksson, P., E. Jakobsson, and A. Fredriksson, (**2001)** "Brominated flame retardants: a novel class of developmental neurotoxicants in our environment?" *Environ Health Perspect,* **109** (9): pp. 903-908.

[110] Fernlof, G., I. Gadhasson, K. Podra, P.O. Darnerud, and A. Thuvander, (**1997)** "Lack of effects of some individual polybrominated diphenyl ether (PBDE) and polychlorinated biphenyl (PCB) congeners on human lymphocyte functions *in vitro*." *Toxicol Lett,* **90** (2-3): pp. 189-197.

[111] Schmidt, S., P. Fortnagel, and R.M. Wittich, (**1993)** "Biodegradation and transformation of 4,4'- and 2,4-dihalodiphenyl ethers by *Sphingomonas sp*. strain SS33." *Appl Environ Microbiol,* **59** (11): pp. 3931-3933.

[112] Rayne, S., M.G. Ikonomou, and M.D. Whale, (**2003)** "Anaerobic microbial and photochemical degradation of 4,4'-dibromodiphenyl ether." *Water Res,* **37** (3): pp. 551-560.

[113] Gerecke, A.C., P.C. Hartmann, N.V. Heeb, H.P. Kohler, W. Giger, P. Schmid, M. Zennegg, and M. Kohler, (**2005)** "Anaerobic degradation of decabromodiphenyl ether." *Environ Sci Technol,* **39** (4): pp. 1078-1083.

[114] Robrock, K.R., M. Coelhan, D.L. Sedlak, and L. Alvarez-Cohent, (**2009)** "Aerobic biotransformation of polybrominated diphenyl ethers (PBDEs) by bacterial isolates." *Environ Sci Technol,* **43** (15): pp. 5705-5711.

[115] Schmidt, S., R.M. Wittich, D. Erdmann, H. Wilkes, W. Francke, and P. Fortnagel, (**1992)** "Biodegradation of diphenyl ether and its monohalogenated derivatives by *Sphingomonas sp*. strain SS3." *Appl Environ Microbiol,* **58** (9): pp. 2744-2750.

[116] Kim, Y.M., I.H. Nam, K. Murugesan, S. Schmidt, D.E. Crowley, and Y.S. Chang, (**2007)** "Biodegradation of diphenyl ether and transformation of selected brominated congeners by *Sphingomonas sp*. PH-07." *Appl Microbiol Biotechnol,* **77** (1): pp. 187-194.

[117] Pfeifer, F., H.G. Truper, J. Klein, and S. Schacht, (**1993)** "Degradation of diphenylether by *Pseudomonas cepacia* Et4: enzymatic release of phenol from 2,3-dihydroxydiphenylether." *Arch Microbiol,* **159** (4): pp. 323-329.

[118] Schauer, F., K. Henning, H. Pscheidl, R.M. Wittich, P. Fortnagel, H. Wilkes, V. Sinnwell, and W. Francke, (**1995)** "Biotransformation of diphenyl ether by the yeast *Trichosporon beigelii* SBUG 752." *Biodegradation,* **6** (2): pp. 173-180.

[119] Takahashi, A., T. Agatsuma, M. Matsuda, T. Ohta, T. Nunozawa, T. Endo, and S. Nozoe, (**1992)** "Russuphelin A, a new cytotoxic substance from the mushroom *Russula subnigricans* Hongo." *Chem Pharm Bull (Tokyo),* **40** (12): pp. 3185-3188.

[120] Takahashi, A., T. Agatsuma, T. Ohta, T. Nunozawa, T. Endo, and S. Nozoe, (**1993)** "Russuphelins B, C, D, E and F, new cytotoxic substances from the mushroom *Russula subnigricans* Hongo." *Chem Pharm Bull (Tokyo),* **41** (10): pp. 1726-1729.

[121] Hall-Stoodley, L., J.W. Costerton, and P. Stoodley, (**2004)** "Bacterial biofilms: from the natural environment to infectious diseases." *Nat Rev Microbiol,* **2** (2): pp. 95-108.

[122] Hoffman, L.R., D.A. D'Argenio, M.J. MacCoss, Z. Zhang, R.A. Jones, and S.I. Miller, (**2005)** "Aminoglycoside antibiotics induce bacterial biofilm formation." *Nature,* **436** (7054): pp. 1171-1175.

[123] Karatan, E. and P. Watnick, (**2009)** "Signals, regulatory networks, and materials that build and break bacterial biofilms." *Microbiol Mol Biol Rev,* **73** (2): pp. 310-347.

[124] An, D. and M.R. Parsek, (**2007)** "The promise and peril of transcriptional profiling in biofilm communities." *Curr Opin Microbiol,* **10** (3): pp. 292-296.

[125] Rice, S.A., M. Givskov, P. Steinberg, and S. Kjelleberg, (**1999)** "Bacterial signals and antagonists: the interaction between bacteria and higher organisms." *J Mol Microbiol Biotechnol,* **1** (1): pp. 23-31.

[126] Caiazza, N.C. and G.A. O'Toole, (**2004)** "SadB is required for the transition from reversible to irreversible attachment during biofilm formation by *Pseudomonas aeruginosa* PA14." *J Bacteriol,* **186** (14): pp. 4476-4485.

[127] Toutain, C.M., N.C. Caizza, M.E. Zegans, and G.A. O'Toole, (**2007)** "Roles for flagellar stators in biofilm formation by *Pseudomonas aeruginosa*." *Res Microbiol,* **158** (5): pp. 471-477.

[128] Klausen, M., A. Aaes-Jorgensen, S. Molin, and T. Tolker-Nielsen, (**2003)** "Involvement of bacterial migration in the development of complex multicellular structures in *Pseudomonas aeruginosa* biofilms." *Mol Microbiol,* **50** (1): pp. 61-68.

[129] O'Toole, G.A. and R. Kolter, (**1998)** "Flagellar and twitching motility are necessary for *Pseudomonas aeruginosa* biofilm development." *Mol Microbiol,* **30** (2): pp. 295-304.

[130] Vallet, I., J.W. Olson, S. Lory, A. Lazdunski, and A. Filloux, (**2001)** "The chaperone/usher pathways of *Pseudomonas aeruginosa*: identification of fimbrial gene clusters (cup) and their involvement in biofilm formation." *Proc Natl Acad Sci U S A,* **98** (12): pp. 6911-6916.

[131] Ryder, C., M. Byrd, and D.J. Wozniak, (**2007)** "Role of polysaccharides in *Pseudomonas aeruginosa* biofilm development." *Curr Opin Microbiol,* **10** (6): pp. 644-648.

[132] Izano, E.A., M.A. Amarante, W.B. Kher, and J.B. Kaplan, (**2008)** "Differential roles of poly-N-acetylglucosamine surface polysaccharide and extracellular DNA in

*Staphylococcus aureus* and *Staphylococcus epidermidis* biofilms." *Appl Environ Microbiol,* **74** (2): pp. 470-476.

[133] Kaplan, J.B., C. Ragunath, N. Ramasubbu, and D.H. Fine, (**2003)** "Detachment of *Actinobacillus actinomycetemcomitans* biofilm cells by an endogenous beta-hexosaminidase activity." *J Bacteriol,* **185** (16): pp. 4693-4698.

[134] Kaplan, J.B., C. Ragunath, K. Velliyagounder, D.H. Fine, and N. Ramasubbu, (**2004)** "Enzymatic detachment of *Staphylococcus epidermidis* biofilms." *Antimicrob Agents Chemother,* **48** (7): pp. 2633-2636.

[135] Xavier, J.B., C. Picioreanu, S.A. Rani, M.C. van Loosdrecht, and P.S. Stewart, (**2005)** "Biofilm-control strategies based on enzymic disruption of the extracellular polymeric substance matrix--a modelling study." *Microbiology,* **151** (Pt 12): pp. 3817-3832.

[136] Davies, D.G. and C.N. Marques, (**2009)** "A fatty acid messenger is responsible for inducing dispersion in microbial biofilms." *J Bacteriol,* **191** (5): pp. 1393-1403.

[137] Stewart, P.S. and J.W. Costerton, (**2001)** "Antibiotic resistance of bacteria in biofilms." *Lancet,* **358** (9276): pp. 135-138.

[138] Spoering, A.L. and K. Lewis, (**2001)** "Biofilms and planktonic cells of *Pseudomonas aeruginosa* have similar resistance to killing by antimicrobials." *J Bacteriol,* **183** (23): pp. 6746-6751.

[139] Lunsdorf, H., I. Brummer, K.N. Timmis, and I. Wagner-Dobler, (**1997)** "Metal selectivity of *in situ* microcolonies in biofilms of the Elbe river." *J Bacteriol,* **179** (1): pp. 31-40.

[140] Baldi, F., N. Ivosevic, A. Minacci, M. Pepi, R. Fani, V.V. Svetlicic, and V.V. utic, (**1999)** "Adhesion of acinetobacter venetianus to diesel fuel droplets studied with *in situ* electrochemical and molecular probes." *Appl Environ Microbiol,* **65** (5): pp. 2041-2048.

[141] MacDonald, I.R., G. Bohrmann, E. Escobar, F. Abegg, P. Blanchon, V. Blinova, W. Bruckmann, M. Drews, A. Eisenhauer, X. Han, K. Heeschen, F. Meier, C. Mortera, T. Naehr, B. Orcutt, B. Bernard, J. Brooks, and M. de Farago, (**2004)** "Asphalt volcanism and chemosynthetic life in the Campeche Knolls, Gulf of Mexico." *Science,* **304** (5673): pp. 999-1002.

[142] Macedo, A.J., U. Kuhlicke, T.R. Neu, K.N. Timmis, and W.R. Abraham, (**2005)** "Three stages of a biofilm community developing at the liquid-liquid interface between polychlorinated biphenyls and water." *Appl Environ Microbiol,* **71** (11): pp. 7301-7309.

[143] Kirk, J.L., L.A. Beaudette, M. Hart, P. Moutoglis, J.N. Klironomos, H. Lee, and J.T. Trevors, (**2004)** "Methods of studying soil microbial diversity." *J Microbiol Methods,* **58** (2): pp. 169-188.

[144] Konopka, A., L. Oliver, and R.F. Turco, Jr., (**1998)** "The Use of Carbon Substrate Utilization Patterns in Environmental and Ecological Microbiology." *Microb Ecol,* **35** (2): pp. 103-115.

[145] Kim, J.S., J.B. Joo, H.Y. Weon, C.S. Kang, S.K. Lee, and C.S. Yahng, (**2002)** "FAME analysis to monitor impact of organic matter on soil bacterial populations." *Journal of Microbiology and Biotechnology,* **12** (3): pp. 382-388.

[146] Muyzer, G., E.C. de Waal, and A.G. Uitterlinden, (**1993)** "Profiling of complex microbial populations by denaturing gradient gel electrophoresis analysis of polymerase chain reaction-amplified genes coding for 16S rRNA." *Appl Environ Microbiol,* **59** (3): pp. 695-700.

[147] Muyzer, G., (**1999)** "DGGE/TGGE a method for identifying genes from natural ecosystems." *Curr Opin Microbiol,* **2** (3): pp. 317-322.

[148] Ercolini, D., (**2004)** "PCR-DGGE fingerprinting: novel strategies for detection of microbes in food." *J Microbiol Methods,* **56** (3): pp. 297-314.

[149] Liu, W.T., T.L. Marsh, H. Cheng, and L.J. Forney, (**1997)** "Characterization of microbial diversity by determining terminal restriction fragment length polymorphisms of genes encoding 16S rRNA." *Appl Environ Microbiol,* **63** (11): pp. 4516-4522.

[150] Fagervold, S.K., J.E. Watts, H.D. May, and K.R. Sowers, (**2005)** "Sequential reductive dechlorination of meta-chlorinated polychlorinated biphenyl congeners in sediment microcosms by two different *Chloroflexi* phylotypes." *Appl Environ Microbiol,* **71** (12): pp. 8085-8090.

[151] Kruger, M.C. and D.F. Horrobin, (**1997)** "Calcium metabolism, osteoporosis and essential fatty acids: a review." *Prog Lipid Res,* **36** (2-3): pp. 131-151.

[152] Abraham, W.R., C. Hesse, and O. Pelz, (**1998)** "Ratios of carbon isotopes in microbial lipids as an indicator of substrate usage." *Appl Environ Microbiol,* **64** (11): pp. 4202-4209.

[153] Kohring, L.L., D.B. Ringelberg, R. Devereux, D.A. Stahl, M.W. Mittelman, and D.C. White, (**1994)** "Comparison of phylogenetic relationships based on phospholipid fatty acid profiles and ribosomal RNA sequence similarities among dissimilatory sulfate-reducing bacteria." *FEMS Microbiol Lett,* **119** (3): pp. 303-308.

[154] Webster, G., L.C. Watt, J. Rinna, J.C. Fry, R.P. Evershed, R.J. Parkes, and A.J. Weightman, (**2006)** "A comparison of stable-isotope probing of DNA and phospholipid fatty acids to study prokaryotic functional diversity in sulfate-reducing marine sediment enrichment slurries." *Environ Microbiol,* **8** (9): pp. 1575-1589.

[155] Kaneda, T., (**1991)** "Iso- and anteiso-fatty acids in bacteria: biosynthesis, function, and taxonomic significance." *Microbiol Rev,* **55** (2): pp. 288-302.

[156] Lambe, D.W., Jr., K.P. Ferguson, and W.R. Mayberry, (**1982)** "Characterization of *Bacteroides gingivalis* by direct fluorescent antibody staining and cellular fatty acid profiles." *Can J Microbiol,* **28** (4): pp. 367-374.

[157] Moss, C.W., (**1981)** "Gas-liquid chromatography as an analytical tool in microbiology." *J Chromatogr,* **203**: pp. 337-347.

[158] Veys, A., W. Callewaert, E. Waelkens, and K. Van den Abbeele, (**1989)** "Application of gas-liquid chromatography to the routine identification of nonfermenting gram-negative bacteria in clinical specimens." *J Clin Microbiol,* **27** (7): pp. 1538-1542.

[159] Stahl, P.D. and M.J. Klug, (**1996)** "Characterization and differentiation of filamentous fungi based on fatty acid composition." *Appl Environ Microbiol,* **62** (11): pp. 4136-4146.

[160] Brondz, I., I. Olsen, and M. Sjostrom, (**1989)** "Gas chromatographic assessment of alcoholyzed fatty acids from yeasts: a new chemotaxonomic method." *J Clin Microbiol,* **27** (12): pp. 2815-2819.

[161] Gunasekaran, M. and W.T. Hughes, (**1980)** "Gas-liquid chromatography: a rapid method for identification of different species of Candida." *Mycologia,* **72** (3): pp. 505-511.

[162] Miller, K.J., (**1985)** "Effects of temperature and sodium chloride concentration on the phospholipid and fatty acid compositions of a halotolerant *Planococcus sp*." *J Bacteriol,* **162** (1): pp. 263-270.

[163] Moss, C.W., M.A. Lambert, and W.H. Merwin, (**1974)** "Comparison of rapid methods for analysis of bacterial fatty acids." *Appl Microbiol,* **28** (1): pp. 80-85.

[164] Fang, J., M.J. Barcelona, and J.D. Semrau, (**2000)** "Characterization of methanotrophic bacteria on the basis of intact phospholipid profiles." *FEMS Microbiol Lett,* **189** (1): pp. 67-72.

[165] Welch, D.F., (**1991)** "Applications of cellular fatty acid analysis." *Clin Microbiol Rev,* **4** (4): pp. 422-438.

[166] Vestal, J.R. and D.C. White, (**1989)** "Lipid analysis in microbial ecology: quantitative approaches to the study of microbial communities." *Bioscience,* **39** (8): pp. 535-541.

[167] Orita, M., H. Iwahana, H. Kanazawa, K. Hayashi, and T. Sekiya, (**1989)** "Detection of polymorphisms of human DNA by gel electrophoresis as single-strand conformation polymorphisms." *Proc Natl Acad Sci U S A,* **86** (8): pp. 2766-2770.

[168] Schwieger, F. and C.C. Tebbe, (**1998)** "A new approach to utilize PCR-single-strand-conformation polymorphism for 16S rRNA gene-based microbial community analysis." *Appl Environ Microbiol,* **64** (12): pp. 4870-4876.

[169] Callon, C., C. Delbes, F. Duthoit, and M.C. Montel, (**2006)** "Application of SSCP-PCR fingerprinting to profile the yeast community in raw milk Salers cheeses." *Syst Appl Microbiol,* **29** (2): pp. 172-180.

[170] Mohr, K.I. and C.C. Tebbe, (**2006)** "Diversity and phylotype consistency of bacteria in the guts of three bee species (*Apoidea*) at an oilseed rape field." *Environ Microbiol,* **8** (2): pp. 258-272.

[171] He, J., Z. Xu, and J. Hughes, (**2005)** "Analyses of soil fungal communities in adjacent natural forest and hoop pine plantation ecosystems of subtropical Australia using molecular approaches based on 18S rRNA genes." *FEMS Microbiol Lett,* **247** (1): pp. 91-100.

[172] Junca, H. and D.H. Pieper, (**2004)** "Functional gene diversity analysis in BTEX contaminated soils by means of PCR-SSCP DNA fingerprinting: comparative diversity assessment against bacterial isolates and PCR-DNA clone libraries." *Environ Microbiol,* **6** (2): pp. 95-110.

[173] Schmalenberger, A. and C.C. Tebbe, (**2003)** "Bacterial diversity in maize rhizospheres: conclusions on the use of genetic profiles based on PCR-amplified partial small subunit rRNA genes in ecological studies." *Mol Ecol,* **12** (1): pp. 251-262.

[174] Delbes, C., M. Leclerc, E. Zumstein, J.J. Godon, and R. Moletta, (**2001)** "A molecular method to study population and activity dynamics in anaerobic digestors." *Water Sci Technol,* **43** (1): pp. 51-57.

[175] Hunter, R.C. and T.J. Beveridge, (**2005)** "High-resolution visualization of *Pseudomonas aeruginosa* PAO1 biofilms by freeze-substitution transmission electron microscopy." *J Bacteriol,* **187** (22): pp. 7619-7630.

[176] Cao, T., H. Tang, X. Liang, A. Wang, G.W. Auner, S.O. Salley, and K.Y. Ng, (**2006)** "Nanoscale investigation on adhesion of *E. coli* to surface modified silicone using atomic force microscopy." *Biotechnol Bioeng,* **94** (1): pp. 167-176.

[177] Kodjikian, L., C. Burillon, G. Lina, C. Roques, G. Pellon, J. Freney, and F.N. Renaud, (**2003)** "Biofilm formation on intraocular lenses by a clinical strain encoding the ica locus: a scanning electron microscopy study." *Invest Ophthalmol Vis Sci,* **44** (10): pp. 4382-4387.

[178] El Nemr, A. and A.M. Abd-Allah, (**2004)** "Organochlorine contamination in some marketable fish in Egypt." *Chemosphere,* **54** (10): pp. 1401-1406.

[179] El Nemr, A., T.O. Said, A. Khaled, A. El Sikaily, and A.M. Abd-Allah, (**2003)** "Polychlorinated biphenyls and chlorinated pesticides in mussels collected from the Egyptian Mediterranean coast." *Bull Environ Contam Toxicol,* **71** (2): pp. 290-297.

[180] Khaled, A., A. El Nemr, T.O. Said, A. El-Sikaily, and A.M. Abd-Alla, (**2004)** "Polychlorinated biphenyls and chlorinated pesticides in mussels from the Egyptian Red Sea coast." *Chemosphere,* **54** (10): pp. 1407-1412.

[181] Saad, M.A.H., S.R. McComas, and S.J. Eisenreich, (**1985)** "Metals and chlorinated hydrocarbons in surficial sediments of three nile Delta lakes, Egypt." *Water, Air, & Soil Pollution,* **24** (1): pp. 27-39.

[182] Harry, M., B. Gambier, and E. Garnier-Sillam, (**2000)** "Soil conservation for DNA preservation for bacterial molecular studies." *European Journal of Soil Biology,* **36** (1): pp. 51-55.

[183] Mullis, K.B., (**1990)** "The unusual origin of the polymerase chain reaction." *Sci Am,* **262** (4): pp. 56-61, 64-55.

[184] Chenna, R., H. Sugawara, T. Koike, R. Lopez, T.J. Gibson, D.G. Higgins, and J.D. Thompson, (**2003)** "Multiple sequence alignment with the clustal series of programs." *Nucleic Acids Res,* **31** (13): pp. 3497-3500.

[185] Tamura, K., J. Dudley, M. Nei, and S. Kumar, (**2007)** "MEGA4: molecular evolutionary genetics analysis (MEGA) software version 4.0." *Mol Biol Evol,* **24** (8): pp. 1596-1599.

[186] Saitou, N. and M. Nei, (**1987)** "The neighbor-joining method: a new method for reconstructing phylogenetic trees." *Mol Biol Evol,* **4** (4): pp. 406-425.

[187] Mosmann, T., (**1983)** "Rapid colorimetric assay for cellular growth and survival: application to proliferation and cytotoxicity assays." *J Immunol Methods,* **65** (1-2): pp. 55-63.

[188] Olsen, G.J., D.J. Lane, S.J. Giovannoni, N.R. Pace, and D.A. Stahl, (**1986)** "Microbial ecology and evolution: a ribosomal RNA approach." *Annu Rev Microbiol,* **40**: pp. 337-365.

[189] Peters, S., S. Koschinsky, F. Schwieger, and C.C. Tebbe, (**2000)** "Succession of microbial communities during hot composting as detected by PCR-single-strand-conformation polymorphism-based genetic profiles of small-subunit rRNA genes." *Appl Environ Microbiol,* **66** (3): pp. 930-936.

[190] Schmalenberger, A., F. Schwieger, and C.C. Tebbe, (**2001)** "Effect of primers hybridizing to different evolutionarily conserved regions of the small-subunit rRNA gene in PCR-based microbial community analyses and genetic profiling." *Appl Environ Microbiol,* **67** (8): pp. 3557-3563.

[191] Bassam, B.J. and P.M. Gresshoff, (**2007)** "Silver staining DNA in polyacrylamide gels." *Nat Protoc,* **2** (11): pp. 2649-2654.

[192] Nielsen, A.T., T. Tolker-Nielsen, K.B. Barken, and S. Molin, (**2000)** "Role of commensal relationships on the spatial structure of a surface-attached microbial consortium." *Environ Microbiol,* **2** (1): pp. 59-68.

[193] Schachter, B., (**2003)** "Slimy business--the biotechnology of biofilms." *Nat Biotechnol,* **21** (4): pp. 361-365.

[194] Matz, C., T. Bergfeld, S.A. Rice, and S. Kjelleberg, (**2004)** "Microcolonies, quorum sensing and cytotoxicity determine the survival of *Pseudomonas aeruginosa* biofilms exposed to protozoan grazing." *Environ Microbiol,* **6** (3): pp. 218-226.

[195] Hammel, K.E., P.J. Tardone, M.A. Moen, and L.A. Price, (**1989)** "Biomimetic oxidation of nonphenolic lignin models by Mn(III): new observations on the oxidizability of guaiacyl and syringyl substructures." *Arch Biochem Biophys,* **270** (1): pp. 404-409.

[196] Barr, D.P. and S.D. Aust, (**1994)** "Pollutant degradation by white rot fungi." *Rev Environ Contam Toxicol,* **138**: pp. 49-72.

[197] Macedo, A.J., K.N. Timmis, and W.R. Abraham, (**2007)** "Widespread capacity to metabolize polychlorinated biphenyls by diverse microbial communities in soils with no significant exposure to PCB contamination." *Environ Microbiol,* **9** (8): pp. 1890-1897.

[198] Pelz, O., M. Tesar, R.M. Wittich, E.R. Moore, K.N. Timmis, and W.R. Abraham, (**1999)** "Towards elucidation of microbial community metabolic pathways: unravelling the network of carbon sharing in a pollutant-degrading bacterial consortium by immunocapture and isotopic ratio mass spectrometry." *Environ Microbiol,* **1** (2): pp. 167-174.

[199] Vonderheide, A.P., K.E. Mueller, J. Meija, and G.L. Welsh, (**2008)** "Polybrominated diphenyl ethers: causes for concern and knowledge gaps regarding environmental distribution, fate and toxicity." *Sci Total Environ,* **400** (1-3): pp. 425-436.

[200] Macedo, A.J., T.R. Neu, U. Kuhlicke, and W.-R. Abraham, "Adaptation of microbial communities in soil contaminated with polychlorinated biphenyls, leading to the transformation of more highly chlorinated congeners in biofilm communities." *Biofilms*.

[201] Bumpus, J.A., (**1989)** "Biodegradation of polycyclic hydrocarbons by *Phanerochaete chrysosporium*." *Appl Environ Microbiol,* **55** (1): pp. 154-158.

[202] Collins, P.J., M. Kotterman, J.A. Field, and A. Dobson, (**1996)** "Oxidation of anthracene and benzo[a]pyrene by laccases from *Trametes versicolor*." *Appl Environ Microbiol,* **62** (12): pp. 4563-4567.

[203] Hammel, K.E., W.Z. Gai, B. Green, and M.A. Moen, (**1992)** "Oxidative degradation of phenanthrene by the ligninolytic fungus *Phanerochaete chrysosporium*." *Appl Environ Microbiol,* **58** (6): pp. 1832-1838.

[204] Kotterman, M.J., H.J. Rietberg, A. Hage, and J.A. Field, (**1998)** "Polycyclic aromatic hydrocarbon oxidation by the white-rot fungus *Bjerkandera sp*. strain BOS55 in the presence of nonionic surfactants." *Biotechnol Bioeng,* **57** (2): pp. 220-227.

[205] Valli, K., H. Wariishi, and M.H. Gold, (**1992)** "Degradation of 2,7-dichlorodibenzo-p-dioxin by the lignin-degrading basidiomycete *Phanerochaete chrysosporium*." *J Bacteriol,* **174** (7): pp. 2131-2137.

[206] Dietrich, D., W.J. Hickey, and R. Lamar, (**1995)** "Degradation of 4,4'-dichlorobiphenyl, 3,3',4,4'-tetrachlorobiphenyl, and 2,2',4,4',5,5'-hexachlorobiphenyl by the white rot fungus *Phanerochaete chrysosporium*." *Appl Environ Microbiol,* **61** (11): pp. 3904-3909.

[207] Takada, S., M. Nakamura, T. Matsueda, R. Kondo, and K. Sakai, (**1996)** "Degradation of polychlorinated dibenzo-p-dioxins and polychlorinated dibenzofurans by the white rot fungus *Phanerochaete sordida* YK-624." *Appl Environ Microbiol,* **62** (12): pp. 4323-4328.

[208] Zhou, J., W. Jiang, J. Ding, X. Zhang, and S. Gao, (**2007)** "Effect of Tween 80 and beta-cyclodextrin on degradation of decabromodiphenyl ether (BDE-209) by White rot fungi." *Chemosphere,* **70** (2): pp. 172-177.

[209] Davey, H.M., (**2011)** "Life, Death and in-Between: Meanings and Methods in Microbiology." *Appl Environ Microbiol*.

[210] Joner, E.J., A. Johansen, A.P. Loibner, M.A. de la Cruz, O.H. Szolar, J.M. Portal, and C. Leyval, (**2001)** "Rhizosphere effects on microbial community structure and dissipation and toxicity of polycyclic aromatic hydrocarbons (PAHs) in spiked soil." *Environ Sci Technol,* **35** (13): pp. 2773-2777.